VOLCANISM OF THE EASTERN SNAKE RIVER PLAIN, IDAHO:

A Comparative Planetary Geology Guidebook

VOLCANISM OF THE EASTERN SNAKE RIVER PLAIN, IDAHO:
A Comparative Planetary Geology Guidebook

Edited by

Ronald Greeley
Department of Geology and Center for Meteorite Studies
Arizona State University
Tempe, Arizona 85281

and

John S. King
Department of Geological Sciences
State University of New York at Buffalo
Amherst, New York 14226

August 1977

Prepared for the Office of Planetary Geology
National Aeronautics and Space Administration
Washington, D.C.

Cover:
Low oblique aerial view of King's Bowl lava field.

PREFACE

This guidebook was prepared for the Planetary Geology Field Conference on Basaltic Volcanism, Snake River Plain, Idaho, sponsored by the Office of Planetary Geology, National Aeronautics and Space Administration, Washington, D. C. The guide and the conference are part of a continuing series designed to show the differences and similarities of the terrestrial planets.

A great many people have contributed to the publication of this guidebook. We thank first our colleagues who are working on the Snake River Plain for their helpful discussions, including S. Oriel, M. Kuntz, R. Holcomb, H. Protsky, and H. Covington. For reviews of various chapters, we thank C. Hodges, P. Spudis, S. Oriel, E. Theilig, and C. Langway. Assistance in figure preparation and editorial procedures was provided by D. Stroud, P. Spudis, R. Papson, E. Theilig, C. Wilbur, M. Womer, and C. Greeley.

R. Greeley and J. S. King, 1977

TABLE OF CONTENTS

1. INTRODUCTION

Ronald Greeley
Dept. of Geology and
Center for Meteorite Studies
Arizona State University
Tempe, Arizona 85281

John S. King
Dept. of Geological Sciences
State University of
New York at Buffalo
Amherst, New York 14226

1. INTRODUCTION

Ronald Greeley
Dept. of Geology and
Center for Meteorite Studies
Arizona State University
Tempe, Arizona 85281

John S. King
Dept. of Geological Sciences
State University of
New York at Buffalo
Amherst, New York 14226

The Planetary Geology Field Conference on the central Snake River Plain was conceived and developed to accomplish several objectives. Primarily, field conferences are sponsored by the National Aeronautics and Space Administration to draw attention to aspects of terrestrial geology that appear to be important in interpreting the origin and evolution of extraterrestrial planetary surfaces. Another aspect of this conference, however, is to present results of recent research in a region. Within the last decade several investigations have been initiated, including work by the organizers and associated graduate students, other university investigators, studies conducted by the National Reactor Test Facility, and a major geological-geophysical investigation by the U. S. Geological Survey (Geologic Division, Denver, Colorado). A final objective of this conference is to bring together investigators of diverse backgrounds who share a common interest in the Snake River Plain.

Exploration of the inner Solar System has shown that the Moon, Mars, Mercury, and possibly Venus, have experienced volcanism during their evolution. More specifically, basaltic lavas (or lavas with comparable properties) appear to cover substantial areas of the terrestrial planets. Thus, it has become clear that an understanding of the physical and chemical processes of basaltic volcanism is essential to the derivation of the histories for the inner planets. Basaltic volcanism, however, is an extremely complex topic, requiring the effort of many different disciplines.

The ideal sequence of planetary exploration begins with reconnaissance unmanned missions, followed by more comprehensive survey missions, samples returned by unmanned spacecraft, and, ultimately, manned exploration by scientists. Given the present level of space exploration, it is doubtful that this sequence will be completed for the terrestrial planets in this century. Thus, to interpret the geological histories of the planets, we must rely primarily on remote sensing methods and studies of possible Earth analogs supplemented by occasional returned samples.

The Snake River Plain appears to be similar in surface morphology to many volcanic regions on the Moon, Mars, and possibly Mercury (see Chapters 2 and 14). The Snake River Plain is comparable in size to many of the extraterrestrial regions observed on these planets and affords the opportunity to study at close hand the various relationships of the rocks to the surface morphology. Moreover, the Plain has been subjected to nonvolcanic processes, such as sapping, "burst" floods, and aeolian (wind) processes that are probably in many ways comparable to Mars. Therefore, the Snake River Plain, in combination with the relatively good state of preservation, the lack of forests or other heavy vegetation, and the good network of jeep trails, is an area nearly ideal for analog studies.

Because of limitations in time, resources, and manpower, the field conference and this guidebook are restricted primarily to the central and eastern Snake River Plain (Figs. 1-1 and 1-2). As discussed in Chapter 4, the western Snake River Plain is distinct in age, structure, and petrology from the central and eastern parts of the plain. Moreover, the enormous distances required to cover all of the plain would either make the conference too long or would result in rather superficial treatment.

Consequently, we have chosen to concentrate on the geology of a part of the plain north of American Falls, Idaho

FIGURE 1-1. Physiographic diagram of part of western United States showing setting of the Snake River Plain (arrow). (From U. S. Geological Survey, 1968.)

(Fig. 1-3). This area displays most of the relationships that are important in understanding the Snake River Plain and the style of volcanism involved in its evolution. Field trips to this area will be supplemented with a trip to Craters of the Moon National Monument, and with an air tour over the central and eastern portions of the plain.

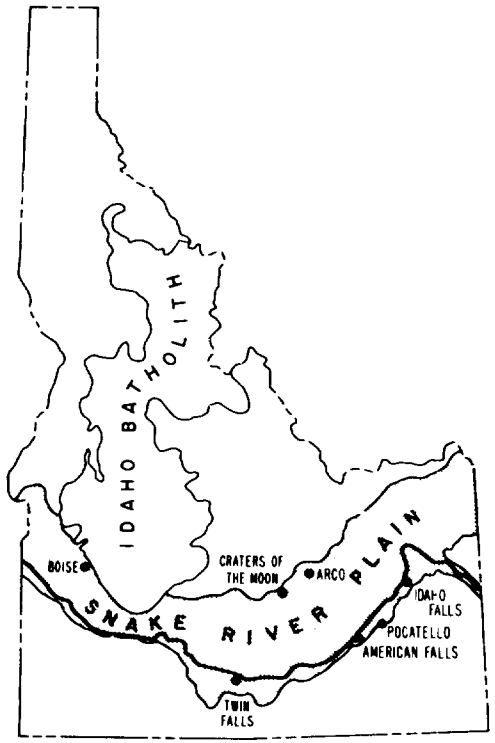

FIGURE 1-2. Outline map of Idaho showing Snake River Plain.

This guidebook includes descriptions of many more areas than will be included during the conference. Their inclusion, however, is intended to provide a broader information base and to encourage visits to the Snake River Plain after the conference. We caution, however, that many of the sections contained herein are in the form of progress reports and are subject to later revision.

REFERENCES

U. S. Geological Survey, 1968. Sheet 59, "Physiography," of National Atlas.

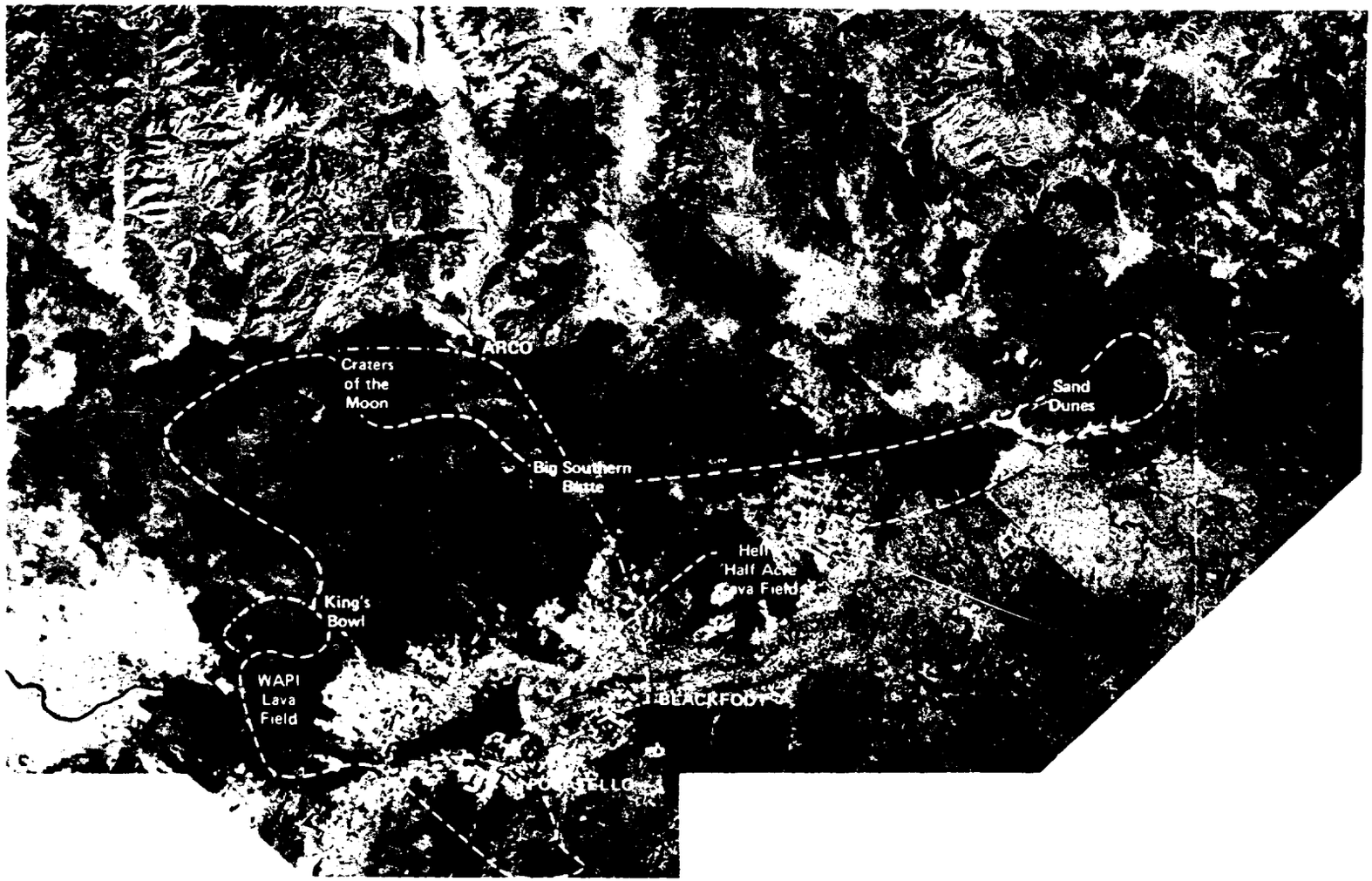

FIGURE 1-3. Mosaic of ERTS images showing the Snake River Plain and identifying areas discussed in this guide. Dashed line indicates approximate flight path for aerial reconnaissance; dot-dash line indicates roads to be used for field trips to King's Bowl–Wapi area and to Craters of the Moon.

2. VOLCANIC MORPHOLOGY

Ronald Greeley
Department of Geology and
Center for Meteorite Studies
Arizona State University
Tempe, Arizona 85281

2. VOLCANIC MORPHOLOGY

Ronald Greeley
Department of Geology and
Center for Meteorite Studies
Arizona State University
Tempe, Arizona 85281

Planetary exploration of the inner solar system has been active for more than a decade. The level of exploration has not been equal for all the planets missions range from photographic flybys of Mercury, through orbiters and unmanned landings on some planets, to manned landings on and samples returned from the Moon. As a result of this exploration, evidence abounds to demonstrate that volcanism has played an important role in the origin and modification of planetary surfaces.

Volcanism on the Moon is demonstrated by photogeology and returned samples that include vesicular basalt (Fig. 2-1), confirming earlier interpretations that the dark lunar maria are vast lava flows (Fig. 2-2). Similar rock textures and flow fronts are also visible on Mars (Figs. 2-3 and 2-4) and lava-like plains occur on Mercury. The spectacular shield volcano on Mars, Olympus Mons, is readily recognized as volcanic (Fig. 2-5) and recent radar images suggest similar constructional landforms on Venus (Malin and Saunders, 1977). Chapter 15 shows some of the volcanic features observed on the planets and illustrates that planetary exploration has reached the stage where it is not enough simply to recognize the presence of volcanism on the planets. Rather, it is critical to the derivation of geological histories to be able to interpret the styles of volcanism, modes of eruption, and general volcanic histories that were involved in the origin and evolution of planetary surfaces.

FIGURE 2-1. A highly vesicular olivine basalt (sample 15016) returned from the Moon by the Apollo 15 astronauts from near the Hadley rille. (after Taylor, 1975; NASA photograph S 71-45477).

The best approach to volcanic history is to combine detailed fieldwork with laboratory studies. Such an approach is presently not possible except for Earth and a few localities on the Moon from which samples have been returned. Thus, we must resort to remote sensing methods, primarily photogeology, supplemented by other techniques, such as spectral analyses, from which interpretations can be drawn. In this chapter, consideration is given to the parameters that govern volcanic morphology.

The styles of volcanism and eruptive histories displayed on planetary surfaces can be determined to some degree through the interpretation of the volcanic landforms. Variations in certain volcanic parameters, such as rate of eruption and volatile content cause distinctive styles of eruption (Hawaiian, Strombolian, etc.), which in turn can lead to distinctive landforms (shield volcanoes, cinder cones, etc.).

FIGURE 2-2. View northward across Mare Imbrium on the Moon as seen by the Apollo 15 astronauts, showing multiple lava flows, each about 30 m thick. The great length of these flows, some exceed 1000 km in length, is indicative of high rates of effusion, extremely low viscosities by comparison with lava flows on Earth, and low thermal conductivities. (NASA Apollo 15 frame AS 15-1556).

FIGURE 2-3. View of the martian surface obtained by Viking Lander 1 showing numerous vesicular rocks considered to be volcanic in origin. (NASA photograph #11-722).

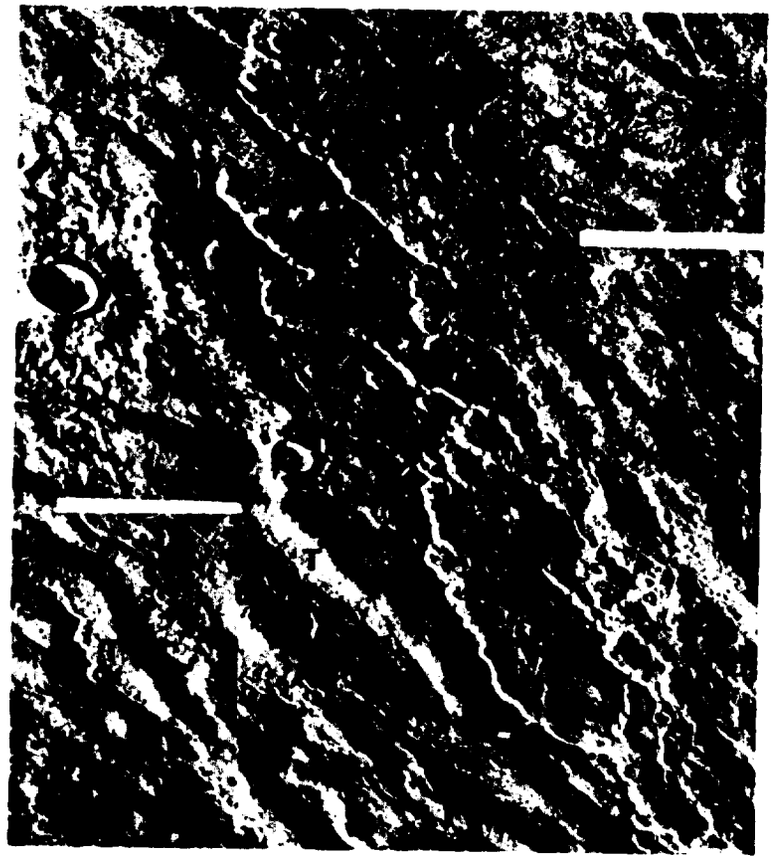

FIGURE 2-4. Viking Orbiter mosaic showing an oblique view across the flank of Alba Patera, one of the large constructs on Mars. The area shown is built of numerous flood-type lava flows - the sheet-like masses indicated by 'F' , and lava flows fed through lava tubes ('T'); flow direction is indicated by the arrow. Possible volcanic domes, some with summit craters, are also visible (small arrow); alternatively, these features may be a class of impact crater. Area of mosaic is about 130 km by 150 km. (after Carr and others, 1977; Viking Orbiter frames 7 B 22 to 27).

FIGURE 2-5. Shaded airbrush relief map of Olympus Mons, the 600 km-diameter shield volcano on Mars. High resolution images show that the shield is constructed of multiple lava flows, often of the tube-and-channel-fed variety. Viking Orbiter images show that many of the flows are superimposed on the bounding scarp and extend hundreds of km across the surrounding plains. (map courtesy of the U.S. Geological Survey).

Distinctive volcanic landforms are clues to styles of volcanism involved in their formation and provide insight into the physical processes of eruption.

This concept has been used for many years on the planets for obvious structures such as shield volcanoes, possible composite cones, and cinder cones, but it is only recently that more refined and complex interpretations have been attempted. Application of the techniques requires a comprehensive understanding of volcanic processes and familiarity with the associated landforms. This approach has not been needed to any great extent by geologists studying volcanoes on Earth, where it is generally possible to conduct field work, and the geomorphology of volcanic landforms as related to eruptive processes has not been studied extensively. Recently, such studies have been undertaken primarily by planetary geologists and, because basaltic volcanism appears to be prevalent on the terrestrial planets, the emphasis has been on basaltic terrains.

VOLCANIC MORPHOLOGY

The pristine forms of volcanoes and volcanic deposits are the result of many complex parameters (Table 2-1). The term volcanic *construct* refers here to the accumulation of volcanic products and includes classic stratovolcanoes, basaltic plains, cinder cones, and similar features. The factors controlling the morphology of volcanic constructs are: 1) style of eruption, 2) proportions of liquids, solids, and gases in the eruptives, 3) viscosities and composition of the lava, 4) vent characteristics, 5) rate and duration of effusion, and 6) pre-flow topography, and to some extent, structure.

Styles of Eruption

Volcanoes have long been classified according to their activity (Table 2-2). Several classifications of volcanic eruptions have been derived, as discussed by Rittmann (1962), Macdonald (1972), Bullard (1976), and others. Table 2-3 is a modification of a classification from Macdonald; it is arranged by increasing explosiveness from relatively quiet basaltic flood eruptions through the sometimes violent ultravulcanian eruptions. Also listed are gas eruptions and fumarolic activity, neither of which produce significant landforms, at least on Earth. Most of the categories of volcanic activity shown in the classification are based on historic eruptions or on volcanoes that are currently active.

TABLE 2-1

FACTORS INFLUENCING THE MORPHOLOGY OF VOLCANIC CONSTRUCTS*

Style of eruption (strombolian, Plinian, etc.)

Proportion of liquids (lava), gases and solids (tephra)

Viscosity of Lava
- Temperature
- Composition
- Amount and State of Volatiles
- Degree of Crystallization
- Character of Flows (e.g., laminar, turbulent)

Vent Characteristics (shape, number, arrangement)

Rate and Duration of Effusion

Pre-flow Topography

* Factors are interrelated.

Volcanic morphology is directly linked to style of eruption—basaltic flood eruptions produce great volumes of hot fluid lava that spread out as flat sheets that often become ponded: strombolian activity involves repeated eruptions of tephra and pasty lava that are ejected relatively short distances from the vent and deposited subaerially to form cinder cones. Peléean eruptions involve thick, pasty block lava flows in relatively low volumes that form dome volcanoes. Flow surfaces of block lavas are often characterized by coarsely "corded," or festooned textures on large scales (Fig. 2-6). Plinian and rhyolitic flood eruptions can produce widespread

ash flows that are deposited as relatively smooth plains. Characteristic surface features of ash flows at scales that could be recognized on aerial photographs are not known, and thus the photogeologic identification of widespread ash flows on planetary surfaces remains difficult.

Proportions of Liquids, Gases, and Solids

The three types of materials produced by volcanic eruptions are liquids (lava), gases (on Earth, mostly steam), and solids (pyroclastics, or *tephra* in the form of ash, lapilli, blocks, bombs, etc.). The higher the proportion of lava erupted, the lower the profile of the resulting volcanic edifice; increases in the amount of ejected solids steepen the construct, as in the case of composite cones, the largest of which are stratovolcanoes. Volatiles released from the magma on eruption often cause fire fountaining and the formation of cinder and spatter cones. If the volatile content is low, or if the volatiles remain in solution in the lava until the flow is emplaced, the volatiles enhance the fluidity of the lava, as discussed below.

TABLE 2-2

CLASSIFICATION OF VOLCANOES (MODIFIED FROM RITTMANN, 1962)

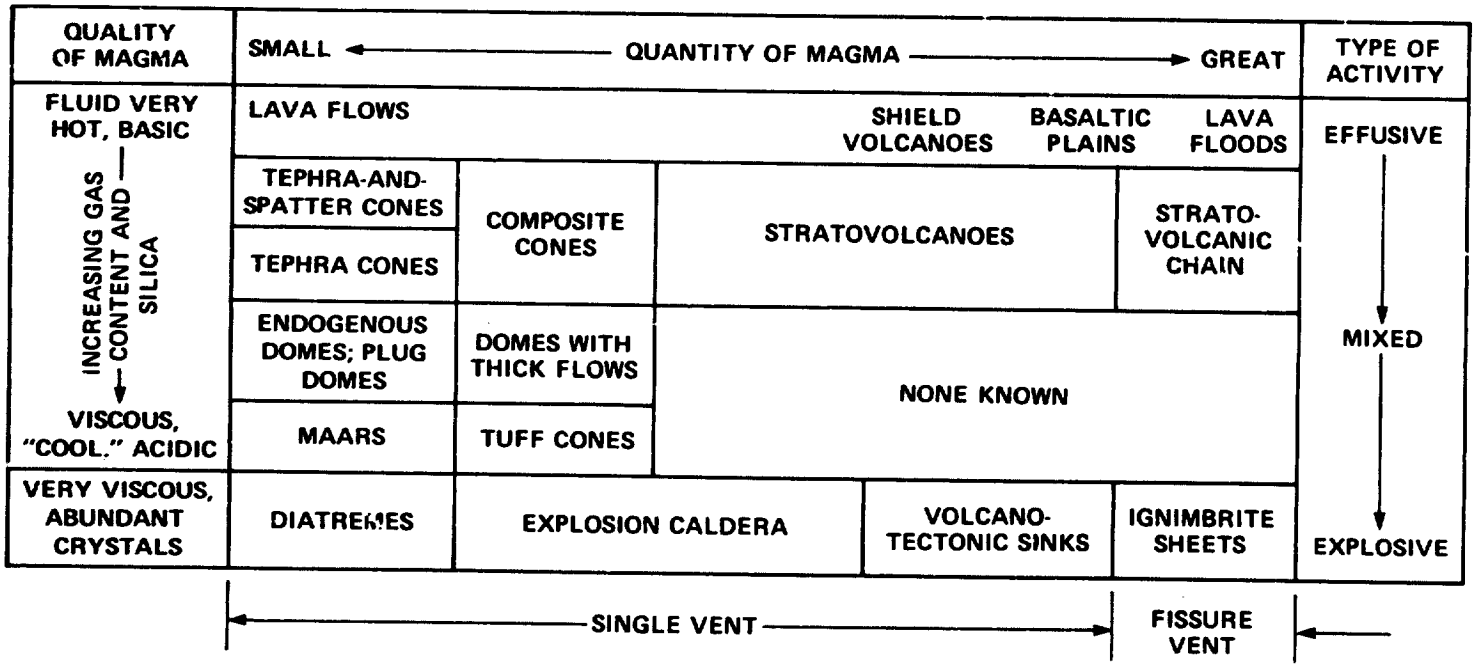

TABLE 2-3. Classification of volcanic eruptions (modified after Macdonald 1972)

Eruption type	*Physical nature of the magma*	*Character of explosive activity*	*Nature of effusive activity*	*Nature of dominant ejecta*	*Structures built around vent*
Basaltic flood	Fluid	Very weak ejection of very fluid blebs; little lava fountaining	Voluminous wide-spreading flows of very fluid lava	Cow-dung bombs and spatter; very little ash	Small spatter cones and ramparts of limited extent; broad lava plain
"Plains" or Icelandic (sensu stricto)	Fluid	Weak ejection of very fluid blebs, little lava fountaining	Moderately wide spreading flows of thin sheets, often through lava tubes and channels	Cow-dung bombs and spatter; very little ash	Very broad flat lava cone, (shields) which frequently coalesce, some spatter cones
Hawaiian	Fluid	Weak ejection of very fluid blebs; lava fountains	Thin, often extensive flows of fluid lava, frequently involving lava tubes and/or channels.	Cow-dung bombs and spatter; very little ash	Spatter cones and ramparts; very broad flat lava cones
Strombolian	Moderately fluid	Weak to violent ejection of pasty fluid blebs	Thicker, less extensive flows of moderately fluid lava; flows may be absent	Spherical to fusiform bombs; cinder; small to large amounts of glassy ash	Cinder cones
Vulcanian	Viscous	Moderate to violent ejection of solid or very viscous hot fragments of new lava	Flows commonly absent; when present they are thick and stubby; ash flows rare	Essential, glassy to lithic, blocks and ash; pumice	Ash cones, block cones, block-and-ash cones
Peléean	Viscous	Like Vulcanian, commonly with glowing avalanches	Domes and/or short very thick flows; may be absent	Like Vulcanian	Ash and pumice cones; domes
Plinian (exceptionally strong Vulcanian)	Viscous	Paroxysmal ejection of large volumes of ash, with accompanying caldera collapse	Ash flows, small to very voluminous; may be absent	Glassy ash and pumice	Widespread pumice lapilli and ash beds; generally no cone building
Rhyolitic flood	Viscous	Relatively small amounts of ash projected upward into the atmosphere	Voluminous wide-spreading ash flows; single flows may have volume of tens of cubic miles	Glassy ash and pumice	Flat plain, or broad flat shield, often with caldera
Ultravulcanian	No magma	Weak to violent ejection of solid fragments of old rock	None	Accessory and accidental blocks and ash	Block cones; block-and-ash cones
Gas eruption	No magma	Continuous or rhythmic gas release at vent	None	None; or very minor amounts of ash	None
Fumarolic	No magma	Essentially nonexplosive weak to moderately strong long-continued gas discharge	None	None; or rarely very minor amounts of ash	Generally none; rarely very small ash cones

FIGURE 2-6a. Vertical aerial photograph of Big Glass Mountain, a rhyolite obsidian flow complex in the Medicine Lake Highlands, east of Mount Shasta. The steep flow fronts, rugged-relief surfaces, and stubby character of the flows are typical of silicic block flows, as are the large scale 'festoons' on the flow surface. (U.S. Forest Service Photograph DDC-3P-28; July, 1955.)

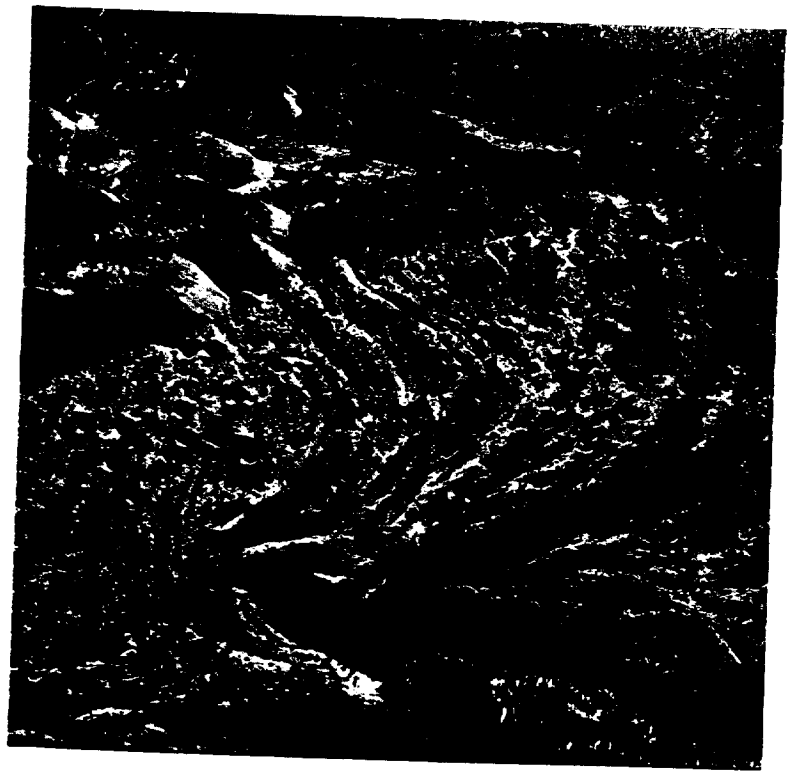

FIGURE 2-6b. Oblique aerial view of Big Glass Mountain. Road in upper right corner indicates scale. (NASA-Ames photograph by W. Quaide, September, 1968.)

Viscosity of Lava

One of the most complex parameters governing volcanic morphology is the viscosity of the lava. Flows that are fluid will spread relatively farther from their vent, forming flat or low-profile constructs, whereas more viscous flows tend to pile up near the source and form dome volcanoes. The viscosity of the lava is controlled primarily by temperature, composition, amount and state of volatiles, degree of crystallization, and flow characteristics (laminar, turbulent, etc.), most of which are interdependent. Relatively few valid measurements of lava viscosities have been made in the field. Macdonald (1972) compiled published results for field estimates of viscosity and shows values ranging from 2×10^3 poise at eruptive temperatures of 1100°C for Hawaiian lavas, to 1×10^{12} poise for rhyolitic lava in Alaska erupted at 800°C. Most of the values obtained in the field are for basalt flows and are model-dependent estimates based on rate of flow in channels. Such estimates require that the depth and shape of the channel be known, which is seldom the case.

The inverse relationship of viscosity to temperature is readily seen in Fig. 2-7. The relations are shown as curves derived from a model of Shaw (1972) in which viscosity as a function of temperature can be determined from the composition of cooled lavas. Even the most fluid terrestrial lavas are not as fluid as some lunar lavas. As determined from laboratory measurements of simulated lunar materials, Murase and McBirney (1970) estimated that basalts in Mare Tranquillitatis were 10 poise at 1400°C. Figure 2-7 shows values for various lunar lavas compared to Columbia Plateau flood basalts and some basalt flows in Hawaii.

The difficulty with estimates of viscosity based on lava composition and laboratory measurements of viscosity is that current methods do not take into account volatile content or the state of the volatiles. Typically, large amounts of volatiles *in solution* in the magma decrease the viscosity, but as the volatiles come out of solution, viscosity can increase. Macdonald (1972) gives an excellent example of the effect: water containing liquid soap in solution is rather fluid, but as soon as the mixture is agitated, soap bubbles form and the resulting frothy mass becomes more viscous. If devolatilization occurs in lavas without vesiculation, the increase in viscosity could be less.

The effect of composition on viscosity is governed largely by the proportion of silica and alkalies. On a molecular scale, silica forms complex three-dimensional networks which can

greatly retard flow and increase the viscosity of lava. Thus, high silica lava flows such as rhyolite and dacite tend to be thick and pasty, whereas low silica lavas such as basalt are more fluid.

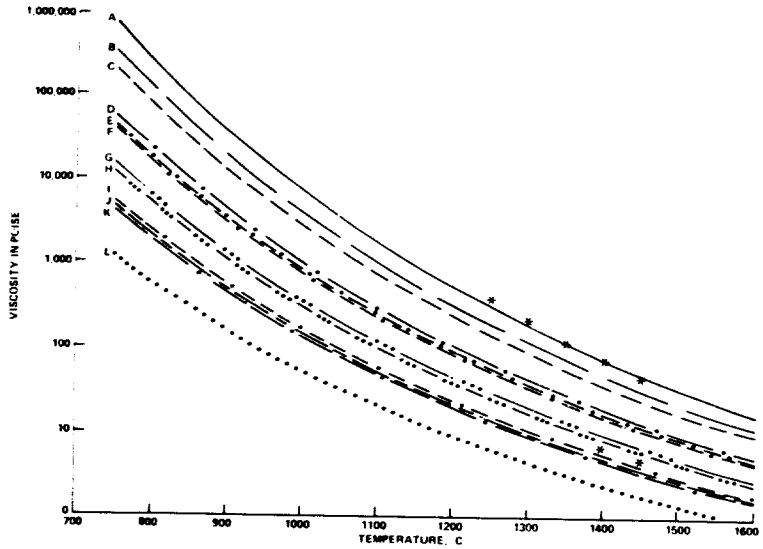

*FIGURE 2-7. Temperature-viscosity curves for some terrestrial and lunar basalts, derived from data of Shaw (1972); asterisks represent laboratory measurements of viscosity. A–Columbia River basalt, (Murase and McBirney, 1970) *=measured viscosity; B–Cave Basalt, Mount St. Helens, Washington: C– average Keaiwa Flow, Hawaii; D–average Mauna Ulu basalt Hawaii; E–Apollo 12 alumina basalt (sample 12038); F–Apollo 15 quartz basalt (sample 15076); G–Apollo 12 quartz basalt (sample 12052); H–simulated lunar basalt (Murase and McBirney, 1970) *=measured viscosity; I– Apollo 12 olivine basalt (sample 12009); J–average Apollo 11 'low potassium' basalt, and Apollo 15 olivine basalt (sample 15555); K–average Apollo 11 'high potassium' basalt; L–Apollo 17 high titanium basalt (sample 71005).*

Vent Characteristics

The size, number, arrangement, and, to some degree, the shape of volcanic vents influence the morphology of volcanoes. Vents are commonly either central (e.g., craters) or linear (fissures, Fig. 2-8). Central vents are typical of cones, shields, and domes, whereas linear vents characterize plateaus or plains. These generalizations are greatly oversimplified, however, and other factors, such as the scale of the vent system and the volume of materials erupted, must also be considered. For example, Mauna Loa is a shield volcano having a prominent central vent, the summit caldera Mokuaweoweo. The great mass of the shield, however, includes not only lavas from the central vent, but also substantial accumulations from small-volume fissure flows erupted on the flanks (Fig. 2-9).

Fissure systems that feed basaltic flood eruptions and major rhyolitic ash flows can be very large. The vent system that fed the Yakima Basalt, one of the many flood basalt flows making up the Columbia River Plateau, is more than 130 km long (Fig. 2-10; Swanson and others, 1975) and evidently was nearly continuously eruptive along its entire length. Eruptions from large fissures seldom occur more than once from the same fissure but rather, the rising magma for subsequent eruptions appears to create new fissures commonly parallel or sub-parallel to previous fissures. This characteristic may partly account for the formation of plateaus rather than prominent constructional ridges.

"Point-source" vents commonly occur along small fissures of the type observed on the flanks of Mauna Loa and other shield volcanoes, and along other small fissures such as the King's Bowl Rift, Idaho. These "point-source" eruptions often form small spatter and cinder cones (Fig. 2-11).

Pre-flow Topography

Pre-flow topography also can influence the surface morphology of lava flows. Depressions such as valleys and craters obviously control the emplacement of lava flows.

FIGURE 2-8. View westward along a small fissure and flow that formed in November, 1973, in Hawaii on the east rift zone of Kilauea volcano. Pauahi Crater is in the background. (photograph by Ronald Greeley, University of Santa Clara, November, 1973).

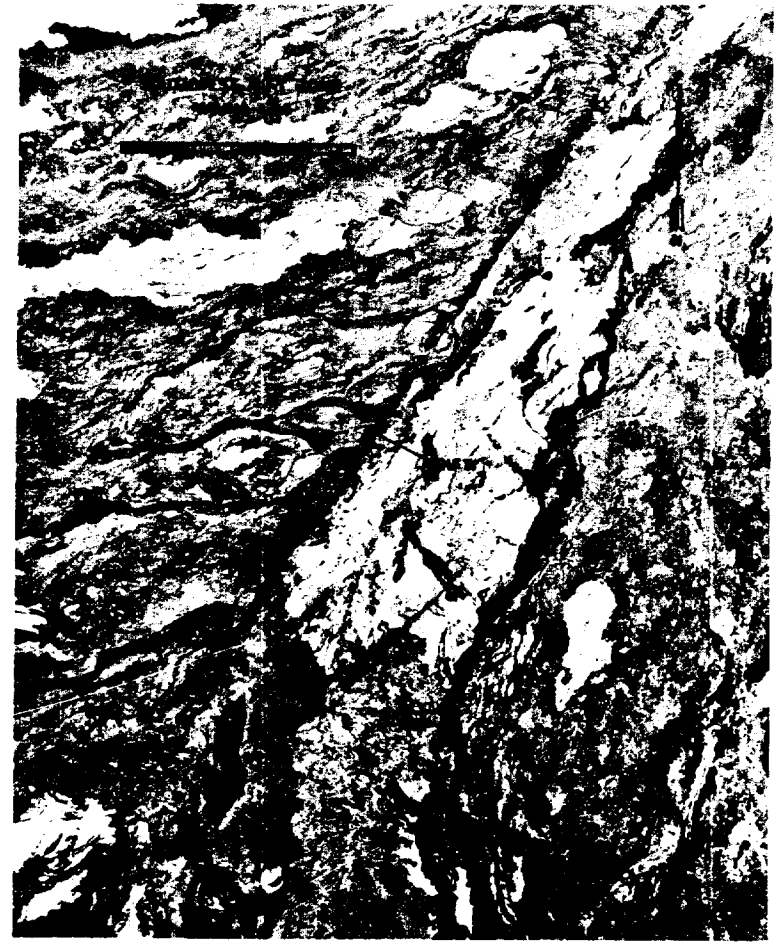

FIGURE 2-9. Southwest rift zone of Mauna Loa shield volcano, Hawaii, showing a prominent fissure, or rift, and associated flows. (U.S. Department of Agriculture photograph).

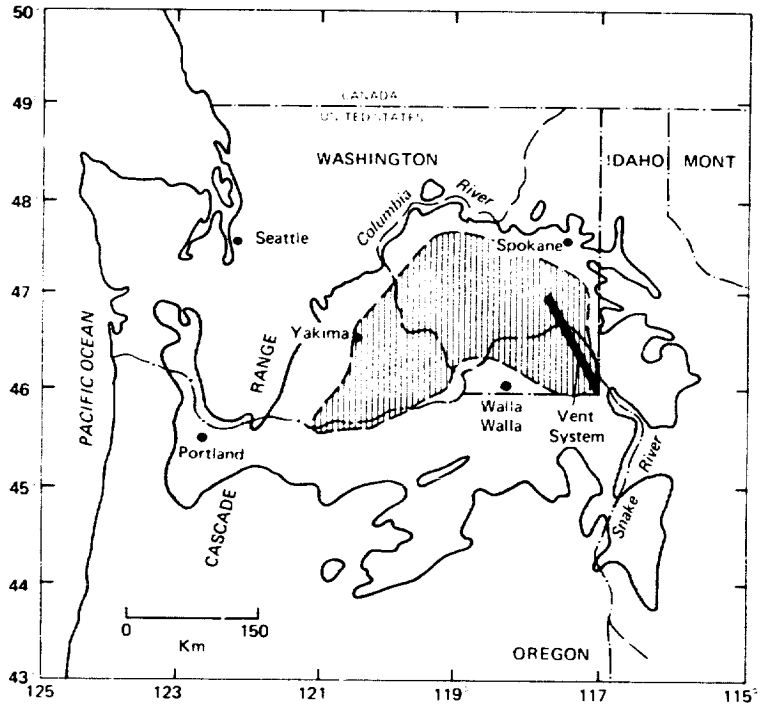

FIGURE 2-10. Sketch map showing original extent of the Roza Member of the Yakima Basalt, the location of the Roza vent system, and the margin of the Columbia Plateau basalts (stipple pattern). (after Swanson and others, 1975).

Even after pre-flow topography is buried, it can affect the flow morphology. Valley floors usually contain the thickest and frequently most active part of a lava flow. In flows containing lava tubes, the tubes often develop in the thickest part of the flow; hence, the axis of the tube coincides with the pre-flow valley floor and collapsed lava tubes mark the location of the former valleys. This effect probably does not result, however, in flows filling shallow valleys.

Buried pre-flow topography can also affect flow surface morphology by controlling differential settling of the lava after its emplacement. Some settling is caused by shrinkage during cooling, but much settling appears to result from devolatilization (Holcomb and others, 1974). Some basalt flows may contain more than 50 percent volatiles by volume, and as degassing takes place, the level of the flow surface subsides, leaving "bath tub" rings around the edges. As the surface is lowered over pre-flow positive features, such as ridges or crater rims, differential settling by the lava can produce an imprint of the underlying structure on the surface; a particularly striking extra-terrestrial example is shown on Mars by Viking Orbiter images (Fig. 2-12).

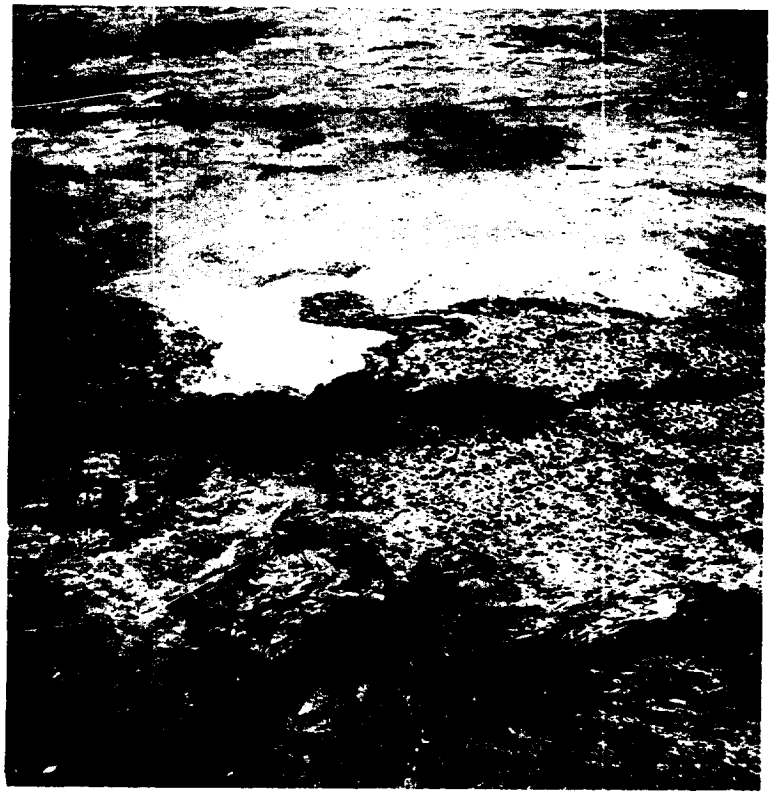

FIGURE 2-11. Oblique aerial view westward across South Grotto, King's Bowl lava field, showing spatter cones along the fissure and lava flows. Highest spatter rampart is about 10 m high. (NASA-Ames photograph by Ronald Greeley, 1969).

FIGURE 2-12. Viking Orbiter 1 image of the border region of the volcanic plains and the heavily cratered terrain on Mars near the crater Pickering, showing flows that have partly buried a crater and that have flowed into a graben. Note the ridge that 'shows through' the overlying flow, even after it has been covered by the lava. (North is to the left; area of photograph is about 109 km by 144 km, Viking Orbiter Frame 56 A 14.)

Another type of pre-flow topographic imprint formed in Hawaii during the filling of Alae Crater by lavas erupted from Mauna Ulu in the late 1960's and early 1970's (Holcomb and others, 1974). Despite the lava burial of the former crater to a depth of tens of meters, the outline of its rim remained visible as a slight scarp, partly as a result of repeated filling and partial drainage of lava from the crater through lava tubes.

Rate and Duration of Effusion

The rate of effusion is the most important factor governing the length of lava flows, according to a recent study by Walker (1973). High rates of effusion result in extensive, far-reaching flows (Fig. 2-13) that are "simple" in character (i.e., composed of a single cooling unit), typified by flood basalts, whereas low rates of effusion produce lavas piled up layer upon layer, forming "compound" flows (see Walker, 1972, for discussion of simple and compound lava flows, and Chapter 4), typified by Hawaiian and basaltic "plains" type volcanism.

The rate of effusion may be calculated as the volume of lava per unit time from the first eruption to the last eruption, including both periods of activity and intervening periods of quiescence. Alternatively, the rate of effusion may be calculated as the volume of lava per unit time only during actual eruption. Thus, the duration of the eruption is closely related to rate. For example, an eruption of short duration but high rate produces a lava flow morphology different than an eruption of long duration but low rate.

BASALTIC LANDFORMS

Basaltic landforms are the most diverse of volcanic structures, perhaps reflecting the wide range of values for the parameters that influence volcanic morphology. Basaltic lavas range from highly fluid to very viscous flows, whereas dacites or other silicic lavas are almost always thick and pasty.

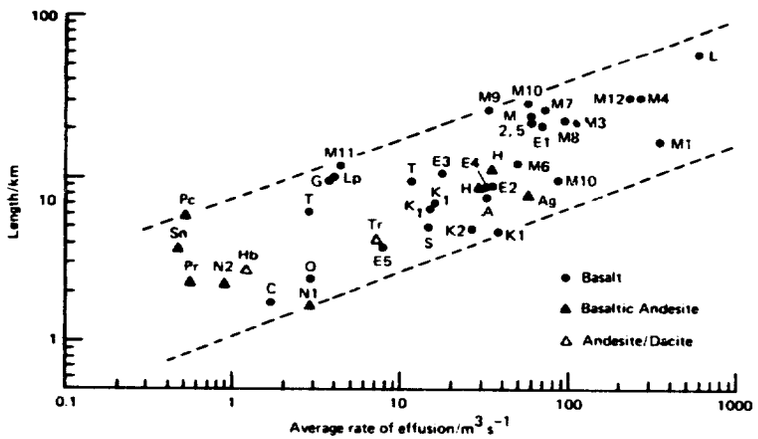

FIGURE 2-13. Plot of lava length against average effusion rate for lava eruptions (mostly basaltic) on various volcanoes. Basaltic lavas, ● : A, Askja 1961 (Iceland); C, Cerro Negra 1968; E, Etna (1, 1669; 2, 1911; 3, 1923; 4, 1928; 5, 1971); G, Gituro 1948 (Congo); K, Kilauea (1, 1955; 2, 1965); L, Laki, 1783 (Iceland); Lp, La Palma 1585; M, Mauna Loa (1, 1851; 2, 1852; 3, 1868; 4, 1887; 5, 1907; 6, 1916; 7, 1919; 8, 1926; 9, 1935; 10, 1942; 11, 1949; 12, 1950); O, Oosima 1951; T, Tenerife 1705; S, Sakurajima 1946. Basaltic andesite lavas, ▲ : Ag, Mt Agung 1963 (Bali); H, Hekla (1, 1845/6; 2, 1947); N, Ngauruhoe (1, 1949; 2, 1954); Pc, Pacaya 1961 (Guatemala); Pr, Paricutin (first 8 months 1945); Sn, Santiaguita (Guatemala). Andesite/dacite lavas, △ : Hb, Hibok-Hibok 1948; Tr, Trident 1953 (after Walker, 1973).

Basaltic flow textures and small surface features have been described by Wentworth and Macdonald (1953), Macdonald (1967), and in a geologic guidebook to Hawaii (Greeley, 1974). Surface features and large constructs are illustrated in Green and Short (1971). Table 2-4 lists the main types of basaltic constructs, gives the styles of their eruptions, and notes typical surface textures.

Flood basalts form extensive, often thick flows erupted at very high rates from fissure vents and produce vast basalt plateaus, typified by the Columbia Plateau (Fig. 2-10). The Yakima Basalt on the Plateau has been studied extensively and serves an an example of a flood basalt (Swanson and others, 1975). The Yakima Basalt includes the Roza Member (1500 km^3) erupted from a linear vent system more than 130 km long and several kilometers wide, and several other members. Vent areas are difficult to identify because they are buried by their own flows; however, dikes and remnants of small pyroclastic cones help to define the general fissure zones, particularly for the less extensive Ice Harbor flows. Eruption rates for the Ice Harbor flows are estimated to have been 2 x 10^{-3}km^3/day and are comparable to those of Kilauea and Mauna Loa, whereas the rate for the Roza Member with an estimated rate of 1 km^3/day was three orders of magnitude higher. Hundreds of cubic kilometers of lava were apparently erupted during a period of at most two or three weeks (Swanson and others, 1975). Throughout most of its 40,000 km^2 extent, the Roza Member consists of a single, simple cooling unit that must have been ponded as vast lava lakes over much of the area, taking years to solidify, as indicated by massive columnar jointing. Lava tubes, lava channels, and other large scale flow features are lacking, either because they did not form or because they were destroyed by activity within the emplaced lavas, such as lava lake circulation. A review of the literature reveals that there are virtually no lava tubes or channels in the other flood basalts of the Columbia Plateau.

Table 2-4. Basaltic volcanoes. (after Greeley, 1976)

Volcanic landform	*Eruptive style*	*Typical texture*	*Comments*
1. Flood basalt plateau	Fissure eruption, high volume-highly fluid; few flow features	Pahoehoe Massive, dense, low vesicularity; vertical jointing	Common on planetary surfaces (1)
2. Basalt "plains"	Fissure and central vent, moderately high volume and rate; fluid lavas; lava tubes and channels	Pahoehoe, tube and toe-fed, aa, variable textures, from massive to vesicular; vertical joints and horizontal platy units	Common on planetary surfaces (2)
3. Basaltic ash plains	Explosive	Pumiceous	Rare
4. Shield volcanoes	Central vent with associated fissures; high rate, moderate volume, fluid lavas, lava tubes and channels	Pahoehoe, tube and toe-fed, vesicular, platy jointing	Common on planetary surfaces (2)
5. Composite cones	Central vent, explosive alternating with flows, tubes and channels infrequent	Pyroclastics and vesicular to dense flows; pahoehoe and aa	Commonly associated with plate subduction zones (3)
6. Cinder cones	Explosive, infrequent flows	Pyroclastics	Common on planetary surfaces (2)
7. Domes	Central vent, low volume, low rate, viscous lavas	Block flows	Rare

(1) Earth, Moon, Mars, Mercury; (2) Earth, Moon, Mars; (3) Earth, Mars (?)

The only surface features of large size preserved on the Roza flow are "sag-flowouts," described by McKee and Stradling (1970) as circular depressions and hills, surrounded by concentric dikes (some more than 250 m across) that appear to have formed by crustal foundering (Fig. 2-14). Recent field studies, however, indicate that some structures may result from phreatic activity after flow emplacement (Hodges, 1977).

Volcanic shields (Fig. 2-5) are produced by relatively high rates of eruption, but the total volumes of lava per eruption sequence are lower than those for flood basalts and the vents are commonly central rather than linear. The nature of the shield-forming eruptions is markedly different from that of flood eruptions. For example, at Mauna Ulu, a small shield volcano in Hawaii, eruptions were sporadic with short stages of quiescence during an eruptive period of five years and produced thin, tube-fed flows. Average flow unit thicknesses for Mauna Ulu and other Hawaiian shield volcanoes is about 5 m, in contrast to 10 to 30 m thick flows in the Columbia Plateau. Rapid outbursts of high volume but short duration also occur on shield volcanoes, as evidenced by the 17 hour summit eruption of Mauna Loa in 1975 (Tilling, personal communication).

Basaltic plains combine some of the characteristics of both flood basalts and shield volcanoes and are tentatively considered (Greeley, 1976) a separate category of volcanic construct, as discussed more fully in Chapter 3. Basaltic plains are typified by the Snake River Plain. This region is made up of lava flows about 10 m thick, erupted from both central vents that produced small coalescing lava shields (termed *low shields*), and short fissures that formed thin sheet-flows; the combined thickness of all flows exceeds 1500 m (LaFehr and Pakiser, 1962) in some places. In size and surface feature morphology, the Snake River Plain resembles some of the smaller lunar maria. As with shield volcanoes, flow features such as lava tubes and lava flow channels are relatively common on basaltic plains.

Composite cones, such as Mt. Shasta in northern California and Mt. Mayon in the Philippines, are steep-sided volcanoes surrounding central vents. As the term suggests, they are composed of a combination of alternating lava flows and tephra deposits, reflecting alternating styles of eruption

from Hawaiian-type to strombolian. The great size (commonly 10-20 km across) is attributed to the eruptive phase that produced lava flows extending many kilometers from the vent. The steep slopes result from the tephra phase, in which cinders accumulate at or near their angle of repose—about 30°. *Parasitic* cinder cones are common on the flanks of composite cones. The accumulations of tephra, both at the summit and in *parasitic* cones, are "welded" together by lava flows, eventually forming the great mass of the composite cone.

As is evident in Table 2-2, volcanic constructs are gradational from one type to the next. Some examples are intermediate between flood lava flows, basaltic "plains," shield volcanoes, and composite cones. The forms may vary spatially and temporally. Thus, one must be wary of assigning too quickly a volcanic style of eruption and mode of lava flow emplacement from the surface morphology—the surface observed may represent only the latest phase of a complex volcanic evolution.

FIGURE 2-14. Stereoscopic aerial photographs showing "sag flowouts," east southeast of Odessa, Washington; larger structure at the bottom is about 500 m across. (U.S. Department of Agriculture photographs AAO-3LL-79, 80.)

SUMMARY

Basaltic lava flows can form many types of constructs (Table 2-4): the largest forms—and the ones commonly observed on spacecraft images of the planets—are flood basalts, basaltic "plains," shield volcanoes, and composite cones, discussed above. Other basaltic features, such as cinder-and-spatter cones, are small accessory or parasitic features that occur with shield volcanoes, basaltic plains, and, rarely, flood basalts.

Shield volcanoes are recognizable by their general topographic form and the presence of small fissures, rift zones, parasitic cinder cones, and various other vent structures such as pit craters, and summit calderas. Shield volcanoes are built of fluid lavas, typically (but not exclusively) basaltic in composition, which are erupted at relatively high rates of effusion; as exemplified by the Hawaiian shield volcanoes, eruptions tend to be sporadic, with intervening periods of quiescence, or low activity, and involve essentially the same vent or vent system repeatedly. These eruptions produce multiple flow units that are thin and commonly fed through lava tubes and lava channels. Shield-forming eruptions of the Hawaiian type have been described as "leaking" from small, shallow reservoirs (Swanson and others, 1975).

Flood lava flows lack flow surface features such as lava tubes and channels. Traces of linear vent systems may be preserved, although typically they are buried by their own products. The long sheet-like flows observed on Mars and the Moon (i.e., the Imbrium flows) are flood lavas. Only basaltic lavas are known to erupt as floods, although in theory magmas of other compositions with similar physical properties could produce similar flows. Flood eruptions represent extremely high rates of effusion from large, deep storage reservoirs. In contrast to the "leaky" style of eruption that forms shield volcanoes, flood eruptions are probably episodic (Swanson and others, 1975), seldom using the same fissure vent more than once per episode.

Basaltic "plains" combine the flow types of shield volcanoes—thin, multiple flow units often emplaced by lava tubes and channels, central vent eruptions, pit craters—with the large-scale flat topography of flood basalts and the arrangement of some of the central vents along major rift systems. Even though the vents are dominantly central, building low-profile coalescing shields, the use of the same vent for a long period of time (as is the case in Hawaii) does not occur. Eruptions are probably sporadic with rates of effusion comparable to those in Hawaiian eruptions.

Composite cones are characterized by: 1) steep profiles and conical shape, 2) parasitic cones, some of which are large in comparison to the main construct, and 3) summit calderas and rift zones. Style of eruption involves production of lava flows—some from Hawaiian-type eruptions -and tephra. The alternating accumulation of these materials leads to the steep slopes characteristic of composite cones. Typically, composite cones are constructed of andesitic lavas, sometimes grading into more silicic compositions.

The interpretation of volcanic processes, based on the morphologies of the constructs, is difficult, particularly on planets where the chemical and physical properties of the magmas are virtually unknown. Studies of terrestrial volcanoes offer the only means of gaining some insight into extraterrestrial volcanology until more complete exploration is feasible.

REFERENCES

Bullard, F. M., 1976. *Volcanoes of the Earth:* University of Texas Press, Austin, 579 p.

Carr, M. H., K. R. Blasius, R. Greeley, J. E. Guest and J. B. Murray, 1977. Some martian volcanic features as viewed from the Viking Orbiters, in press, Jour. Geophys. Research.

Greeley, R. (ed.), 1974. Geologic guide to the Island of Hawaii—A field guide for comparative planetary geology. NASA CR 152416, 257 p.

Greeley, R., 1976. Modes of emplacement of basaltic terrains and an analysis of mare volcanism in the Orientale Basin: Proc. Lunar Sci. Conf. 7th, p. 2747-2759.

Greeley, R., D. Storm and C. Wilbur, 1976. Frequency distribution of lava tubes and channels on Mauna Loa volcano, Hawaii: Geol. Soc. Amer. Abs., vol. 8, p. 892.

Green, J. and N. M. Short, 1971. *Volcanic Landforms and Surface Features–A photographic atlas and glossary:* Springer-Verlag, New York.

Hodges, C. A., 1977. Basaltic ring structures of the Columbia Plateau, in press.

Holcomb, R. T., D. W. Peterson, and R. I. Tilling, 1974. Recent landforms at Kilauea Volcano–A selected photographic compilation: in Greeley, R., ed., Geologic Guide to the Island of Hawaii, NASA CR 152416, p. 50-86.

LaFehr, T. R. and D. H. Pakiser, 1962. Gravity, volcanism and crustal deformation in the eastern Snake River Plain, Idaho: U. S. Geol. Survey Prof. Paper 450 D, p. D76-D78.

McKee, B. and D. Stradling, 1970. The sag flowout: a newly described volcanic structure. Bull. Geol. Soc. Amer., vol. 81, p. 2035-2044.

Macdonald, G. A., 1967. Forms and structures of extrusive basaltic rocks in Basalts: The Poldervaart Treatise on Rocks of Basaltic Composition, vol. 1, Interscience Publ. John Wiley and Sons, New York.

Macdonald, G. A., 1972. *Volcanoes:* Prentice-Hall, Inc., Englewood Cliffs, New Jersey, 510 p.

Malin, M. C. and R. S. Saunders, 1977. Surface of Venus: Evidence of diverse landforms from radar observations: Science, vol. 196, p. 987-990.

Murase, T. and A. R. McBirney, 1970. Viscosity of lunar lavas: Science, vol. 167, p. 1491-1493.

Rittman, A., 1962. Volcanoes and their activity: Interscience Publ., John Wiley and Sons, New York, 305 p.

Shaw, H. R., 1972. Viscosities of magmatic silicate liquids: an empirical method of prediction: Amer. Jour. Sci., vol. 272, p. 870-893.

Swanson, D. A., T. L. Wright and R. T. Helz, 1975. Linear vent systems and estimated rates of magma production and eruption for the Yakima Basalt on the Columbia Plateau. Amer. Jour. Sci., vol. 275, p. 877-905.

Taylor, R. S., 1975. *Lunar Science: A Post Apollo View*, Pergamon Press, New York, 372 p.

Walker, G. P. L., 1972. Compound and simple lava flows and flood basalts. Bull. Volcano., vol. 35, p. 579-590.

Walker, G. P. L., 1973. Lengths of lava flows. Phil. Trans. R. Soc. London A, vol. 274, p. 107-118.

Wentworth, C. K. and G. A. Macdonald, 1953. Structures and forms of basaltic rocks in Hawaii: U. S. Geol. Survey Bull. 994, 98 p.

3. BASALTIC "PLAINS" VOLCANISM

Ronald Greeley
Department of Geology and
Center for Meteorite Studies
Arizona State University
Tempe, Arizona 85281

3. BASALTIC "PLAINS" VOLCANISM

Ronald Greeley
Department of Geology and
Center for Meteorite Studies
Arizona State University
Tempe, Arizona 85281

Analysis of the morphology of the central Snake River Plain and comparisons with other basaltic regions lead to the conclusion that the plain may represent a distinctive style of volcanism that combines aspects of both flood basalts and classic basaltic shield volcanoes. Although traditionally included in the Columbia Plateau and generally considered a plateau basalt region, the central Snake River Plain—and regions similar to it—is considered sufficiently different from flood basalts in the characteristics of the flows and the resulting surface morphology (and, therefore, also different in the style of volcanism involved in its formation) to warrant its consideration as a distinctive class. The expression *basaltic "plains"* has been tentatively proposed (Greeley, 1976) for this intermediate type of volcanic region.

Several authors have recognized the distinctive character of the central and eastern Snake River Plain in comparison to the Columbia Plateau. In many respects, the Snake River Plain is more akin to southeastern Oregon and the Modoc Plateau of California (Fig. 3-1) than to the flood basalts of the Columbia Plateau. The geochemical uniqueness (Figs. 3-2 and 3-3) of the plain has been addressed by Waters (1961), Powers (1960), Jones (19), Leeman (1974, 1975) and others. The differences in the lava flow morphology of the plain and the Columbia Plateau are discussed by Greeley and King (1975) and in Chapter 4 of this guidebook. Thus, there are several independent lines of evidence that show the Snake River Plain is unlike the Columbia Plateau and the inference

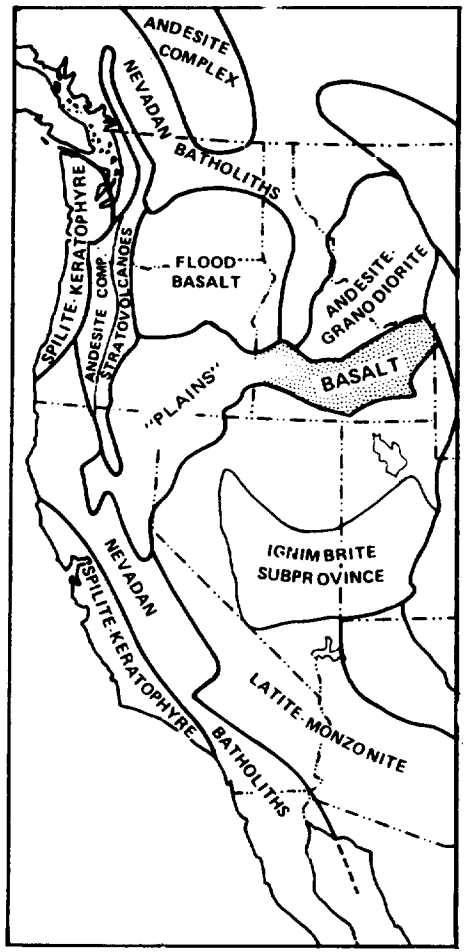

FIGURE 3-1. Map of the western United States showing major igneous provinces; note that the Snake River Plain of Idaho (shaded area) is more closely related to the basaltic regions of southeast Oregon and northeastern California than to the flood basalts of southeastern Washington and northeastern Oregon. (Modified from Eardley, 1962.)

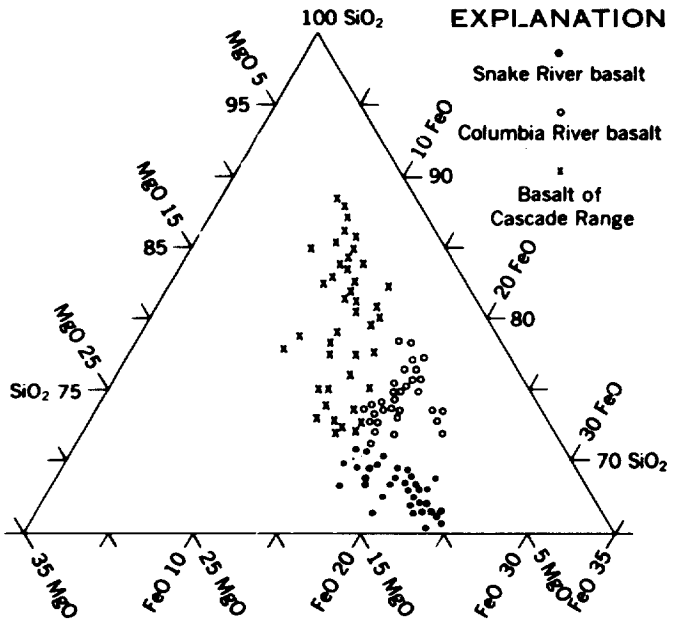

FIGURE 3-2. Ratios between SiO_2, MgO, and total iron plus manganese in some basalts of the northwestern United States. Data plotted are weight percent of SiO_2, MgO, and sum of FeO + 0.9 Fe_2O_3 + MnO computed to 100 percent. (after Powers, 1960)

is drawn that the style of volcanism and modes of lava flow emplacement were also different.

Investigations of basalt regions outside the Snake River Plain suggest that not all basaltic plains are the result of "typical" flood-type eruptions. Walker (1972), for example, proposed the terms *compound lava flows* and *simple lava flows* to distinguish differences in modes of emplacement and in morphology. Walker builds on the recognition by Nichols (1936) that many lava flows can be separated into *flow units* that represent individual "gushes" of lava, but which are all part of the same eruptive sequence. Compound lava flows consist of multiple flow units that range from 5 cm to more than 10 m thick, although most are in the 50 cm to 5 m range. Most pahoehoe lavas are of the compound type; aa lavas occur in both compound and simple flows. Although the interval between emplacement of flow units can be very short, lava crusts typically develop that are sufficiently thick to preserve the individuality of the unit. Thus, compound lava flows are made up of a sequence of thin units which, to some degree, behave as individual cooling units (Fig. 3-4).

In contrast to compound lava flows, simple lava flows consist of single, typically thicker, flow units that are essentially single cooling bodies. Walker (1972) attributes the difference primarily to the rate of effusion; a low rate leads to the development of compound flows, a high rate (flood eruptions) produces simple flows. Thus, determination of the predominant flow type in any one region would enable the prevailing rate (high versus low) of effusion to be estimated.

Another difference between the proposed "plain" type province and classic flood basalts and basaltic shields is the proposal of Noe-Nygaard (1968) to distinguish a sub-category of shield volcanoes for which he proposed the term *shield volcano of scutulum type* (from the Latin *scutulum*, the diminutive of *scutum*, = shield). In studies of the basalt flows of the Faroe Islands, Noe-Nygaard identified very flat shield volcanoes having slope angles of about $1/2^{o}$. The shields described are about 15 km across and are estimated to consist of less than 7 km^3 of lava, made up of compound lava flows. Similar flat shields occur in Iceland. Mauna Iki in Hawaii, constructed from eruptions in 1926, has a similar morphology and is of comparable dimensions. Macdonald (1972, p. 195-196) uses the term *lava cone* to describe Mauna Iki and similar low-profile shields.

It is primarily the small size and low profile of these shields that led Noe-Nygaard and Macdonald to separate the "scutulum" or "lava cone" type shields from Hawaiian and major Icelandic shield volcanoes. To prevent confusion with composite *cones* and to avoid the awkward phrase *shield volcano of scutulum type*, the term *low shield* is proposed to describe this category of volcano. Low shield volcanoes are

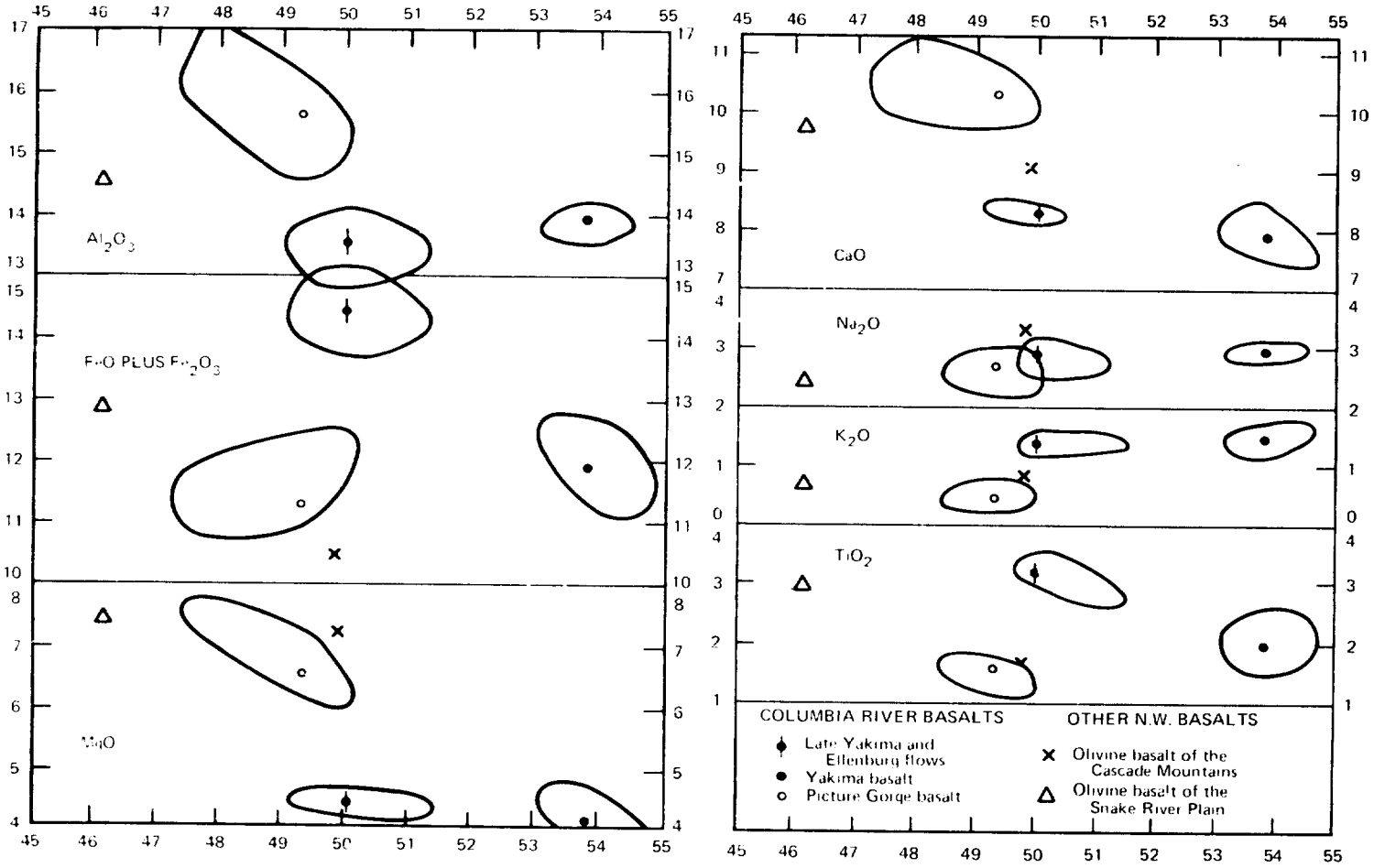

FIGURE 3-3. Variation diagram for basaltic rocks of the Pacific northwest, showing the distinctive character of the Snake River Plain basalts. Spaces enclosed by lines show areas within which chemical analyses fall. (from Waters, 1961.)

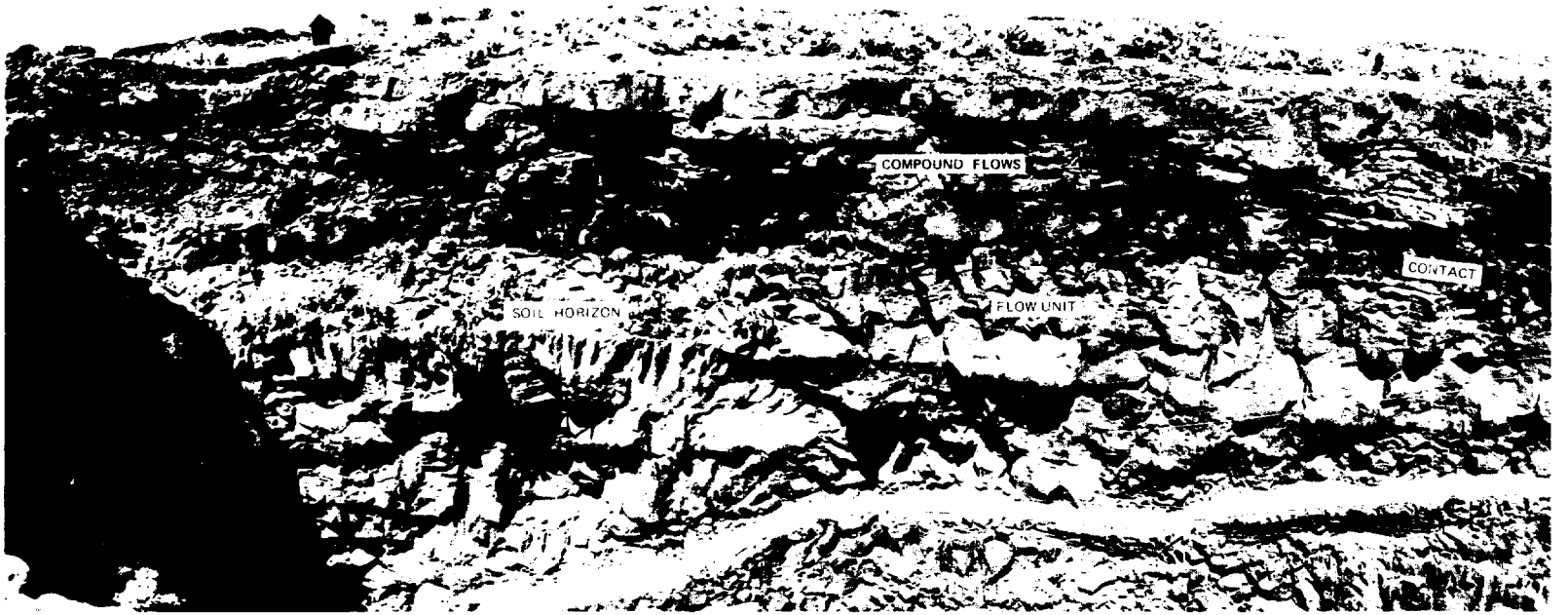

FIGURE 3-4. Panoramic view of the east wall of King's Bowl, showing lava flows typical of the Snake River Plain; compound lava flows consist of multiple, typically thin flow units.

typical of the Snake River Plain, and regardless of the term applied, they appear to represent a distinctive form of volcanism.

The foregoing discussion suggests that, first, the Snake River Plain is petrologically and morphologically distinct from the Columbia Plateau, and hence is not a classic flood basalt region, and second, that the shields making up most of the plain are not of the classic Hawaiian or Icelandic type, but are distinctive constructs. Moreover, other basaltic regions, such as parts of the Modoc Plateau of California, appear to share characteristics with the Snake River Plain and may also represent a style of volcanism intermediate between flood basalt eruptions and major shield-building eruptions. In the sections that follow, the Snake River Plain is described and compared with flood basalts and shield volcanoes.

FLOW TYPES

The prevailing flow type in the Snake River Plain is pahoehoe basalt that was emplaced as compound lava flows in the form described by Walker (Fig. 3-4). Cross sectional exposures of lava flows are rather limited in the central and eastern Snake River Plain because of the lack of erosion. Although some flows are exposed in the walls of summit craters, they are probably not typical for the main bodies of the flows that make up the plains away from the vents. When rare exposures are found away from the vents, flow units average about 1 to 5 m thick. Compound flow thicknesses, or the total of all flow units for a given eruptive sequence, may be 35 m or more thick, as in the Hell's Half Acre field (see Chapter 7) or the Wapi Field (see Champion, 1973, and Chapter 8).

Fresh surfaces of the pahoehoe flows are typically rather hummocky, with local relief as much as 10 m (Fig. 3-5). So-called *collapse depressions* (Hatheway, 1971) are common on some flows (Fig. 3-6). Also present are *pressure plateaus, pressure ridges, and flow ridges* (Fig. 3-7; see also Chapter 8). These structures are all typical of compound lava flows and apparently result from the manner in which the flows advance through a series of budding toes, described by Wentworth and Macdonald (1953) and others. Weathering of the flow surface features and accumulation of wind-blown sediments in low-lying parts result in a smoothing of the surface relief to the degree that in older flows only remnants of the prominent features, such as some ridges, are visible.

Local relief is also formed by flow fronts. Flows that encroach topographically high structures, such as tuff cones and other constructs "freeze" in place, and a shallow depression results between the flow front and the pre-flow feature.

FIGURE 3-5. Photograph of the flow front of the Wapi lava field, showing typical surface relief of 5 to 10 m; arrows mark flow front contact; open arrow indicates figure for scale.

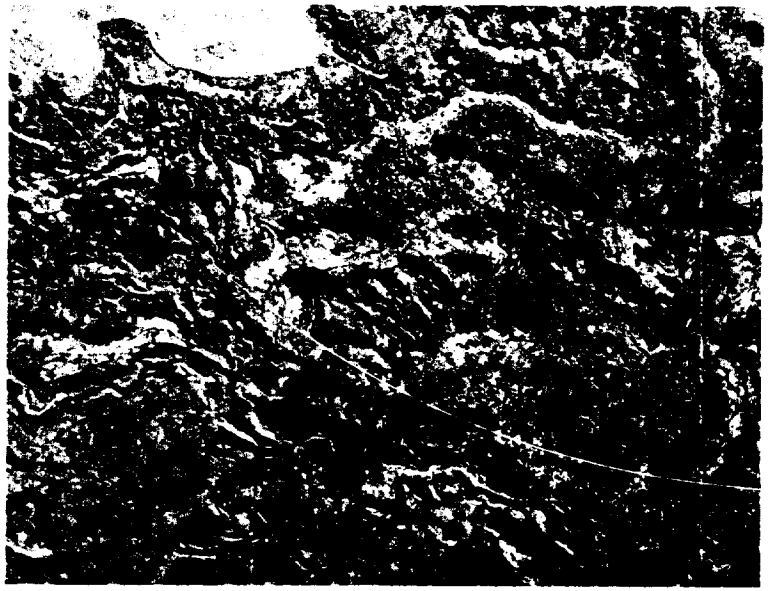

FIGURE 3-6. Vertical aerial photograph of part of the Wapi lava field showing pressure plateau (flat, upper surface) and some collapse depressions (arrows) formed on the plateau. (NASA-Ames photograph 878-3A-3, October, 1968.)

Aa flows are also present in the Snake River Plain. Some are of considerable extent, such as the aa flow complex erupted from fissures in Craters of the Moon (Fig. 3-8) that covers 150 km^2. Some aa flows appear to be of the simple lava flow type, emplaced as a single surge of lava. However, they are relatively thin, similar to the individual pahoehoe flow units of the compound lava flows and emplacement of comparatively viscous aa over so large an area is problematical. Observations made on Mt. Etna in collaboration with J. Guest on active flows suggest the process involved. In 1975, a series of pahoehoe flows was erupted on the north flank of the volcano. In the final stages of emplacement, however, the texture of the flow surface changed abruptly to aa. Moreover, some of the active flow on Etna was through lava tubes and

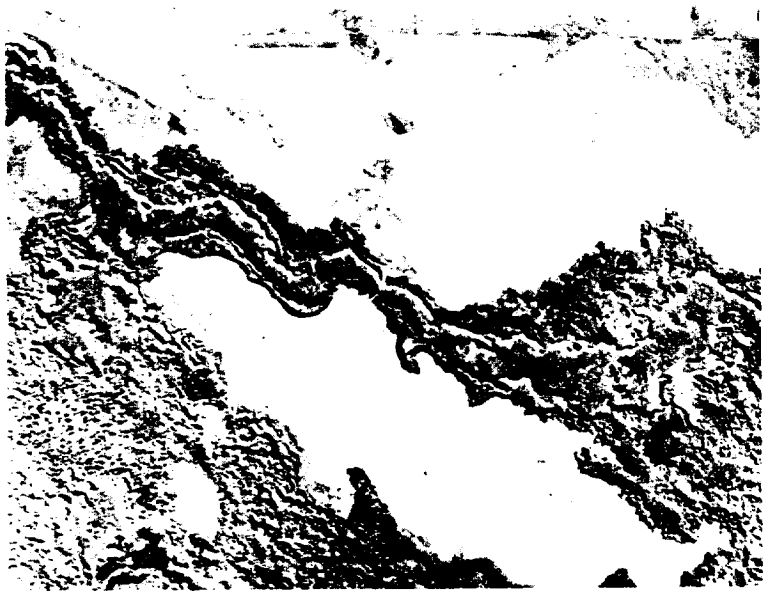

FIGURE 3-7. Vertical aerial photograph of the eastern margin of the Wapi flow, showing 'flow ridge' (Champion, 1973, and Chapter 8), which formed parallel to the direction of flow. Dark areas are flow units of the Wapi field; light areas are the older flows. (NASA-Ames photograph 878-5-7; October, 1968).

after the flows cooled, it appeared that lava tubes had formed in aa -in conflict with widely held views that lava tubes form nearly exclusively in pahoehoe flows. The tubes, however, formed during the pahoehoe stage and were preserved within the flow after the surface texture had converted to aa. Such tubes appear to be very infrequent, but their occurrence does explain the presence of lava tubes in aa.

Some of the large, thin aa flows in the Snake River Plain may, like those on Etna, have been erupted and essentially emplaced as pahoehoe but transformed to aa in the final stages of flow. Although the concept is difficult to substantiate for prehistoric flows, some flows on the plain suggest this possibility, as shown in Figure 3-9.

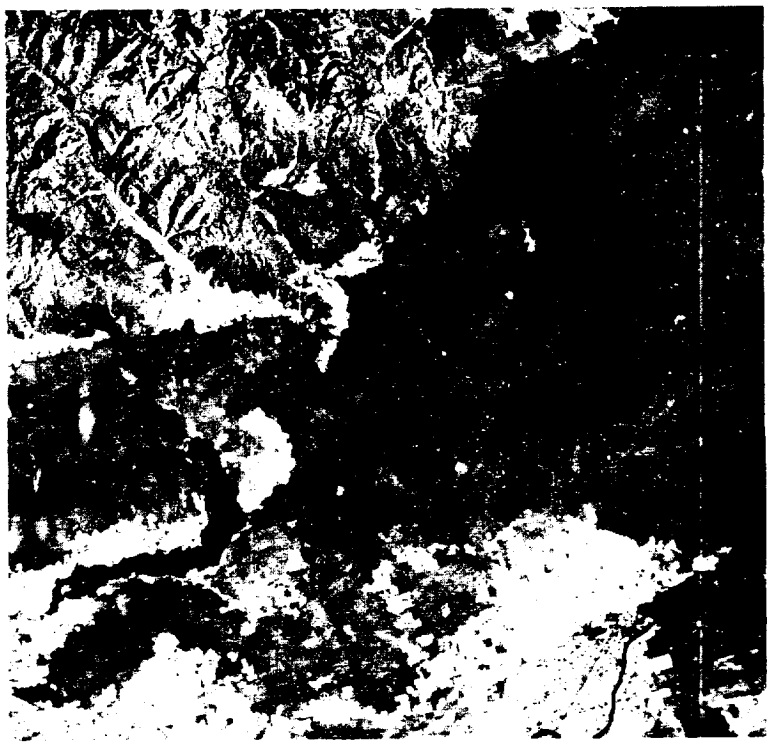

FIGURE 3-8. ERTS images of the central Snake River Plain; youngest flows show as dark patches: Craters of the Moon flows (upper right corner) are mostly fissure-fed; 'angle-shaped' flow on the left is the Shoshone Ice Cave lava field, emplaced mostly through lava tubes and channels; and the Wapi lava field (right-hand side), a low shield. All of the flows are compound flows, composed of multiple flow units.

LAVA TUBES

The role of lava tubes and channels in the emplacement of some basalt flows is poorly understood. A recent study (Greeley and others, 1976) of Mauna Loa shows that more than 80 percent of the flows exposed on the surface at least partly involved flow through lava tubes and channels in their

FIGURE 3-9. Vertical aerial photograph of a small basalt flow erupted southeast of Big Southern Butte; vent area is marked with an arrow. Flow surface exhibits both pahoehoe and aa flow textures; emplacement of most of the flow is considered to have taken place essentially in the pahoehoe state, then in the final stages of emplacement, the lava transformed to aa. Incomplete transition is indicated by irregular slabs of pahoehoe (light-toned surfaces). Similar flow transition has been observed in active flows on Mt. Etna and in Hawaii. (U.S. Department of Agriculture photograph CXN-4R-106; October, 1[illegible].

emplacement. Lava tubes, and to a lesser extent channels, transport lavas efficiently great distances from their vents. Lava tube systems longer than 20 km are common in many areas on Earth and structures interpreted as lava tube systems on the Moon and Mars exceed 100 km in length.

The distinction between tubes and channels is that tubes are hollow tunnels within flows and have free-standing roofs upon cooling and draining of the lava; channels typically are non-roofed, open rivers of lava that frequently have crustal slabs on their surfaces, but the slabs do not form free-standing roofs after the lava drains. In active flows, tube roofs and channel crusts prevent heat loss and enable the flow to remain mobile longer than in flows lacking these features.

Lava tubes and channels develop in Hawaiian-type eruptions in which the rate of effusion is moderately high (e.g., 10 to 100 m^3s^{-1}; Walker, 1973) but not as high as in flood eruption. Predictably, there are no known lava tubes in the Yakima Basalt or comparable flood lava flows of the Columbia Plateau. Tube formation also seems enhanced by sporadic eruption, involving multiple flow units with intervening periods of quiescence. This kind of activity was typical for the approximately six-year history of Mauna Ulu, Hawaii, a low shield having complex networks of lava tubes (Greeley, 1970, 1971; Peterson and Swanson, 1974).

Although lava tubes and channels are predominantly constructional features in that they emplace lava flows, they can also erode by melting and "plucking" of flows previously emplaced by the lava tube and also pre-flow terrain. Complex sequences of construction and erosion by multiple flow units can develop in this type of flow, illustrated in Figure 3-10. Although hypothetical, this diagram is based on surveys of lava tube systems in the western United States and on observations of active flows on Mt. Etna and in Hawaii (Greeley, 1970, 1971).

Lava tubes also played an important role in the emplacement of some of the flows in the Snake River Plain. Although they are not as common as in Hawaiian flows, some of the tubes in the plain appear to be larger than those in Hawaii. A preliminary survey of part of the central plain indicates that more than a fifth of the flows involved lava tubes and channels.

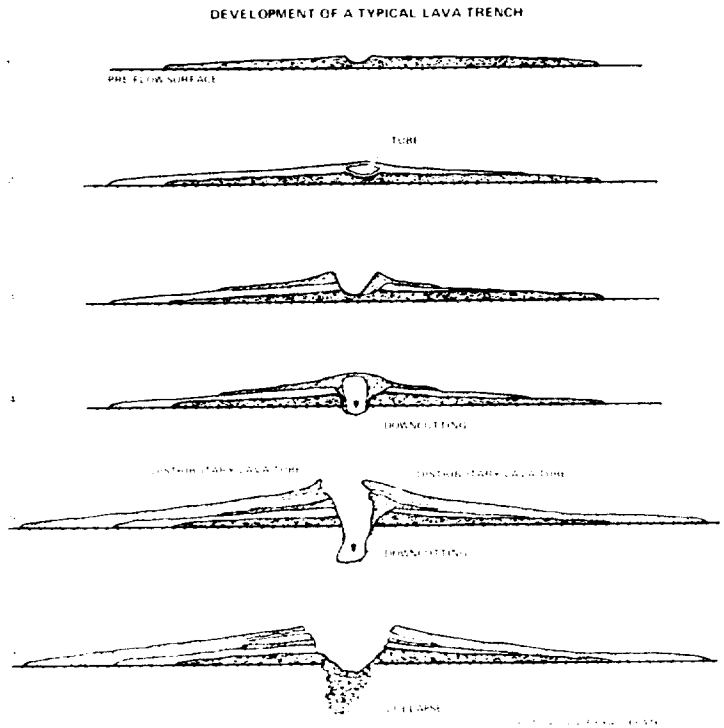

FIGURE 3-10. Sequence to show some of the stages in the development of a tube-fed compound lava flow. Stage 1 is a single flow unit emplaced by a shallow lava channel; stage 2 involves a second flow unit, in which lavas flowed down the previous channel and formed a roof. Stage 3 includes a third flow unit that was turbulent and formed a large channel; continued eruption of the same flow resulted in the formation of a roof, with downward erosion by melting and physical removal of some of the previous flow and preflow rocks. In stage 5 a fourth flow unit was erupted at a high rate; it initially used the previous tube as the feeding conduit, but because the volume of lava was large, the previous tube was destroyed and an open-flow channel developed, segments of which may have become roofed; overflow from the channel formed distributary lava tubes and small channels. Stage 6 marks the end of eruption with collapse of roofed segments by bank collapse.

Although this sequence is hypothetical, elements of each stage are based on observations of active lava tubes and channels and studies of cooled structures.

TYPES OF CONSTRUCTS ON THE SNAKE RIVER PLAIN

The regional geology of the eastern and central Snake River Plain is described in several reports, including Russell (1902) and Stearns and others (1938, 1939) and summarized in Chapter 4. Aspects of the plain pertinent to this discussion are described by Stearns (1928), Murtaugh (1961), Trimble and Carr (1961), Niccum (1969), Prinz (1970), Greeley and King (1975a,b), and LaPointe (1975, 1977).

The central and eastern Snake River Plain is formed by the accumulation of lavas in four main types of constructs. The term *construct* refers to any major accumulation of lava flows and other volcanic products. The four types are: 1) *low shields*, 2) *fissure flows*, 3) *major tube flows*, and 4) *intracanyon flows*. The relationships of these constructs are shown diagrammatrically in Figures 3-11 and 3-12. Although flood-type flows may also be present in the plain, none are exposed or documented.

Low Shields

Most of the central and eastern Snake River Plain is built up of multiple low shields, typified by the Wapi and Hell's Half Acre lava field. These fields are simply the uppermost and youngest of a complex series of coalescing low shields and other constructs that have an accumulated thickness of more than 1500 m (LaFehr and Pakiser, 1962) in some parts of the plain.

The Wapi lava field covers more than 300 km^2 and is a compound lava flow consisting of pahoehoe lavas of the "degassed" variety (Swanson, 1973). Lava toes, collapse depressions, flow ridges, and pressure ridges are common, but no lava tubes have been found on the main part of the field (Champion, 1971). The areal extent of the Wapi, one of the larger young flows on the plain, is considerably less than the 40,000 km^2 Roza Member of the Yakima Basalt (Swanson and others, 1975), a classic flood basalt.

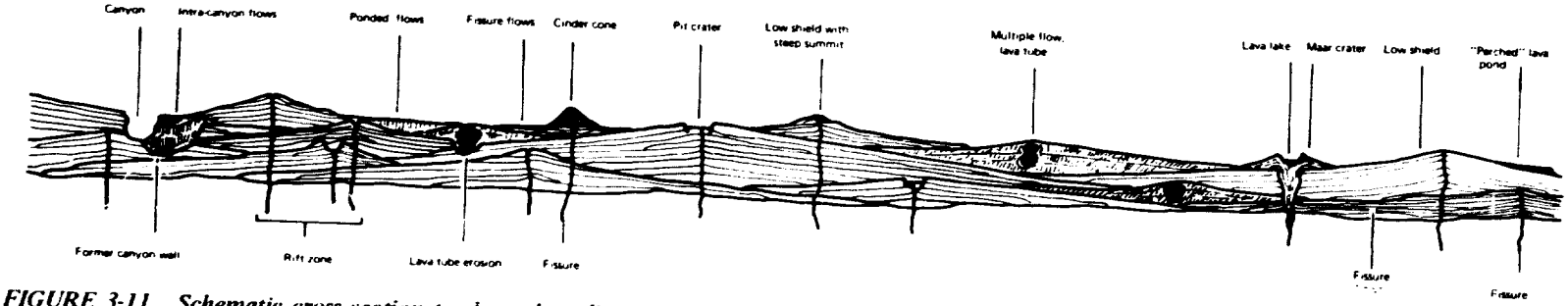

FIGURE 3-11. Schematic cross section to show the salient features of a 'plains' basalt region, typified by the central Snake River Plain. The vertical scale and surface relief are greatly exaggerated in order to show detail that would otherwise be lost. The predominant lava is pahoehoe basalt in the form of flow units that seldom exceed 5 to 10 m in thickness. The primary constructional forms are: 1) low shields, many of which have summit pit craters; the summits of most low shields are marked by steeper profiles than the rest of the construct, resulting partly from last-stage, low volume eruptions of aa lava; 2) flows fed by large lava tubes that wind between coalescing low shields; multiple eruptions often use the same lava tube as the conduit to feed advancing flow fronts and to add 'second stories' above previous flows and tubes; in some instances lava tubes may entrench into older flows by erosion; 3) fissures produce thin flows with relatively low surface gradients; the flows may be pahoehoe or aa, some of which are emplaced by networks of small tubes and channels; 'point source' eruptions along fissures can result in infrequent cinder-and-spatter cones; 4) flows more than 10 m thick are occasionally found in 'plains' type regions; these may represent flood-type eruptions, but more frequently, they are the result of lava ponding in low-lying regions and as intracanyon flows (left side of diagram); regardless of origin, thick flows are infrequent and appear to contribute comparatively little to the total volume of the 'plains' region; and 5) maar craters that result from ground water and magma interactions.

In profile (Fig. 3-13) the Wapi low shield displays two prominent slopes: the main part of the shield has slopes less than $1/2^{o}$, whereas the summit region steepens to about 5^{o}. The same type of profile is seen at Hell's Half Acre and older low shields on the plain. As older shields are encroached by subsequent flows from other sources, the steeper "upper story" often remains unburied.

The steeper summit for low shields can be explained partly by the nature of the flows that make up the summit region. As at Pillar Butte, the summit region for the Wapi low shield (see Chapter 8), has a high proportion of short, low-volume aa flows that piled up, elevating the vent. In comparison to the pahoehoe flow of the main field, the aa flows were more viscous and may represent the final stages of eruption. However, the complex sequence of development from steep cone to low shield to spatter rampart, observed during the short history of Mauna Ulu, would caution against assuming that earlier, steeper summit regions might not be buried at Pillar Butte.

In addition to steeper profiles, the summits of many of the low shields are marked by one or more irregular craters, commonly pit craters. Many of these show evidence of multiple collapse (Fig. 3-14) and were source vents for large lava tubes or channels (Fig. 3-15). Rarely, spatter ramparts, built of pasty agglutinate, occur at the summit (Fig. 3-16).

The summit vent regions in the Snake River Plain show an asymmetry toward the northside of the low shield. This is accounted for by the regional topographic slope to the south. Flows erupted from central vents tended to flow south, rather than north, resulting in the "offset" of the vent and summit region with respect to the shield in plan view.

Many low shields appear to be aligned in distinctive rift zones, with shields along each zone roughly contemporaneous in age. An example is the Inferno Chasm rift zone (Greeley and King, 1975b and Fig. 3-17). The aligned shields may represent a style of fissure eruption in which effusion was localized at various points along the fissure. Individual shields, however, are built of flow units of a magnitude akin

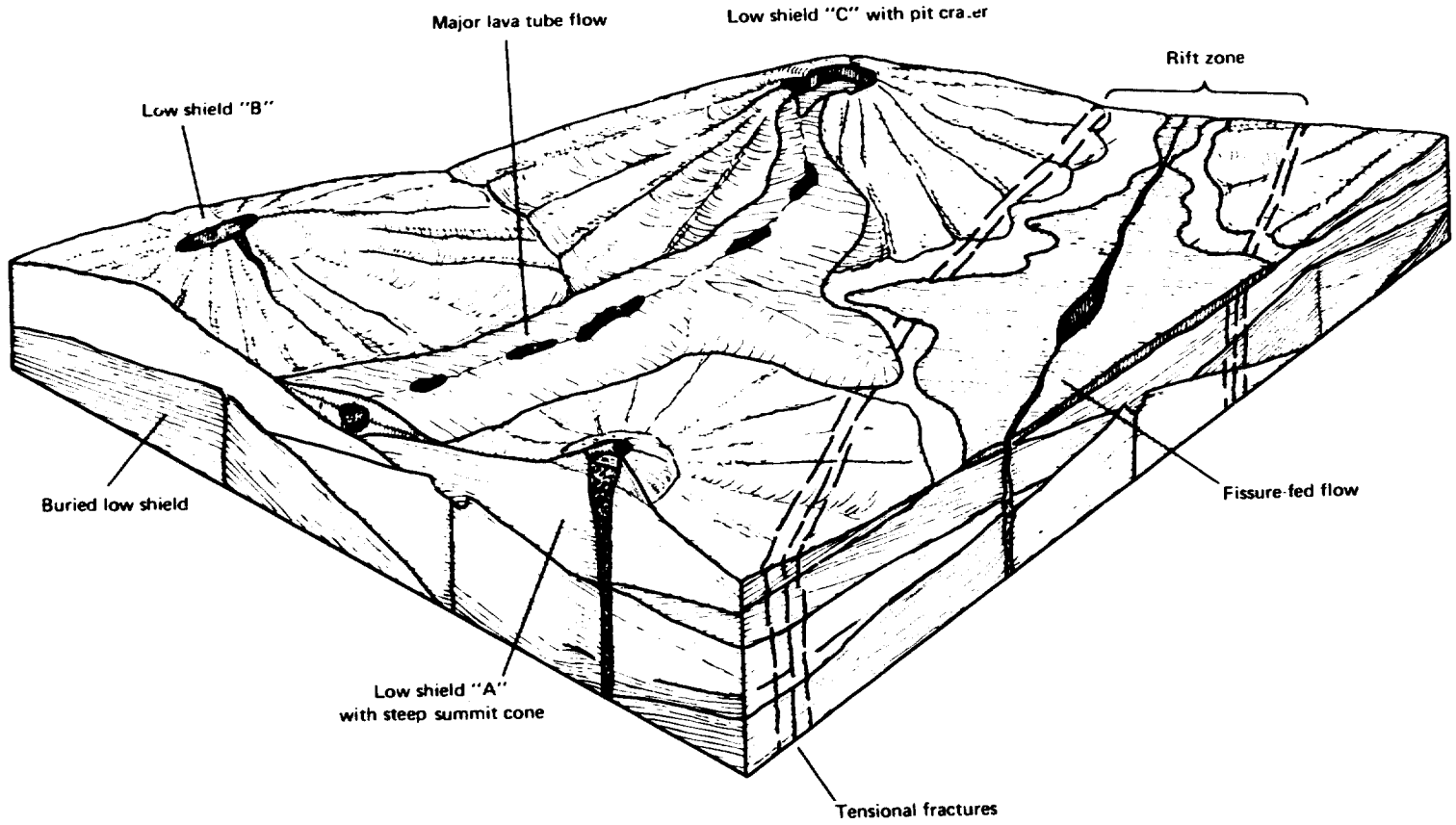

FIGURE 3-12. Block diagram showing the relationship of low shields, major lava tube flows, and fissure flows.

to Hawaiian activity. For some unknown reason, once the low shields on the plain reached a maximim size, the eruption vent shut off, with subsequent eruptions occurring elsewhere.

Fissure Flows

Most fissure vents are associated with rift zones. Typically, fissure flows in the central and eastern Snake River Plain are compound, or multiple flow units. The two youngest fissure flows on the plain are the King's Bowl flow, and flows in the Craters of the Moon where two flow units have been dated by C^{14} methods at 2085 $\pm$ 85 and 2255 $\pm$ 60 years before present (Bullard, 1971). The King's Bowl Flow has been dated by C^{14} methods at 2130 $\pm$ 130 years before present (Prinz, 1970). Craters of the Moon flows (see Chapter 13) consist of several aa and pahoehoe flows erupted from the fissures along the Great Rift (Fig. 3-8) and cover nearly 1500 km^2. This is the largest fissure flow identified on the plain, but its magnitude is much less than that of typical flood basalt flows on the Columbia Plateau.

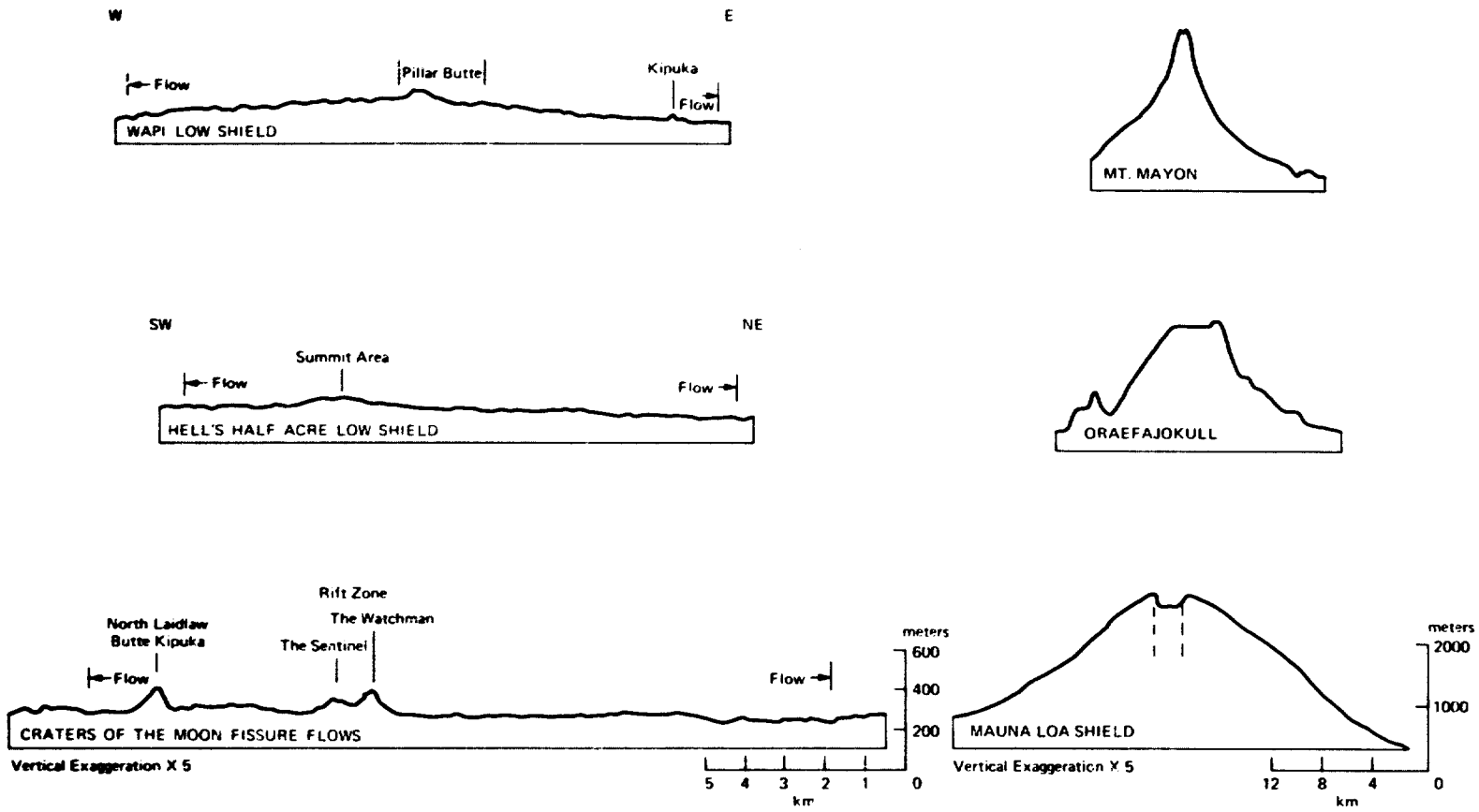

FIGURE 3-13a. Topographic profiles comparing Icelandic and Hawaiian shield volcanoes, a composite cone, and low shield volcanoes of the Snake River Plain; note the difference in scales for comparisons.

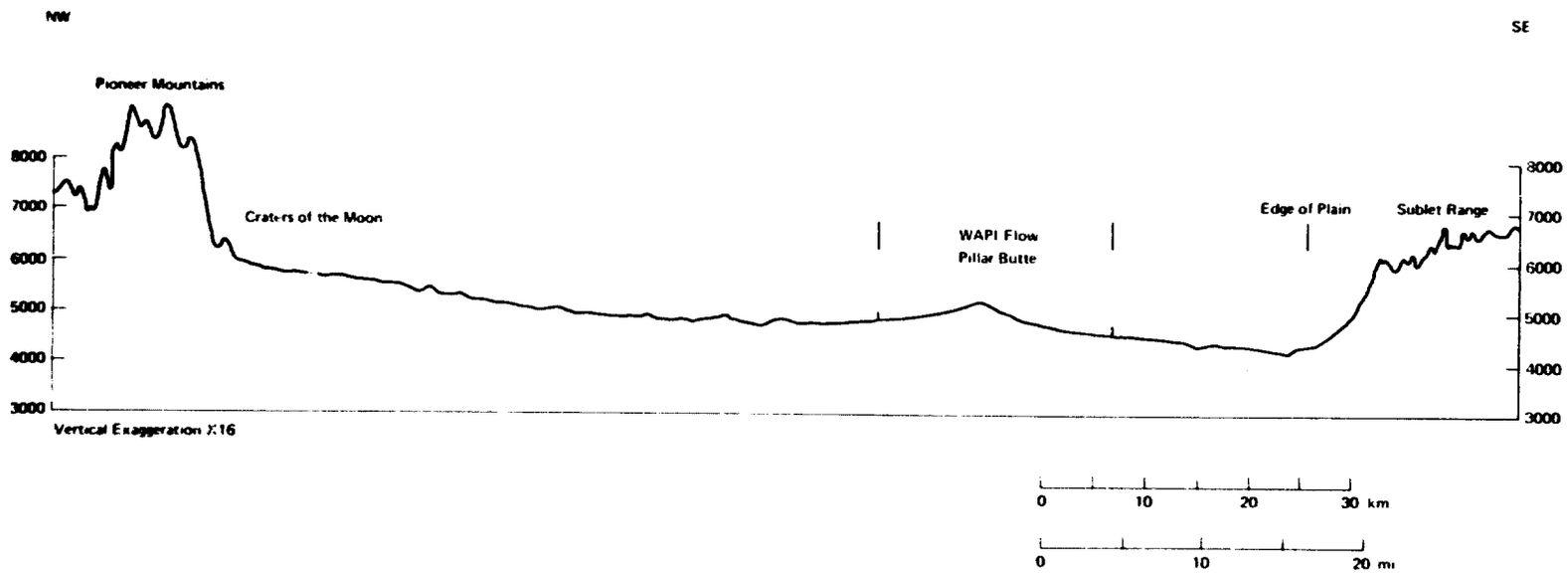

FIGURE 3-13b. Topographic profile across the Snake River Plain showing the region slope to be southeast and the Wapi low shield.

The King's Bowl flow covers only about 3 km^2 and consists of several flow units (Greeley and King, 1975a), some of which were ponded as small lava lakes (see Chapter 11). Thickness of individual flows is less than about 1.5 m, although some of the lava lakes may have been more than 4 m deep in places. The King's Bowl flow was erupted from a prominent fissure (Fig. 3-18); in some places the feeder dike is exposed (Fig. 3-19).

Although the main characteristic of fissure flows is the nearly continuous effusion of lava along several kilometers or more of the fissure, eruption at "point-sources" along the fissure may occur either independently or contemporaneously with fissure effusion, producing small spatter cones, or rarely, substantial cinder cones, as in Craters of the Moon (Fig. 3-20). Phreatic eruption may also occur along fissures when rising magma encounters ground water, as at King's Bowl (Fig. 3-18). Such "point source" structures are scarce on the plain and contribute little to the total accumulation of volcanic materials.

Major Lava Tube Flows

Lava tubes 0.5 to 5 m across are abundant in low shield and fissure flows. Major lava tube flows, however, are emplaced by tubes typically larger than 10 m across. The resulting construct is a compound flow that is long, narrow,

FIGURE 3-14. Vertical aerial photograph of Wildhorse Corral (illumination from the east, or right side of the photograph). The vent is about 52 m deep and 1 km long, its length being oriented north-south on the Inferno Chasm rift zone. Wildhorse Corral appears to have a complex eruptive history, indicated by terraces within the crater walls and multiple flow units, some of which were tube-fed. (from Greeley and King, 1975a; NASA-Ames photograph 951, 8-15, 17; May, 1969).

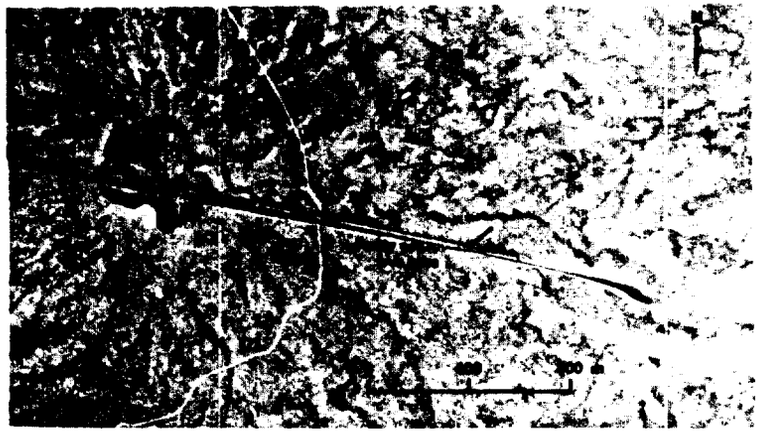

FIGURE 3-15a. Vertical aerial photograph of an unnamed pit crater (left side of photograph), about 2.5 km north of Mosby Well, Idaho, that was the source for a major lava tube flow; lava tube can be traced eastward more than 5 km through a series of collapses that show as dark holes. (U.S. Geological Survey photograph GS SWEZ 6-206; September, 1971).

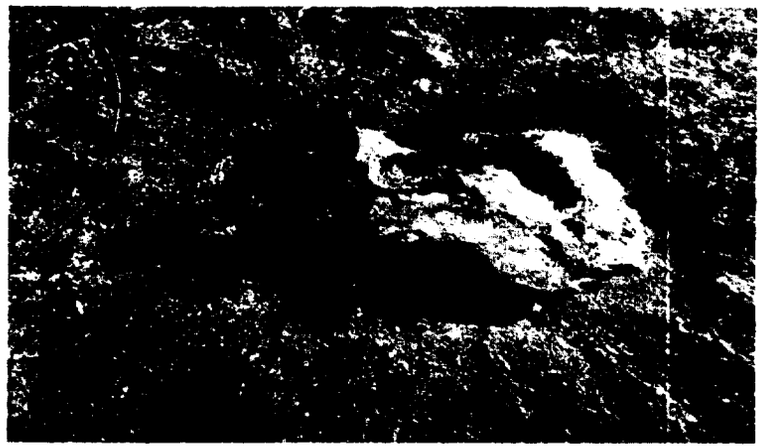

FIGURE 3-15b. Irregular pit crater, shown in Figure 3-15a; illumination is from the lower left. (photograph by Ronald Greeley, University of Santa Clara, 1971).

FIGURE 3-16. Low-altitude oblique view northward to the Pillar Butte area, the summit vent region for the Wapi low shield. The knob on the horizon is Pillar Butte, a spatter rampart associated with the summit vents. Dark patches are aa flows; a large pressure ridge is visible at the bottom of the photograph. (NASA-Ames photograph by Mike Lowas, 1969)

and somewhat sinuous, demonstrating the control exerted by pre-flow topography. Although the sources for the tubes are not always obvious, examples can be cited in which low shields, pit craters (Fig. 3-15), and possibly fissures were sources for major lava tube flows.

Bear Trap lava tube northwest of King's Bowl and Shoshone Ice Cave (lava tube) and their associated flows are examples of this class of construct on the plain. Bear Trap is an older, partly buried compound flow, whereas Shoshone Ice Cave flow (Fig. 3-21) is one of the youngest, fresh flows on the plain. The name Shoshone Ice Cave refers to a segment of the lava tube that has been developed as a tourist attraction; it is part of a complex lava tube *lava* channel system, which during active flow, *involved* both roofed and unroofed segments. Many of the formerly roofed parts, however, have collapsed, leaving open trenches that are continuous with the open channel segments. The compound flows associated with the Shoshone lava tube system cover

FIGURE 3-17. Oblique aerial view northeastward across vents of the Inferno Chasm rift zone (Inferno Chasm vent just out of view to the right). (from Greeley and King, 1975a).

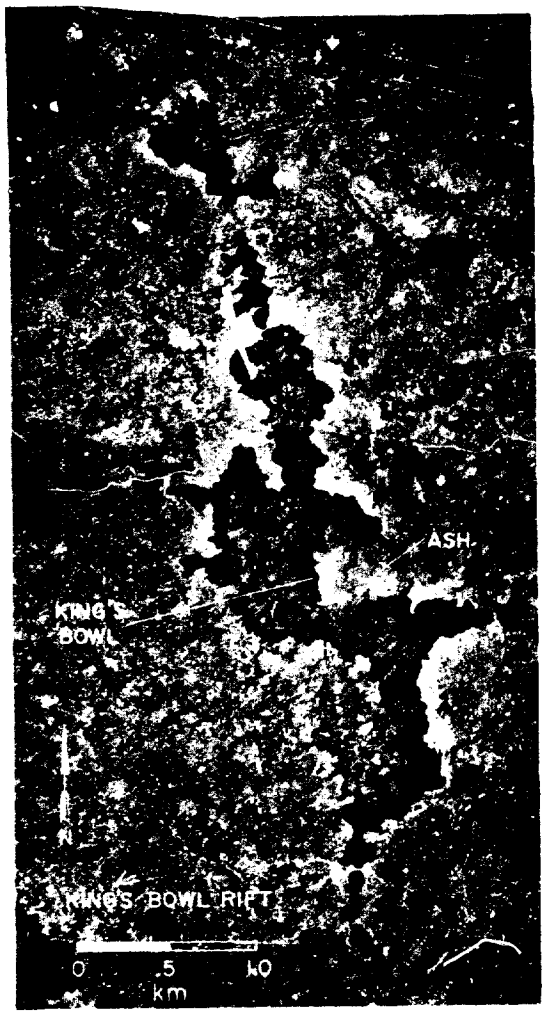

FIGURE 3-18. Vertical aerial photograph of the King's Bowl rift and the King's Bowl lava field, a compound lava flow fed by the main fissure. A phreatic eruption and subsequent collapse created King's Bowl (see Chapter 9), the elongate crater on the fissure; prevailing winds from the west (left) at the time of the eruptions carried ash and other fine particles eastward from the fissure. (U. S. Department of Agriculture Photograph.)

FIGURE 3-19. View of one of the feeding dikes along the main fissure at King's Bowl lava field. (photograph by James Papadakis).

about 210 km^2 and consist of both aa and pahoehoe flow units. Numerous small distributary lava tubes are preserved, some of which can be traced directly from the main tube. Small distributary lava tubes and channels were important in the conduction of lavas away from the main tube and contributed to the development of a subtle topographic arch along the axis of the main tube, typical of many lava tubes.

Bear Trap lava tube and the flows associated with it (Fig. 3-22) make up one of several tube-flow systems that originate in the vicinity of the King's Bowl rift and flow westward. The tube can be traced more than 21 km by a series of collapsed segments and is then buried by Holocene basalt flows from Craters of the Moon (Greeley and King, 1975). The axial trace of the tube is defined by a broad topographic swell which, to some degree, has controlled the emplacement of subsequent lava flows. Although most of the lava tube system

FIGURE 3-20. Low oblique aerial view of cinder-and-spatter cones aligned on a fissure in Craters of the Moon National Monument. (photograph by Ronald Greeley, University of Santa Clara, 1972).

FIGURE 3-21. Vertical aerial photograph of the main vent region (upper left) for the Shoshone Ice Cave lava flow, a compound lava flow consisting of pahoehoe and aa flow units, many of which were fed through lava tubes. Parts of the collapsed lava tube are visible as dark spots. Side road and parking area west (left) of the main highway (U.S. Highway 93) mark Shoshone Ice Cave, a segment of the lava tube open to the public. (U.S. Department of Agriculture photograph CVR-1KK-157, 158).

FIGURE 3-22. View of the interior of Bear Trap lava tube, part of a lava tube system more than 13 km long that fed a major compound lava flow.

is collapsed, there are two uncollapsed segments close to the Arco–Minidoka road that are readily accessible. Although the total extent of the flows associated with Bear Trap lava tube cannot be determined because the flanks of the tube-arch and distal end of the flows are buried, the exposed part of the flow is estimated to be about 60 km^2.

In contrast to the voluminous lavas in low shields and the large fissure-flows, major lava tube flows are small. However, these flows contribute substantially to maintaining the flatness of the plain in that they "fill-in" the low-lying region between adjacent, coalescing low shields (Fig. 3-12).

Intracanyon Flows

Several rivers cut the Snake River Plain, forming deep canyons (Fig. 3-23). Although the most notable is the canyon of the Snake River, several tributary canyons are also impressive. During the relatively short history of the plain, older canyons apparently existed, but their presence is now mostly

FIGURE 3-23. Low oblique aerial view northeastward of Twin Falls on the Snake River near Kimberley, Idaho. (NASA-Ames photograph by Ronald Greeley, 1969).

obscured by lava flows. Outcrops exposed by erosion along the present Snake River show that lavas spilled into the canyons, forming *intracanyon flows*, some of which ponded to depths exceeding 30 m. Columnar jointing and entablature structures are evidence for possible ponding of the flow prior to cooling. Sources for intracanyon flows may have been low shield, fissures, or major lava tubes. A tube-fed intracanyon flow occurs in the western Snake River Plain, mapped by Howard and Shervais (1973).

Because exposures of intracanyon flows in the central and eastern Snake River Plain are rather limited, their significance in the accumulation of lavas in the plain cannot be assessed fully. Intracanyon flows, however, are probably of relatively limited areal extent and may not be very representative for the plain as a whole.

Miscellaneous Vent Structures and Flows

Relatively minor accumulations of lava flows and other volcanic products occur on the plain and on the margins of the plain. These features include tuff-and-cinder cones, such as China Cap (Fig. 3-24), and maar craters such as Sand Crater (also known as Twin Buttes, Fig. 3-25), and Split Butte (see Chapter 12). Cinder and spatter cones are rare and appear to be associated with fissures, as discussed above. Some elongate vents and flows may be aligned over fissures and may be transitional between fissure flows and low shields associated with rift zones.

Some flows from tubes, central vents, or fissures formed natural levees and developed into lava lakes. The lakes may have been centered over the vent, as at King's Bowl (Fig. 3-18 and Chapter 11) and Split Butte (Chapter 12), or they may have formed "perched" lava ponds (Holcomb and others, 1974) on the flanks of construct (Figs. 3-17 and 3-26).

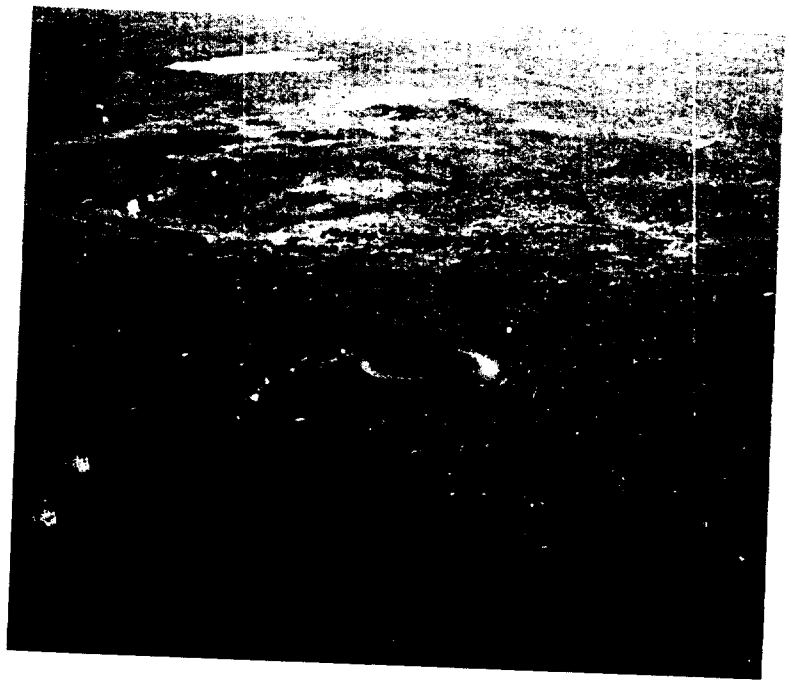

FIGURE 3-24. Oblique aerial view southwestward across China Cap, a small scoria cone about 385 m across that is 14 km southwest of Big Southern Butte. This nearly perfectly circular cone contains a crater 30 m deep. The rim is composed mostly of scoria with some blocks and bombs and at least one layer of agglutinate Like Split Butte and Sand Butte, the flanks of China Cap have been partly buried by younger lava flows, creating a distinctive moat-like ring around the cone where the flow front solidified. (Photograph by R. Greeley, University of Santa Clara, 1970.)

DISCUSSION AND SUMMARY

A style of volcanism, informally termed "plains" volcanism, is intermediate in character between eruptions of flood lava flows and of shield volcanoes. Distinctions of style are based on thickness, extent, and other properties of the flows for each type of eruption and on gross geomorphology of the three types of constructs.

As used here, the term *flood eruption* is restricted to the production of flows that exceed 20-30 m thickness and that are erupted at very high rates of effusion; flood eruptions produce "simple" flows that are single-body cooling units, typified by the Roza Member of the Yakima Basalt in the Columbia Plateau (Swanson and others, 1975). These flows lack well-defined surface flow features such as lava tubes and lava channels. Vent systems are long, narrow fissures that are seldom active for more than one eruption. Vent structures, such as cinder and spatter cones, typically are not preserved on the surface.

FIGURE 3-25. Oblique aerial view northeastward across Sand Butte, a tephra cone 1.2 km in diameter that contains a 650 m crater. Although most of the inner and outer slopes are covered with vegetation, several outcrops show the outward-dipping tephra layers that make up the cone. Sand Butte is astride a north-south fissure along which flow has occurred, and which has given rise to other vents, such as the series of low spatter ramparts in the upper left part of the photograph. The lower flanks of the cone have been covered by pahoehoe flows, identified here by the hummocky surface and pressure ridges. (From Greeley and King, 1975a.)

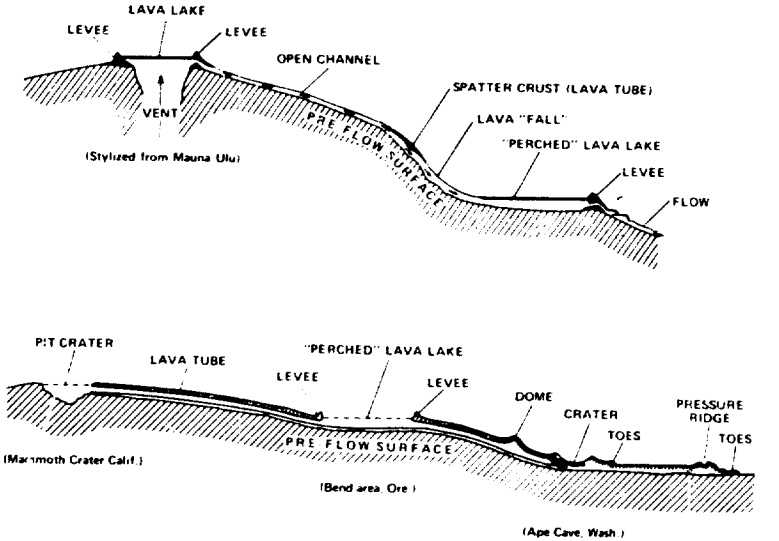

FIGURE 3-26. Hypothetical diagrams based on observations, showing "perched" lava ponds on steep and gentle slopes and their relation to lava tubes.

Large shield volcanoes of the Hawaiian and Iceland type are formed by relatively quiet lava outpourings, erupted more slowly than in flood eruptions. The flows typically are compound and emplaced through tubes. Flows are erupted predominantly from central vents—hence the formation of the shield—but can also emanate from fissures.

In contrast, basaltic "plains" regions, typified by the Snake River Plain, combine aspects of both flood eruptions and shield-forming eruptions. The Snake River Plain is built of four types of constructs: low shields (small, low profile, central vent volcanoes), major tube-fed lava flows, fissure-fed flows, and intracanyon flows, all of which coalesce and interweave in space and time. Although low shields are the predominant structure, eruptions appear to have been limited inasmuch as the shields never reached the enormous proportion of the large Hawaiian shield volcanoes.

The definition of "plains" volcanism is tentative and requires additional study to determine if the classification is warranted. The recognition of distinctive volcanic styles, and hence volcanic histories, is pertinent to planetary geology, and discrimination of "plains" volcanism may be useful for unravelling surface histories for the planets.

REFERENCES

Bullard, F. M., 1971. Volcanic history of the Great Rift, Craters of the Moon National Monument, South-central Idaho: Geol. Soc. Amer. Abs. with Programs, vol. 3, no. 3, p. 234.

Champion, D. E., 1973. The relationship of large scale surface morphology to lava flow direction, Wapi lava field, southeastern Idaho: Unpubl. Master's Thesis, Univ. New York at Buffalo, 44 p.

Eardley, A. J., 1962. *Structural Geology of North America:* Harper and Row, Publ., New York, 2nd ed., 743 p.

Greeley, R., 1971. Observations of actively forming lava tubes and associated structures, Hawaii: Modern Geology, vol. 2, p. 207-223.

Greeley, R., 1972. Additional observations on actively forming lava tubes and associated structures, Hawaii: Modern Geology, vol. 3, p. 157-160.

Greeley, R., 1976. Modes of emplacement of Basaltic terrains and an analysis of mare volcanism in the Orientale Basin: Proc. Lunar Sci. Conf. 7th, p. 2747-2759.

Greeley, R. and J. S. King, 1975a. Geologic field guide to the Quaternary volcanics of the south-central Snake River Plain, Idaho: Idaho Bur. Mines and Geology Pamphlet No. 160, 49 p.

Greeley, R. and J. S. King, 1975b. Rift zones in the south-central Snake River Plain, Idaho: Geol. Soc. Amer., Abs., vol. 7, p. 610-611.

Greeley, R., D. Storm, and C. Wilbur, 1976. Frequency distribution of lava tubes and channels on Mauna Loa volcano, Hawaii: Geol. Soc. Amer. Abs., vol. 8, p. 892.

Hatheway, A. W., 1971. Lava tubes and collapse depressions: Unpubl. Ph.D. dissertation, Univ. Arizona, 353 p.

Holcomb, R. T., D. W. Peterson, and R. I. Tilling, 1974. Recent landforms at Kilauea Volcano: A selected photographic compilation in Greeley, R., ed., Geologic Guide to the Island of Hawaii, NASA CR 152416, p. 49-86.

Howard, K. A. and J. W. Shervais, 1973. Geologic map of Smith Prairie, Elmore County, Idaho: U. S. Geol. Survey, Misc. Geol. Inv. Map I-818.

Jones, R. W. 1970. Comparison of Columbia River basalts and Snake River Plains basalts: Proc. Second Columbia River Basalt Symp., Eastern Wash. State College, p. 209-221.

LaPoint, P. J. I., 1975. Photogeologic study of volcanic and structural features of the eastern Snake River Plain, Idaho: Geol. Soc. Amer., Abs. with Programs, vol. 7, no. 5, p. 620.

LaPoint, P. J. I., 1977. Preliminary photogeologic map of the eastern Snake River Plain, Idaho: U. S. Geol. Survey, MF-850.

Leeman, W. P., 1974. Part I—Petrology of basaltic lavas from the Snake River Plain, Idaho, and Part II—Experimental determination of partitioning of divalent cations between olivine and basaltic liquid: Univ. Oregon, Ph.D. dissertation, 337 p.

Leeman, W. P., 1975. Petrology and origin of Snake River Plain (SRP) olivine tholeiites: Geol. Soc. Amer., Abs. with Programs, vol. 7, no. 5, p. 621-622.

Macdonald, G. A., 1972. *Volcanoes:* Prentice-Hall, Englewood Cliffs, New Jersey, 510 p.

Murtaugh, J. G., 1961. Geology of Craters of the Moon National Monument: Moscow, Idaho Univ., M. S. thesis, 99 p.

Niccum, M. R., 1969. Geology and permeable structures in basalts of the east central Snake River Plain near Atomic City, Idaho: Pocatello, Idaho State Univ., M. S. thesis, 137 p.

Nichols, R. L., 1936. Flow units in basalt: J. Geol., vol. 44, p. 617-630.

Noe-Nygaard, A., 1968. On extrusion forms in plateau basalts. Visindafelag Islendinga, Anniv., vol., Reykjavik, p. 10-13.

Peterson, D. W. and D. A. Swanson, 1974. Observed formation of lava tubes during 1970-71 at Kilauea Volcano, Hawaii: Studies in Speleology, vol. 2, pt. 6, p. 209-224.

Powers, H. A., 1960. A distinctive chemical characteristic of Snake River Basalts of Idaho: U. S. Geol. Survey Prof. Paper 400-B, p. 298.

Prinz, M., 1970. Idaho rift system, Snake River Plain, Idaho: Geol. Soc. Amer. Bull., vol. 81, p. 941-947.

Protska, H. J., P. Eaton, and S. Oriel, 1976. Cordilleran Thermotectonic Anomaly: II. Interaction of ar intraplate chemical plume mass and related mantle diapir (abs.): Geol. Soc. America Ann. Mtg., Abs. with Programs, p. 1055.

Russell, T. C., 1902. Geology and water resources of the Snake River Plains of Idaho: U. S. Geol. Survey Bull. 199, 192 p.

Stearns, H. T., 1928. Craters of the Moon National Monument, Idaho: Idaho Bur. Mines and Geology Bull. 13, 57 p.

Stearns, H. T., L. Crandall, and W. G. Steward, 1938. Geology and groundwater resources of the Snake River Plain in southeastern Idaho: U. S. Geol. Survey Water Supply Paper 774, 268 p.

Stearns, H. T., L. L. Bryan, and L. Crandall, 1939. Geology and water resources of the Mud Lake region, Idaho, including the Island Park area: U. S. Geol. Survey Water Supply Paper 818, 125 p.

Swanson, D. A., 1973. Pahoehoe flows from the 1969-1971 Mauna Ulu eruption, Kilauea Volcano, Hawaii: Geol. Soc. Amer. Bull., vol. 84, p. 615-626.

Swanson, D. A., T. L. Wright, and R. T. Heltz, 1975. Linear vent systems and estimated rates of magma production and eruption for the Yakima Basalt on the Columbia Plateau: Amer. J. Sci., vol. 275, p. 877-905.

Trimble, D. E. and W. J. Carr, 1961. Late Quaternary history of the Snake River Plain in the American Falls region, Idaho: Geol. Soc. America Bull., v. 72, no. 12, p. 1739-1748.

Walker, G. P. L., 1972. Compound and simple lava flows and flood basalts: Bull. Volcan., vol. 36, p. 579-590.

Waters, A. C., 1961. Stratigraphic and lithologic variations in the Columbia River Basalt: Am. Jour. Sci., vol. 259, p. 583-611.

Wentworth, C. K. and G. A. Macdonald, 1953. Structures and forms of basaltic rocks in Hawaii: U. S. Geol. Surv. Bull. 994, 98 p.

4. REGIONAL SETTING OF THE SNAKE RIVER PLAIN, IDAHO

John S. King
Department of Geological Sciences
State University of New York at Buffalo
Amherst, New York 14226

4. REGIONAL SETTING OF THE SNAKE RIVER PLAIN, IDAHO

John S. King
Department of Geological Sciences
State University of New York at Buffalo
Amherst, New York 14226

Although lava flows and features of the central and eastern Snake River Plain are the focus of this field conference, examination of the regional setting may provide a perspective useful to those unfamiliar with the Plain. For convenience, the broad picture developed here will be concentrated on the State of Idaho with ultimate resolution to the Snake River Plain.

PHYSIOGRAPHIC FRAMEWORK

Idaho consists of some 216,300 km^2 of diverse physiography and geology (Fig. 4-1). It is best classified as mountainous, for areas of high relief dominate the northern, central, and far southern parts of the State. The irregular eastern boundary of Idaho, adjoining Montana, lies along the crest of mountain ranges. Throughout much of its course of more than 560 km, it follows the high peaks of the Bitterroot Mountains, and in the south, along the continental divide, a location which reflects the history of the Idaho Territory in the 1860's (Wells, 1974).

Mountain ranges in the panhandle region of the State extend southward to the generally west-flowing Salmon River at about 45°30' N latitude, about the middle of the State. To the south lie the Salmon River Mountains with many peaks in excess of 3050 m (10,000 ft). Due south of the Salmon River Mountains are the Sawtooth Mountains and extending southeast from the central Salmon River Mountain

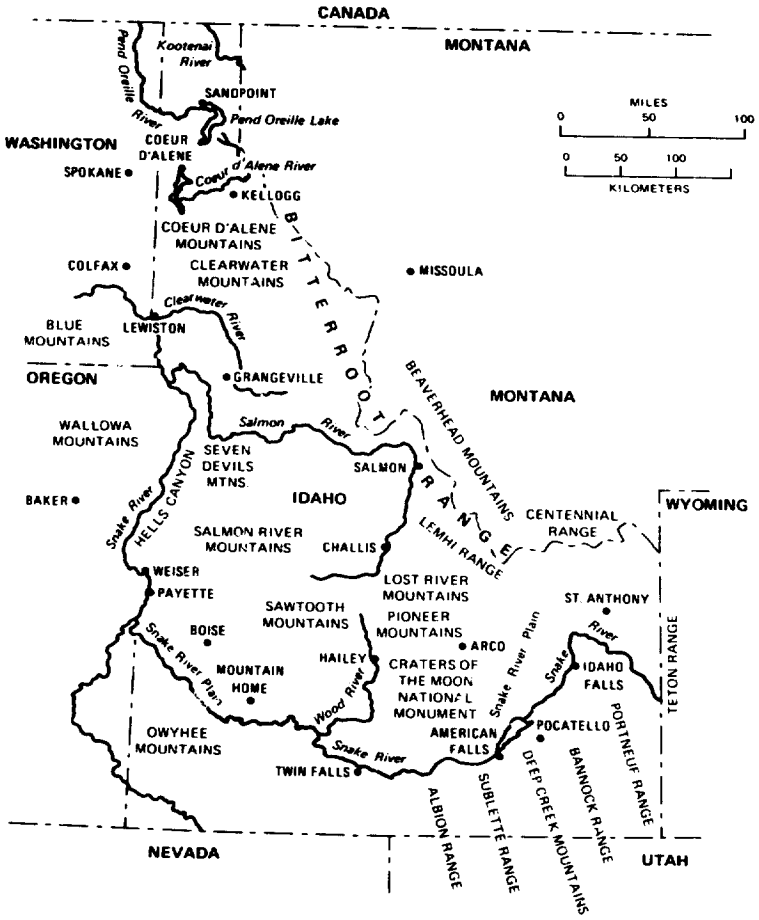

FIGURE 4-1. Map of Idaho showing Snake River Plain and other physiographic features (after McKee, 1972).

"core" is a series of parallel ranges which from west to east are the Pioneer, Lost River, Lemhi, and Beaverhead Ranges. The highest point in Idaho is Borah Peak (12,622 ft) in the Lost River Range. In the southeastern part of the State, south of the Snake River is a series of mountain ranges which trend generally northwest. From east to west these are the Portneuf Range, east of Pocatello, the Bannock Range, the Deep Creek Mountains, the Sublette Range, and the generally north-south trending Albion Range. Many elevations in th region exceed 2750 m. The Owyhee Mountains with hig peaks ranging in elevation from 1825 to 2440 m are locate in the southwestern part of the State.

Cutting a swath 65–100 km wide across this region of mountain terrain is the Snake River Plain physiographic province which dominates southern Idaho. This is a broad, flat, arcuate depression which is concave to the north and covers some 49,200 km^2, nearly one quarter of the total area of the State. It extends about 645 km west from the Yellowstone Plateau to the Idaho–Oregon border where it adjoins the Columbia Plateau. It is bordered on the south by the Basin and Range Province and on much of the north by the Northern Rocky Mountain Province. Elevations on the Snake River Plain diminish from the east (1350–1525 m) to the west (900–1200 m).

GEOLOGIC FRAMEWORK

A variety of rock types of all geologic ages crop out in Idaho and, although on first view a patchwork pattern emerges, there is nonetheless resolvable order. All of the rocks in the State may be placed in three general categories from Precambrian to Recent (Fig. 4-2).

1) Precambrian rocks occur mostly north of the Snake River Plain and are dominant in the northern panhandle region of the State. However, they also crop out to the south in the Bitterroot Range but are covered by younger rocks before coming in contact with volcanic rocks of the Snake

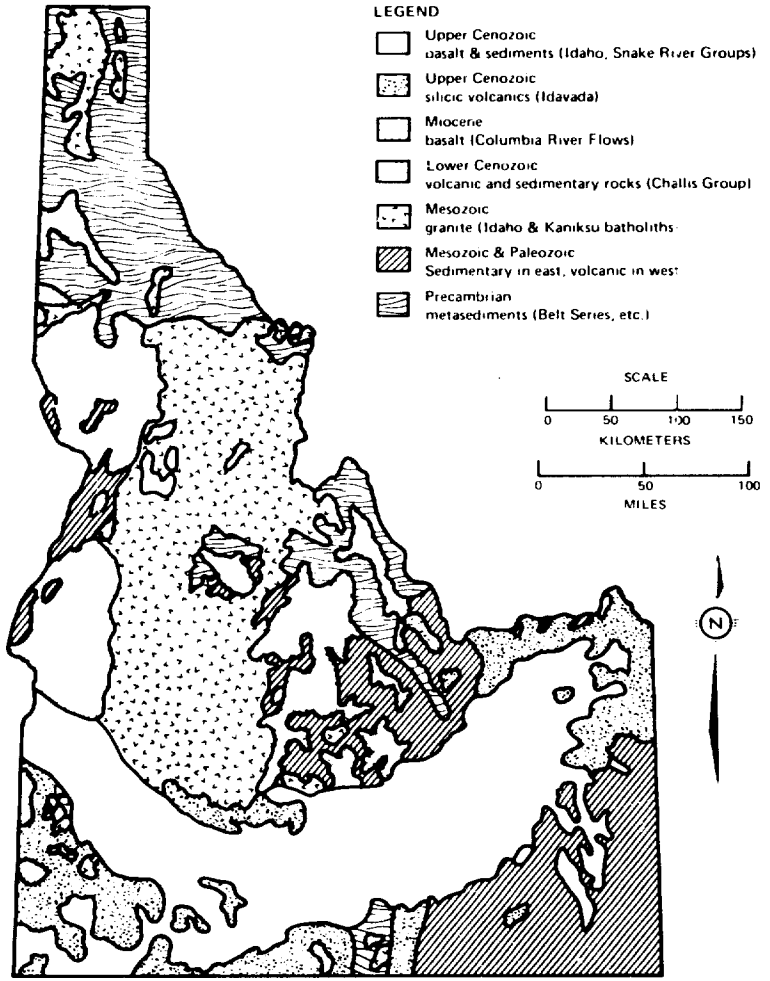

FIGURE 4-2. Geologic sketch map of Idaho (after McKee, 1972).

River Plain Province. Precambrian metamorphic and plutonic rocks south of the Snake River are generally confined to the Albion Range at about 113°30' longitude, although young Precambrian rocks are exposed in the Bannock Range. There are two types of Precambrian rocks in Idaho: a metamorphic basement complex of gneisses and schists, such as those which occur in the central and southern Albion Range (Armstrong and Hills, 1967), and younger, weakly to non-metamorphosed rocks such as the siltstones and argillites of the Belt Series and the quartzites and argillites of the younger Brigham Group. Belt-type rocks are the dominant Precambrian units in Idaho.

2) Paleozoic and Mesozoic sedimentary rocks crop out in the southeastern part of the state. They occur both north and south of the Snake River Plain and rocks representing every Paleozoic period are present in southeastern Idaho (McKee, 1972). Central Idaho is dominated by the Idaho batholith which is made up of granitoid rocks of Mesozoic and early Tertiary age. The Idaho batholith extends north from the Snake River Plain for more than 400 km and is 80–110 km wide.

3) The younger rocks of Idaho are dominated by several volcanic series, many of which are associated with interlayered fluvial and lacustrine sediments. The oldest of these series is the Challis Volcanics of probable Eocene age. The Challis Volcanics consist mainly of andesite but some associated basalts and rhyolites, as well as interlayered sediments are also present. For the most part, Challis Volcanics are located east of the Idaho batholith and north of the Snake River Plain (Fig. 4-2).

The Columbia River Basalts are younger than the Challis Volcanics and lie in western Idaho, mostly north of the Snake River Plain. This basalt contains interlayered lake beds.

The Idavada Volcanics are of Early to Middle Pliocene age and are composed primarily of welded ash flows. The Idavada Volcanics are exposed in the southwestern part of the State where they border the Snake River Plain Province. Silicic rocks of this age are generally considered to be the "basement" of the Snake River Plain (Stone, 1967).

Two younger volcanic series complete the generalized stratigraphic column: the Idaho Group of Early Pliocene to Middle Pleistocene age, and the youngest volcanic series, the Snake River Group of Late Pleistocene to Holocene age. The Idaho Group is made up of siliceous ash beds associated with some basalt flows while the Snake River Group is composed mainly of basalt flows. Both of these younger series contain intercalated lake and stream deposits. The Idaho and Snake River Groups are the dominant units of the Snake River Plain.

SNAKE RIVER PLAIN

The Snake River Plain was early concluded to be, because of its low relief, a regional downwarp that has been filled with basalt. Kirkham (1931) believed that subsidence of the plain may have been caused by removal of deep magma from both this region and the Columbia Plateau region to the west. Recent studies have demonstrated, however, that the Snake River depression is made up of two structurally dissimilar segments which join in the vicinity of Twin Falls at about 114°30' longitude.

The western Snake River Plain is a complex graben bounded on both the north and south by systems of normal faults (Malde and Powers, 1962; Hill and others, 1961). Malde (1965) estimated 2745 m of displacement since Early Pliocene along the faults on the north side of the western plain.

The structure of the eastern Snake River Plain is less clearly defined. The idea of a downwarp proposed by Kirkham has not been entirely dismissed. Malde (1965) located northeast trending faults on the north side of the plain in the vicinity of Twin Falls, but these are of limited extent and cannot be traced far to the northeast. Truncation of the southeast trending mountain ranges arrayed along the north side of the Snake River Plain suggests faulting. Hot

springs along both boundaries of the eastern plain compared to the lack of such springs in the interior region is suggested as evidence for the presence of bounding faults (Schoen, 1974). The gravity relief in the eastern plain is in marked contrast with high gravity anomalies characteristic of the western plain (LaFehr and Pakiser, 1962) and anomalies normal to the trend of the eastern Snake River Plain may reflect near-surface relief. The grain of this geophysically-defined structure agrees with structural trends in the Basin and Range Province to the south, and may mean that basin and range type structure is buried beneath the plain (Schoen, 1974).

Geological and geophysical data suggest that the eastern Snake River Plain is an extension of a zone defined by the alignment of the Yellowstone calderas and the Island Park caldera west of the Park. Eaton and others (1975) concluded that the Yellowstone plateau volcanic field and the eastern Snake River Plain were contiguous and shared a common ancestry of volcanism and tectonism (Fig. 4-3). They further suggested that a magma chamber may be present beneath the Yellowstone rhyolite plateau and have acted as a volcanic focus, perhaps related to a subcrustal plume, that has migrated northeastward relative to the North American plate and parallel to the axis of the eastern Snake River Plain over the last 15 million years (since Late Miocene). However, this interpretation has more recently been altered by Eaton and others (1976) and Protska and others (1976) who now include the region in a zone of high heat flow extending from southeastern California to Idaho and Montana. It is suggested that this anomaly is the result of late Cenozoic interaction between an uranium and thorium-rich plume and subducted oceanic lithosphere.

Idaho Rift System

The Idaho Rift System is a a series of aligned vents and discontinuous fractures that extend from the northern margin of the Snake River Plain in the vicinity of Craters of the

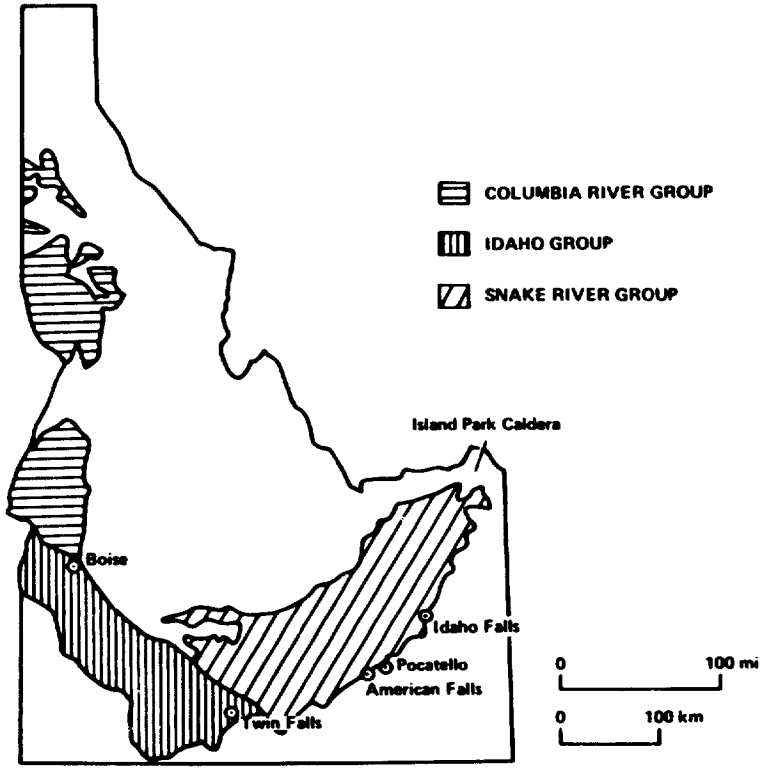

FIGURE 4-3. Idaho map showing the major Cenozoic basalt groups.

Moon National Monument southeastward to the Wapi lava field (Fig. 4-4) where the fractures either terminate or are obscured by the young lavas of the Wapi flow. Many of the fractures of the Idaho Rift System have served as conduits for lava. The Idaho Rift System was originally referred to as the Great Rift but was redesignated by Prinz (1970) when he divided the system into several rift sets (Fig. 4-5) of differing trends:

1. The Great Rift set trends N 35°W and is defined within Craters of the Moon National Monument by an alignment of vents. No open cracks are exposed in the Monument;

FIGURE 4-4. ERTS image of the central Snake River Plain showing three of the youngest lava fields in the region, flows associated with Craters of the Moon National Monument, the Wapi lava field, and the King's Bowl lava field.

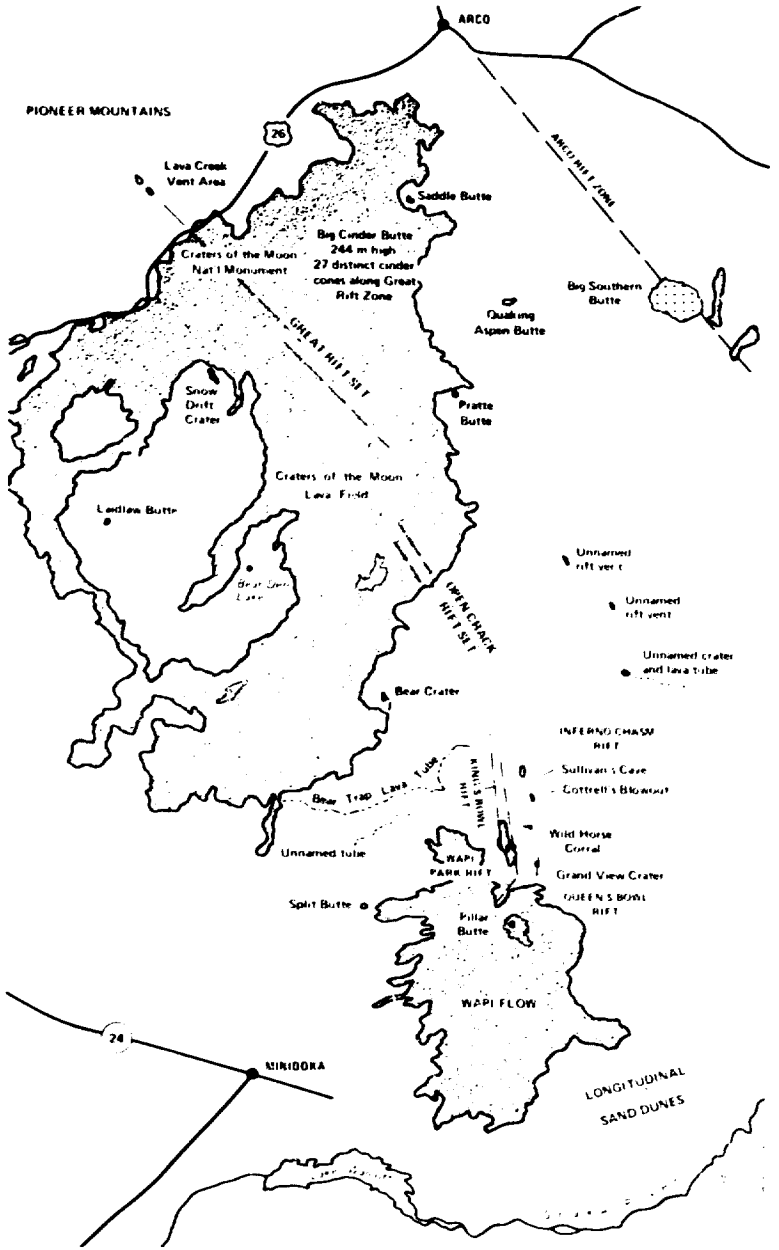

FIGURE 4-5. Map of the general area shown in Figure 4-4, showing the major features along the Idaho Rift System (after Prinz, 1970).

however, open fissures are present southeast of the Monument but lack associated lava flows. An open fissure located north of the Snake River Plain in the Pioneer Mountains which parallels the trend of the Great Rift set has been described by Anderson (1929). This fracture suggests extension of the Great Rift set beyond the limits of the Snake River Plain (Fig. 4-5).

2. The Open Crack rift set trends N 30°W and has no extrusives associated with it (Fig. 4-6).
3. The King's Bowl rift set trends N 10°W and has some small flows associated with it (Fig. 4-7). Prinz (1970) included the Queen's Bowl rift set here and projected it north into Inferno Chasm, Cottrell's Blowout and Wildhorse Corral (Fig. 4-5).
4. The Wapi rift set is inferred to trend north-south beneath Pillar Butte and extend parallel to the long dimension of the Wapi flow.

Several rift sets of different trends and ages have been recognized in the King's Bowl area (Greeley and King, 1975a):

1. The King's Bowl rift is the youngest of these rift sets and is defined by a discontinuous 1.5 m to 2.5 m wide fissure flanked on both sides by sets of narrow tensional cracks. The King's Bowl rift trends N 10°W. To the south of King's Bowl (Fig. 4-5), the flanking fractures on the east side of the rift are traceable to and beneath a tongue of the Wapi flow.
2. The Queen's Bowl rift, which trends N 10°E, is an older tensional set, as evidenced by greater weathering of basalt exposed in the fractures and a heavier cover of vegetation.
3. The Inferno Chasm rift which appears to be the oldest of these rift sets, is a zone defined by an alignment of several prominent volcanic vents including Inferno Chasm, Cottrell's Blowout and Wildhorse Corral. This set trends N 4°W.

FIGURE 4-6. Vertical aerial photograph of the Open Crack rift set of the Idaho Rift System, south of Craters of the Moon National Monument. This rift set was apparently "dry" with no apparent eruption associated with it. Area of photograph 2.4 km by 3.6 km. (U. S. Geological Survey Photograph GS SWEZ 8-75, October 1971).

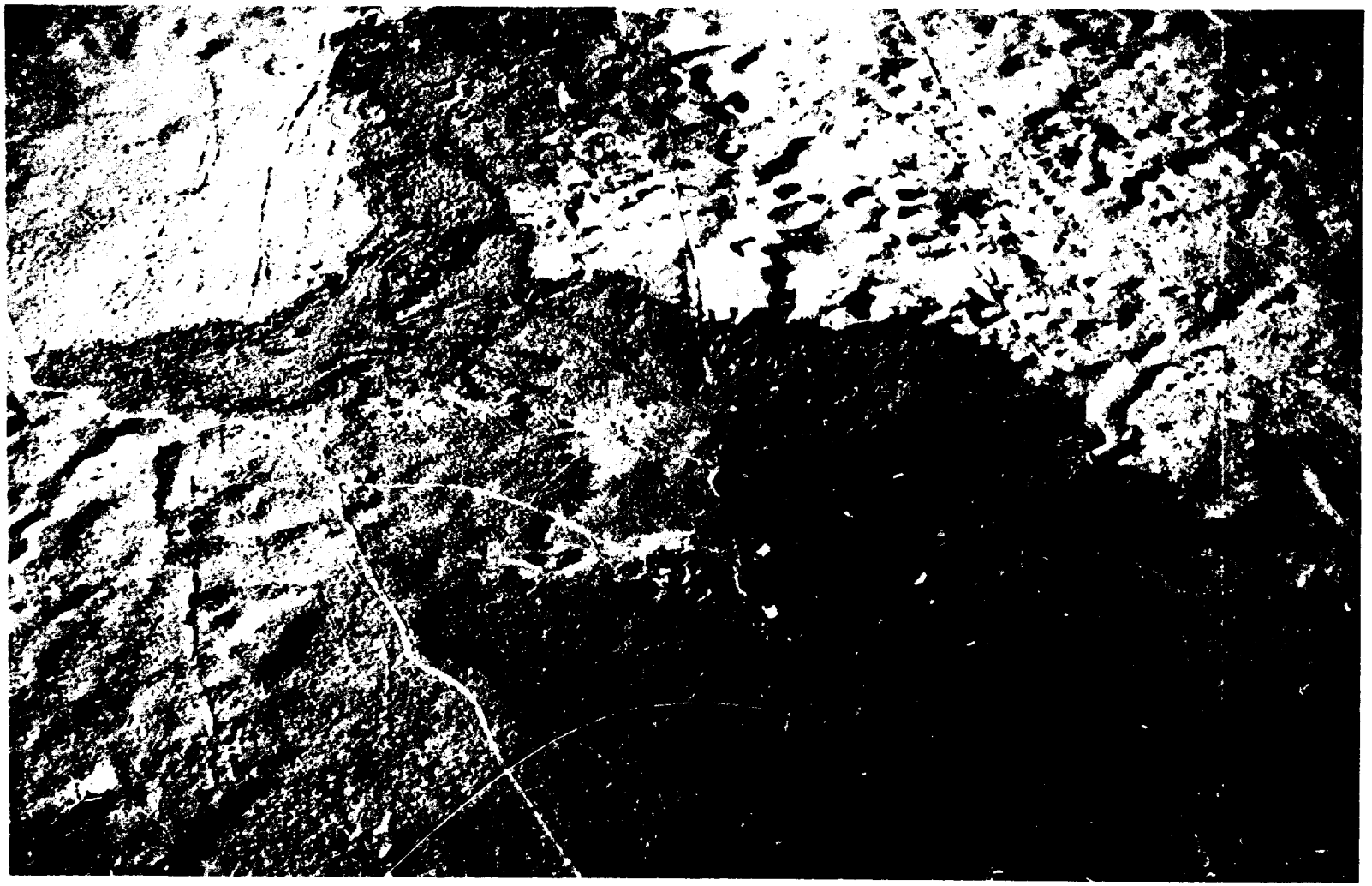

FIGURE 4-7. Low oblique aerial view of the King's Bowl rift, showing the young fissure-fed flows (dark area) and King's Bowl, a phreatic eruption crater on the fissure. Note the extensional fractures that parallel the fissure. (From Greeley and King, 1975b.)

A possible additional rift is defined by an alignment of vents in Wapi Park on the north side of the Wapi lava flow.

The trends of the rift sets range from N 10°E (Queen's Bowl rift of Greeley and King, 1975a) to N 35°W (Great Rift set of Prinz, 1970). The rifts are tensional fractures which collectively approximate the trend of basin and range structures north and south of the plain. In this sense they may be the surface expression of renewed basement faulting related to basin and range structure beneath the lava flows of the Snake River Plain (Leeman, 1974; Schoen, 1974).

Silicic Volcanic Constructs

Basalt is the dominant surface rock of the eastern and central Snake River Plain, but in a group of three prominent volcanic features close to the central axis of the plain south of Arco, two features are not basaltic, and the third, Middle Butte, is defined by tilted basalt which is believed to be a cap overlying a silicic plug. Big Southern Butte and East Butte are both composed of silicic rocks and their origin has long been controversial. They have been interpreted as kipukas or stepptoes (Russell, 1902) and as blocks of older rock faulted to their present position (Stearns and others, 1938). More recently, Schoen (1974) has suggested that these features were emplaced as viscous silicic domes, possibly derived from remobilized silicic material underlying the basalt of the Snake River Plain. He points out that the tilted basalt flow which caps Middle Butte stands at an anomalously high elevation compared to surrounding flows. The nearest location of a flow showing equal elevation and similar attitude to the Middle Butte flow is 128 km distant to the northeast. From this Schoen concludes that the basalt cap on Middle Butte is a plate which has been pushed up to its present elevation and orientation by emplacement of a plug of younger silicic rock. More attention will be given to East, Middle, and Big Southern Buttes in another paper in this conference guide (Chapter 6).

Snake River Basalts

All of the features which will be seen during the Volcanic Conference are developed in basalts of the Snake River Group which are of late Pleistocene to Holocene age. These basalts differ markedly in origin from the Miocene basalts of the Columbia River Group to the west. The Columbia River basalts were extruded from fissures whereas Snake River Group lavas erupted from centers which were probably rift controlled, but which changed locations repeatedly through time. Thus the present build up of the basaltic succession represents a composite of overlapping and coalescing flows from a variety of vents (Fig. 4-8). The distinction between the two basaltic provinces is discussed in Greeley (1976) and Chapter 3.

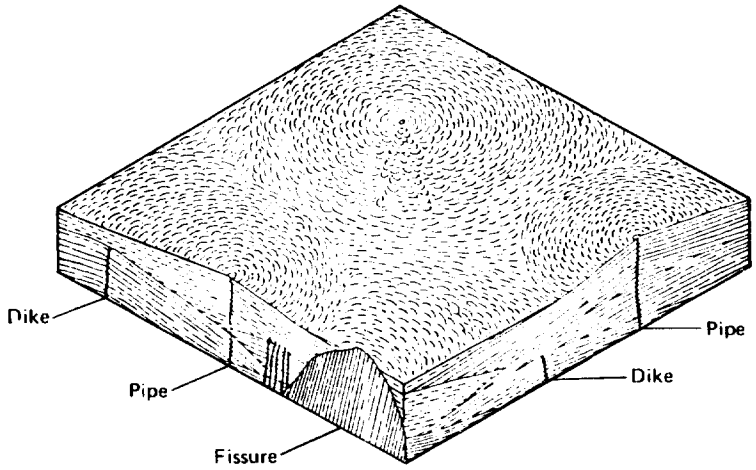

FIGURE 4-8. Diagram illustrating the structure of a typical lava plain or plateau. (From Macdonald, 1972, after Rutten, 1964.)

Most of the Snake River basalts represent highly mobile pahoehoe flows (Stone, 1967). Snake River lavas must have been extremely fluid as the flows spread great distances from their vents (Lindgren, 1898). Furthermore, shields of many of the vents are large (up to 16 km) but of low relief (60–90 m) reflecting discharge of a very fluid lava (Russell, 1902). Stearns and others (1938) noted an abundance of low shields (about 30 m high) with associated flows which cover areas up to 77 km^2 also suggesting a very fluid lava. However, it has recently been pointed out that the rate of effusion is an important variable which must be considered in the evaluation of the extent of lava flows. Thus even viscous material can be carried farther from the vent if the effusion rate is continuously high (Walker, 1972).

The Snake River Group lavas are olivine tholeiites which are fairly uniform in mineralogy, chemistry, and texture (Stone, 1967). They are characterized chemically as being low in SiO_2 and total alkalis and having a high total iron content. The average Snake River lava apparently began to crystallize at about 1175°C and crystallization was complete with a reduction of 150°C (Stone, 1967). Leeman (1974) indicated from a study of the McKinney basalt, which is a member of the Snake River Group, that the lavas were erupted at 1190° to 1200°C. According to Stone (1967), the first phase to crystallize was olivine, but it was quickly joined by plagioclase and all principal phases were crystallizing simultaneously with a temperature drop of 35°–50°. The texture of the basalt indicates that crystallization generally occurred subsequent to termination of movement of the flow. Had crystallization taken place during flow, subalignment of elongate grains such as feldspar laths would be expected. However, such alignment is not common and, for the most part, the inequant mineral grains show random orientation.

The total thickness of basalts of the eastern Snake River Plain is not known. LaFehr and Pakiser (1962) suggest thickness variations of the basalts of from several hundred to over 1500 m. Test holes drilled at the National Reactor Testing Station south of Arco penetrated 456 m below the surface and were still in Snake River Group basalts (Walker, 1964). Electrical resistivity data determined on a line between Blackfoot and Arco are interpreted to indicate a maximum depth of 1830 m for basalts of the eastern Snake River Plain (Zohdy and Stanley, 1972, 1973).

Estimates of the thicknesses of individual flows of Snake River Group basalts are variable. Russell (1902) estimated flows to be from 45–75 m thick. Stone (1967) states that "the flows range in thickness from 10–60 feet (3–18 m), averaging 30 feet (9 m), but may reach several hundred feet in thickness where they fill canyons." Champion (1973) estimated the average thickness of the Wapi field (made up of several flow units), which is one of the most recent of the Snake River Group lavas, at about 32 m, and Leeman (1974) characterized the Snake River basalts as thin flows from 3 to 10 m in thickness. Accurate flow thicknesses are difficult to establish in light of the petrologic similarity of the lavas as well as the overlap of flows from different vents. Coupled with this, flow units, representing different but overlapping surges of material from the same vent tend to mask any textural boundary differences between flows. The areal extent of many flows which have spread out on a low gradient surface indicate that the flows were extremely fluid and this, in turn, suggests that the average thickness of the flows is not great, possibly in the range of 1 m to 10 m.

The uniformity of petrology and the lack of widespread natural incisions through the flows as well as a lack of well data makes correlation of all but the younger surface flows of the eastern Snake River Plain difficult. Stratigraphic columns can be determined locally as at the King's Bowl or in Wildhorse Corral, but it is difficult to extend that control laterally. Moreover, flow thicknesses determined near their vents are probably not typical of the main part of the flow. Most flows have vesicular tops and narrower vesicular bases (Stone, 1967) which is a useful criterion for differentiation of flows. Soil horizons are also useful as flow dividers but are not always continuous. Also, Stearns and Macdonald (1942),

based on observations at Haleakala in Hawaii, have shown that "pseudo" soil horizons can result from the migration of ground water through rubbly zones within a single lava flow. Such a pseudo horizon, marked by an abundance of reddish friable material would, in such a case, not indicate a flow contact, but rather a physically distinct zone within a single flow. Additionally, the present surface of the flows is undulating and significant local relief is found around pressure ridges and collapse depressions. Assuming a similar surface expression for earlier flows and noting the present accumulation patterns of windborne deposits, a significant period of time appears to be necessary to develop a widespread, continuous soil horizon. Loess accumulates in low and protected regions on the surface and builds up slowly. If insufficient time intercedes between flows, the loessal accumulation remains discontinuous and of only local significance in flow correlation. Some success at correlation of the surface flows has been made by intensive stereoscopic study of aerial photos noting slopes, textural variations, and flow fronts. This type of analysis allows geologic mapping of the surface units and provides insight into the complex overlap and coalescence of flows from various vents (Greeley and King, 1975b; LaPoint, 1975).

Stearns and others (1938) mapped some 300 vents on the Snake River Plain east of 115° longitude and extrapolated this figure to a total of 400 for the entire plain. In their mapping they were unable to locate any widespread structural patterns defined by the vents although many short chains of vents were found. Most of the vents are low shields from which lava erupted quietly. There are notable local exceptions to this pattern of eruption, however, which indicate more violent phreatic eruptions. King's Bowl on the King's Bowl rift set is one of these. It has an extensive field of ejecta as well as an area of ash accumulation. Split Butte is another such vent and, although apparently less explosive than the King's Bowl event, the Split Butte mound is made up dominantly of a rampart of layered tephra (Greeley and King, 1975b; Womer, 1977 and Chapter 12). Both of these vents no doubt erupted as they did owing to interaction of the lava with ground water.

Age of the Plain and Lavas

The Snake River Plain is interpreted by Stone (1967) to have developed since the Pliocene Epoch. Eaton and others (1975), based largely on K-Ar da ng of volcanic units along the margins of the eastern plain (Armstrong, Leeman and Malde, 1975), project the volcanic and tectonic history of the eastern plain back about 15 million years. They suggest that a magma body, which is still molten, underlies the Yellowstone Plateau, and, in their interpretation, this present position of volcanism ". . . represents the active end of a system of similar volcanic foci that has migrated progressively northeastward for 15 million years. . . " This migration is envisioned to have started at the southwestern end of the eastern Snake River Plain and followed slowly along the trace of the eastern plain. The parallelism of the structural grain of exposed Precambrian rocks elsewhere in the Rocky Mountain region with the direction of movement has suggested control by Precambrian structures (Eaton and others, 1975).

Age determinations for the younger flows of the eastern Snake River Plain are not abundant. Bullard (1976) reports two dates from burned sage destroyed by one of the Holocene flows in Craters of the Moon National Monument which bracket in a 2100–2300 year age range. Flows which issued from the King's Bowl rift have also been dated by C^{14} methods on burned sage roots found in the base of the flow at the Crystal Ice Cave as 2130 ± 130 years (Prinz, 1970). Kuntz (1977) has obtained C^{14} dates from disseminated charcoal and organic material in soils beneath the older North Robbers and Cerro Grande flows as 11,940 ± 300 and 10,780 ± 300 C^{14} years respectively and an age of 4100 ± 200 C^{14} years on the Hell's Half Acre flow. He also feels that at least 10 other flows in the same vicinity are less

than 50,000 years old. These ages are all considerably younger than the youngest eruptive events in the Yellowstone region (150,000–70,000 years) indicated by Eaton and others (1975). Although their hypothesized eruptive sequence has been qualified by suggesting that rhyolitic volcanism followed eruption of tholeiitic lava at each focus and was followed in turn by basalts which have ". . . continued to erupt virtually to the present," there seems to be some lack of supporting evidence for this in many of the basalt and rhyolite sequences of the central plain.

SUMMARY

The Snake River Plain is a prominent physiographic region which occupies nearly one fourth of the total area of the State of Idaho. It contrasts markedly with the surrounding terrain in that it is characterized by low topographic relief and stands at low elevation in respect to the surrounding ranges. The Snake River Plain has developed since Late Miocene–Pliocene. The base of the Snake River depression can be considered to be the Idavada Volcanic Series or time-equivalent silicic rocks which crop out along the edge of the plain.

The Snake River Plain is structurally divisible into two parts. The western plain is interpreted on both geophysical and geological evidence to be a graben. The eastern plain, however, is more difficult to interpret; it may be a regional downwarp at least partially bounded by faults, or it may be the result of the migration of some shallow subsurface volcanic focus over the past 15 million years or possibly a combination of these causes.

REFERENCES

Anderson, A. L., 1929. Lava Creek Vents, Butte County: Northwest Science, vol. 3, p. 13-19.

Armstrong, R. L. and F. A. Hills, 1967. Rb-Sr and K-Ar Geochronologic Studies of Mantled Gneiss Domes, Albion Range, Southern Idaho, USA: Earth and Planetary Letters, vol. 3, p. 114-124.

Armstrong, R. L., W. P. Leeman and H. R. Malde, 1975. K-Ar dating Quaternary and Neogene volcanic rocks of the Snake River Plain, Idaho: Amer. Jour. Sci., vol. 275, p. 225-251.

Bullard, F., 1976. Volcanoes. University of Texas Press, Austin, 330 p.

Champion, D. E., 1973. The relationship of large scale surface morphology to lava flow direction, Wapi lava field, southeastern Idaho: Unpublished M. A. Thesis, State Univ. of New York, Buffalo, 44 p.

Eaton, G. P. and R. L. Christiansen, H. M. Iyer, A. M. Pitt, D. R. Mabey, H. R. Blank, Jr., I. Zietz, M. E. Gettings, 1975. Magma beneath Yellowstone National Park: Science, vol. 188, p. 787-796.

Eaton, G. P., H. Protska, S. Oriel, and K. Pierce, 1976. Cordilleran Thermotectonic Anomaly: I. Geophysical and geological evidence of coherent late Cenozoic intraplate magmatism and deformation (abs.): Geol. Soc. America Annual Meeting, Abstracts with Programs, p. 850.

Greeley, R., 1976. Modes of emplacement of basalt terrains and an analysis of mare volcanism in the Orientale Basin: Proc. Lunar Sci. Conf. 7th Annual, p. 2747-2759.

Greeley, R. and J. S. King, 1975a. Rift zones in the south-central Snake River Plain, Idaho: Geol. Soc. America, Abs. with Program (Rocky Mountain Section), vol. 7.

Greeley, R. and J. S. King, 1975b. Geologic field guide to the Quaternary volcanics of the south-central Snake River Plain, Idaho: Pamphlet No. 160, Idaho Bureau of Mines and Geology, 49 p.

Hill, D. P., H. L. Baldwin, Jr., and L. C. Pakiser, 1961. Gravity, volcanism and crustal deformation in the Snake River Plain, Idaho: U. S. Geol. Survey Prof. Paper 424-B, p. B248-B250.

Kirkham, V. R. D., 1931. Snake River Downwarp: Jour. Geol., vol. 39, p. 465-482.

Kuntz, M. A., 1977. Extensional faulting and volcanism along the Arco Rift Zone, eastern Snake River Plain, Idaho (abs.): Geol. Soc. America, Rocky Mountain Sectional Meeting, Missoula.

LaFehr, T. R. and D. H. Pakiser, 1962. Gravity, volcanism and crustal deformation in the eastern Snake River Plain, Idaho: U. S. Geol. Survey Prof. Paper 450D, p. D76-D78.

LaPoint, P. J. I., 1975. Photogeologic study of volcanic and structural features of the eastern Snake River Plain, Idaho (abs.): Geol. Soc. America, Rocky Mountain Sectional Meeting, Abstracts with Programs, p. 620.

Leeman, W., 1974. Petrology of basaltic lavas from the Snake River Plain, Idaho, Ph.D. Dissertation, Univ. of Oregon, 337 p.

Lindgren, W., 1972. Geologic Atlas of the U. S.: Boise Folio No. 45, 11 p.

Macdonald, G. A., 1977. Volcanoes: Prentice-Hall, Englewood Cliffs, 510 p.

Malde, H. E., 1965. Snake River Plain: in Wright, H. E. and D. G. Frey, eds., The Quaternary of the United States, p. 255-263.

Malde, H. E. and H. A. Powers, 1962. Upper Cenozoic stratigraphy of western Snake River Plain, Idaho: U. S. Geol. Survey Prof. Paper 596, 52 p.

McKee, B., 1972. Cascadia: McGraw Hill Book Co., 394 p.

Prinz, M., 1970. Idaho rift system, Snake River Plain, Idaho: Geol. Soc. America Bull., vol. 81, p. 941-947.

Protska, H. J., G. P. Eaton and S. S. Oriel, 1976. Cordilleran Thermotectonic Anomaly: II. Interaction of an intraplate chemical plume mass and related mantle diapir (abs.): Geol. Soc. America Annual Meeting, Abstracts with Programs, p. 1055.

Russell, T. C., 1902. Geology and water resources of the Snake River Plains of Idaho: U. S. Geol. Survey Bull. 199, 192 p.

Schoen, R., 1974. Part III. Geology, in Robertson, J. B., R. Schoen and J. T. Barraclough, Influence of liquid waste disposal on the geochemistry of water at the National Reactor Testing Station, Idaho: U. S. Geol. Survey Open File Report, IDO 22053, 231 p.

Stearns, H. T., L Crandall and W. G. Steward, 1938. Geology and groundwater resources of the Snake River Plain in Southeastern Idaho: U. S. Geol. Survey Water Supply Paper 774, 268 p.

Stearns, H. T. and G. A. Macdonald, 1942. Geology and ground water resources of the island of Maui, Hawaii: Hawaii Division of Water and Land Development, Bull. 7, p. 61-113.

Stone, G. T., 1967. Petrology of Upper Cenozoic basalts of the Snake River Plain, Ph.D. Dissertation, Univ. of Colorado, 392 p.

Walker, E. H., 1964. Subsurface geology of the National Reactor Testing Station, Idaho: U. S. Geol. Survey Bull. 1133E, 22 p.

Walker, G. P. L., 1972. Compound and simple lava flows and flood basalts: Bull. Volcanologique, vol. 35, p. 1-12.

Wells, M. W., 1974. Origins of the name "Idaho" and how Idaho became a territory in 1863: in Etulain, R. W. and B. W. Marley, The Idaho Heritage, Idaho State University Press, 230 p.

Womer, M. B., 1977. A study of the ash rings of Split Butte, a maar crater of the south-central Snake River Plain, Idaho: Unpubl. Master's Thesis, State Univ. of N. Y. at Buffalo, 53 p.

Zohdy, A. A. R., and W. D. Stanley, 1972. Profiles of deep electrical soundings on the Snake River Plain, Idaho, (abs.): Geol. Soc. America, p. 423.

Zohdy, A. A. R. and W. D. Stanley, 1973. Preliminary interpretation of electrical sounding curves obtained across the Snake River Plain from Blackfoot to Arco, Idaho: U. S. Geol. Survey Open File Report, 3 p.

5. AERIAL GUIDE TO THE GEOLOGY OF THE CENTRAL AND EASTERN SNAKE RIVER PLAIN

Ronald Greeley
Department of Geology and
Center for Meteorite Studies
Arizona State University
Tempe, Arizona 85281

5. AERIAL GUIDE TO THE GEOLOGY OF THE CENTRAL AND EASTERN SNAKE RIVER PLAIN

Ronald Greeley
Department of Geology and
Center for Meteorite Studies
Arizona State University
Tempe, Arizona 85281

One of the objectives of this field conference is to acquaint planetologists with plains-type basaltic volcanism through field trips to key features on the Snake River Plain. Within the available time, however, it will not be possible to visit on the ground more than just a few selected localities. This air tour has been designed to cover the major features that are not included in the ground trips and to give an aerial perspective to the features that will be visited. There is, however, another reason for the air tour. The interpretation of planetary surfaces and the derivation of the geological histories for the planets involves primarily photogeology. Thus, planetologists must have an appreciation for geologic features and relations as viewed "remotely." Moreover, most of the volcanic features on the Snake River Plain are rather low relief and large, and it is only from the air that they can be placed in perspective.

The air tour will be of approximately three to four hours duration. Figure 5-1 shows the general path of the flight which originates at the Pocatello airport. The tour and this guide are segmented into seven "legs." It must be emphasized that weather and other conditions at the time of the flight will govern both the sequence and the actual flight path.

NOTES FOR PHOTOGRAPHERS

Taking photographs from airplanes is often a frustrating exercise. This short section describes some factors to consider in photographing geologic features during the air tour.

A camera with adjustable shutter speeds and lens openings is recommended. For black and white film intended for enlarging, Plus X is suggested; if only 2X or 3X enlargements are planned, the faster Tri-X is suggested. For color slides or prints, High Speed Ektachrome is suggested.

Lighting conditions for aerial photography are tricky at best and are even more difficult over dark basalt flows. For cameras with built-in light meters, be certain that the meter is "seeing" the desired subject. Pictures are often underexposed because the meter measured mostly the sky. To get the proper exposure for dark lava flows, tip the camera (or the light meter) so that is "sees" only the ground and no sky. The picture can be composed after the proper light reading is obtained. For particularly interesting features, it is a good idea to "bracket" the exposure, using one "f" stop above and one "f" stop below the nominal value. The price of film is the least expensive part of the trip!

A haze, or UV filter, is also recommended. If a polarizing filter is used, watch for reflection produced by the polarizing effect of the airplane window. In addition, bring a soft cloth or tissue to wipe the window. Extra film is a good investment. Invariably, film runs out before the flight is over. If you are prone to motion sickness, your colleagues would appreciate your taking Dramamine (or something similar) *prior* to the flight (generally it doesn't do much good to take the medication after you begin to feel queasy). The dips, turns, and banks of the reconnaissance flight can bring problems even to the staunchest flier.

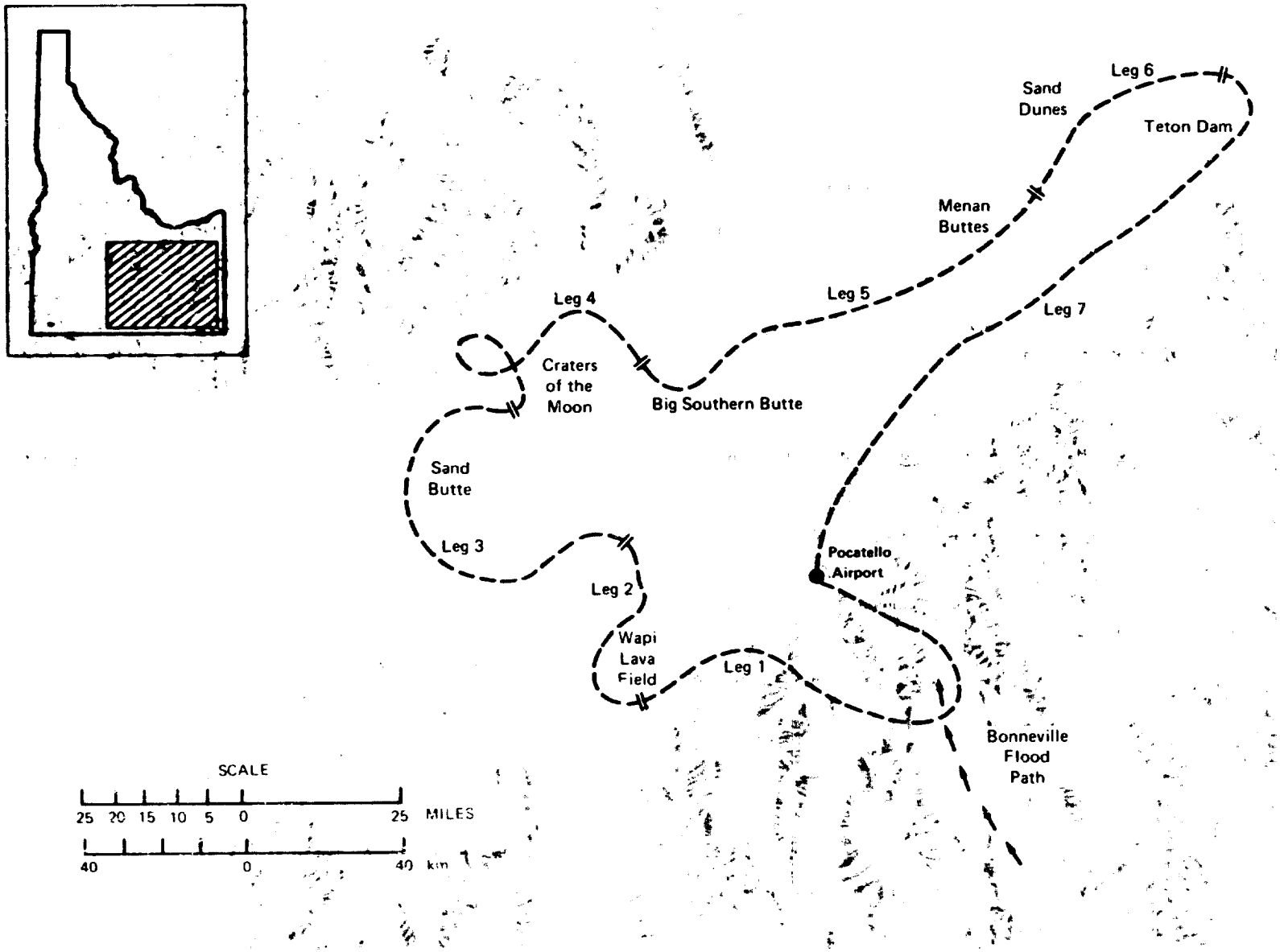

FIGURE 5-1. Map of southeastern Idaho showing flight path over the central and eastern Snake River Plain.

SUMMARY OF FLIGHT

LEG 1 follows the valley of the Portneuf River upstream, southward toward Utah. This valley was the waterway for the Bonneville flood, the spillover of ancient Lake Bonneville into the Snake River drainage system that occurred about 30,000 years ago during the Pleistocene. The flight will then cross westward over the mountains that bound the plain on the south. These mountains are mostly eroded pre-Tertiary sedimentary and metamorphic rocks with some Tertiary silicic volcanics. The leg ends with a view of the ancient channelway (Lake Channel) of the Snake River that was abandoned as a result of the Bonneville flood.

LEG 2 begins near the Snake River and includes views of the Wapi Lava Field and sand dunes, some of which have been covered by young basalt flows. The flight path includes Split Butte–a maar crater that contained a lava lake–and ends with an overview of the southern end of the Idaho Rift System, one of the major structural elements on the Snake River Plain. Phreatic craters, pit craters, low-shield constructs, fissures, and fracture zones will be viewed.

LEG 3 parallels the Bear Trap Lava Tube for about 20 km, then turns north, for a view of Sand Butte, a well-preserved maar crater and tuff ring situated over a fissure. Numerous low shields, typical of the plain, will be seen.

LEG 4 begins near the southern end of the Great Rift System in Craters of the Moon National Monument and includes views of the extensive cinder cones and young flows within the Monument, including one flow that erupted in the Pioneer Mountains, immediately north of the plain. The flight path then turns eastward and crosses Big Lost River and Little Lost River–streams which "disappear" into the porous basalt flows.

LEG 5 begins near Big Southern Butte, a steptoe, or kipuka, of silicic volcanics and includes views of several young basalt flows, lava tube systems, and pressure ridges. The flight path then swings northeastward to Menan Buttes, twin craters on Henry's Fork River.

LEG 6 covers several large, active sand dune fields in the northeast part of the plain. One field includes "climbing" dunes that cross Juniper Buttes, a series of small volcanic mountains. The flight path also includes well preserved low shields, lava tubes, and pit craters.

LEG 7 begins with an overflight of the Teton Dam failure site and the channel of the waterway created by the rapid release of water. The flight path then follows the Snake River downstream, diverts over Hell's Half Acre lava field, and ends at the Pocatello Airport.

REFERENCES

Koscielniak, D. E., 1973. Aeolian deposits on a volcanic terrain near St. Anthony, Idaho: M.S. Thesis, Univeristy of New York at Buffalo, 28 p.

Kuntz, M., 1977. Extensional faulting and volcanism along the Arco Rift zone, eastern Snake River Plain: Geol. Soc. Amer. Abs. with program (Rocky Mountain Section), vol. 9 pp. 740-741.

FIGURE 5-2. Oblique aerial view southward up the pathway of the Bonneville flood (arrow indicates flow direction) in the vicinity of Inkom; white strips near arrow are scour-lines in the basalt, caused by the flood. (Photograph by Ronald Greeley, University of Santa Clara, June, 1977.)

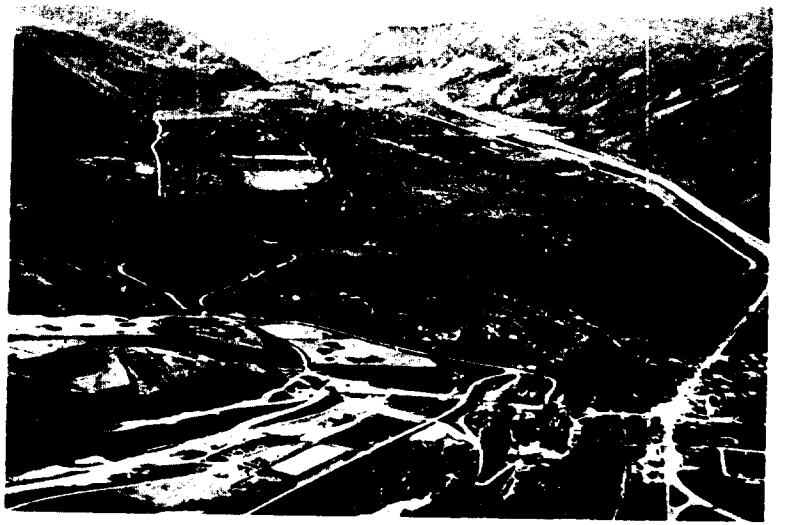

FIGURE 5-3. View downstream of the area shown in Figure 5-2, toward the "narrows." (Photograph by Ronald Greeley, University of Santa Clara, June, 1977.)

FIGURE 5-4. Oblique aerial view of American Falls (right) and American Falls Reservoir and dam. (Photograph by Ronald Greeley, University of Santa Clara, June, 1977.)

FIGURE 5-5. Vertical aerial photograph of area between American Falls and the Wapi lava field, showing irrigated crop land (dark fields) and dry land farming (mostly wheat, light and medium gray areas); irregularly-shaped dark areas are rocky areas that often correspond to pressure ridges on the partly weathered lava flows. Area of photograph 2.4 km by 3.6 km. (U. S. Geological Survey Photograph GS SWEZ 1-188; August, 1971.)

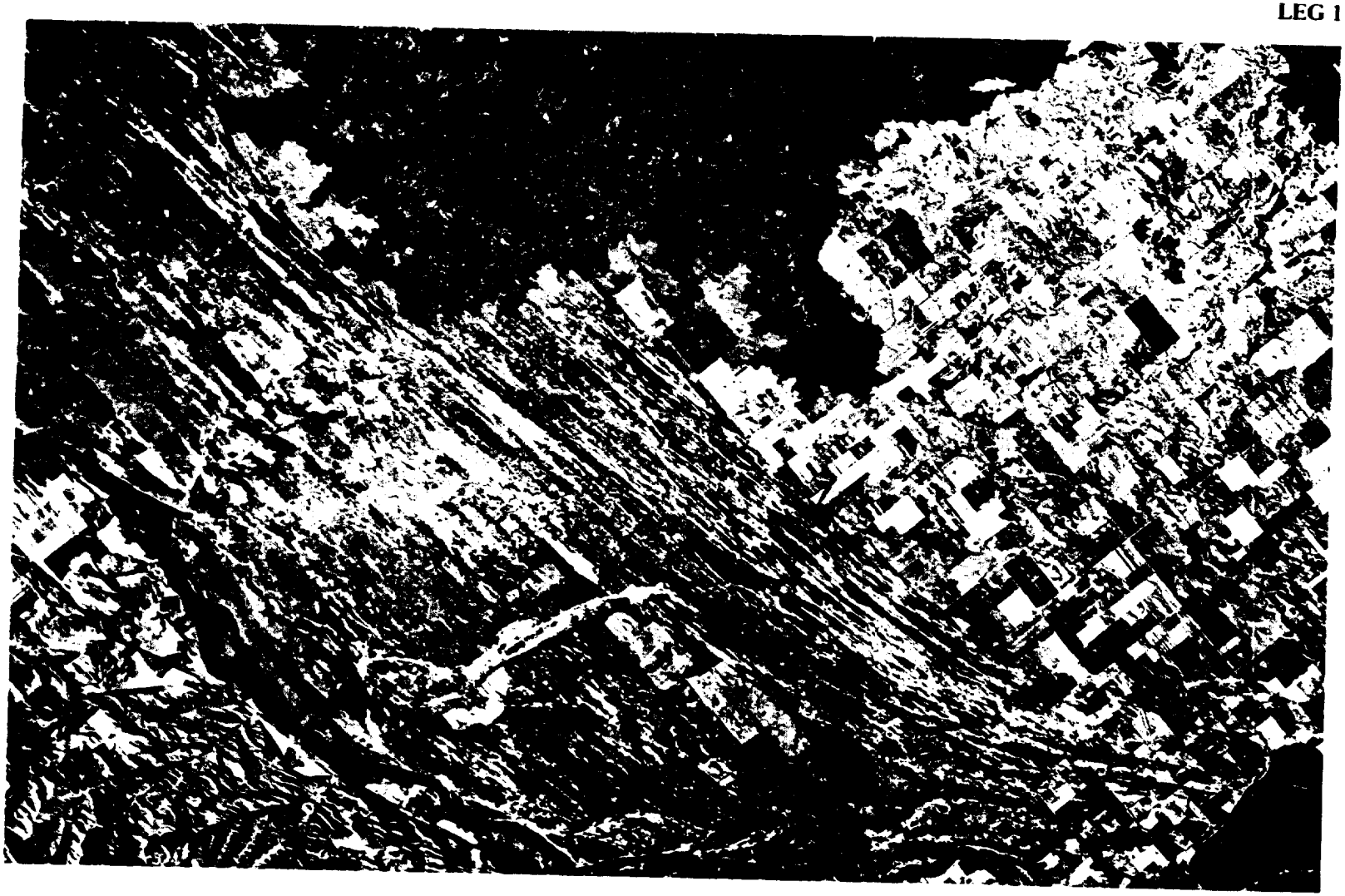

FIGURE 5-6. High altitude (U-2 aircraft) photograph of the Snake River (lower part of the picture) sand dune field truncated by the Wapi lava field (top of picture) and a segment of the ancient channel (arrow) for the Snake River. American Falls reservoir is in the lower right. (NASA-Ames Photograph 72-186, frames 5709, 5710, October, 1972.)

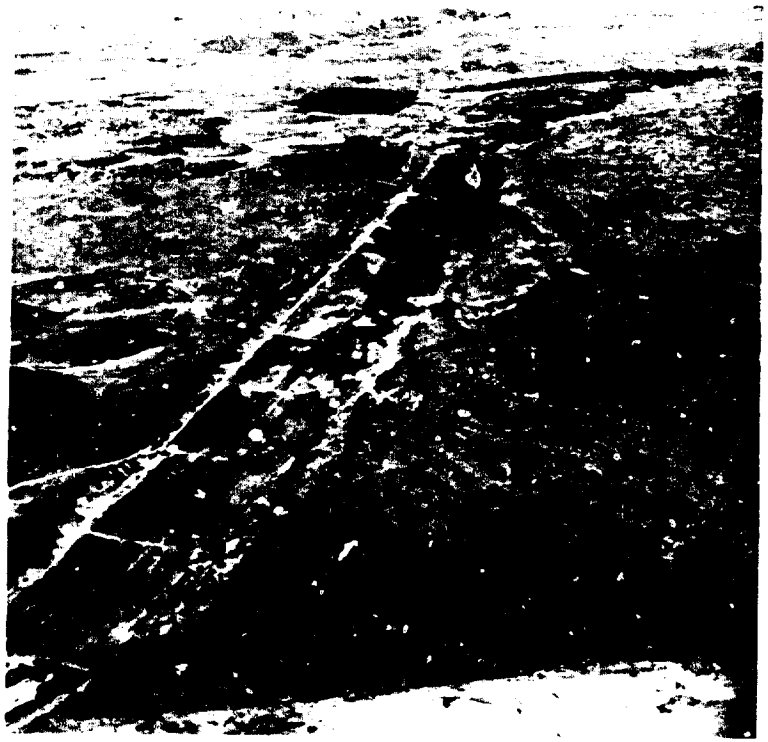

FIGURE 5-7. Low oblique view southward down Lake Channel; note the straight wall on the east (left) side, which may reflect structural control (Photograph by Ronald Greeley, University of Santa Clara, June 1977.)

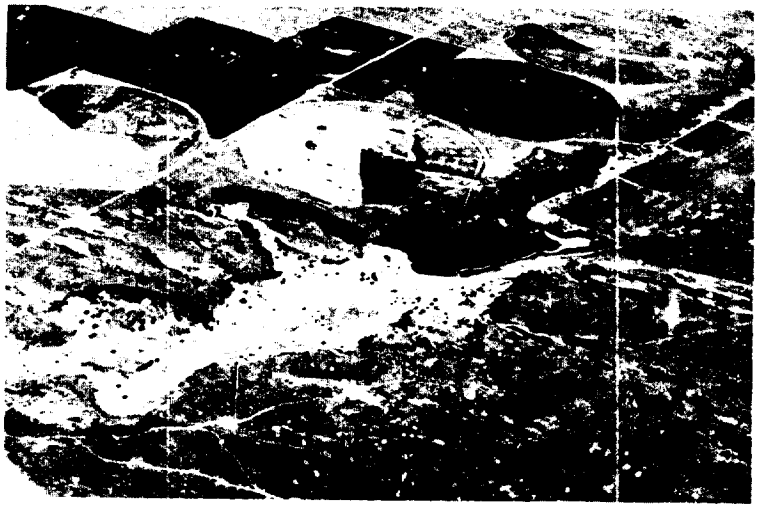

FIGURE 5-8. Oblique view southeastward of the upper end of Lake Channel, showing scalloping that may result partly from sapping processes; white deposits are wind-blown sands. Circular areas are the result of revolving irrigation systems. (Photograph by Ronald Greeley, University of Santa Clara, June, 1977.)

FIGURE 5-9. Detail of area shown in Figure 5-8. (Photograph by Ronald Greeley, University of Santa Clara, June, 1977.)

FIGURE 5-10. Vertical aerial photograph of the southern margin of the Wapi lava field (dark area), showing longitudinal sand dunes that are partly covered by lavas. A small vent is in the middle of the picture. North is to the left; area of photograph is 2.2 km by 3.2 km. (U. S. Geological Survey Photograph GS SWEZ 1-11, August, 1971.)

LEG 1

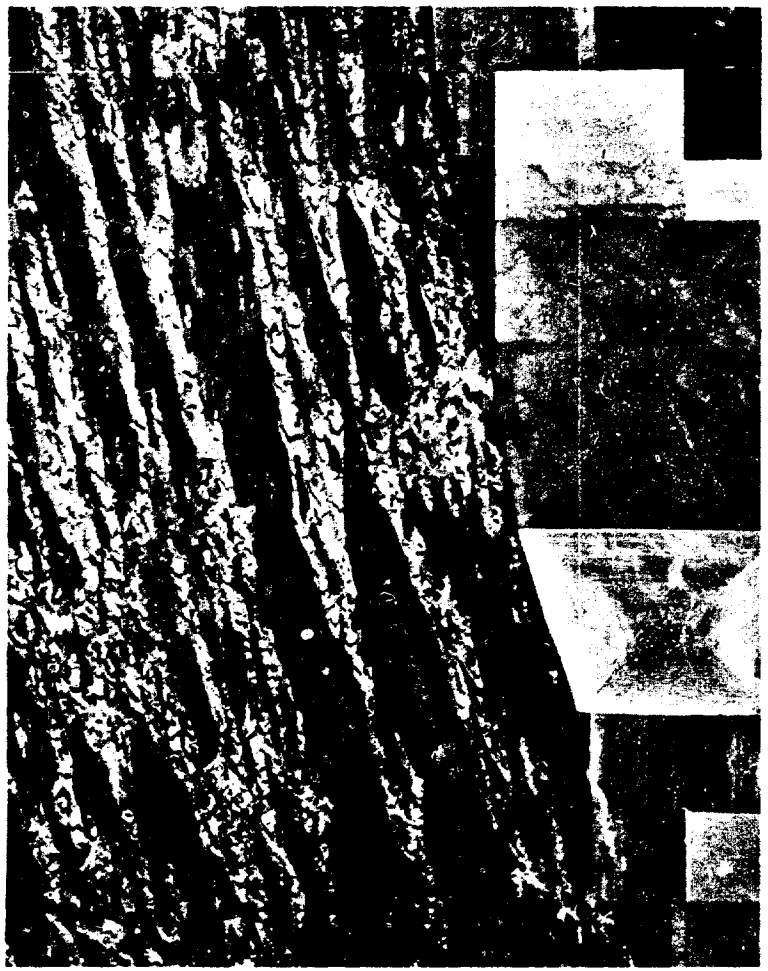

FIGURE 5-11. Vertical aerial photograph of the area west of American Falls and immediately north of the Snake River, showing longitudinal-parabolic dunes. Area of photograph is 2.2 km by 3.4 km. (U. S. Geological Survey Photograph GS SWEZ 1-06, August, 1971.)

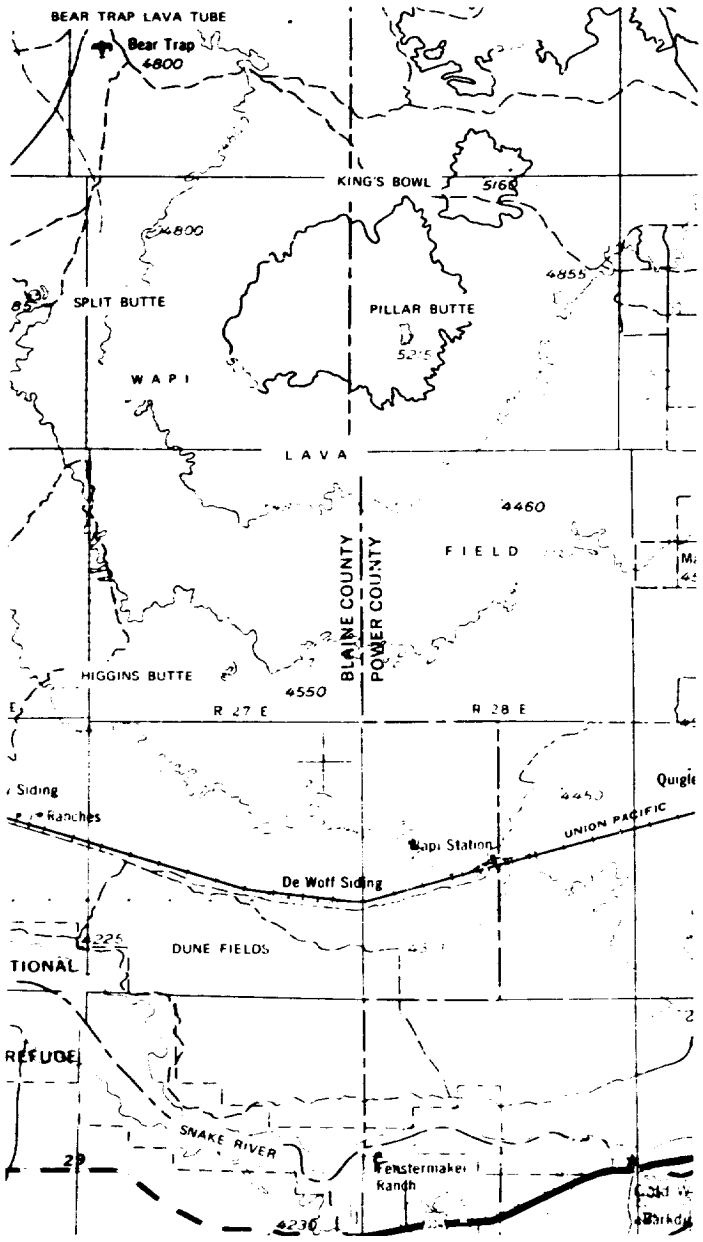

FIGURE 5-12. Index to LEG 2.

LEG 2

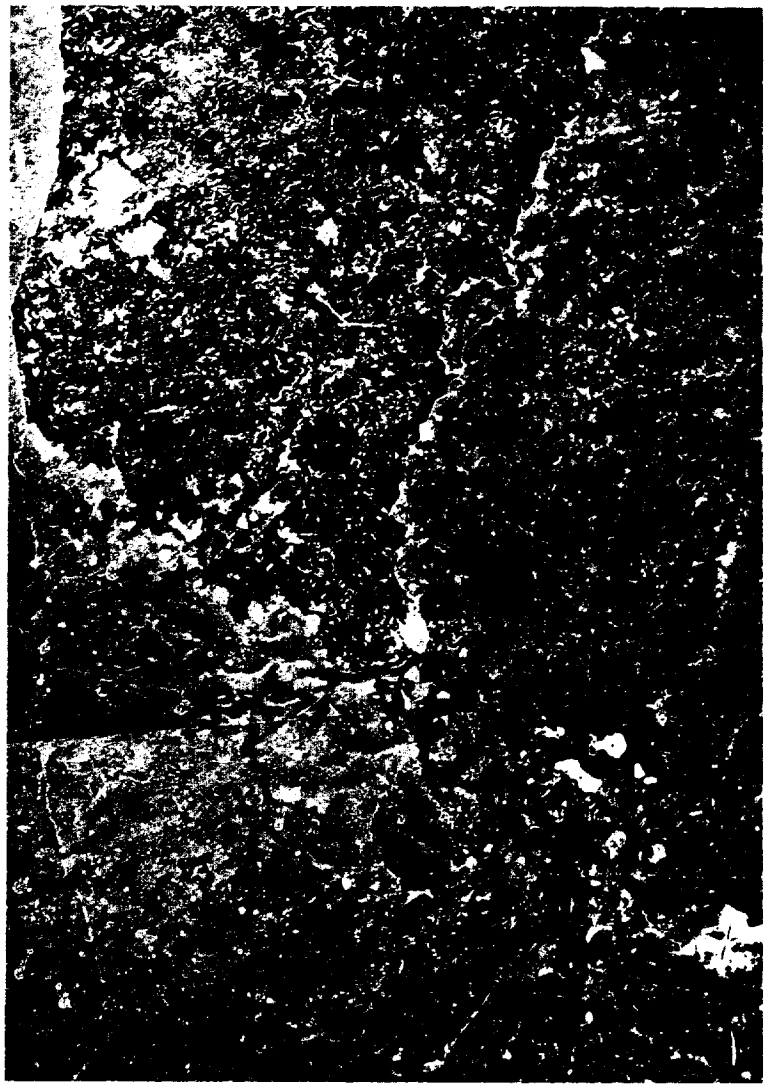

FIGURE 5-13. Mosaic of vertical aerial photographs northeast of Lake Walcott, showing effect of prairie fires on discernibility of lava flow textures. Textures are least obvious on unburned areas (light gray, top); an old burn is on the bottom of photograph; the latest burn (right middle, dark area), occurred a few months before the photograph was taken. Most of both burns were contained by jeep trails. Area of photograph is 3.5 km by 5.1 km. (U. S. Geological Survey Photograph GS SWEZ 1-244, October, 1971.)

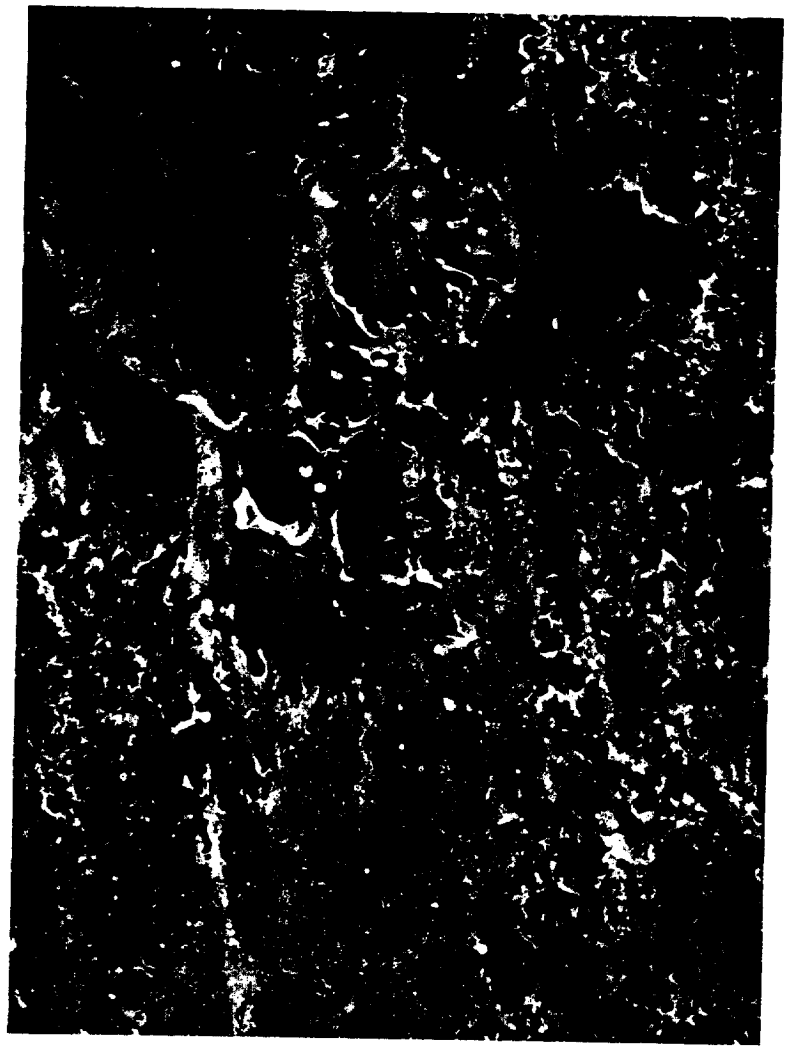

FIGURE 5-14. Vertical aerial photograph, 10 km north of Burley, showing streaks of wind-blown particles deposited on pahoehoe basalt flows. Area of photograph is about 2.5 km by 3.6 km. North is to the top (U. S. Geological Survey Photograph GS SWEZ 1-233, October, 1971.)

LEG 2

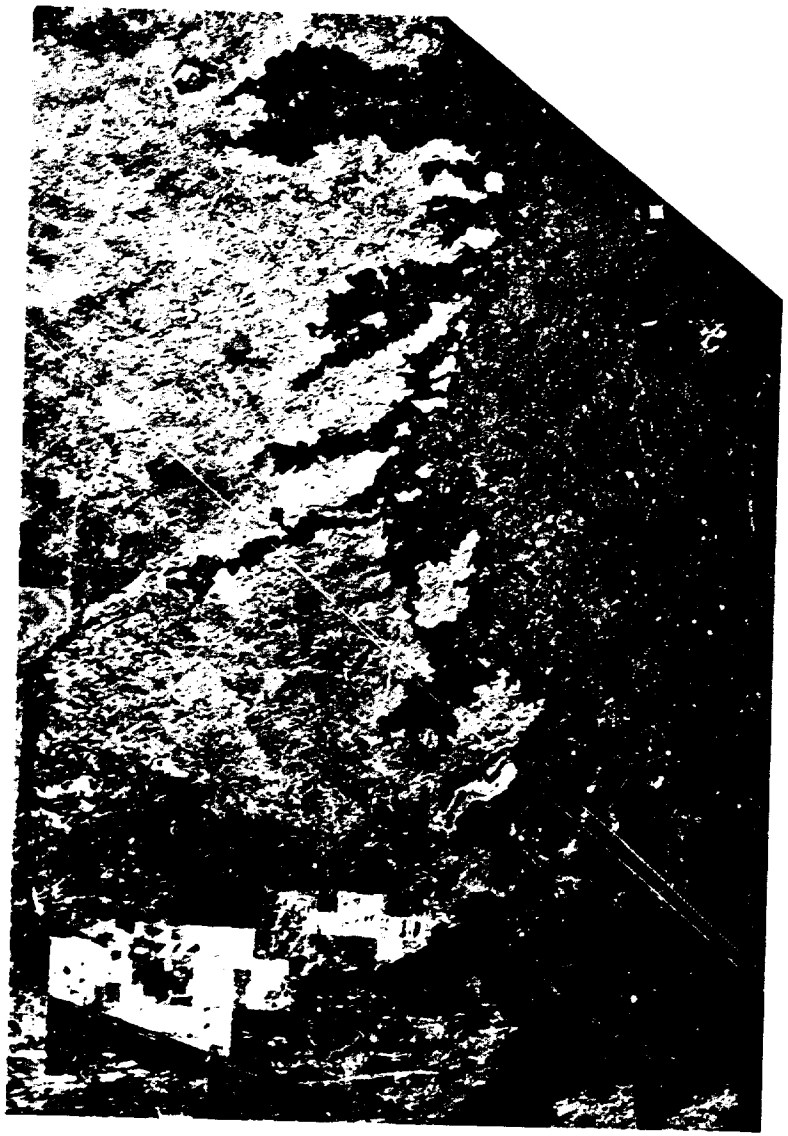

FIGURE 5-16. Oblique aerial view of Split Butte, a maar that contained an inner lava lake (see Chapter 12). (Photograph by Ronald Greeley, University of Santa Clara, July, 1971.)

FIGURE 5-15. High altitude (U-2 aircraft) photograph of the western edge of the Wapi Lava Field (dark area on the right), older flow (light gray), and Split Butte (crater at top of picture). Area of photograph 14.3 km by 18.5 km. (NASA-Ames Photograph 72-186, frame 5716, October, 1972.)

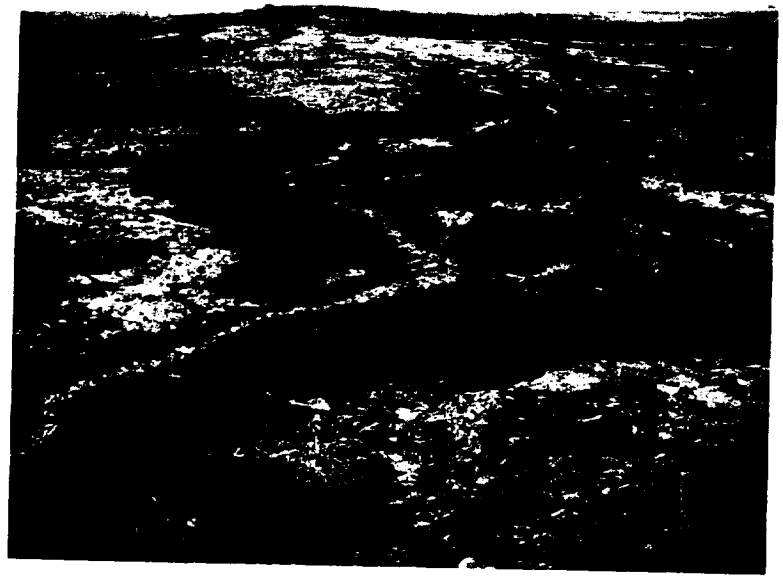

FIGURE 5-18. Oblique aerial view northward toward the summit of Pillar Butte (the knob on the horizon) on the Wapi lava field. Dark area is aa; light areas, including the sinuous channel down the middle of the aa flow, are composed of pahoehoe flows. (NASA-Ames Photograph by M. Lovas, 1970.)

FIGURE 5-17. Low oblique aerial photograph of a small cinder cone and crater that have been breached by Wapi lavas. (Photograph by Ronald Greeley, University of Santa Clara, July, 1971.)

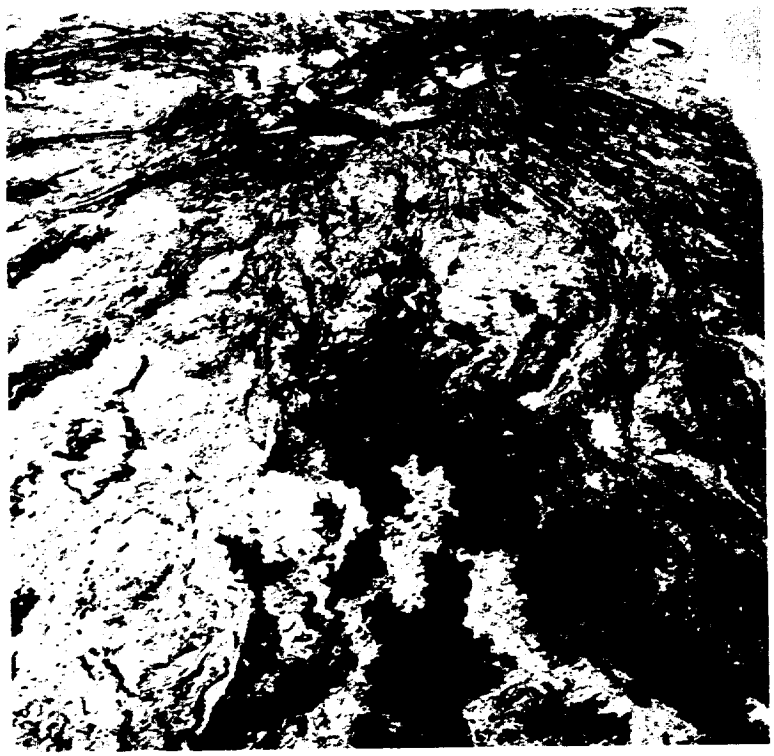

FIGURE 5-19. View northward toward Pillar Butte summit vents; numbers correspond to stations. Note the numerous lava channels near the summit; dark areas are aa flows, light areas are generally pahoehoe. Station 7 is the entrance to a small lava tube. (Photograph by Ronald Greeley, University of Santa Clara, June, 1977.)

FIGURE 5-20. Vertical aerial photograph of Pillar Butte area, the summit vent region of the Wapi low shield and Wapi Park (top of photograph), the vent region for an older, partly buried low shield. As is typical of the low shields in the Snake River Plain, the vent regions are steeper and frequently form kipukas, or unburied "islands" or, as here, a "peninsula" in younger flows. Area of photograph is 2.8 km by 4.2 km. (U. S Geological Survey Photograph GS SWEZ 1-182, August, 1971.)

FIGURE 5-21. Vertical aerial photograph of the King's Bowl lava field, which consists of multiple, fissure-fed flows. (U. S. Department of Agriculture photograph CYN 7B, August, 1946.)

FIGURE 5-22. Oblique aerial view southwestward across South Grotto, the southern end of the King's Bowl lava field, and spatter cones on the fissure; numbers mark perched lava lakes. (Photograph by Ronald Greeley, University of Santa Clara, June, 1977.)

FIGURE 5-23. Oblique aerial view southwestward of King's Bowl, a phreatic explosion crater on the main fissure. (Photograph by Ronald Greeley, University of Santa Clara, June, 1977.)

FIGURE 5-24. Oblique aerial view of Creon's Cave area, the north end of the King's Bowl lava field, showing numerous lava lakes (flat, light-toned areas). (Photograph by Ronald Greeley, University of Santa Clara, June, 1977.)

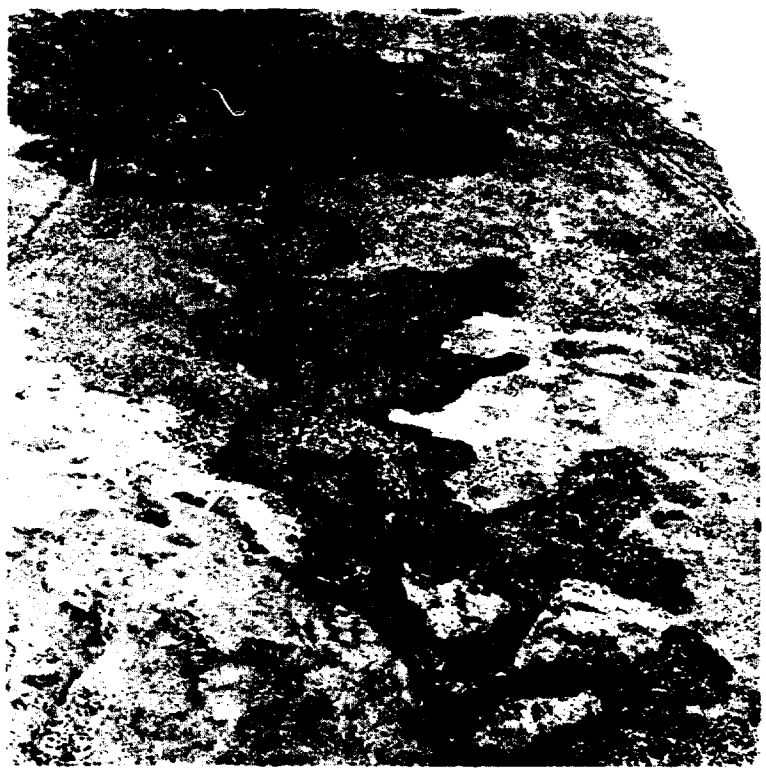

FIGURE 5-25. Low-altitude oblique aerial view southward of the north end of the King's Bowl lava field. (Photograph by Ronald Greeley, University of Santa Clara, June, 1977.)

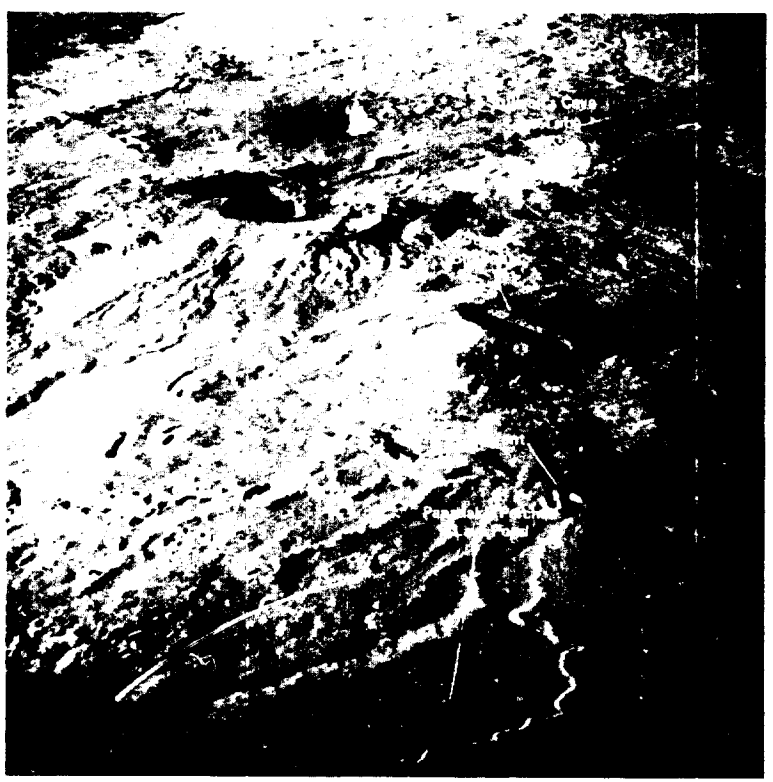

FIGURE 5-26. Low oblique aerial view northeastward across the Inferno Chasm Rift zone (from Greeley and King, 1975).

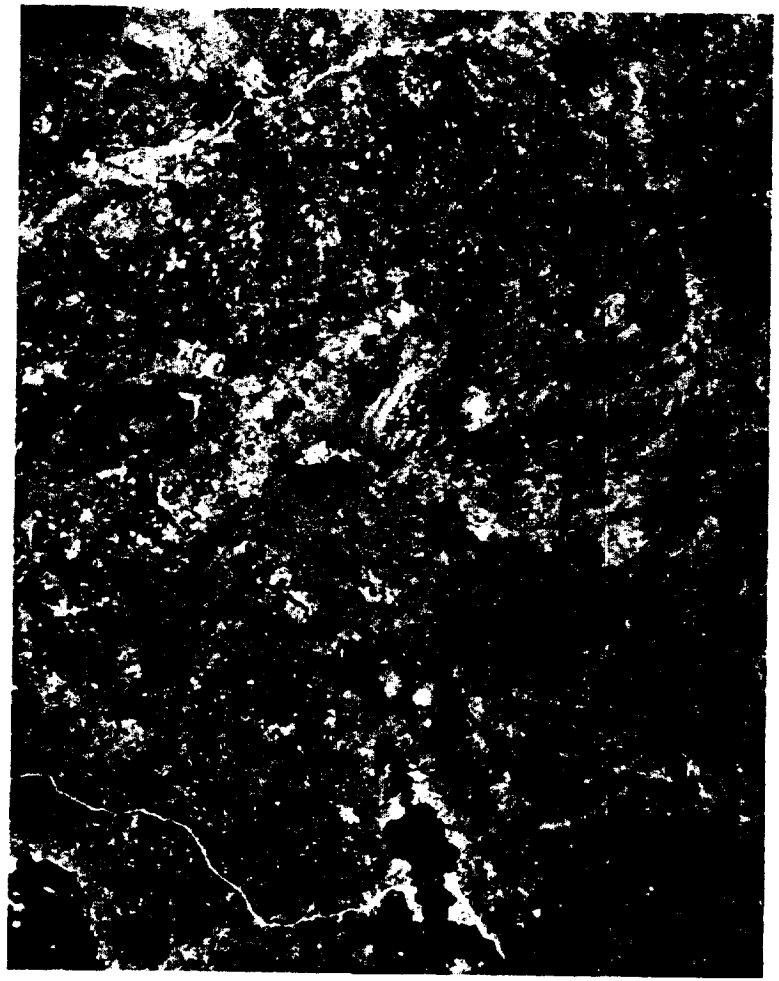

FIGURE 5-27. Vertical aerial photograph of the King's Bowl area (King's Bowl lava flow is in left middle part of picture), north along the Inferno Chasm rift zone (bottom), showing Inferno Chasm, Papadakis perched lava pond, Cottrell's Blowout, and Wildhorse Corral; part of the Bear Trap lava tube is visible in the upper right corner (arrow). Area of photograph is 6.6 km by 10.2 km. (U. S. Geological Survey Photograph GS-VCTZ, 2-190, August, 1971.)

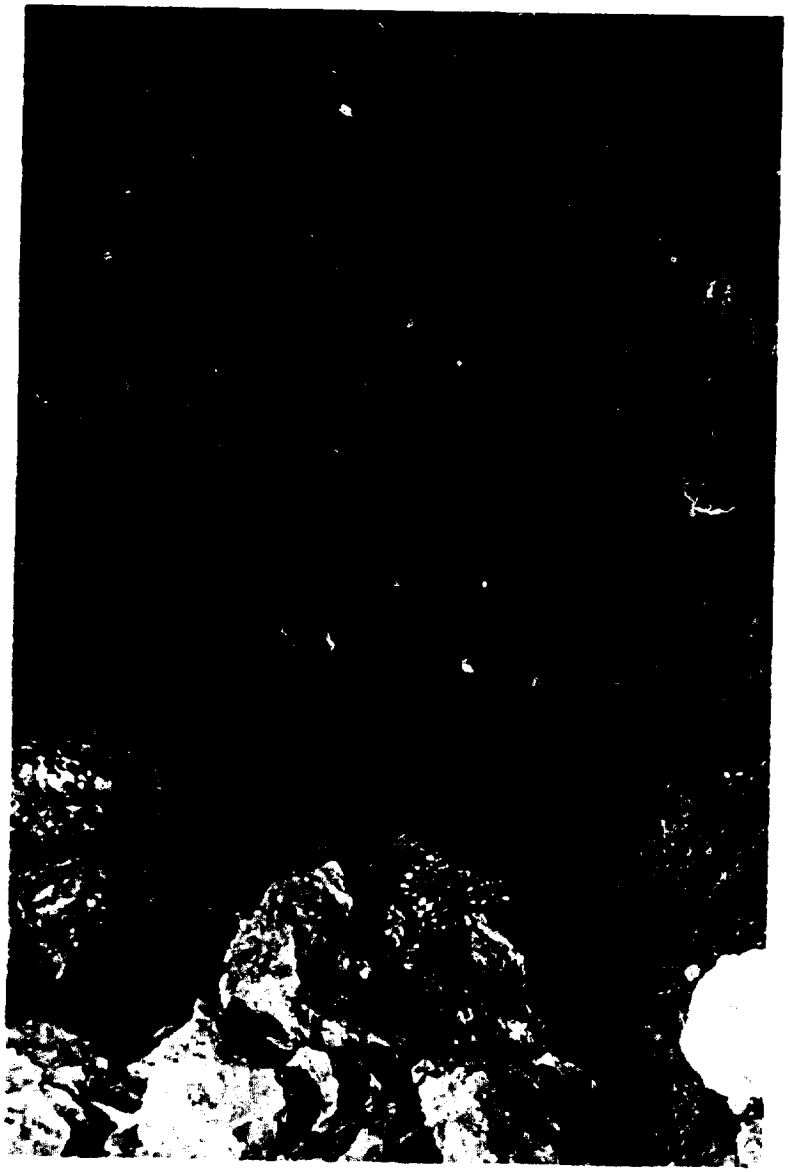

FIGURE 5-28. View of the interior of Sullivan's Cave, part of a lava tube on the southeast flank of Wildhorse Corral. Large blocks on the floor have collapsed from the ceiling. Figure in background is measuring height to the ceiling using a helium-filled balloon. (NASA-Ames Photograph by Mike Lovas, 1968.)

FIGURE 5-29. Oblique aerial view eastward across Inferno Chasm (illumination from the left). The circular vent toward the top of the photograph is about 175 m in diameter and 21 m deep. It is one of several vents that make up the Inferno Chasm rift. In addition to the principal flow channel, two other channels are visible on the south (right) flank of the crater. Cracks at the bottom of the photograph are part of the set of tensional fractures on the east side of the King's Bowl rift. (Photograph by Ronald Greeley, University of Santa Clara, 1970.)

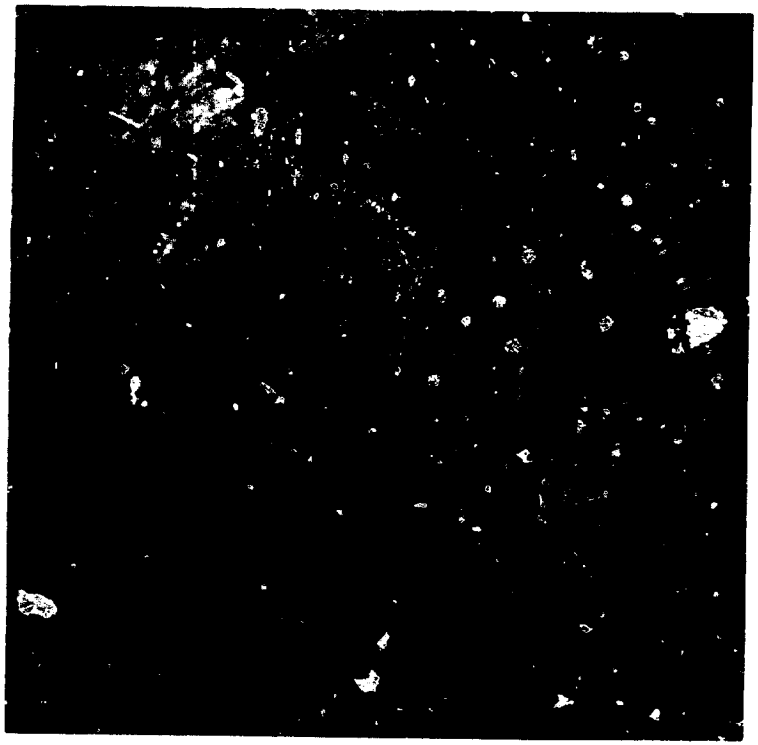

FIGURE 5-30. Oblique aerial view across Papadakis perched lava pond; flow fronts associated with the pond are at the bottom of photograph.

FIGURE 5-31. Landsat (ERTS) image of the Wapi lava field (lower right) and Craters of the Moon flows; Leg 3 begins near Bear Crater (1), continues along Bear Trap lava tube (2) to Split Butte (3) and ends at Craters of the Moon (4). Area of image is 110 km by 80 km.

LEG 3

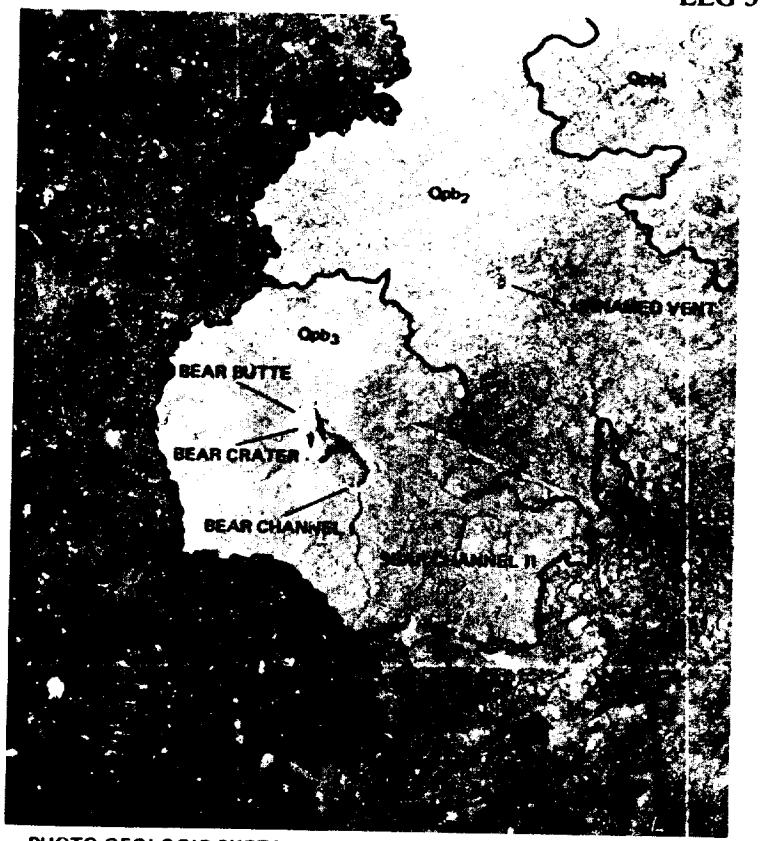

PHOTO-GEOLOGIC SKETCH MAP OF BEAR BUTTE SHIELD VOLCANO
R. GREELEY, 1972

0 1 2 3 4
km

QUATERNARY
- RECENT — Qrb — BASALT, MOSTLY PAHOEHOE; FROM CRATERS OF THE MOON
- PLEISTOCENE (?) — Qpb1 — BASALT, PAHOEHOE; POSSIBLY FROM FLOWS ASSOCIATED WITH THE IDAHO RIFT
- PLEISTOCENE (?) — Qpb2 — *BASALT, PAHOEHOE, ERUPTED FROM UNNAMED VENT
- PLEISTOCENE (?) — Qpb3 — *BASALT, PAHOEHOE OF THE BEAR BUTTE SHIELD VOLCANO

*MAY BE CONTEMPORANEOUS

*CONTACTS NOT FIELD CHECKED

FIGURE 5-32. Geological sketch map of Bear Butte.

FIGURE 5-33. Oblique aerial view of Bear Crater and associated lava channel. (Photograph by Mike Lovas, July, 1971.)

FIGURE 5-34. Low oblique aerial photograph of Bear Crater; crater is about 60 m deep. (Photograph by Ronald Greeley, University of Santa Clara, 1972.)

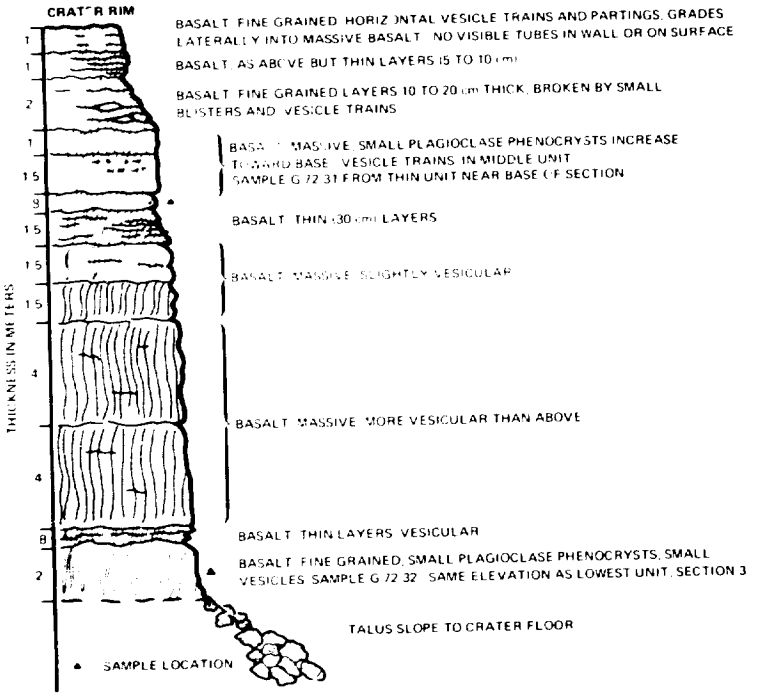

FIGURE 5-35. Measured section from the wall of Bear Crater, showing thin flow units typical of low shields on the Snake River Plain.

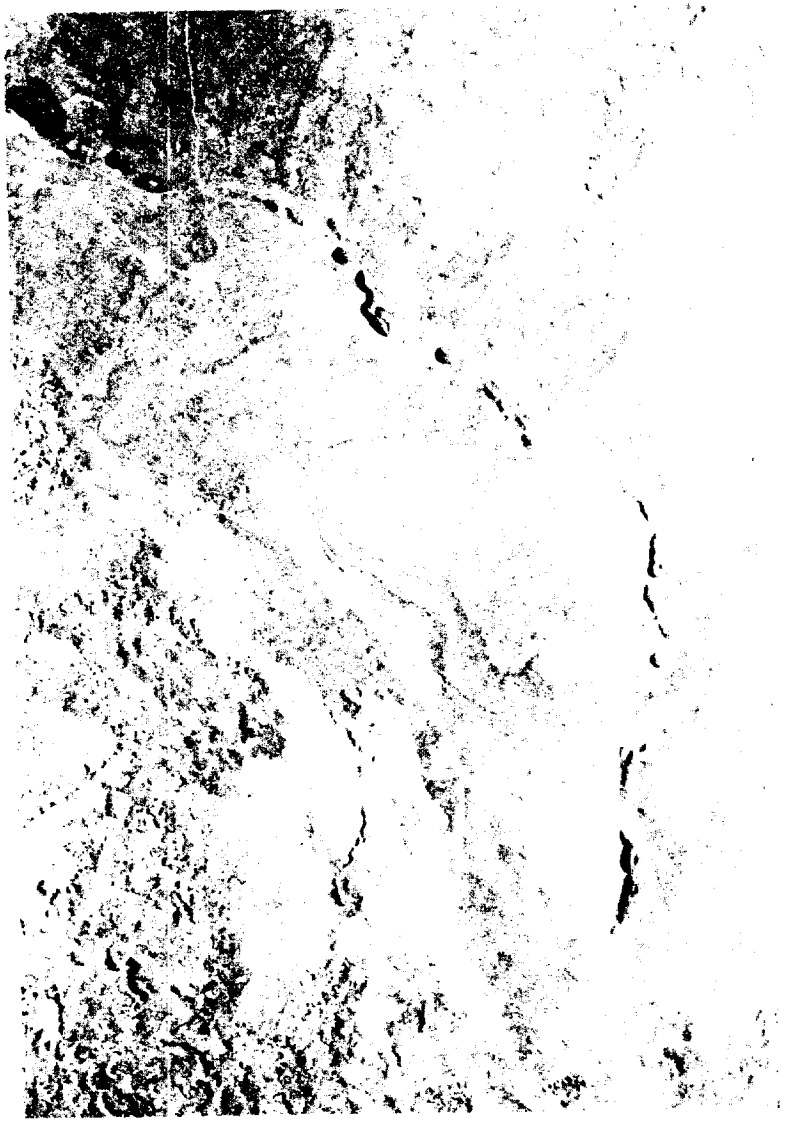

FIGURE 5-36. Vertical aerial photograph of the western end of Bear Trap lava tube; area of photograph 1.8 km by 2.7 km. (U. S. Geological Survey Photograph GS-SWEZ 8-19, October, 1971.)

FIGURE 5-37. Low-altitude oblique aerial view of Bear Trap lava tube showing collapsed portions and incipient fractures; road (upper right) indicates scale. (NASA-Ames Photograph by Ronald Greeley, 1969.)

FIGURE 5-38. Entrance to an uncollapsed segment of Bear Trap lava tube. (NASA-Ames Photograph by James Papadakis, 1969.)

FIGURE 5-39. Vertical aerial photograph of Sand Butte, southwest of Craters of the Moon National Monument. Area of photograph is 2.0 km by 3.0 km. (U. S. Geological Survey Photograph GS SWEZ 8-58, October, 1971.)

FIGURE 5-40. Low oblique aerial view northward of Sand Butte, a 900 m diameter maar crater formed on a fissure. Note the shallow moat formed between the maar tuff cone and the younger flows that encroach the flanks of the cone. (Photograph by Ronald Greeley, University of Santa Clara, 1972.)

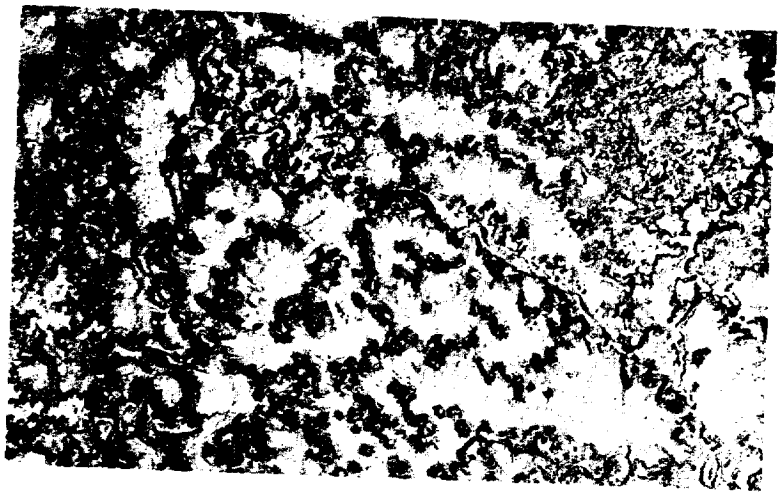

FIGURE 5-41. Aerial photograph of area 10 km SSE of Carey, showing variation in pahoehoe surface textures on the 1 to 5 m scale and circular collapse depressions. (North is to the right.) Area of photograph is 2.0 km by 1.3 km. (U. S. Geological Survey Photograph GS SWEZ 6-80, September, 1971.)

FIGURE 5-42. Vertical aerial photograph of Snowdrift Crater, the summit crater for a low shield southwest of Craters of the Moon National Monument. Area of photograph is 2 km by 2.8 km. (U.S. Geological Survey Photograph GS-SWEZ 9-194, November, 1971.)

FIGURE 5-43. Landsat (ERTS) view of area covered by Leg 4. After leaving Sand Butte (1), flight trends eastward toward the south end of the Great Rift in Craters of the Moon National Monument (toward 2), then follows the rift northwestward toward the monument headquarters (3); then leg ends near Big Southern Butte (just out of picture, near (4).

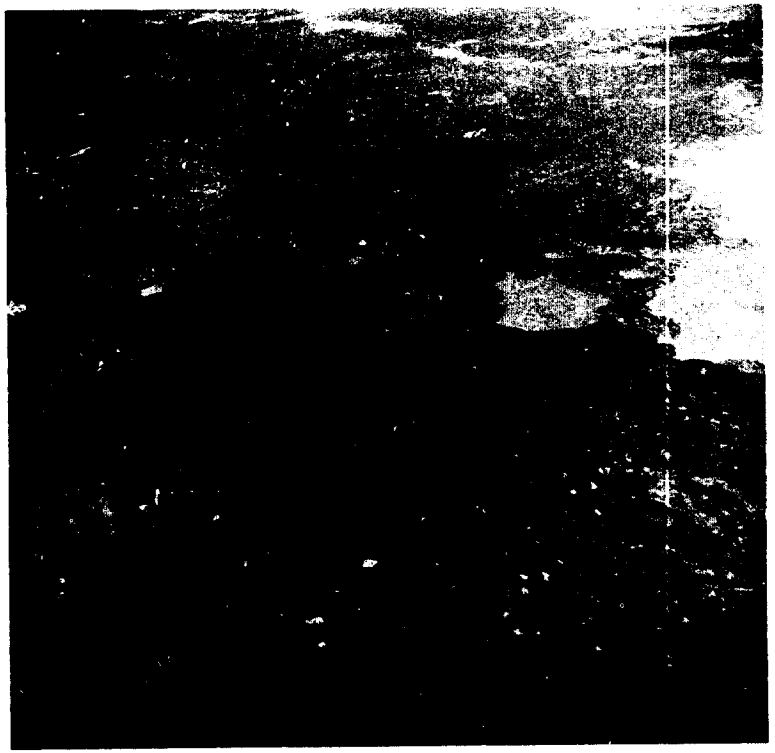

FIGURE 5-44. Low oblique aerial view of one of the main fissure-fed aa flows erupted from the Great Rift, Craters of the Moon National Monument. (NASA-Ames Photograph by Mike Lovas, 1969.)

FIGURE 5-45. Low oblique aerial view of aa flows (dark patches) and older pahoehoe flows, some of which contain pressure plateaus and collapse depressions; area is at the south end of Craters of the Moon National Monument. (NASA-Ames Photograph by Mike Lovas, 1969.)

FIGURE 5-46. Oblique aerial view of aa flow in Craters of the Moon National Monument. Trail crossing the end of the flow leads to the Cave Area. (Photograph by Ronald Greeley, University of Santa Clara, June, 1977.)

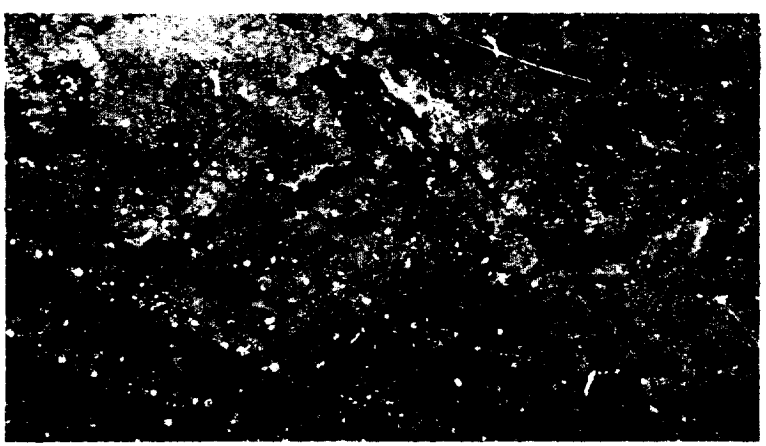

FIGURE 5-47. Vertical aerial photograph of the southern end of the Great Rift in Craters of the Moon National Monument, showing cinder and spatter cones on the fissure. Area of photograph is 3.9 km by 1.7 km. (U. S. Geological Survey Photograph GS SWEZ 3-50, September, 1971.)

FIGURE 5-48. Oblique aerial view of the Great Rift. (Photograph by Ronald Greeley, University of Santa Clara, June, 1977.)

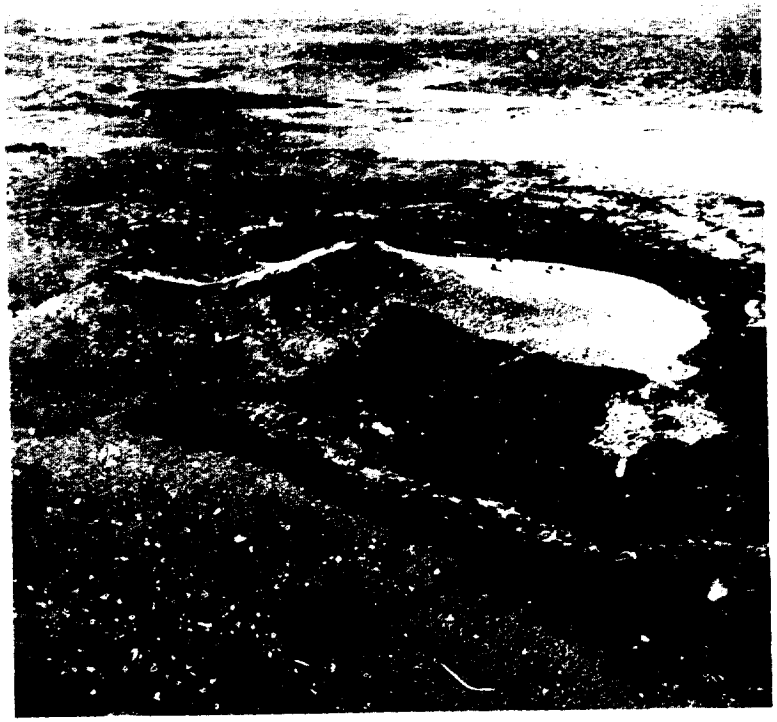

FIGURE 5-49. View northward along the Great Rift across Watchman cinder cone. (Photograph by Ronald Greeley, University of Santa Clara, June, 1977.)

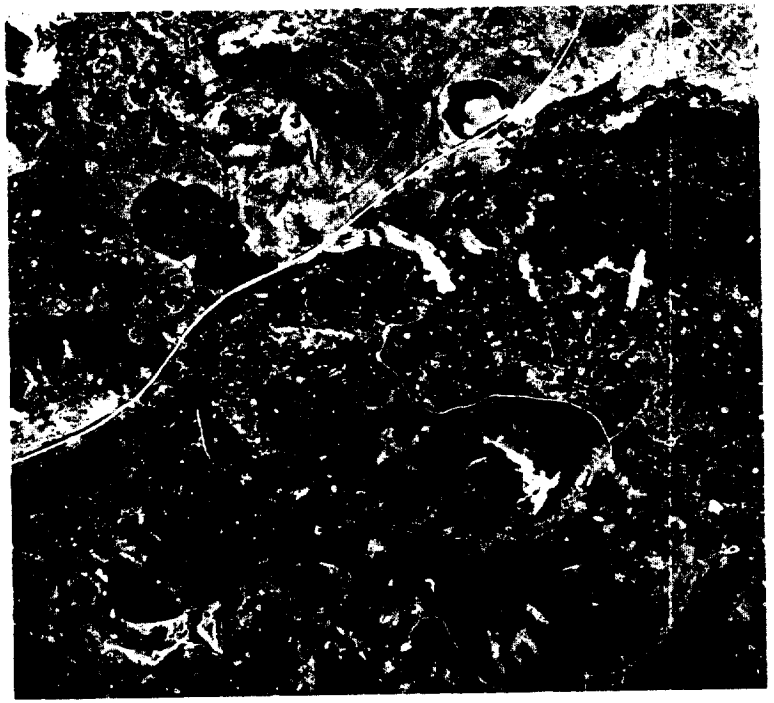

FIGURE 5-50. Vertical aerial photograph of the north end of Craters of the Moon National Monument: Visitor Center (1), Highway Flow (2), Sunset Cone (3), Grassy Cone (4), Big Craters (5), and North Crater (6).

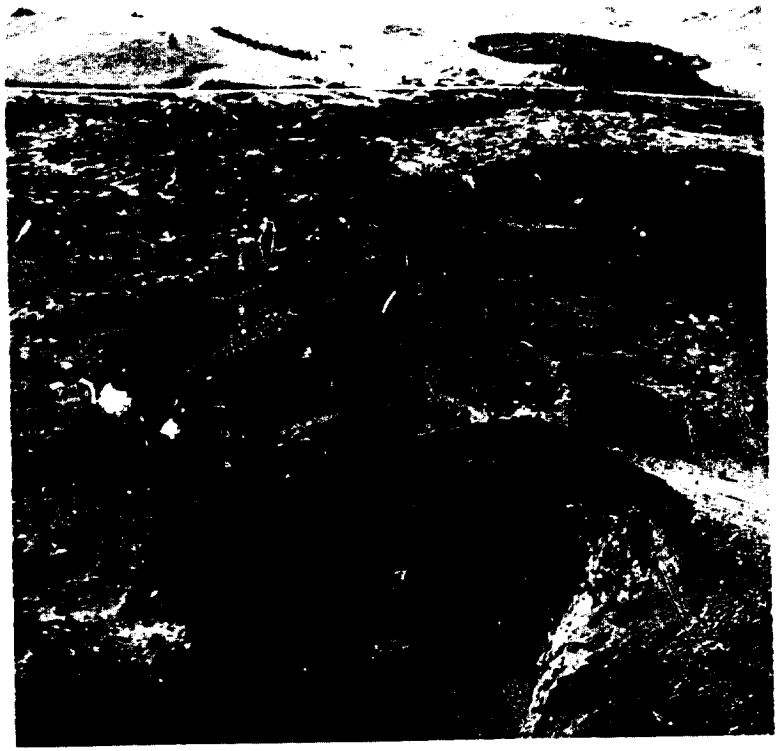

FIGURE 5-51. Low oblique aerial photograph northward across the Big Craters area cinder cones; Highway Flow is in upper right. (Photograph by Ronald Greeley, University of Santa Clara, June, 1977.)

FIGURE 5-52. Oblique aerial view of a flow in the Craters of the Moon area, showing transition from pahoehoe (light plate-like areas) to aa (dark areas). (Photograph by Ronald Greeley, University of Santa Clara, June, 1977.)

FIGURE 5-53. Aerial view of an unusual pahoehoe to aa transition. (Photograph by Ronald Greeley, University of Santa Clara, June, 1977.)

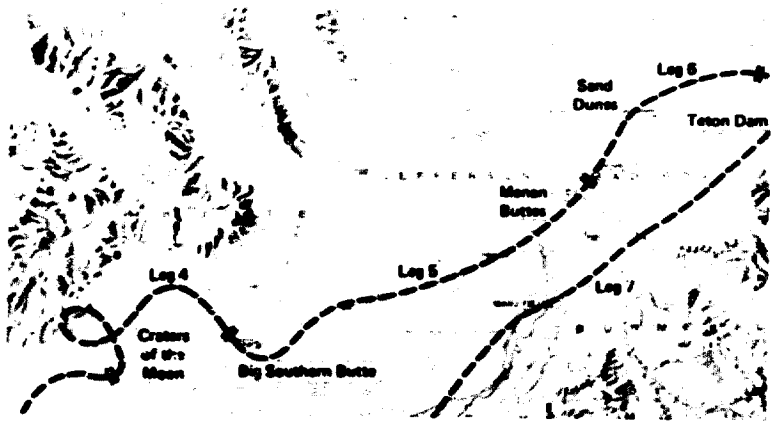

FIGURE 5-54. Index map of Leg 5.

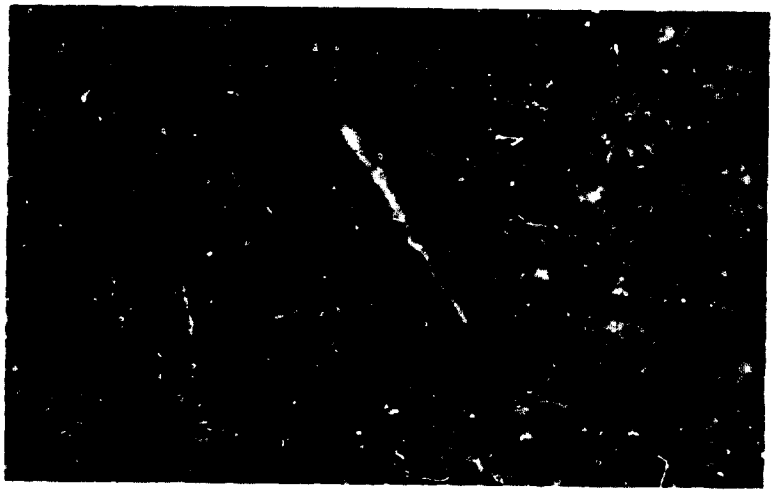

FIGURE 5-56. Vertical aerial photograph of a slot-shaped vent 24 km south southwest of the Big Southern Butte area; note the short channel that flows southwest of the vent. Area of photograph is 1.5 km by 1.0 km. (U. S. Geological Survey Photograph GS SWEZ 6-138, September, 1971.)

FIGURE 5-55. Low oblique aerial view of the northeast flank of Big Southern Butte and one of the linear vents of the Arco rift zone (Kuntz, 1977), identified by the row of spatter cones and basalt flows. White line in foreground is a jeep trail. (NASA-Ames Photograph by Ronald Greeley, May, 1969.)

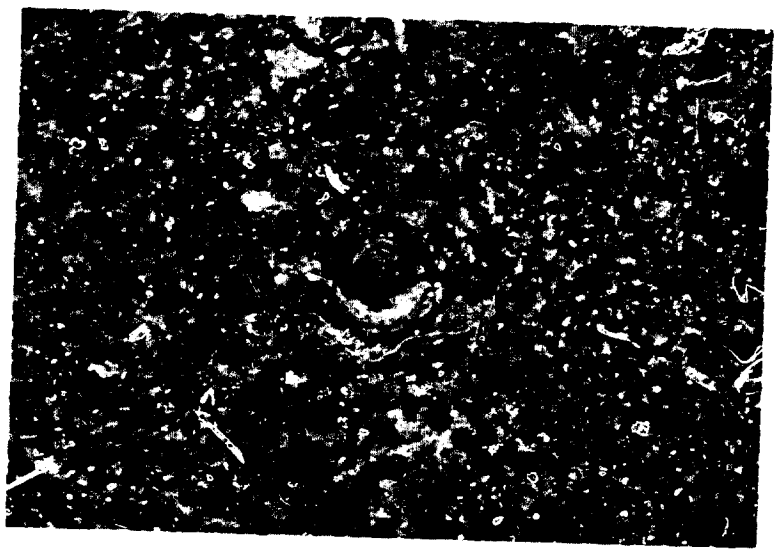

FIGURE 5-57. Vertical aerial photograph of China Cap, 270 m diameter cinder-and-tuff cone southeast of Big Southern Butte. Area of photograph is 2.0 km by 1.4 km. (U. S. Geological Survey Photograph GS SWEZ 6-40, September, 197 .)

FIGURE 5-58. Vent complex east of Cedar Butte and Big Southern Butte. The aligned vents north of the crater may be associated with a fissure or they may be rootless vents, perhaps associated with a lava tube. The dark area is a large pressure plateau. Area of photograph is 2.7 km by 3.6 km. North is to the top. (U. S. Department of Agriculture Photograph CXN-3R-209, September, 195 .)

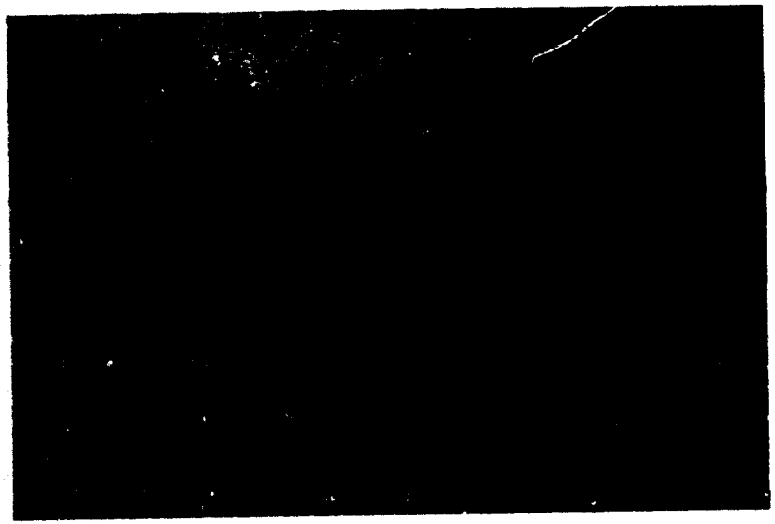

FIGURE 5-59. Part of pressure plateau shown in previous figure; note dimple-shaped crater. (Photograph by Ronald Greeley, University of Santa Clara, June, 1977.)

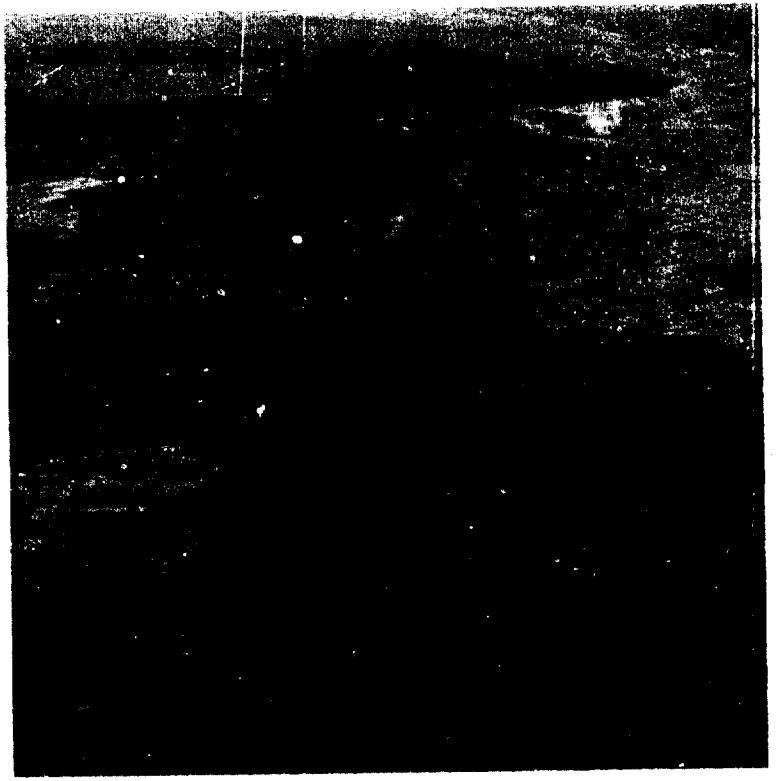

FIGURE 5-60. Oblique aerial view of a summit pit crater and partly collapsed lava tube, east of Cedar Butte (seen in background). (Photograph by Ronald Greeley, University of Santa Clara, June, 1977.)

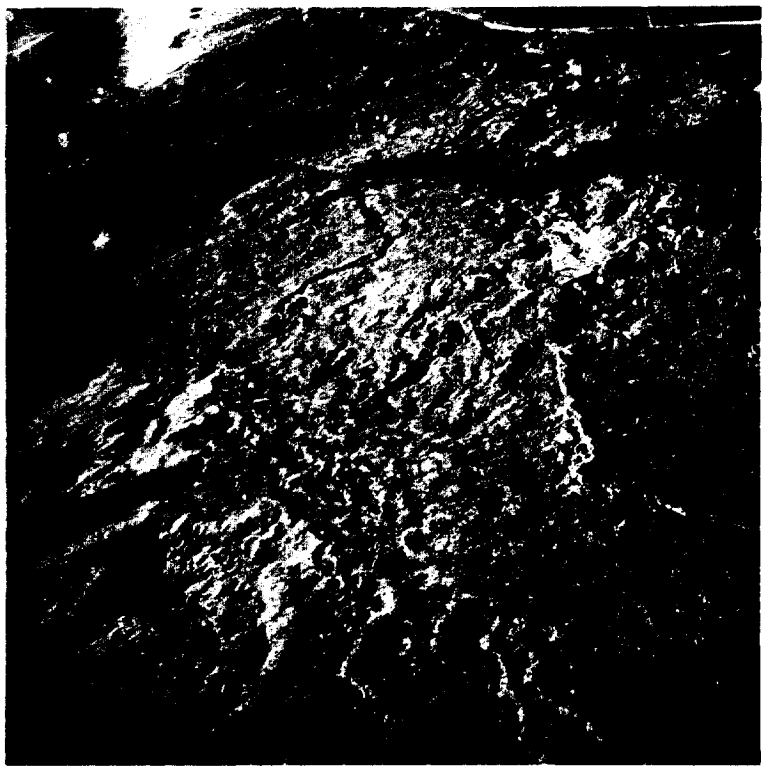

FIGURE 5-61. View of the lava tube system shown in Figure 5-60 and a pressure ridge-channel feature (right side of photograph). (NASA-Ames Photograph by Ronald Greeley, 1969.)

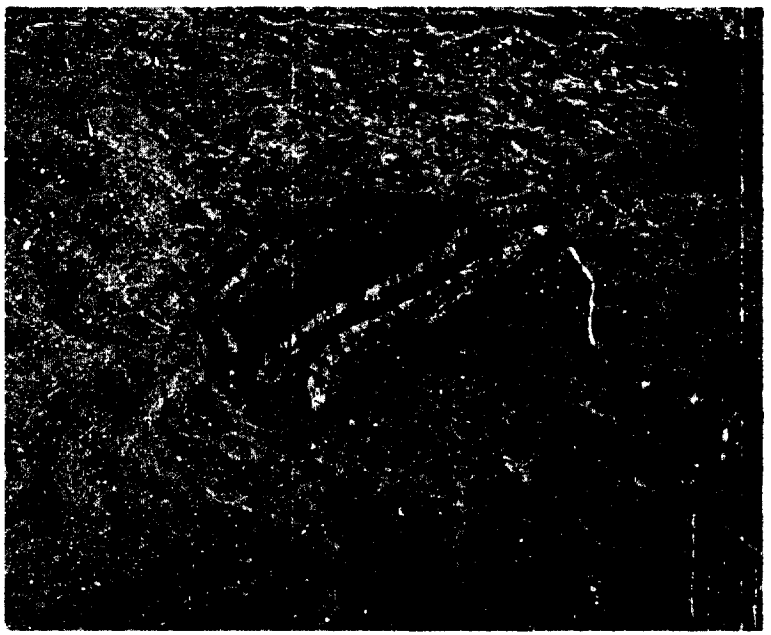

FIGURE 5-62. Pressure plateau several hundred meters long, east of Big Southern Butte. (Photograph by Ronald Greeley, University of Santa Clara, June, 1977.)

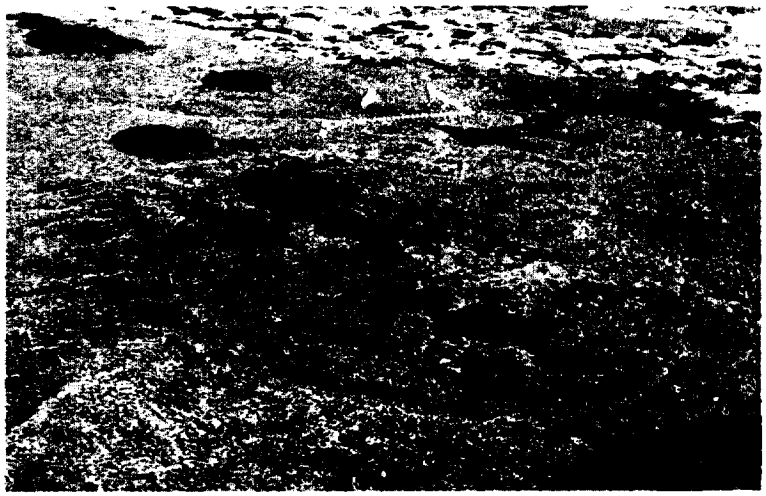

FIGURE 5-63. Low altitude oblique photograph of a chain of craters associated with a lava tube; note raised rim craters in upper left. (NASA-Ames Photograph by Mike Lovas, 1969.)

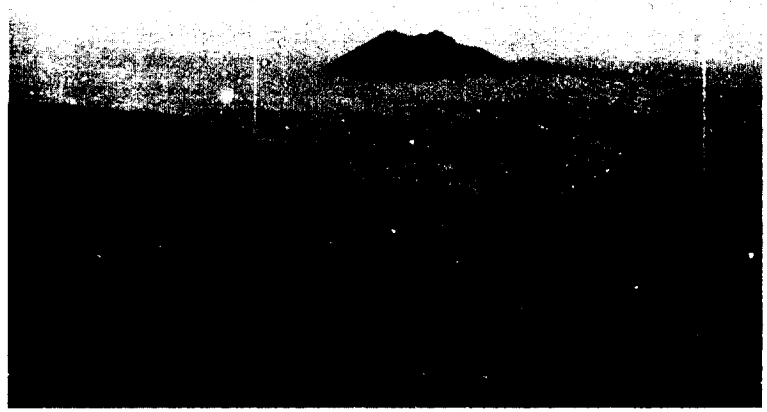

FIGURE 5-64. View northward toward East Butte, a 300 m high silicic dome volcano surrounded by basalt flows. Middle Butte is the dark mass on the left, a structurally uplifted block composed of basaltic lavas. The crater in middle of the view marks the summit vent for a small construct that appers to post-date the uplift of Middle Butte. (Photograph by Ronald Greeley, University of Santa Clara, June, 1972.)

LEG 5

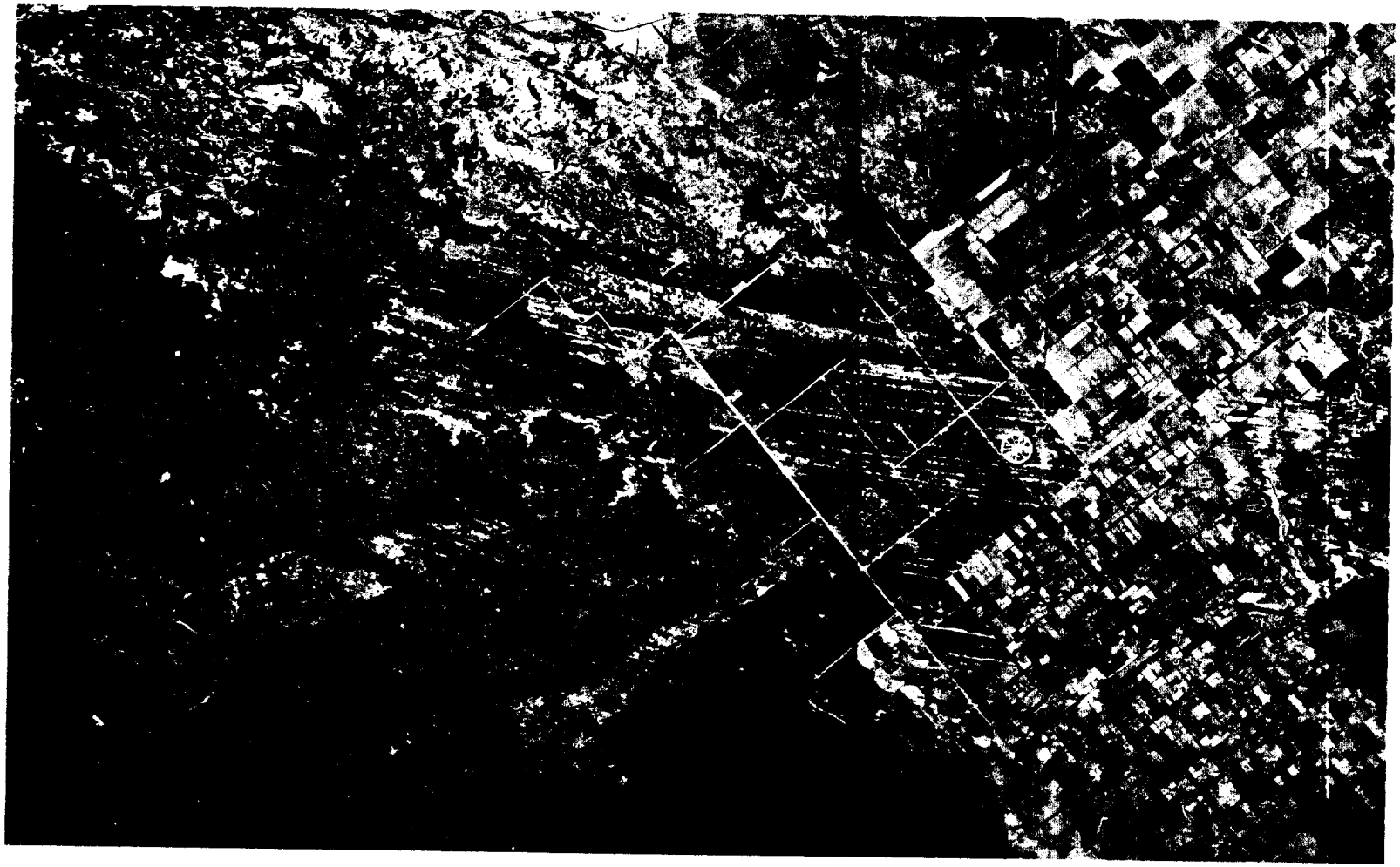

FIGURE 5-65. High altitude (U-2 aircraft) vertical photographs in the Circular Butte area, showing young lava flows and prominent aeolian streaks. Area of photographs is 36.1 km by 22.7 km. (NASA-Ames Photographs 72-186, frames 5741, 5743, October, 1972.)

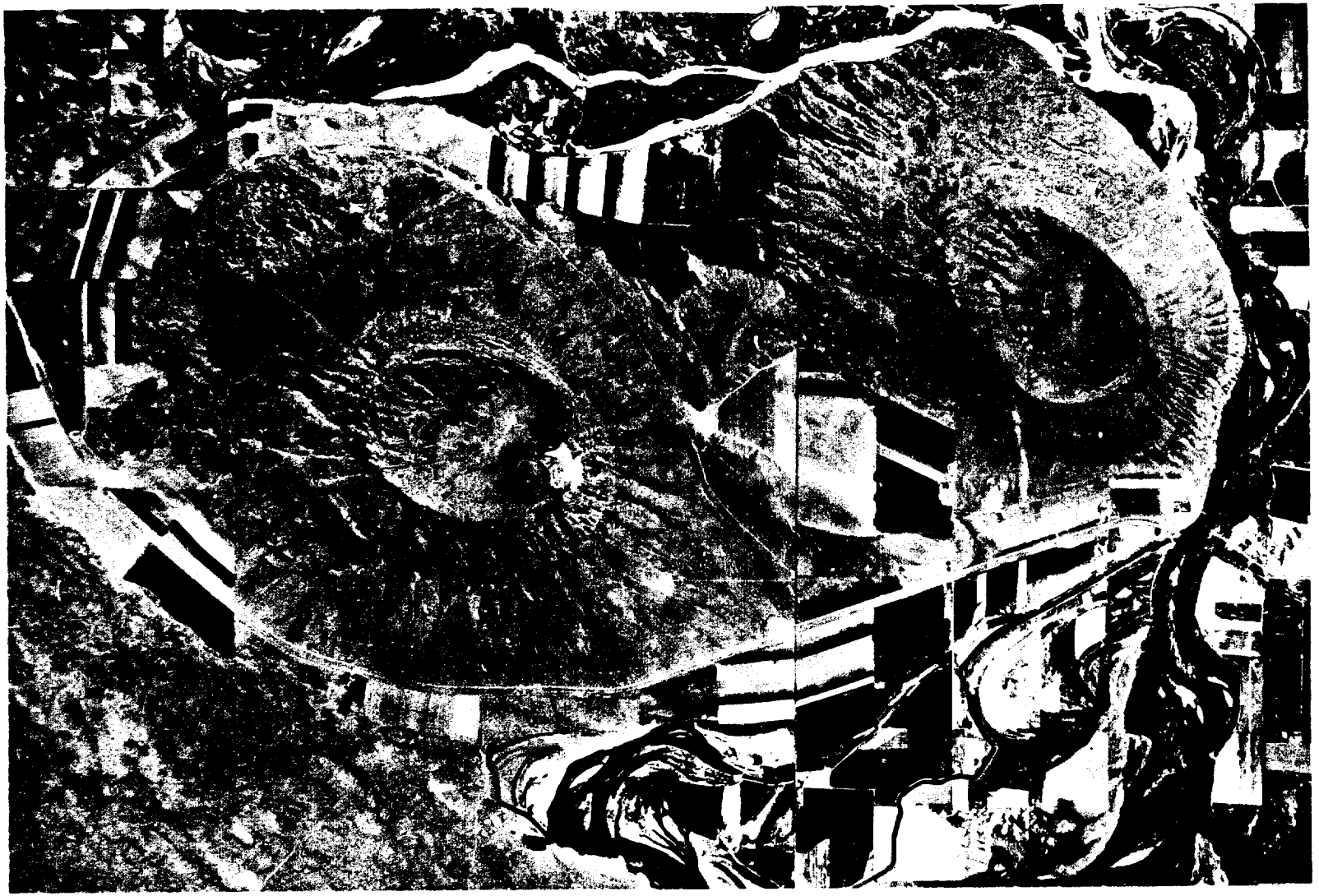

FIGURE 5-66. Vertical aerial view of Menan Buttes, "twin" cones on the Teton and Snake Rivers near Menan. The summit craters are about 900 m and 760 m across; these constructs stand about 150 m above the surrounding plain. (U.S. Department of Agriculture Photographs CXS-6AA-50 and 51, July, 1960.)

FIGURE 5-67. Oblique aerial view across Menan Buttes. (NASA-Ames Photograph by Mike Lovas, 1969.)

FIGURE 5-68. Mosaic of high-altitude (U-2 aircraft) photographs of sand dune field west of town of St. Anthony (arrow). Compare with map of Figure 5-69. Area of mosaic is 38 km by 24 km; north is to the upper right. (NASA-Ames Photographs 72-186, 5694-5696, October, 1971.)

LEG 6

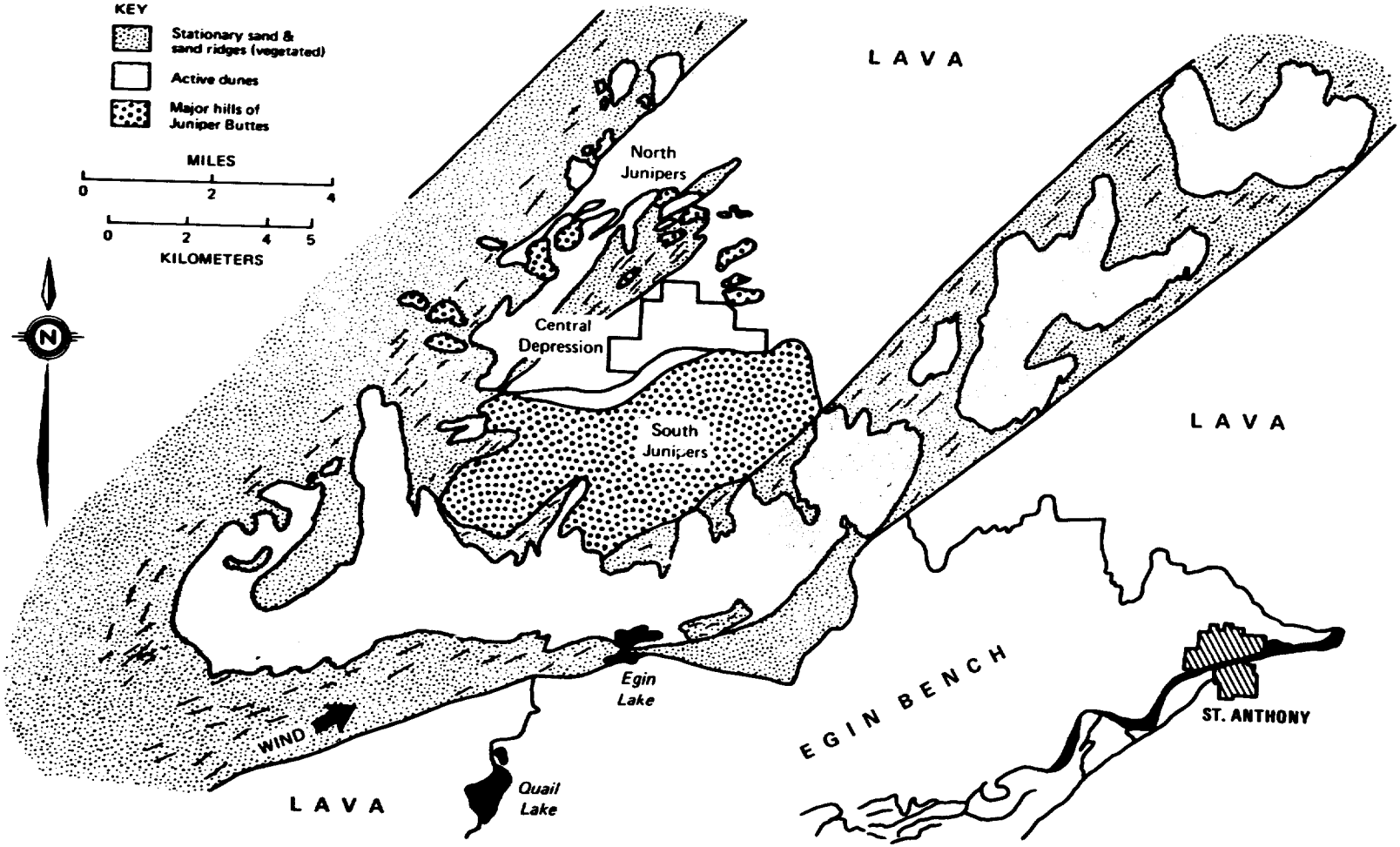

FIGURE 5-69. Sketch map showing major dune fields and their relation to Juniper Buttes (after Koscielniak, 1973).

FIGURE 5-70. Vertical aerial photograph of "lobate," or imbricating dunes at North Junipers. Area of photograph is about 4.3 km by 3.4 km. (U.S. Department of Agriculture Photograph CXR-11AA-33, 34, June, 1960.)

FIGURE 5-71. Oblique aerial view of dunes shown in Figure 5-70. (Photograph by Ronald Greeley, University of Santa Clara, 1972.)

FIGURE 5-72. High oblique view eastward toward Juniper Buttes and a field of parabolic dunes migrating northeastward. Note the trailing "tails" of the dunes that have been stabilized by vegetation. Jeep trail in foreground indicates scale. (Photograph by Ronald Greeley, University of Santa Clara, June, 1972.)

FIGURE 5-73. Oblique aerial view of the southeast side of the "climbing dunes," St. Anthony dune field. Although the prevailing direction of dune migration is toward the northeast (toward the upper right), notice that the slip face along the dune crests indicates a wind from the northeast; 180° reversals in wind direction are common in the Snake River Plain after a storm. (Photograph by Ronald Greeley, University of Santa Clara, July, 1971.)

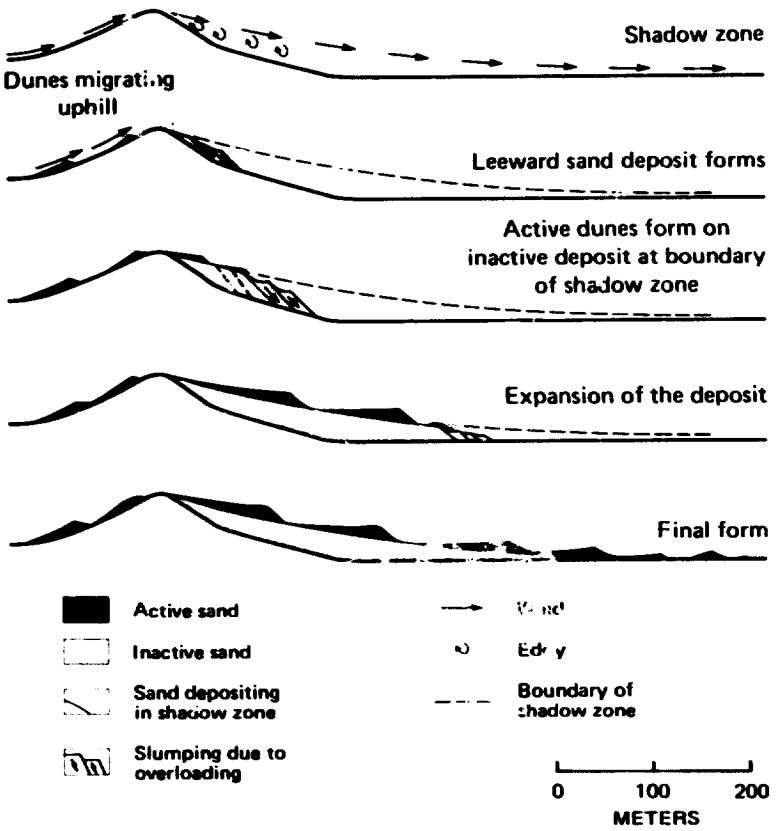

FIGURE 5-74. Sequential diagram showing development of overlapping dunes at Juniper Buttes (after Koscielniak, 1973).

FIGURE 5-75. View southward across two dune elements of the "climbing" dunes of Juniper Buttes, where the dunes have crossed the volcano complex. (Photograph by Ronald Greeley, University of Santa Clara, July, 1971.)

FIGURE 5-76. Oblique aerial view of part of the "climbing" dunes at Juniper Buttes; migration direction is toward the viewer. Note the imbricating arrangement of dunes within the complex. (Photograph by Ronald Greeley, University of Santa Clara, July, 1971.)

FIGURE 5-77. View northeastward across "dune crater" (arrows define crater rim), a small pit crater formed in basalt. The crater has been overrun by an active parabolic dune complex that has left "tails" of sand draped across the crater. Dune migration is northwestward (toward the upper left). The active dune field is visible as the white zone on the left side of the photograph. The small mountain in the right background is a Tertiary silicic volcanic complex. (Photograph by Ronald Greeley, University of Santa Clara, 1973.)

FIGURE 5-78. Low altitude oblique view of active parabolic (or "hairpin") dunes; direction of migration is northward (toward the upper right). (Photograph by Ronald Greeley, University of Santa Clara, July, 1971.)

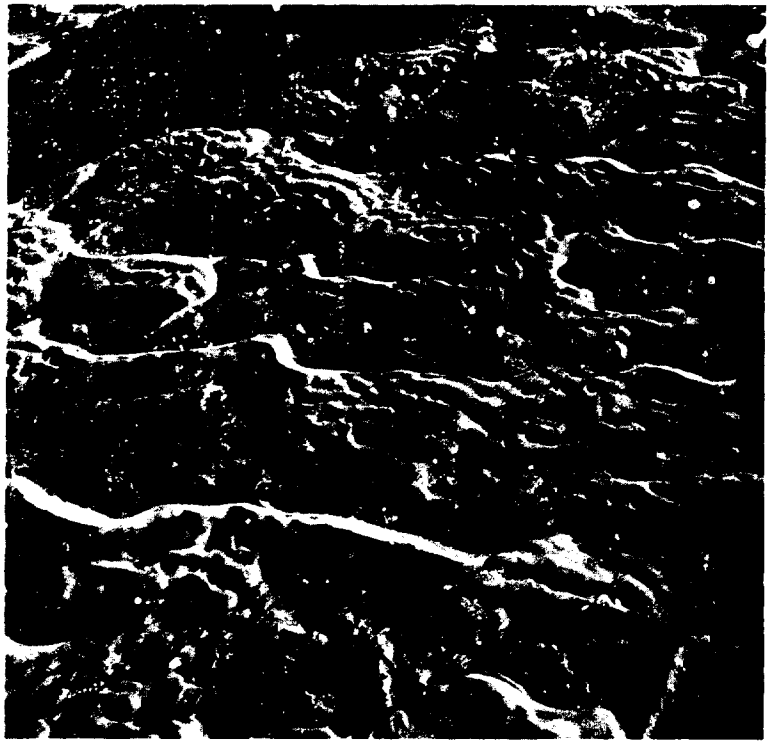

FIGURE 5-79. Low altitude oblique view of transverse dunes in the St. Anthony field, where the field migrated across a basalt flow; a basalt pressure ridge is marked with an arrow. (Photograph by Ronald Greeley, University of Santa Clara, July, 1971.)

FIGURE 5-80. Low altitude oblique view of an interdune area within the St. Anthony dune field. The surface over which the dunes are passing is a fresh basalt flow; the flow texture is rough aa with local relief up to 4 m. (Photograph by Ronald Greeley, University of Santa Clara, July, 1971.)

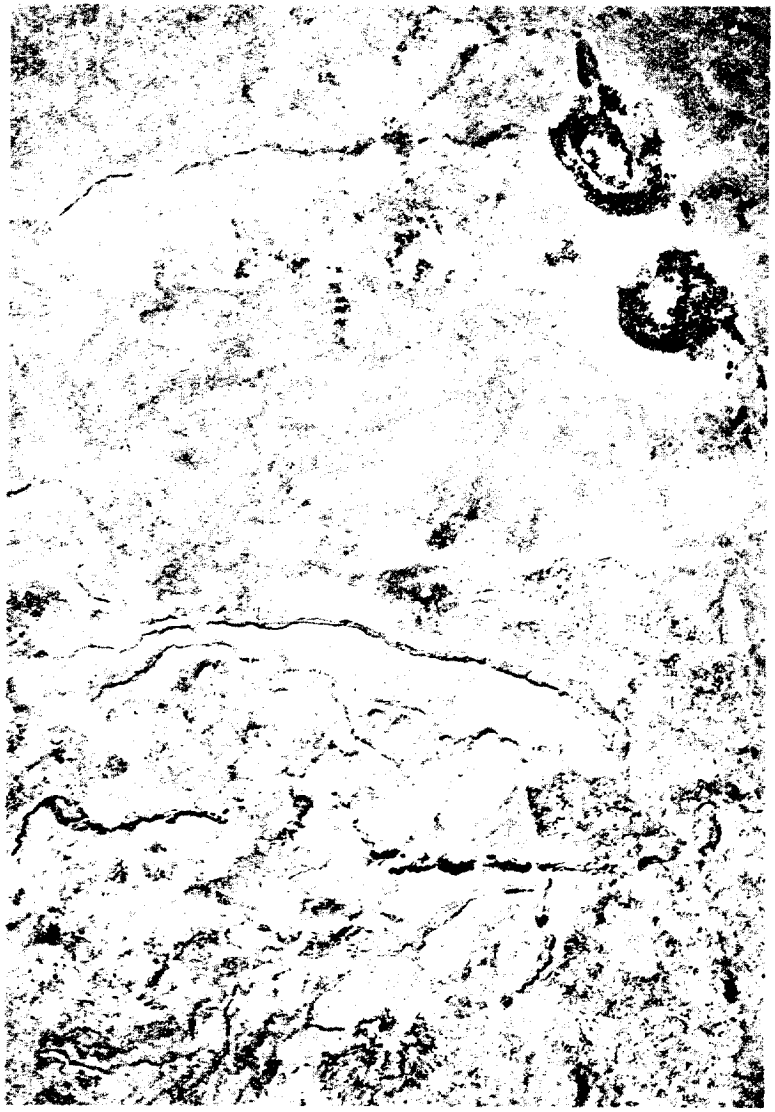

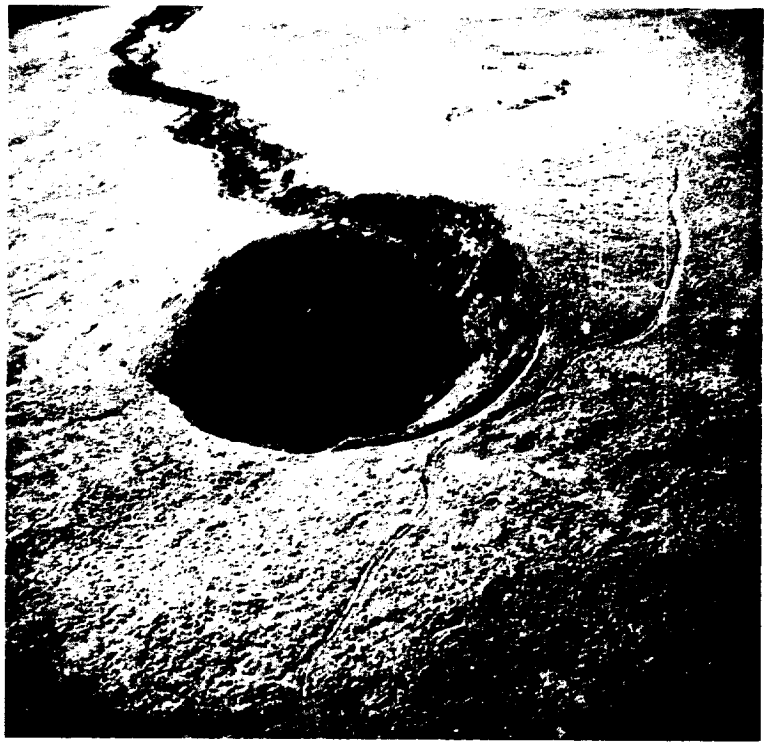

FIGURE 5-82. Low oblique aerial view of pit crater and collapsed lava tube shown in previous figure. (Photograph by Ronald Greeley, University of Santa Clara, 1971.)

FIGURE 5-81. Vertical aerial photograph of "The Junipers," twin pit craters about 35 km north northwest of St. Anthony; the northern most (top) pit crater has a collapsed lava tube associated with it (trends west). The lower part of the photograph shows a partly collapsed lava tube system and a large lava channel. Area of photograph is 2.3 km by 3.4 km. (U. S. Department of Agriculture Photograph CXR-11AA-88, June, 1960.)

FIGURE 5-83. Vertical aerial photograph of a pit crater and lava tube–lava channel. Note the numerous cut-off branches and parallel lava tubes along the main structure. Area of photograph 2.8 km by 4.6 km. (U. S. Department of Agriculture Photographs CXR-8AA-106, 108, June, 1960.)

FIGURE 5-84. Leg 7 extends from the sand dune fields and lava flows west of St. Anthony (1) to the airport at Pocatello (2). Main features of interest include the boundary of the Snake River Plain and the mountains to the southeast, channels, oxbow lakes, and other features related to the Snake River, and Hell's Half Acre lava field (3) (see Chapter 7).

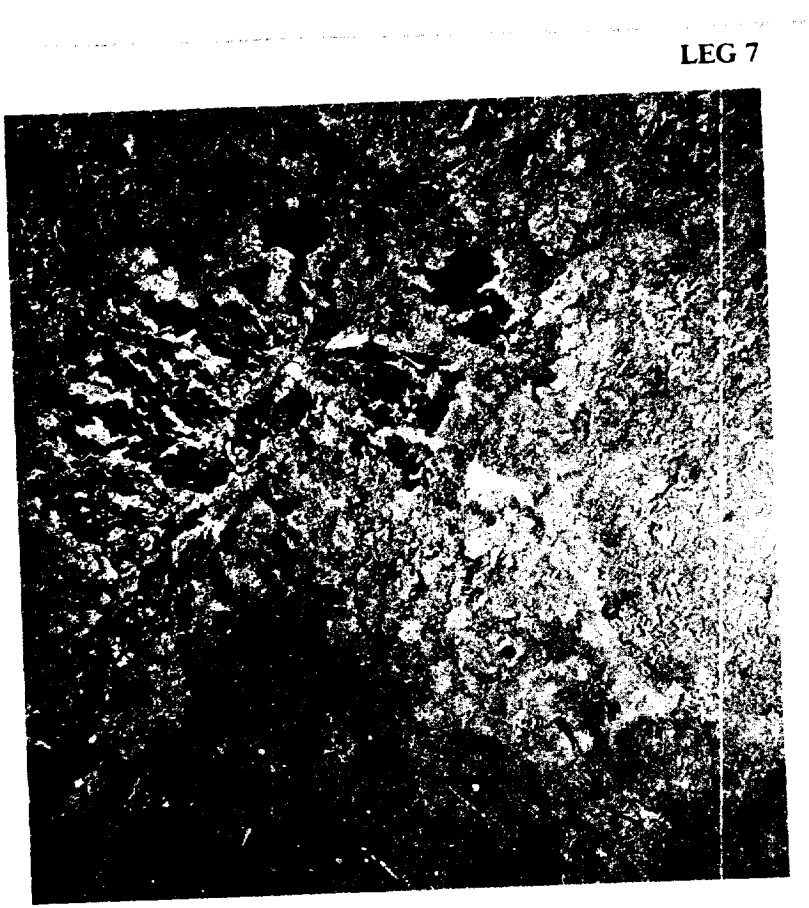

FIGURE 5-85. Vertical aerial photograph of the summit region of Hell's Half Acre lava field, southwest of Idaho Falls. (U. S. Geological Survey Photograph GS-SWEZ 7-77, October, 1971.)

6. BIG SOUTHERN, MIDDLE, AND EAST BUTTES

Dallas B. Spear
Department of Geological Sciences
State University of New York at Buffalo
Amherst, New York 14226

6. BIG SOUTHERN, MIDDLE, AND EAST BUTTES

Dallas B. Spear
Department of Geological Sciences
State University of New York at Buffalo
Amherst, New York 14226

Three conspicuous buttes rise above the relatively flat accumulations of Plio-Pleistocene and younger basaltic flows of the eastern Snake River Plain between Arco and the Idaho Falls–Blackfoot areas (Fig. 6-1). These prominent landmarks, known as Big Southern, Middle, and East Buttes in their order from southwest to northeast, can be seen from distances of 150 km or more.

Big Southern Butte, the largest of the three, rises 760 m above the surrounding plain. It has a diameter of 8 km at its base and is somewhat elongated in a northwest-southeast direction. Middle Butte, located 19 km east-northeast of Big Southern, is 1.6 km in diameter and 335 m high. East Butte is situated 3 km east of Middle Butte, has a diameter of 3.4 km at its base, and rises 300 m above the surrounding basaltic flows. Big Southern Butte and East Butte are rhyolitic domes whereas Middle Butte is an upraised block of stratified basalt.

The origin of the buttes has long been an enigma. Russell (1902) was the first geologist to visit the buttes and offer an interpretation. He believed Big Southern and East Buttes to be steptoes, ancient rhyolitic volcanoes surrounded by a sea of basalt. He recognized Middle Butte as a fault block, but offered no further comments concerning its significance. Stearns and others (1938) suggested that East and Middle Buttes represent fault blocks of older rock uplifted and eroded. Subsequent eruptions of basalt left the two buttes as steptoes.

Schoen (1974) interpreted the silicic buttes to be relatively young rock emplaced as viscous plugs and domes. He

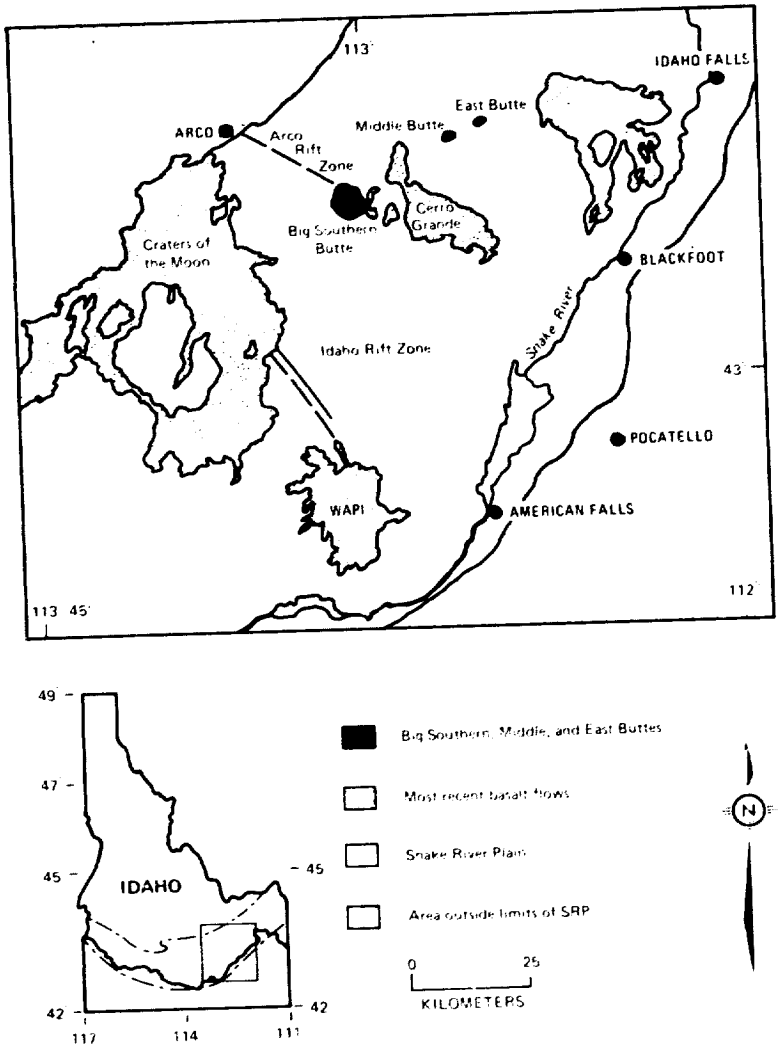

FIGURE 6-1. Central Snake River Plain showing relation of Big Southern Butte, Middle Butte, and East Butte to other features on the plain.

cites evidence from well logs, gravity and resistivity studies, and K-Ar dating to support his interpretation. He believed the source of the silicic magma to be remobilized rhyolitic basement.

Armstrong and others (1975) report K-Ar dates of .30± .02 MY and .6 ± .01 MY for Big Southern and East Buttes respectively. They state that Middle Butte could not be dated precisely because of contamination with atmospheric argon but is still relatively young (1.9 ± 1.2 MY). Schoen (1974) and Armstrong and others (1975) suspect that the basalt of Middle Butte was pushed up by a younger, still concealed rhyolitic dome.

The chronological development presented above has been drawn from reports dealing with regional geology. The authors of those reports undoubtedly were struck by the unique problem these prominent buttes present but did not conduct detailed studies of the buttes. Therefore, an investigation was initiated in 1976 to study the geology of the buttes and the surrounding area, and to establish both petrologically and structurally, the relationship of Big Southern Butte, Middle Butte, and East Butte to the basaltic flows which comprise the surrounding area. The objective of this paper is to present some observations made during, and subsequent to, a brief field season in 1976; it is not meant to be a final report on the area.

BIG SOUTHERN BUTTE

Preliminary mapping has shown that Big Southern Butte consists of two coalescing cumulo domes, each which may have had more than one intrusive center (Figs. 6-2, 6-3, 6-4). The division into two domes is based on overall morphology and characteristic differences in respective rock types. The domes are aligned along a N 45 W trend with the southeasterly dome having formed first. The relative ages of the two domes are inferred from unconformable relationships of respective rock types exposed in a roadcut near the top of the butte.

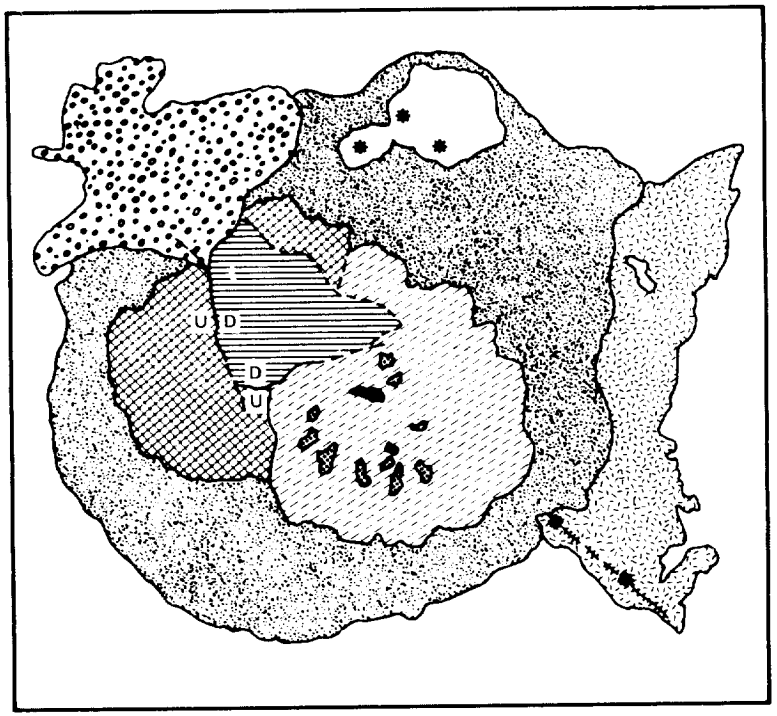

FIGURE 6-2. Geologic sketch map of Big Southern Butte.

FIGURE 6-3. High oblique aerial view southeast along the Arco rift zone (Kuntz, 1977) toward Big Southern Butte, a 760 m-high silicic plug volcano surrounded by basalt flows. Arrows mark linear vent systems of the rift zone. (NASA-Ames photograph by Ronald Greeley, May, 1969.)

FIGURE 6-4. High altitude vertical aerial photograph of Big Southern Butte; North Robbers flow is on the east flank (right side) of the Butte. (Army Map Service frame 4417; 1953).

The first-formed dome is characterized by lavender-gray spherulitic, lithoidal rhyolite grading to a light gray rhyolite in the upper parts of the section. Flow banding is common. The rock is composed of microcrystalline quartz and alkali feldspar intergrowths. Small (less than 1 mm) phenocrysts of quartz are very rare. Mafic minerals are also rare; magnetite is present as small equant grains (less than 0.1 mm) and a dark green clinopyroxene is a very rare component. Devitrification spherulites are abundant and show some chloritization.

Numerous and varied breccias are found on the slopes of Big Southern Butte in association with the first-formed dome. Most are interpreted to be crumble breccias based on criteria summarized by Parsons (1969). Crumble breccias form as a dome expands and grows and appear as non-sorted, non-bedded angular clasts in a fine-grained matrix. Average sizes of the clasts in the breccias at Big Southern Butte vary

from one outcrop to another but generally are 5 to 10 cm; clasts range in size from less than 1 cm to over 1 m.

In addition to the breccias, banded spherulitic obsidian, light dirty-gray pumice, and a honey-brown glassy welded tuff are found associated with the first-formed dome. The obsidian is relatively widespread in occurrence but limited in outcrop. It is interpreted to represent the rapidly cooled upper margin of the dome. The pumice and the glassy welded tuff are minor rock types but might suggest some vent activity.

It is believed that the development of the first-formed dome was primarily by internal expansion. Attitudes of flow banding generally document flow outward from the center of the dome. Also the distribution of crumble breccias supports a gradually expanding dome.

The younger dome of Big Southern Butte does not show the variability in outcrop as is seen in the older dome. It is composed of a white massive rhyolite, mineralogically similar to the other dome but lacking the abundant spherulites. There is only minor flow banding and breccias are not common. In general the younger dome is very homogeneous in appearance, although some upper portions of the rhyolite are hydrothermally altered with small intricate caverns and patterns formed by solution and wind. A few small basaltic inclusions, presumably torn from the conduit during the ascent of the rhyolite to the surface, are found at one outcrop on the northwestern slope.

Unlike the first-formed dome, a crater may be central to the younger dome. This interpretation is based entirely on morphology. Ascending the road which enters from the north side, one passes through a narrow section which in turn opens up into a large amphitheater about 800 m across. Whether or not this is the vestige of a crater or an erosional feature is yet to be determined. Two thin (10 to 20 cm) ash layers intercalated with nonsorted, poorly consolidated breccias (vulcanian breccias?) overlie the massive white rhyolite and require that a vent was active late in the evolution of Big Southern Butte.

A large section of basalt (at least 300 m) covers most of the northern slope of Big Southern Butte. The section dips uniformly 45°N 45°E. The basalt was pushed up and tilted during the development of the rhyolite domes and therefore is older. A fault, or series of faults, separates the basalt from the rhyolite.

The lower part of the section is extremely altered; some parts are very hard and brittle while others will crumble when struck by a hammer. Presumably migration of magmatic fluids and exsolving gases released during the intrusion of the rhyolite is responsible for the alteration. No mineralization was observed.

Unaltered basalt is found about halfway up the section, but the transition from altered to unaltered basalt was not observed due to scree-covered slopes. Stearns and others (1938) interpreted some of the basalt to be younger than the rhyolite, originating from a cinder cone (?) within the amphitheater of the younger dome. However, as a working hypothesis, this author believes all of the basalt on Big Southern to be older than the rhyolite. The basis for this hypothesis is the uniformity of thickness and dips of the basalt layers from one outcrop to another, the absence of any observable flow lobes, and the lack of clear correlation between the basalt and the possible cinder cone. Hamilton (1965) reports to have observed interlayering of basalt and rhyolite within the basalt section, but at the time of this writing that part of the section had not been visited. A clear understanding of the relationship between the basalt and the rhyolite of Big Southern Butte is very important to understanding its development and history and much work remains to be done in order to unravel that relationship.

EAST BUTTE

East Butte apparently has a simpler history than Big Southern. It is interpreted to be a single cumulo dome (Figs. 6-5, 6-6a) without any evidence for a crater. Attitudes of flow banding indicate flow away from the center in all directions. Breccias were not observed. Inclusions of basaltic and rhyolitic fragments are present in numerous outcrops.

The rock types of East Butte contrast sharply with those of Big Southern Butte. Large (2 to 5 mm) phenocrysts of sanidine, quartz, and minor plagioclase occur in a fine-grained to glassy matrix. Dark greenish-brown clinopyroxene is also present as small phenocrysts. Although megascopically there may be two or three lithologic varieties, mineralogically they are similar, differing primarily in the amount of glass in their matrix.

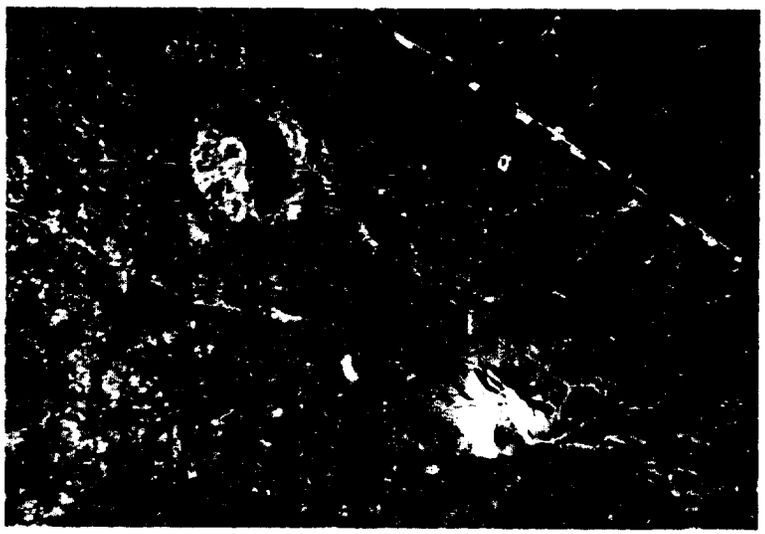

FIGURE 6-5. High altitude (U-2) vertical aerial photograph of Middle Butte (upper left and East Butte (lower right). (NASA-Ames Photograph 72-186, frame 5720; October 1972.)

FIGURE 6-6a. Stereoscopic pair of aerial photographs (turn page 90° for viewing) of East Butte. (U. S. Geological Survey photograph GS-SWEZ 7-83, 84; October, 1971).

MIDDLE BUTTE

Middle Butte is composed entirely of stratified basalt (Figs. 6-6b) that dips about 10° to the south. Although detailed sections have not been described, samples were collected from the scree which mantles the northern side. In thin section the basalt resembles other Snake River Plain basalts containing abundant feldspar, olivine, clinopyroxene, opaques, and interstitial brown glass. Calcite fills vesicles and has replaced some of the glass.

The mechanism responsible for elevating relatively young basalts to form Middle Butte is thought to be the intrusion of viscous silicic magma. Schoen (1974) reports that gravity data can be interpreted to support an hypothesis of rocks with a density less than that of the capping basalt beneath Middle Butte. The fact that Big Southern and East Buttes are silicic domes favors this hypothesis.

STRUCTURAL SETTING OF THE BUTTES

Two fundamental questions arise concerning Big Southern, Middle, and East Buttes: Are the rhyolitic domes genetically related to the Snake River Plain olivine tholeiites? What structural process(es) control their localization? Discussion of the first question will be deferred until a later date after chemical and petrographic data have been evaluated. The question of structural control can only be approached at present by offering some observations which seem to be relevant.

There are two factors which appear to play an important role in the structural control of the domes. One is the presence of rift zones which are normal to the plain (see Prinz, 1970; Greeley and King, 1975). These zones are tensional features characterized by open fractures and lineaments along which many volcanic eruptions can be correlated, particularly some of the most recent. It is generally believed that Basin and Range structural elements, which are thought to underlie the Snake River Plain, may be the controlling

FIGURE 6-6b. Stereoscopic pair of aerial photographs (turn page 90° for viewing) of Middle Butte. (U. S. Geological Survey photograph GS-SWEZ 7-85, 86; October, 1971).

influence of the rift zones (Schoen, 1974). Big Southern Butte lies near the southern end of the Arco Rift Zone (Kuntz, 1977) and is elongated in the direction of the trend of the rift. However, East and Middle Buttes do not lie on any observed lineaments which trend normal to the plain.

The other factor which seems to be important is that the buttes lie along the axis of the Snake River Plain. A well-defined topographic high also coincides with the axis. Karlo and King (1976) identified a broad northeast-southwest trending fracture zone north of the Hell's Half Acre lava field, along which a concentration of vents occur. Moreover, a well-defined lineament can be seen on aerial photographs, trending east-northeast from East Butte. Whether or not fracture trends can be extended along the entire axis of the plain remains to be seen. They are not readily observable in aerial photographs around Big Southern Butte but other factors may be obscuring the fractures. Some workers are not convinced that a major northeast-southwest set of fractures exist and that the lineaments of that orientation are aeolian features (Malde, 1971). Detailed analysis of aerial photographs and field verification will be necessary before it can be firmly stated whether or not a northeast-southwest fracture set exists.

It is too early to offer a model for the evolution of the area under discussion. At present, the interpretation of Schoen (1974) is considered a good working hypothesis.

Acknowledgements

I wish to thank Drs. John S. King, Steven S. Oriel, and Mel A. Kuntz for assistance during this research project. Field support for 1976 was provided by NASA Grant NGR 33-014-108. Topographic maps were supplied by the U. S. Geological Survey.

REFERENCES

Armstrong, R. L., W. P. Leeman, and H. E. Malde, 1975. K-Ar dating, Quaternary and Neogene volcanic rocks of the Snake River Plain, Idaho: American Jour. Sci., v. 275, p. 225-251.

Greeley, R. and J. S. King, 1975. Rift zones in the south-central Snake River Plain, Idaho: Geol. Soc. America, abs. with programs (Rocky Mountain Section), v. 7.

Hamilton, W. C., 1965. Geology and petrogenesis of the Island Park caldera of rhyolite and basalt eastern Idaho: U. S. Geol. Survey Prof. Paper 504–C, 37 p.

Karlo, J. F. and J. S. King, 1976. The dependence of topography on volcanic processes within the eastern Snake River Plain, Idaho: NASA TM X-3364, p. 138-140.

Kuntz, M. A., 1977. Extensional faulting and volcanism along the Arco Rift Zone, eastern Snake River Plain, Idaho: Geol. Soc. Amer., Abs. with Programs (Rocky Mountain Section), vol. 9.

Malde, H. E., 1971. Geologic investigation of faulting near the National Reactor Testing Station, Idaho: U. S. Geol. Survey Open File Report, 167 p.

Parsons, W. H., 1969. Criteria for the recognition of volcanic breccias: Review: Geol. Soc. America Mem. 115, p. 263-304.

Prinz, M., 1970. Idaho Rift System, Snake River Plain, Idaho: Geol. Soc. America Bull., v. 81, p. 941-948.

Russell, I. C., 1902. Geology and water resources of the Snake River Plains of Idaho: U. S. Geol. Survey Bull. 199, 192 p.

Schoen, R., 1974. III. Geology, in J. B. Robertson, R. Schoen, and J. T. Barraclough, Influence of liquid waste disposal on the geochemistry of water at the National Reactor Testing Station, Idaho: U. S. Geol. Survey Open File Report, IDO 22053, 231 p.

Stearns, H. T., L. Crandall, and W. G. Steward, 1938. Geology and groundwater resources of the Snake River Plains in south-eastern Idaho: U. S. Geol. Survey Water Supply Paper 774, 268 p.

7. GEOLOGY OF THE HELL'S HALF ACRE LAVA FIELD

John Karlo
Department of Geology
Central Michigan University
Mount Pleasant, Michigan 48859

7. GEOLOGY OF THE HELL'S HALF ACRE LAVA FIELD

John Karlo
Department of Geology
Central Michigan University
Mount Pleasant, Michigan 48859

In most discussions of Snake River Plain volcanism, the Craters of the Moon volcanic field is preeminent as it is the largest and best known feature within the province. Stearns and others (1938), however, noted that it is only one of several "rift zones" within the Snake River Plain. The objective of this paper is to show diversity of Snake River Plain volcanism by summarizing the geology of the Hell's Half Acre lava field which is dissimilar to the Craters of the Moon lava field and is probably more typical of most of the constructs that constitute the plain.

The Hell's Half Acre lava field is one of several very fresh, large-volume basalt flows of the eastern Snake River Plain. It is located southwest of Idaho Falls and covers approximately 400 sq. km (Fig. 7-1). On the ground, as well as from the air (Fig. 7-2), it is a prominent landmark. Interstate Highway 15 crosses the flow between Idaho Falls and Blackfoot (geologic observation turnoffs are provided on both sides of the highway); U. S. Highway 26 cuts through the southern tip of the field in a roadcut approximately 10 km northwest of Blackfoot, and U. S. Highway 20 skirts around the northern edge of Hell's Half Acre, making its closest approach at 20 Mile Rock approximately 32 km west of Idaho Falls.

It is expected that when Hell's Half Acre is adequately dated, it will be found to be quite young. The surface of the flow shows very little sign of weathering and is almost devoid of aeolian sediment that covers older Snake River Plain flows. Junipers growing on the flow have been dated by tree ring counts that give a minimum age for the flow of approximately 1660 years b.p. (Stearns and others, 1938); a preliminary date for charred material from beneath the Hell's Half Acre flow is 4100 ± 200 years b.p. (Kuntz, personal communication).

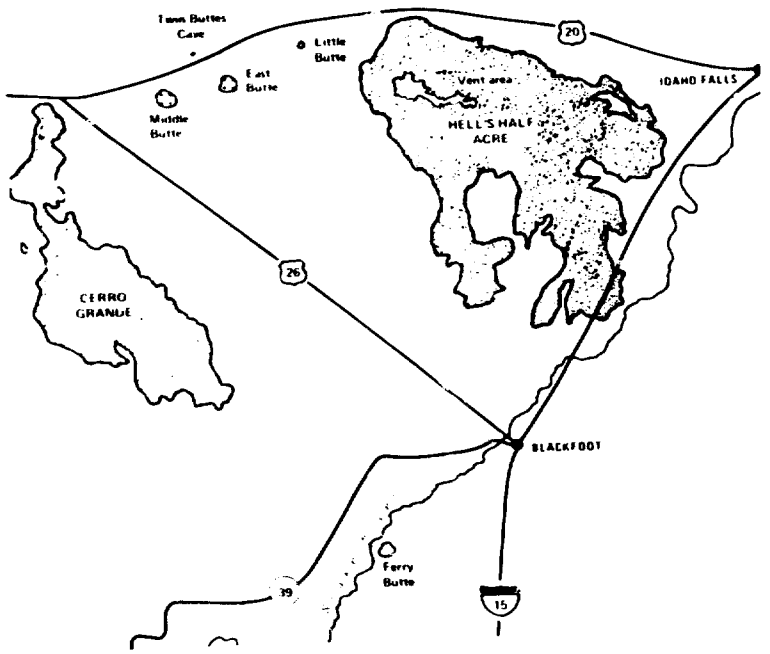

FIGURE 7-1. Index map to Hell's Half Acre lava field.

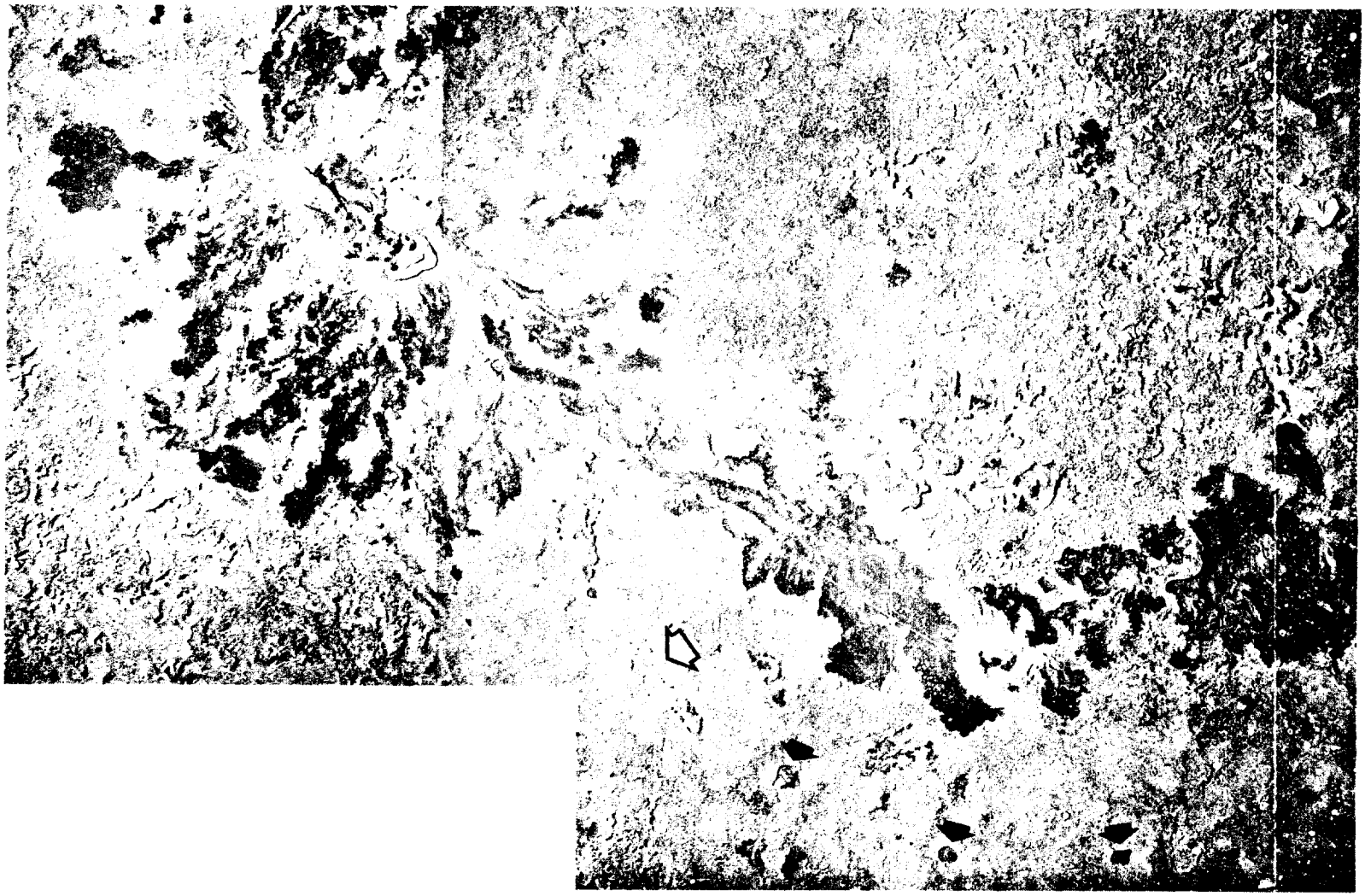

FIGURE 7-2. Mosaic of vertical aerial photographs of the summit vent region of Hell's Half Acre low shield. Dark patches are aa flows. The collapse crater at the summit is about 840 m long and is the result of multiple collapse and lava lake activity. An extensive lava tube can be traced from the summit (open arrow); the raised-rim craters marked by arrows may be associated with the tubes; similar crater-tube relations have been noted in Washington (Greeley and Hyde, 1971). Area of mosaic 4.2 km by 6.2 km. (U.S. Dept. of Agriculture Photographs CXO-1GG-31, 43; May, 1966.)

The basalts of the Hell's Half Acre field are typical of the Snake River Group (see Chapter 4, for stratigraphic nomenclature). Using the definition of Yoder and Tilley (1962), the basalts are olivine tholeiites and are characterized by low silica (46–47%), high total iron (14.5–16% as Fe_2O_3), and low total alkali (3.3–3.4%). Petrologically, the basalts are somewhat intermediate in character and are comprised of 5 to 10 percent modal olivine plus plagioclase phenocrysts in a matrix of olivine, plagioclase, augite and glass. Hell's Half Acre is somewhat unusual among flows of the eastern Snake River Plain in that lavas in some parts of the field have large numbers of olivine gabbro xenoliths that were carried to the surface from depth during eruption (Fig. 7-3). The xenoliths are considerably richer in MgO than the host basalts and may represent differentiates of Snake River Plain basalt.

The flow units comprising the Hell's Half Acre field all apparently originated from a single vent now marked by a small caldera-like central crater (Figs. 7-4 and 7-5). Eruptions involved several distinct phases between which there were apparently no significant time intervals. Stearns and others (1938) observed that most flows in the eastern Snake River Plain originated from solitary vents characterized by short periods of activity. Hell's Half Acre seems to be in accord with this observation.

FIGURE 7-3a. Olivine gabbro xenolith in a flow unit exposed in a summit pit crater at Hell's Half Acre.

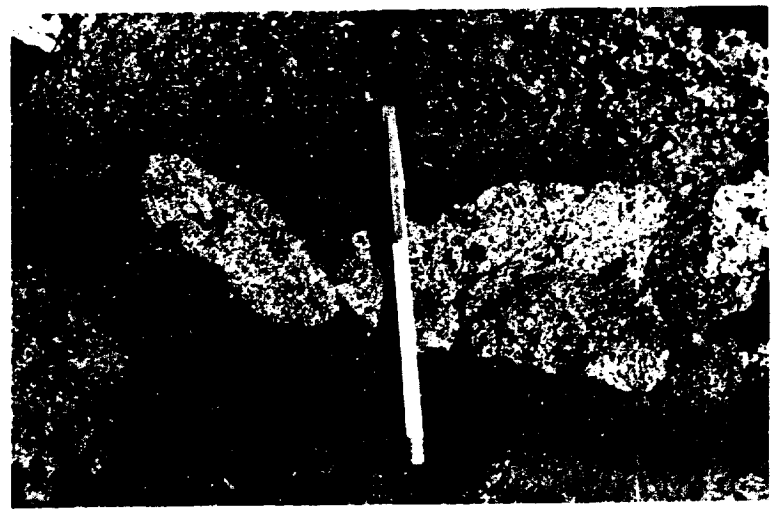

FIGURE 7-3b. Detail of xenolith, showing that xenolith occurs where there is a change in vesicularity in the lava flow.

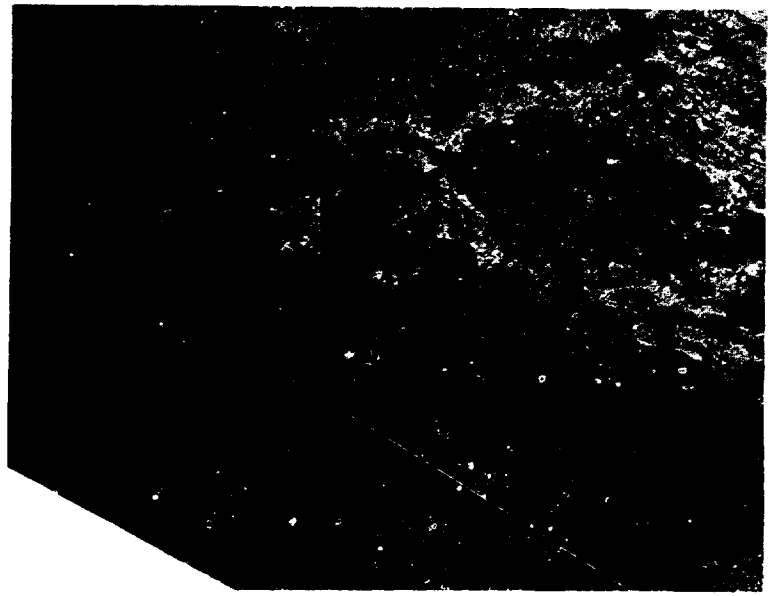

FIGURE 7-4. Oblique aerial view southeastward across the summit vents of Hell's Half Acre field.

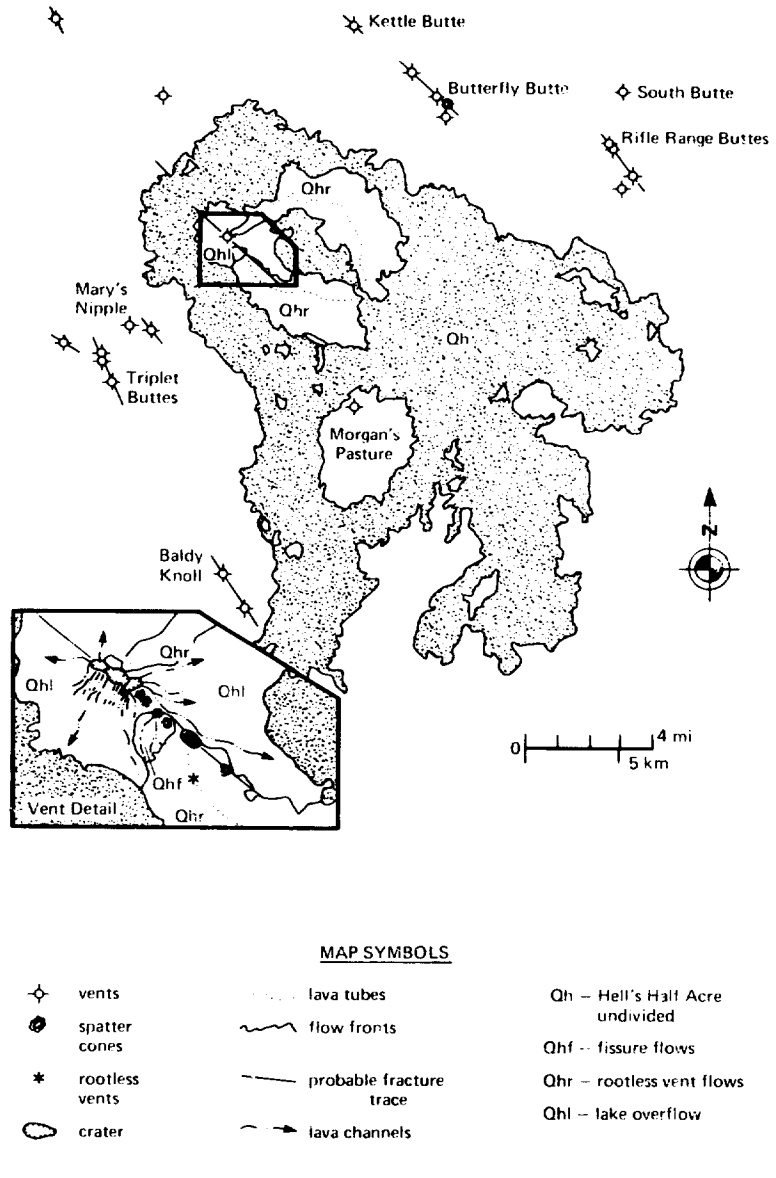

FIGURE 7-5. Geologic sketch map of Hell's Half Acre flow.

STRATIGRAPHIC DIVISIONS

The Hell's Half Acre field can be subdivided into four *"members,"* a member being defined as all of the products of a single phase of eruption. Each member is composed of a number of individual flow units. At Hell's Half Acre, the members are, from oldest to youngest: 1) undifferentiated massive flow units (Qh), 2) fissure eruptives (Qhf), 3) flow units fed by rootless vents (Qhr), and 4) thin, near-vent flow units (Qhl). The distribution of these members is shown in Fig. 7-5. Members 3 and 4, Qhr and Qhl, are related to lava lake activity at the vent.

Member Qh

The oldest member (Qh) is about 10–20 m thick and makes up most of the Hell's Half Acre field. It is dominantly pahoehoe, but small areas of aa are located at the distal ends of some channels. This member consists of only a few overlapping flow units, although delineating the exact extent of each is impossible as flow fronts are not traceable very far. Near flow fronts, the surface topography is extremely rough (Fig. 7-6) and shows well-developed pressure ridges and plateaus, collapse pits, and small pahoehoe toes and ropey textures. Away from the flow fronts, however, the topographic relief becomes very low and approaches a nearly smooth surface almost lacking even the typical ropey pahoehoe structures. A similar observation was made for the Wapi lava field by Champion (1973), but no satisfactory explanation of this characteristic has yet been proposed. Lava tubes and extensive open channels are not found in the Qh member, although distribution paths of the lava are often apparent from surface features visible in aerial photographs. These distribution paths commonly follow depressions which separate older flows. Flow fronts in Snake River Plain lavas are characteristically steep and nearly vertical at ground level, resulting in V-shaped valleys at contacts between relatively fresh lavas. Such valleys often acted as migration channels for lavas from later eruptions.

Member Qhf

Overlying the massive Qh flow units is the Qhf member, which is a sequence of thin fissure-flow units, spatter ramparts, and spatter cones (inset detail, Fig. 7-5). The ramparts and cones mark a single northwest-southeast trending lineament which transects the crater of the Hell's Half Acre vent (Fig. 7-4). The products of this phase of eruption are mainly southeast of the crater but a small area of spatter ramparts is also present on the northwest side. In the southeastern portion of the member, some exceptionally well-developed channels have distributed pahoehoe lavas away from the line of spatter cones. The fracture that served as the conduit for these lavas is considered to be part of a larger fracture zone, inasmuch as a set of parallel open cracks occur along strike just beyond the northwest margin of the Hell's Half Acre field. The vent fracture is vertical and approximately 4 km long with an extensional displacement of about 4 m. The secondary parallel fractures are also extensional but with lengths of only 0.5 to 1 km and displacements of 0.1 to 0.6 m.

FIGURE 7-6. Oblique aerial view of the margin of Hell's Half Acre field.

FIGURE 7-7. Panoramic view of the wall of one of the summit pit craters showing very thin flow units; scarp in the background is the main summit "caldera" wall.

Members Qhr and Qhl

The members Qhr and Qhl are related to lava lake activity at the vent and overlie both the spatter cone lineament and the older massive flow units. The lower member (Qhr) is composed of two broad areas (Fig. 7-5) of pahoehoe lavas fed by rootless vents located along the paths of two lava tubes which extend from the crater at the vent. The upper member (Qhl) is composed of many thin channeled aa and pahoehoe flow units which resulted from repeated lava lake overflows (Fig. 7-2). The uppermost of these flow units can be traced locally back over the edge of the crater where their layering becomes vertical. These Qhl flow units are exposed in cross-section in the scarp-wall of the main crater

(Fig. 7-7) and vary in aggregate thickness from 1 to 5 m. All of the Qhl flow units, because of rapid cooling, contain more glass than other lavas of the Hell's Half Acre field.

GEOLOGY OF THE VENT

The main vent at Hell's Half Acre is marked by a deep central depression with shallow depressions projecting to the northwest and southeast (Figs. 7-4 and 7-8). The deep central depression is formed by pit craters and curvilinear normal faults. The shallow depressions are floored by a lava lake surface (Fig. 7-9) and appear to have formed when drainback from the lake caused the brittle crust to collapse. Vertical glassy layers, with bulbous, clinkery surface textures, and scoring caused by lava lake crust being dragged against still-plastic basalt are evident around most the outer crater scarp (Fig. 7-10). The central depression is also floored by lava lake crust without, however, the evidence of lava "plasticity" at fault scarps. The collapse which produced the central depression apparently occurred after final solidification of the lake crust.

Exposed in the walls of the pit craters (Fig. 7-7) is a series of layers which are interpreted as a succession of four lava lake crusts. The sequence of layers within each crust is the same: each crust is capped by 1 to 2 m of thin (less than 30 cm) layers of scoriaceous lavas with rough lower surfaces and smooth upper surfaces. This thinly layered sequence grades downward into a 2 to 3 m zone, composed of many alternating dense and vesicular subhorizontal layers that are intergradational. This zone protrudes downward into crevices in the underlying thinly layered basalts which mark the top of the next lava lake crust. This sequence of lake crusts suggests a history of fluctuating lake levels.

Within the main crater are many spatter cones and spatter ramparts. Most of the cones are incomplete and are preserved only as small fragments of the original cone structures. The breached structures are commonly flooded by the uppermost lava lake, although some thin, small-volume flows on the lake can be traced back to three of the cones. The arrangement of the cones and the pit craters within the vent forms two lines subparallel to, although not directly in line with, the Qhf-spatter cone lineament (Fig. 7-8). This parallelism suggests that the fracture zone that served as the conduit for the Qhf flow units also served as the conduit for later eruptions.

Along the northeast side of the crater (Figs. 7-4 and 7-8), there is a large (0.3 by 0.2 km) uplifted rectangular block. The displacement is "trap-door" in style with approximately 15 m of upthrow along the southwest side of the block and slight downdrop along its northeast side. On the northeast side, the movement at the trap-door "hinge" was accompanied by considerable crushing. The other faces of the block, northwest and southeast, are cut by numerous slumps.

FIGURE 7-8. Oblique aerial view northwest across summit vent area; black dots mark positions of "cones."

FIGURE 7-9. Panoramic view northwestward across the lava lake surface at the summit region of Hell's Half Acre; Middle Butte (left) and East Butte (right) are on the horizon to the right.

The block is capped by lava lake overflow layers (Qhl) which, because of the rotation, dip markedly northeastward. Around the southeast end of the block, there also are Qhl flow units which show evidence of diversion around the block. The latter flow layers cannot be correlated with the uppermost lake crust. Therefore, the age of faulting of the block, while younger than the beginning of lake activity, is older than the lake crust immediately flooring the crater.

FUMAROLIC DEPOSITS

A late phase of minor vent activity at Hell's Half Acre was fumarolic. Various sulfates are distributed as crusts along fractures and as powdery deposits which fill cavities between flow units in the walls of the vent. Species identified are gypsum, bloedite ($MgSO_4Na_2SO_4 \cdot 4H_2O$), and thenardite ($Na_2SO_4$). Similar deposits of gypsum have been found at Wapi lava field, and jarosite (?) was found at King's Bowl lava field. The timing of sulfate deposition is unclear, but because the sulfates occur within the lava lake flows and are truncated by the lake-collapse scarps, they may be partly synchronous with lake activity.

DISCUSSION

The fractures associated with the Hell's Half Acre field are parallel to a regional tectonic grain. Many workers in different parts of the eastern Snake River Plain (Walker, 1964; Prinz, 1970; Greeley and King, 1975; Karlo, 1976; Kuntz, 1977) have observed that vents are often structurally controlled. Where this has been documented, the dominant orientation of vent-associated fractures, as at Hell's Half Acre, is northwesterly. These fractures appear to be the primary tectonic features of the province and suggest that the direction of maximum extension is along the axis of the plain rather than across it as is commonly believed. The interrelationship between fracturing and volcanism for the plain is conjectural, but it is a reasonable assumption since the fractures appear to have served as lava conduits and since the development of the fractures and volcanism along the fractures were probably synchronous. At Hell's Half Acre, it cannot be demonstrated that the initial volcanism was fracture-controlled but as the extension fracture served as the vent conduit in the later stages of eruption, it is a reasonable probability.

FIGURE 7-10. "Grooved" lava at the scarp of the lava lake.

During the initial phase of eruption, the bulk of the Hell's Half Acre lava (Qh) was emplaced and, although it can be divided into internal flow units, there is no evidence to suggest that it was not essentially a single outpouring of lava. The succeeding fissure eruption phase (Qhf) is suggestive of a renewal of activity and may indicate that eruptive activity drastically decreased after the primary (Qh) eruption phase. The small-volume fissure eruptions of Qhf may represent a reopening of the conduit, perhaps through continued extension of the fracture. In any case, eruption soon became localized along the fracture at the initial vent site in the form of a lava lake whose level fluctuated with surges in activity. An early period of massive overflow from the lake produced two large flow units (Qhr) which were distributed primarily through lava tubes. Periodically, the lake was deflated by drain-back into the conduit with later resurgent activity refilling the lake, similar to the "piston" activity observed at Mauna Ulu in Hawaii (Holcomb and others, 1974). The cone remnants within the vent crater were probably produced during the various episodes of lake refilling. Fluctuations in lake level led to repeated overflows, producing Qhl flow units throughout this stage of eruption. A final deflation of the lake, leading to collapse of the brittle lake crust, produced much of the present vent crater depression which was then locally deepened by the formation of pit craters and subsidence along curvilinear faults.

CONCLUSION

The vagaries of volcanic processes and the large number of vents within the eastern Snake River Plain led to diversity in volcanic "style." Hell's Half Acre is not an unusual volcano for the eastern Snake River Plain and may represent a mid-range in volcanic diversity, although obviously no single volcano can be described as being wholly "typical" of the province. Features such as Craters of the Moon, Menan Buttes, Big Southern Butte, and others, are more widely known

because of their unusual characteristics, and though significant, may not give a representative view of the province. Unfortunately, too few volcanoes have been described in detail and we as yet have only a partial understanding of Snake River Plain volcanism.

REFERENCES

Champion, D. C., 1973. The relationship of large scale surface morphology to lava flow direction, Wapi Lava Field, Southeast Idaho: Master's Thesis, State University of N. Y. at Buffalo, 44 p.

Greeley, R. and J. H. Hyde, 1972. Lava tubes of the Cave Basalt, Mount St. Helens, Washington: Geol. Soc. Amer. Bull., vol. 83, p. 2397-2418.

Greeley, R., and J. S. King, 1975. Rift zones in the south-central Snake River Plain, Idaho: Geol. Soc. Amer. Abs., vol. 7, p. 610-611.

Holcomb, R. T., D. W. Peterson, and R. I. Tilling, 1974. Recent landforms at Kilauea Volcano: in Greeley, R., ed., Geologic Guide to the Island of Hawaii, NASA CR 152416, p. 50-86.

Karlo, J. F., 1976. Orthogonal rifting within the Eastern Snake River Plain, Idaho: Geol. Soc. Amer. Abs., vol. 8, p. 594.

Kuntz, M., 1977. Extensional faulting and volcanism along the Arco Rift Zone, Eastern Snake River Plain, Idaho: Geol. Soc. Amer. Abs., vol. 9.

Malde, H. E. and H. A. Powers, 1962. Upper Cenozoic stratigraphy of Western Snake River Plain, Idaho: Geol. Soc. Amer. Bull., vol. 73, p. 1197-1219.

Prinz, M., 1970. Idaho Rift System, Snake River Plain, Idaho: Geol. Soc. Amer. Bull., vol. 81, p. 941-947.

Stearns, H. T., L. Crandall and W. Steward, 1938. Geology and groundwater resources of the Snake River Plain in Eastern Idaho: U. S. Geol. Survey Water Supply Paper 774, 268 p.

Walker, E. H., 1964. Subsurface geology of the National Reactor Testing Station, Idaho: U. S. Geol. Survey Bull. 1133-F, 22 p.

Yoder, H. S. and C. E. Tilley, 1962. Origin of basalt magmas; an experimental study of natural and synthetic systems: Jour. Pet., vol. 3, p. 343-532.

8. GEOLOGY OF THE WAPI LAVA FIELD, SNAKE RIVER PLAIN, IDAHO

Duane E. Champion
Division of Geological Sciences
California Institute of Technology
Pasadena, California

Ronald Greeley
Department of Geology
Arizona State University
Tempe, Arizona

8. GEOLOGY OF THE WAPI LAVA FIELD, SNAKE RIVER PLAIN, IDAHO

Duane E. Champion
Division of Geological Sciences
California Institute of Technology
Pasadena, California

Ronald Greeley
Department of Geology
Arizona State University
Tempe, Arizona

The Wapi lava field is one of several Holocene and latest Pleistocene volcanic fields on the central Snake River Plain (Fig. 8-1). In many respects, it is typical of the older fields of low shields that make up the present surface of the plain (see Chapter 3). Thus, study of the Wapi low shield is important in understanding the processes involved in the formation of this type of construct.

The Wapi Field covers a large (300 km^2) area that is elongate in the north-south direction and has three prominent lobes extending east, west, and northwest from the main mass of the field. The margin of the field is smooth on the north and east sides; where it ponded against the regional slope of the Snake River Plain on the south and west sides, the margin forms long, lingular flows where it occupies the drainages of small intermittent streams. Generally, the flows of the field have covered a typical plains surface of weathered lava and loess, but at their southern edge, they are superposed on a field of sand dune blowouts (Fig. 8-2) which trend east-northeast from the area around Lake Minidoka to the vicinity of American Falls.

The slope of the Wapi Field is typical of the low shields of the Snake River Plain, over distances of 10 to 20 kilometers, slopes are typically less than one degree. This flat slope is a consequence of the very fluid pahoehoe lavas and relatively high rates of effusion that typify the Snake River Plain. The only area of the field having a steeper slope is in the vicinity of Pillar Butte, the summit region of the field, where the slopes range from 5^o to 7^o.

FIGURE 8-1. Landsat (ERTS) image showing the Wapi lava field (1), Craters of the Moon National Monument (2), Cerro Grande lava field (3), Hell's Half Acre lava field (4), and American Falls Reservoir (5). Area of photograph is 110 km by 120 km.

FIGURE 8-2. High altitude (U-2 aircraft) aerial photograph of the southeast margin of the Wapi Flow (dark area on left) that is superposed on a field of longitudinal sand dunes. Some of the active dunes are crossing the lava field (A); dark patches (B and elsewhere) are aa lavas. Area of photograph is 13.3 km by 12.9 km. (NASA-Ames Photograph 72-186, frame 5710, October, 1972.)

THE WAPI FIELD

The Wapi Field is composed of numerous flow units of pahoehoe lava piled side by side and atop one another, of the type described by Walker (1972) as compound. The presence of many kipukas along the south and west sides of the field suggest that the flows are rather thin (Fig. 8-3). Russell

FIGURE 8-3. Vertical aerial view of a small kipuka (white area) within the Wapi lava field; note also the pressure plateau (A). (NASA-Ames Photograph 878-5-7, October, 1968.)

(1902) states that the average thickness of flows (made of many flow units) on the Snake River Plain is 15 to 25 m and the Wapi Field appears to be typical of this figure, except in the very center of the field and in the vicinity of Pillar Butte where the total thickness may be 100 m. Near the margins of the field, the flow units are larger, tend to have greater local relief (as much as 10 m) and are characterized by large pressure ridges, pressure plateaus (Fig. 8-3) and collapse depressions (Figs. 8-4). This transition of the size of the flows from the periphery to the interior of the field is apparently a function of proximity to the vent area; thus, closer to the vent, many small pahoehoe flows have filled depressions in earlier flows and generally leveled the local relief. This effect is most pronounced toward Pillar Butte.

The lava of the Wapi Field has a filamented pahoehoe texture over 90 percent of its surface, with relatively minor portions broken into slabby pahoehoe or aa lavas.

Surface Features

Pressure ridges (Fig. 8-5) are common on the Snake River Plain. They were described by Russell (1902) as:

> " . . . dome-like ridges, commonly from 10 to 30 feet high, 20 to 70 feet wide, and from 50 to possibly 500 feet long, which are usually cracked open at the top throughout their length, the cracks being open fissures usually 3 to 4 feet wide but sometimes as much as 10 feet. The fissures referred to narrow downward, and the basalt forming their walls is frequently columnar, the columns being at right angles to the outer surfaces of the ridges."

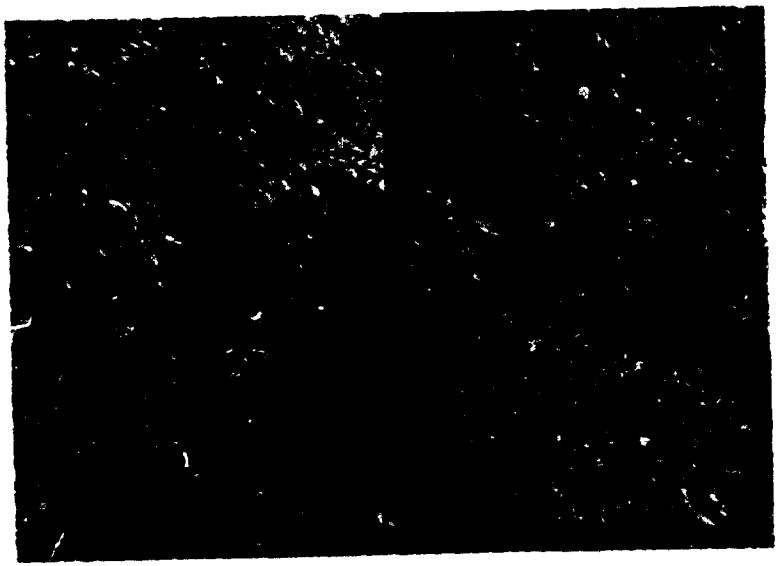

FIGURE 8-4. Stereoscopic pair of aerial photographs showing several collapse depressions on a pressure plateau, Wapi lava field. Area of photograph is 840 m by 1540 m. (NASA-Ames Photograph 878 1-3, 4, October, 1968.)

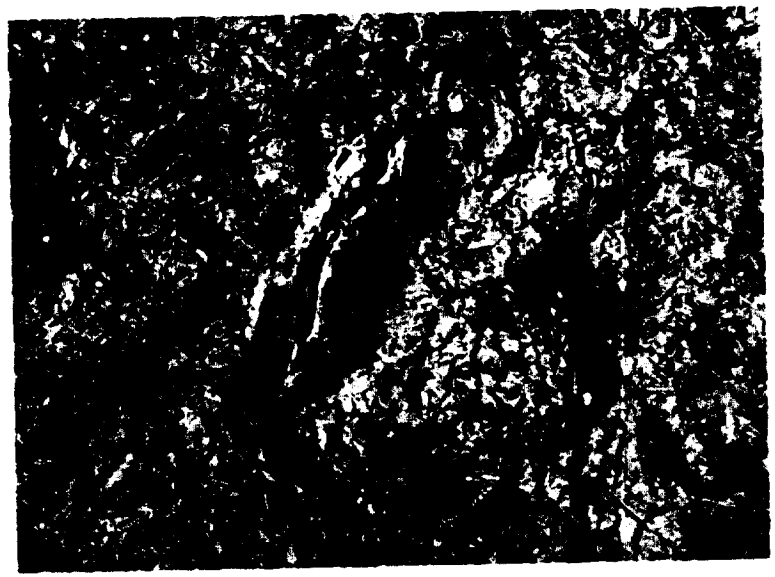

FIGURE 8-5. Low altitude oblique view of a pressure ridge on the Wapi lava field. (Photograph by Ronald Greeley, University of Santa Clara, June, 1977.)

He also noted that these cracked ridges frequently occur in groups with their long axes subparallel. His projected mechanism for the formation of these features was:

> "The similarity between the large ridges on the surfaces of the older sheets of the Snake River lava and the hollow folds, corrugations, etc., observed at the Cinder Buttes [Craters of the Moon], leaves no room for doubting that the former, like the latter, were produced by lateral pressure in the surface portion of a lava flow."

Russell attributed the size of the features to the fact that the parent flow had to move such a great distance over such a relatively flat surface. Russell does not specifically state the relationship between the orientation of the long axes of the pressure ridges to the flow direction, but it generally has been assumed that it is transverse to the principal direction of flow such that frictional drag of the flow underneath causes the crust of the flow to compress into a ridge. Wentworth and Macdonald (1953) state:

> "Many of them [tumuli], particularly those of highly elongate form, and the great majority of pressure ridges, apparently were formed by the horizontal thrusting and buckling of the flow crust caused by the pressure of fluid lava."

Probably the most detailed work on the formation of pressure ridges was carried out on the McCartys Basalt Flow in New Mexico by Nichols (1946). In this study, the relationships between large morphologic features such as pressure ridges and collapse depressions are carefully described over the area of the last 10 km of the flow. Several models based on mechanical studies were advanced to explain the relationships observed. Among the most interesting of Nichols' observations and interpretations that pertain to the Wapi Field are: (1) there are two kinds of cracks in the flow, one is wedge-shaped and is caused by stretching of the lava crust by uplift while another kind is polygonal and caused by thermal contraction of the cooling of the lava; (2) cracks formed in a slowly uplifting and thickening crust would be wedge-shaped as the upper crust would be stretched more than the bottom part of the crust which would have been liquid during all except the last stages of the uplift; (3) pressure ridges can be divided into two types: longitudinal ridges with axes parallel to flow direction (termed here *flow ridges*, Fig. 8-6) and transverse ridges with axes across the direction of flow; (4) the medial cracks in the pressure ridges are

FIGURE 8-6. Oblique aerial view of a "flow ridge," a long, thin projection of the lava field that appears to have been "inflated" into a ridge by lava after the general pattern of the flow was emplaced; jeep trail indicates scale. (NASA-Ames Photograph by Ronald Greeley, 1969.)

empty, although some are filled with "squeeze ups;" and (5) Nichols' rejection of the viscous drag model for the formation of the pressure ridges on the McCartys Flow and proposition of a domical collapse theory to account for them.

Pressure ridges are the most ubiquitous large-scale feature on the Wapi Field and occur in a continuous series of sizes and shapes. They range in length from a nearly continuous 8 km to as short as 10 m. They range in height from 1 to 15 m. Some of the ridges have a rounded domical form, but most are relatively flatsided with sides dipping 30° to 40°. The best-formed and largest pressure ridges occur on the eastern side of the field. The medial cracks of the major pressure ridges invariably lack flowouts and generally are 6 to 10 meters deep, indicating that cracking occurred late in the history of the flow.

The long continuous pressure ridges in the Wapi Field pass laterally into features termed *pressure plateaus* (Figs. 8-3 and 8-4). Pressure plateaus are defined as:

> "A broad area of lava, generally pahoehoe, that has been bodily elevated by the intrusion of new lava into the lower, still congealed part of a flow without the addition of any new lava at the surface." (Gary and others, 1972.)

The pressure plateaus of the Wapi Field are flat areas bordered by scarps. The edges of the plateau dip 30° to 40°, the same as the sides of the pressure ridges. Pressure plateaus range in width from 15 to 200 m.

Collapse depressions (Figs. 8-4 and 8-7) are another class of surface features found in certain areas of the Wapi Field in abundance. The depressions range in size from 1 to 35 m across and are from 2 to 10 m deep. The largest and best-formed of the collapse depressions are on the eastern side of the field. Collapse depressions on the McCartys Flow are described by Nichols (1946) and Hatheway (1971). Many of their observations on collapse depressions on the McCartys Flow and elsewhere coincide with features seen on the Wapi

FIGURE 8-7. Panoramic view of a typical collapse depression on the Wapi lava field; this structure is on the flow between Wapi Park and Pillar Butte. Arrow points to figure for scale.

Field. These observations include: (1) the long axes of the collapse depressions are nearly always parallel to the direction of the flow, and the surface of the flow between the depressions is relatively flat; (2) the scarp that faces in toward a collapse depression often overhangs the depression and the lower lip of the opening is grooved and striated, a phenomenon probably caused at the time of collapse when the lava was still soft and plastic; and (3) collapse depressions commonly have squeeze-ups within them, which are extruded after collapse occurs.

Nichols (1946) states: "These depressions and others are formed by the collapse of the roofs of lava tunnels." The McCartys Flow is in the valley of the Rio San Jose, New Mexico and the bottom of collapse depressions are commonly filled with water and alluvium, which prevents detailed study of the floors and interiors of the depressions. In comparison, the collapse depressions on the Wapi Field can be examined in detail. Of the approximately 100 collapses studied, none were found with any connection to a lava tube system at either the upflow or downflow end of the depression.

From their shape and position, it is apparent that the collapse depressions of the Wapi Field are related to the flow system, but apparently they are not simply collapsed roofs of lava tubes. From observations of striations and squeeze-ups, it is believed that the formation of the depressions occurs relatively early in the flow history, before the flows have solidified.

Age of the Wapi Field

Several workers have attempted to determine the absolute age of the Wapi Field by digging under the edge of the flows and obtaining charcoal from the burned roots of sagebrush overridden by the flows. This is clearly the most viable method, but until recently all attempts have been fruitless. In July, 1977, a charred root sample was found, but the results were not obtained in time for inclusion here.

Stratigraphically, the Wapi flows overlie the southern segments of King's Bowl rift, which in turn have been overlain by the King's Bowl flows, for which a C^{14} date of 2360 ± 150 years B.P. (Valastro and others, 1972) has been obtained. Unfortunately, the King's Bowl lavas and the Wapi lavas are not in contact. From degree of weathering and vegetative cover, the Wapi lavas may be somewhat older than the King's Bowl flows.

Paleomagnetic information from the Wapi Field and other nearby flows may provide an approximate absolute age. Figure 8-8 is a north polar projection of the Earth on which is plotted the virtual geomagnetic poles and 95 percent confidence ovals of several young flows along the Idaho Rift System, some of which are C^{14} dated, and others that are thought to be similar in age.The group of poles, including those obtained for the Trenchmortar Flat, Watchman, and Rattlesnake Butte flows document an extensive eruption episode in Craters of the Moon at about 2100 years B.P. The pole for King's Bowl at 2360 ± 150 years B.P. is in a different position and the Wapi pole is very close to it. The

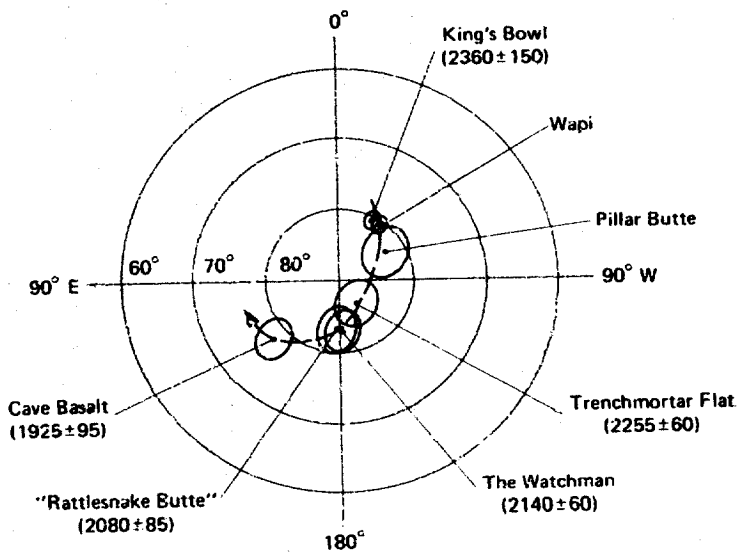

FIGURE 8-8. North Polar projection of Earth showing virtual geomagnetic poles (VGP) and ovals of 95 percent confidence for late Holocene C^{14} dated and undated flows along the Idaho Rift System, Snake River Plain, Idaho. Titles and names of flows, and C^{14} ages in radiocarbon years B.P.

distinction between the virtual geomagnetic pole (VGP) positions of King's Bowl and the flows at approximately 2100 years B.P. allow us to disregard an earlier C^{14} date of 2130 ± 130 years B.P. (Prinz, 1970) as being slightly in error. The dotted arrow shows the progression of VGP positions with time between these two groups. The close similarity between VGP's for King's Bowl and Wapi lavas combined with the close proximity of the vents and the identical orientation of the rift segments along which the eruptions took place (Champion, 1973) suggest they probably formed at the same time.

The short aa flows near the Pillar Butte area have also been sampled to determine any great temporal difference with the flows of the main mass of the field. Samples from

that area have a wider statistical distribution, thus the confidence oval is much larger and the pole position less accurately known. The pole position suggests that the flows in the Pillar Butte area are somewhat younger than the rest of the Wapi Field. Unfortunately, as the Pillar Butte area is topographically higher than the rest of the field, there is a good possibility that they have been rotated slightly during the deflation of the cone after the eruption. The axis of the rotation is in the proper orientation to move the pole for Pillar Butte flows from the position of the Wapi and King's Bowl poles, to the position it occupies. We can only say that at most the Pillar Butte flows are slightly younger (2300 years B.P.) than the Wapi flows, and possibly very nearly the same age.

PILLAR BUTTE

Characteristic for most of the low shields making up the Snake River Plain, the Wapi lava field is capped with a steeper-profiled summit region. For the Wapi Field, the summit region is referred to as *Pillar Butte*. The steep profile is at least partly attributed to the relatively low-volume flows that did not travel very far from the central vent, and the higher proportion of viscous aa flows.

Pillar Butte is a prominent mass of agglutinate and layered flows, possibly injected with dikes; the mass rises some 18 m above the general summit region on the south side. This prominent structure served as a landmark for early travellers along the Oregon Trail, and still serves as a general reference point in the south-central Snake River Plain.

The Pillar Butte summit region contains at least 11 distinctive eruptive centers, identified by pit craters and former lava lakes. Flows from these centers are typically short and often contain small lava tubes and channels. Many of the tubes and channels were used repeatedly by subsequent flows, sometimes forming roofs over previous channels (Fig. 8-9), or draining into older lava tubes through "skylights" (Fig. 8-10). The largest lava tube is Moss Cave (Figs. 8-11 and 8-12).

FIGURE 8-9. View of a small lava channel and lava tube formed in a flow from Pillar Butte; channel was roofed by a subsequent flow to form the lava tube (Station 7).

The age relationships of the Pillar Butte flows to the main mass of the Wapi lava field is not clear everywhere. To the south, the aa flows for Pillar Butte are superposed on the Wapi lavas; however, on the west side of the Pillar Butte region, it appears that the Wapi lavas truncate those of Pillar Butte.

Pillar Butte and the Wapi lava field are among the best preserved low shields on the Snake River Plain and are useful for understanding the style of volcanism involved in their formation. The guide that follows is keyed for a half-day field trip designed to point out the salient features of low shields.

FIGURE 8-10. Drainage of surface flows into Moss Cave lava tube (see Figs. 8-11 and 8-12). (NASA-Ames Photograph by Mike Lovas, 1969.)

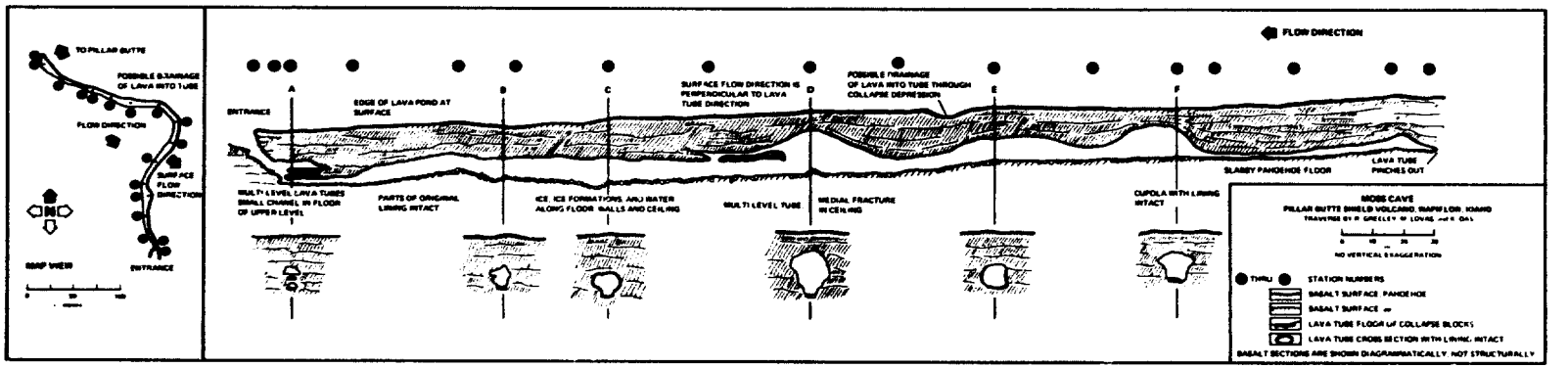

FIGURE 8-11. Diagram of Moss Cave lava tube.

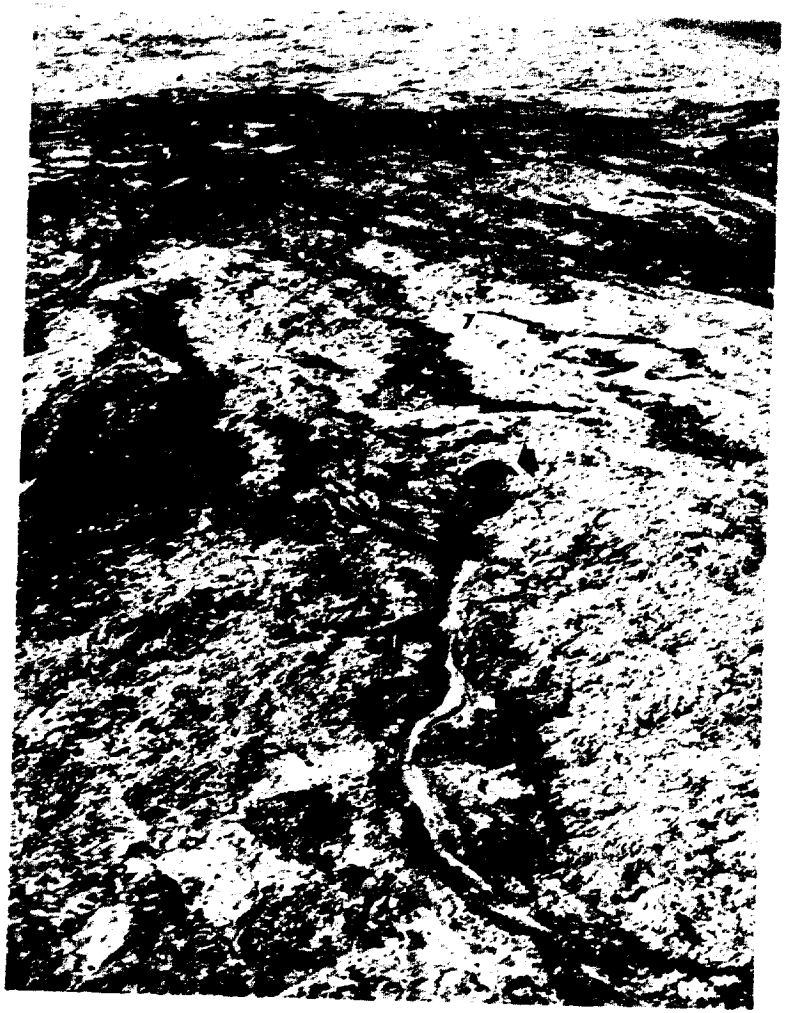

FIGURE 8-12. View northward across the south flank of Pillar Butte, the summit region of the Wapi low shield; arrow marks the entrance to Moss Cave lava tube; "7" refers to station of field guide and indicates location of Figure 8-9. (Photograph by Ronald Greeley, University of Santa Clara, June, 1977.)

GUIDE TO WAPI PARK, THE WAPI FLOW, AND PILLAR BUTTE

This guide is keyed to stations identified in Figure 8-13. The trip begins in an area known as Wapi Park which is reached via a jeep trail off the main American Falls–Crystal Ice Cave road. The trip includes a hike of about 5 km and requires about a half-day; therefore, water should be carried, particularly during summer months.

Wapi Park (Station 1)

Wapi Park is a peninsula-like area (Fig. 8-14), formed by a linear vent that has been almost completely surrounded by lavas of the Wapi Field. The term "park" is commonly applied to kipukas on the Snake River Plain, and there is no implication of recreational "park" qualities. A few small aspen growing along the flow margin in Wapi Park evidently indicate that there is sufficient moisture accumulating to support the growth.

The linear vents at Wapi Park can be projected southwestward through a cinder cone kipuka in the Wapi Field to another linear vent system, Higgins Butte, on the southwest margin of the field. These three, older vents are similar in state of preservation, suggesting contemporaniety and may define a rift system (Greeley and King, 1975).

Using the method of Bullard (1976), a tunnel was excavated beneath the edge of the Wapi Field near Wapi Park and about 200 gm of charcoal were recovered. The sample has been submitted to obtain a C^{14} date for the Wapi flows.

The Wapi Field (Station 2)

This "station" includes the 1.6 km hike from the parking area at Wapi Park to the edge of the Pillar Butte area. **Note:** Because of the lack of large prominent landmarks and the rugged local relief on the lava flows, it is often easy to become disoriented on the Wapi Field. The best landmark in

FIGURE 8-13. Air photo guide to Pillar Butte.

this region is the knob at Pillar Butte; keep slightly to the east (left) of the knob as you walk toward the area and on to Station 3. For the return to the parking area, the vents of Wapi Park are the best landmarks; however, they may be confused with other vents in the area, so become familiar with their form and general position. Note that the parking area is at the south end of the vents.

In the walk across the Wapi lavas, note the hummocky local relief, collapse depressions, squeeze-ups, and pressure ridges. Note also that the local relief changes from low over some of the plateau areas to fairly high (10 m) elsewhere. Imagine what the contact would look like if the Wapi flow were covered with a younger lava flow.

FIGURE 8-14. Vertical aerial photograph of Wapi Park (light-toned area at top of photograph), the vent region of an older low shield that has been partly buried by the younger Wapi lava flows (dark area). Pillar Butte, the summit vent region for the Wapi lava shield, is visible at the bottom of the photograph. The field trip will leave the jeep trail in Wapi Park and proceed cross country over the pahoehoe lavas of the Wapi flow to the Pillar Butte area, a hike of about 1.6 km. Area of photograph is about 2.8 km by 4.4 km. (U S. Department of Agriculture Photograph CYN-7B-106, August, 1946.)

Pillar Butte (Station 3)

This station marks the northwest edge of the Pillar Butte flows which emanate from several small vents (Fig. 8-15) and flow around the west side of Pillar Butte, truncating older flows from the summit vents. The difference in time between the flows may have been only a matter of hours or days. Many of these flows are tube-fed; note the sinuous ridges (tubes) (Fig. 8-16), channels (Fig. 8-17), and "budding" lava toes.

Pillar Butte (Station 4)

Cross the north flank of the Pillar Butte summit region to Station 4, a region of several pit craters and vents that fed the northern part of the Pillar Butte area (Fig. 8-13). Take care in walking across some of the lava flows; many of the flows are *shelly pahoehoe*, a thin-shelled, gassy variety that is fragile and sharp (Fig. 8-18). Shelly pahoehoe is characteristic of near-vent regions where devolatilization of the lava can occur rapidly to form cavernous blisters.

FIGURE 8-15. Panoramic view of small pit crater at Station 3, Pillar Butte summit region.

FIGURE 8-16. View of a small lava tube that originates from pit crater shown in Figure 8-15; figure is standing on the ridge formed along the roof of the tube.

FIGURE 8-17. Small sinuous lava channel associated with the pit crater shown in Figure 8-15.

FIGURE 8-18. Shelly pahoehoe, a glassy variety of lava that is fragile; it is generally restricted to near-vent areas.

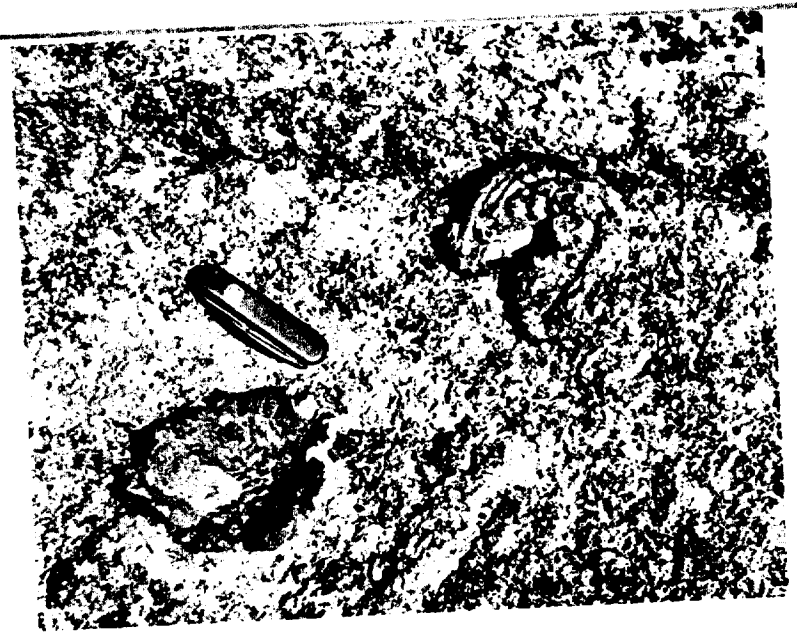

FIGURE 8-19. Two, small cow-dung bombs near the summit of Pillar Butte.

Pillar Butte (Station 5)

Walk from Station 4 toward the east side of the summit region. Some of the lavas are slabby pahoehoe flows consisting of thin, plate-like slabs of lava. Several prominent lava lakes were active in the summit regions. Note the "floors" of the summit crater that represent subsided lava lake surfaces. Cow dung bombs (Fig. 8-19) and spatter are present around many of the former lava lakes.

Pillar Butte (Station 6)

This station marks the top of Pillar Butte, a mass of agglutinate, flows, and possibly dikes, that rises above the summit region (Fig. 8-20). A good perspective of the Pillar Butte flows to the south, as well as the surrounding terrain, can be gained from here. Wapi Park is clearly visible northward as are the trailers at Crystal Ice Cave. Several kipukas can be seen within the Wapi field. On a clear day, the bounding mountains on the north and south sides of the plain are visible.

FIGURE 8-20. Panoramic view of Pillar Butte (right side) and one of the pit craters in the summit region. Figures on left indicate scale.

Pillar Butte (Station 7)

This station marks the general area south of Pillar Butte, and should be visited only if time permits. Features in this area are well-developed lava tubes (Figs. 8-9, 8-21, and 8-22), lava channels, and other flow features such as dribblet spires (Fig. 8-23).

Return to Wapi Park

For the return to the parking area, walk on the west side of Pillar Butte (Figs. 8-24 and 8-25) toward the Wapi Park vents. A scarp forms the west side of Pillar Butte and may represent a fault formed by either subsidence of the flow mass to the west, or uplift of the summit by inflation, or a combination of the two.

Follow essentially the same path back across the Wapi Field to the parking area.

FIGURE 8-21. Ice stalagmites and frozen pond on floor of Moss Cave. Rain, snow-melt, and ice-melt from the winter percolates through the lava tube roof and freezes; ice generally remains year-round despite the high temperatures on the surface in the summer. (NASA-Ames Photograph by Mike Lovas, 1969.)

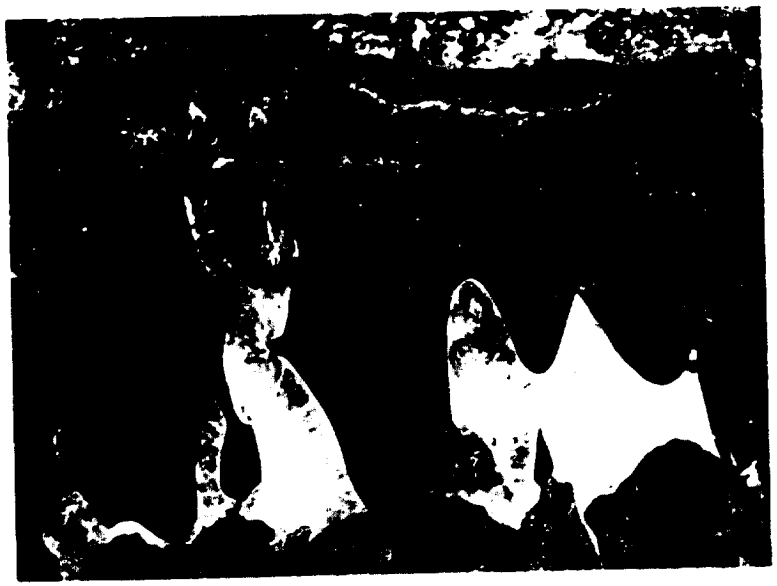

FIGURE 8-22. Ice stalagmites in Moss Cave. Forked-shaped stalagmite is about 30 cm high. (NASA-Ames Photograph by Mike Lovas, 1969.)

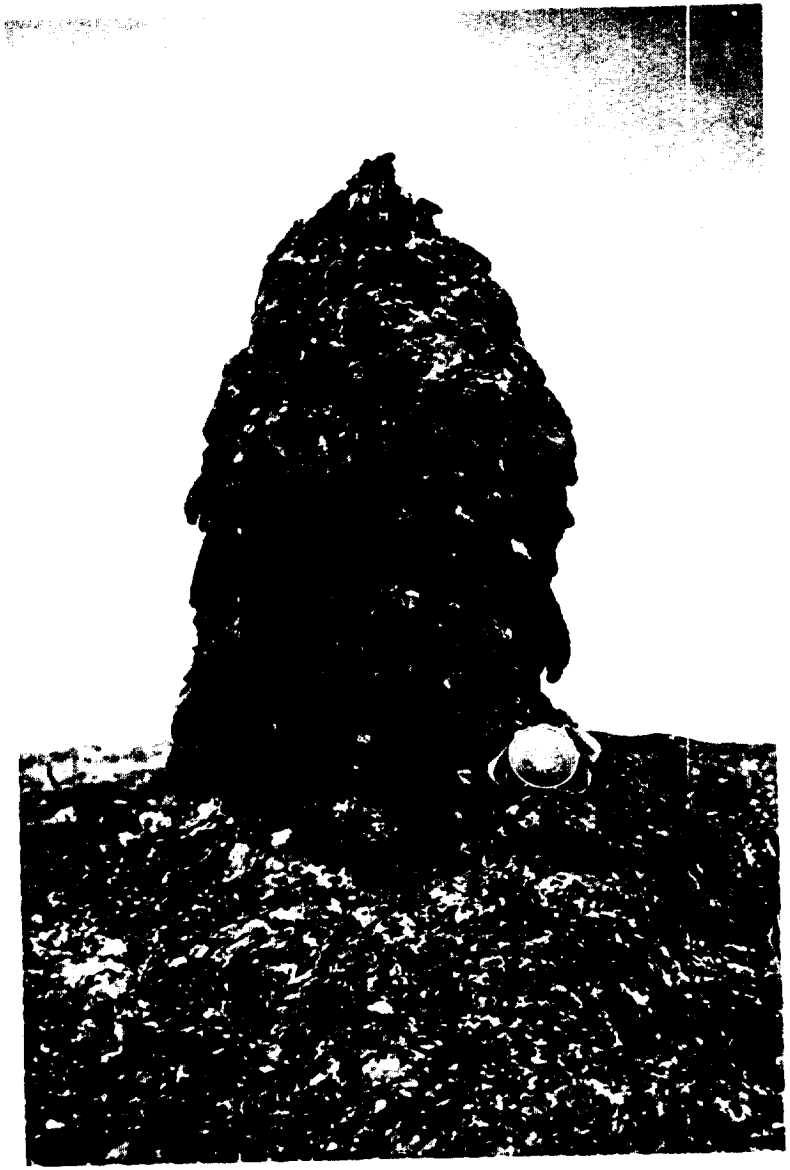

FIGURE 8-23. A dribblet spire (a type of hornito) on the flows south of Pillar Butte; canteen indicates scale.

FIGURE 8-24. View of Pillar Butte from the south end of the summit region; arrow points to figure for scale.

FIGURE 8-25. Panoramic view of a small flow that spilled out of a summit pit crater near Pillar Butte, visible to the right.

REFERENCES

Champion, D. E., 1973. The relationship of large scale surface morphology to lava flow direction, Wapi lava field, SE Idaho: Unpublished Master's Thesis, State University of New York at Buffalo, 44 p.

Greeley, R. and J. S. King, 1975. Geologic guide to the Quaternary volcanics of the south-central Snake River Plain, Idaho: Idaho Bur. Mines Geology, Pamphlet 160, 49 p.

Hatheway, A. K., 1971. Lava tubes and collapse depressions: Unpublished Ph.D. Dissertation, University of Arizona, 353 p.

Nichols, R. L., 1946. McCartys basalt flow, Valencia County, New Mexico: Geol. Soc. Amer. Bull., vol. 57, p. 1049-1086.

Prinz, M., 1970. Idaho Rift System, Snake River Plain, Idaho: Geol. Soc. Amer. Bull., vol. 81, p. 941-948.

Russell, I C., 1902. Geology and water resources of the Snake River Plains of Idaho: U. S. Geol. Survey Bull. 199, 192 p.

Valastro, S., Jr., E. M. Davis, A. G. Zarela, 1972. Radiocarbon, vol. 14, p. 470.

Walker, G. P. L., 1972. Compound and simple lava flows and flood basalts: Bull. Volcan., vol. 36, p. 579-590.

Wentworth, C. K. and G. A. Macdonald, 1953. Structures and forms of basaltic rocks in Hawaii: U. S. Geol. Survey Bull. 994, 98 p.

9. CRYSTAL ICE CAVE AND KING'S BOWL CRATER, SNAKE RIVER PLAIN, IDAHO

John S. King
Department of Geological Sciences
State University of New York at Buffalo
Amherst, New York 14226

9. CRYSTAL ICE CAVE AND KING'S BOWL CRATER, SNAKE RIVER PLAIN, IDAHO

John S. King
Department of Geological Sciences
State University of New York at Buffalo
Amherst, New York 14226

The Idaho Rift system traverses the Snake River Plain in east-central Idaho from the vicinity of Craters of the Moon National Monument south to the Wapi lava field. The rift is a series of sets of discontinuous tension fractures of distinctly different ages and trends (Prinz, 1970; Greeley and King, 1975). One of the youngest of these fracture sets is the King's Bowl rift set which is made up of a discontinuous central fissure up to 2.5 m wide, flanked on both the east and west by additional subparallel tension fractures (Fig. 9-1). The central fissure of the King's Bowl rift set has been the source of several small lava flows, the largest of which covers about 4.5 to 5 km^2 and is considered to have erupted from the fissure in the vicinity of the King's Bowl. King's Bowl is a large oval crater about 85 m long, 28 to 30 m across at its widest, and approximately 30 m deep.

Fractures in the King's Bowl rift can be entered and the rift examined in cross section at several points (Fig. 9-2). A trail descends about 30 m to the bottom of the King's Bowl and a tunnel descends about 46 m along the central fissure into the Crystal Ice Cave which is a collection of ice columns, stalactites, and stalagmites formed in a part of the rift that is relatively shielded from variations in surface temperatures.

The object of this paper is to present and interpret the current knowledge of Crystal Ice Cave, King's Bowl crater, and the rift, as well as to present a brief synopsis of the sequence of events for the King's Bowl lava flow. Certain interpretations will, no doubt, change with the addition of further details from future studies.

FIGURE 9-1. Oblique aerial view northward along King's Bowl rift. South Grotto area is in the foreground, marked by a series of low spatter cones. A series of "perched" lava lakes can be traced eastward (to the right) from South Grotto. Note the en echelon offset in the fissure. Light areas marked by arrows mark zones along the fissure that have been blanketed by tephra erupted from the fissure. (Photograph by Ronald Greeley, University of Santa Clara, 1971.)

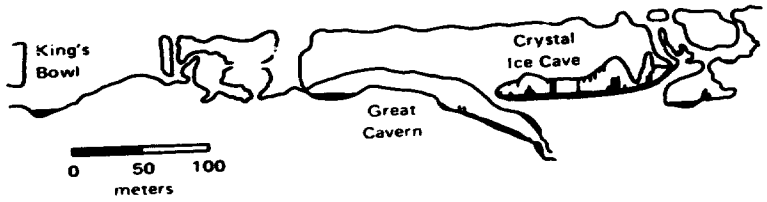

FIGURE 9-2. Longitudinal section of part of Crystal Ice Caves Rift, Idaho, based on sketch by James Papadakis. The King's Bowl is at the southern end of the section shown (from Halliday, 1976).

CRYSTAL ICE CAVE

Crystal Ice Cave displays massive ice formations developed in a large cavity along the King's Bowl rift, set at a depth of about 46 m. It is located on the rift 230 m north of the north end of King's Bowl. Crystal Ice Cave was opened to the public in 1965, and the descent to the ice room allows several excellent views of the walls of the King's Bowl Rift. Particularly noteworthy near the start of the descent are gouges ripped into the wall rock by ejecta being thrown to the surface by volcanic eruption.

History of Crystal Ice Cave

It is reported that spelunkers penetrated the rift to a depth of nearly 245 m, which is the depth of the water table in this area (Prinz, 1970). Entrance into the rift for this exploration was made through South Grotto, a large, prominent spatter cone located on the rift 1.6 km south of King's Bowl. The exact date and specifics of this descent are not well known, as they were never recorded and the descent was made by interested local spelunkers from Aberdeen, Idaho. Nevertheless, this exploration drew attention to the region and in 1956, two local cavers decided to see how deeply they could penetrate the King's Bowl vent itself. They found an opening in the north end of King's Bowl which carried them down to an ice floor. It is reported that the explorers found only one small opening toward the north end of this ice floor and, while the two were investigating this, one of them lost his flashlight down the hole. In attempting to retrieve the light, he entered the hole and descended about 3 m to a point where the passageway opened into a large cavity containing a spectacular array of massive columns, stalactites, and stalagmites of ice. The original designation of the ice cave was Liar's Cave, owing to the fact that the discoverers' story of this ice accumulation located under the lava flows and in the summer heat of the desert was unbelievable to those who had not seen it first hand.

In 1961, a geologist who had an active interest in caving learned of Liar's Cave. James Papadakis came to southern Idaho from Texas to learn more about the ice cave. He reexplored the cave and was so intrigued by what he found that he decided to develop it commercially. The initial access to the cave was through King's Bowl, and in 1964 Papadakis blasted out a trail to the bottom of the crater. However, this only carried visitors down to the ice floor at the north end of the King's Bowl crater – few visitors wished to continue on through the one small opening in the ice floor to complete the descent into the ice cave proper. Thus, Papadakis altered his plan for the cave. He located the pc t on the Great Rift directly above the ice cave and proceeded to blast out a 370 m long tunnel which descends a vertical distance of about 46 m into the ice cave. The tunnel descends

along the King's Bowl rift and makes use of natural openings along the rift wherever possible. It begins from a point above the ice cave and trends north along the rift, crosses the rift at the half way point and "folds" back south along the rift in continuing descent (Fig. 9-3). The opening of this tunnel was a tremendous undertaking, especially when one appreciates that it was accomplished primarily by two individuals — James Papadakis and his father, Louis. Papadakis made several refinements to the ice cave tunnel through the years and it was largely through his efforts that the Great Rift was designated a U. S. National Landmark in 1968. Papadakis sold his interest in the cave in 1975 and major additional developments have been made by the new owners since that time. The most obvious recent addition is the Hanging Balcony, constructed into the rift at the base of the tunnel. As one looks to the south from the Hanging Balcony (Fig. 9-3), the location of the discovery hole is near the top of the cave surmounting a massive flow of ice which slopes down from the roof.

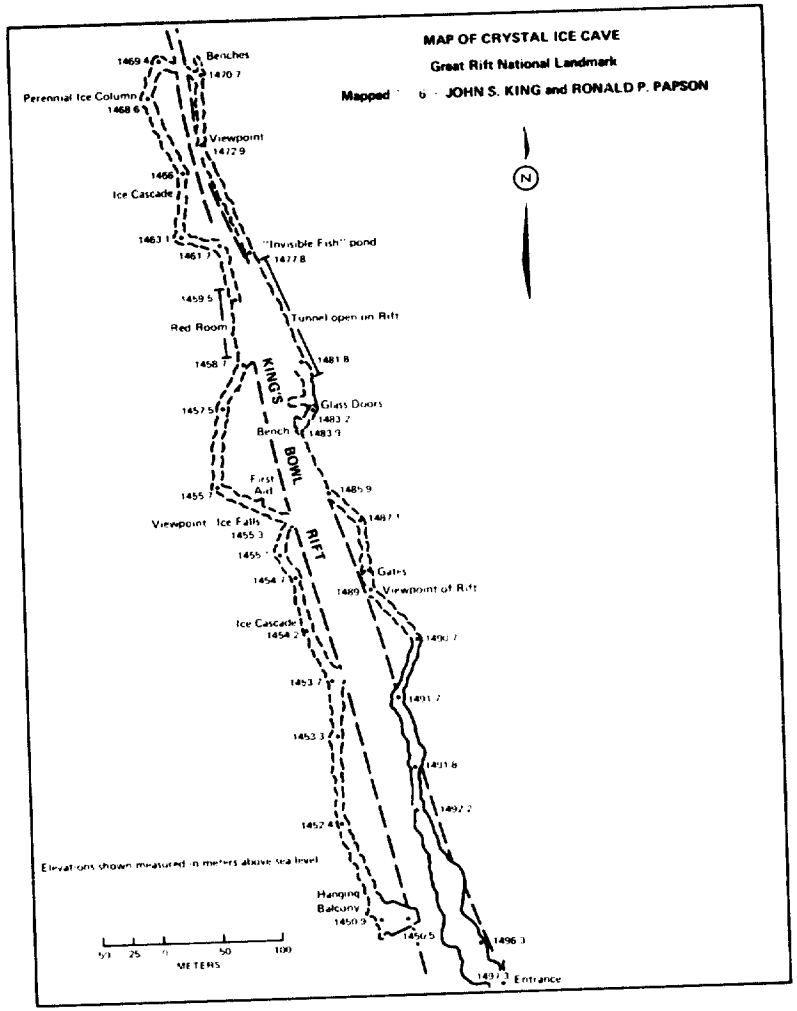

FIGURE 9-3. Map of Crystal Ice Cave. Exaggerated separation, particularly in the south, to permit greater detail. Elevations shown in feet at stations based on control from U.S. Geological Survey Pillar Butte Quadrangle. Total descent from entrance to Hanging Balcony is 153.8 feet.

Formation of the Crystal Ice Cave

Ice is fairly common in lava tubes, but only in areas which receive winter snows. This is quite clearly demonstrated in Hawaii where lava tubes above the snow line on Mauna Kea and Mauna Loa contain ice on their floors while those tubes located below the snow line do not. Snow accumulates on the Snake River Plain in the winter and the open rift provides a protected spot where it can collect and, in some instances, persist throughout the year. The basalt flows are excellent insulators, demonstrated by the manner in which they retain heat under crusts which form over a still fluid and hot flow. The same quality also acts in an opposite sense, and where snow collects in pits in the basalt, under appropriate

conditions, such as protection from contact with the direct rays of the sun, snow and ice can be preserved for long periods of time. The presence of snow in a large protected cavity in the rock causes the ambient temperature in the cavity to be depressed and this, in effect, results in the formation of a natural ice box. Surface water percolating down through the overlying rock and entering this natural ice box is crystallized by the low temperatures in the cave, resulting in the development of ice formation. However, as the ambient temperature of the cave fluctuates ever so slightly around the freezing point, surface water entering the cavity, as well as melt from the previously formed stalactites, can drip down and freeze, resulting in a gradual buildup of stalagmites from the cave floor. In addition, as the humidity in the cave increases, slight fluctuations in temperature should result in condensation of ice from the vapor phase. Such slow accumulation would result in massive ice columns developing over long periods of time (see Chapter 10).

With modest increases in the temperature, many of these columns begin to alter internally and the ice structure tends to become punky or charged with voids. The water released from the columns in this fashion, as well as other water being added from the ceiling of the cave spreads out on the cave floor, either to persist for a time as a water film on the surface of the already accumulated ice, or to recrystallize as a thin, new surface layer on the ice floor (Fig. 9-4).

The process of ice column accumulation depends on: 1) winter snow and subfreezing temperatures at the surface at least during part of the year, 2) a continuing source of surface water either as winter snows, or even rain, which percolates slowly through the overburden and into the cave, 3) an appropriate cavity or opening in which snow and then ice may accumulate, protected from summer's heat and the direct rays of the sun, and, 4) a slightly fluctuating temperature near the freezing point of water in the cavity (the temperature extremes in the Crystal Ice Cave are 29° – 32.5°F). Many types of ice formations develop in this

FIGURE 9-4. Ice stalagmite in Crystal Ice Cave. (Photograph by James Papadakis.)

environment; however, many of the more delicate features are ephemeral and melt away.

The depth to the water table in this region is 245 m (Table 9-1). The water temperature at that depth is 12.8°C and the air temperature above the water is 15.8°C. Clearly the ice accumulation in the Crystal Ice Cave, as well as other settings in the lava flows where ice accumulates is a near-surface phenomenon, resulting from seasonal variations in temperature and climate at the surface.

Age of the Ice Formations

There is no presently known way to determine the age of the ice columns in the Crystal Ice Cave (C. C. Langway, Jr., personal communication). Where ice is datable, ages are based on seasonal variations in oxygen isotope ratios (O^{18}/O^{16}) or radiometric dating techniques, neither of which is apparently applicable to the cave ice. Even lacking exact ages, however, it is not difficult to accept the fact that massive columns such as those in Crystal Ice Cave do not develop in only a few years. Obviously, the process has been going on for some time, but exactly how long remains unknown at this time. The King's Bowl flow is the youngest flow associated with this portion of the rift and is about 2000 years old (Prinz, 1970). Allowing a generous estimate of up to two hundred years for the vent and surrounding areas to cool after their active period, it seems possible that with similar annual weather conditions to those that exist at the present, the accumulation of ice in the Crystal Ice Cave could go back 1700–1800 years, but this remains speculation.

THE KING'S BOWL

King's Bowl crater resulted, at least in part, from an explosive eruption. The prominent lava mounds (Fig. 9-5) situated around King's Bowl outline the limits of a lava lake which was present prior to the King's Bowl explosive event.

TABLE 9-1
WELL LOG FROM THE CRYSTAL ICE CAVE WATER WELL
Driller: George Vollmer
Elevation at surface at well site: 4932 feet (1503.3 meters)
Source: U. S. Geological Survey

FEET		METERS
0 - 15	Lava - broken, gray	0 - 5
15 - 40	Lava - solid, gray	5 - 12
40 - 73	Lava - broken, red	12 - 22
73 - 80	Lava - hard, gray	22 - 24
80 - 125	Lava - broken, red	24 - 38
125 - 135	Lava - hard, gray	38 - 41
135 - 180	Lava - medium hard, red	41 - 55
180 - 195	Lava - hard, gray	55 - 59
195 - 230	Lava - cinder, brown	59 - 70
230 - 245	Lava - hard, gray and red	70 - 75
245 - 252	Lava - hard, gray	75 - 77
252 - 257	Lava - soft, black	77 - 78
257 - 270	Lava - hard, gray	78 - 82
270 - 279	Lava - broken, red	82 - 85
279 - 315	Lava - hard and broken, gray	85 - 96
315 - 328	Lava - broken, red	96 - 100
328 - 335	Lava - hard and broken, gray	100 - 102
335 - 350	Lava - soft, red	102 - 107
350 - 420	Lava - hard, gray	107 - 128
420 - 445	Lava - cinder, red	128 - 136
445 - 460	Lava - clay and cinder, red	136 - 140
460 - 475	Lava - hard, gray	140 - 145
475 - 500	Lava - medium hard, black	145 - 152
500 - 505	Lava - very hard, gray	152 - 154
505 - 530	Lava - medium hard, gray	154 - 162
530 - 560	Lava - hard, red	162 - 171
560 - 565	Lava - soft, red	171 - 172
565 - 595	Lava - hard, gray	172 - 181
595 - 650	Lava - soft, red	181 - 198
650 - 665	Lava - hard, gray	198 - 203
665 - 675	Lava - soft, red and gray	203 - 206
675 - 680	Lava - cinder, red	206 - 207
680 - 705	Lava - medium hard, red	207 - 215
705 - 715	Lava - broken, gray	215 - 218
715 - 735	Lava - broken, red	218 - 224
735 - 765	Lava - hard, gray	224 - 233
765 - 785	Lava - very hard, gray	233 - 239
785 - 800	Lava - cinders and water	239 - 245

Water temperature at 774 ft (236 m), 55°F (12.7°C)
Air temperature above water at 774 ft (236 m), 60.5°F (15.8°C)
pH of water 7.68

FIGURE 9-5. View across the lava lake near King's Bowl, showing several "lava mounds" on the horizon, considered to be remnants of the lava lake levee. (Photograph by John S. King, SUNY at Buffalo.)

Presumably, the source vent for this lava lake was near King's Bowl crater; possible feeder dikes are visible in the Great Rift at the north end of King's Bowl.

The King's Bowl lava lake was probably fairly short-lived. As lava erupted from the vent, it spread out and, as it became more viscous on cooling, it tended to wrinkle and form ridges at the outer limits of flow. This effect, possibly coupled with deflation of the lake at times and small overflows, is believed to have resulted in the development of natural levees which ultimately contained the lake at estimated depths of from 2 – 3 m, as evidenced by withdrawal levels visible on some of the lava mounds. Although most of the lava mounds are considered to be remnants of one of the two levees, there are local exceptions which do not seem to fit this hypothesis and their relationship to the lava lake is not as yet clearly established. The entire array of lava mounds around King's Bowl is locally referred to as "the Circle of Fire."

Liquid lava which flowed from the vent crusted over quickly as it spread outward over the surface. However, the abundance of large squeeze ups west of the rift at King's Bowl (Fig. 9-6) indicate that molten lava remained present beneath the crusted surface and when fractures developed, the still liquid, but apparently cooling and more viscous, material squeezed up and out to the surface where it solidified in the present globular masses.

Liquid lava ultimately overtopped or broke through the containing levee at many points. This phenomenon is characteristic of both levels of the lake. There were large outflow channels associated with both lake levels through which much of the lava drained. However, flow patterns and channels around many individual mounds indicate that lava also flowed out between these levee remnants. The explanation for such a drainage remains obscure, although tumescence of

FIGURE 9-6. View across the lava lake surface showing numerous squeeze ups, some more than 1 m across; lava mounds are in the background. (Photograph by John S. King, SUNY at Buffalo.)

the lake flow prior to the King's Bowl explosive event is a distinct possibility. The distribution of the lava mounds suggests that in some way they were more resistant portions of the levee than the intervening sections which were removed.

The explosive event at King's Bowl followed or may even have contributed to the breakout of the lava lake. In the explosive event, the ejecta consisted of both large blocks and a lapilli-ash. On the west side of the rift, ejecta makes up a block field composed of fragments more than 100 cm close to King's Bowl to 5 to 10 cm at a distance of 245 m in a line due west of King's Bowl. Jaggar (1949) believes that such explosions must be the result of interaction of ground water with magma. In the initial movement of magma to the surface, the lava seals itself off from the water table and maintains that seal by outward pressure as long as its hydrostatic head is above the water table. However, on withdrawal of the lava, water may break into the conduit, resulting in a rapid generation of gas. Jaggar feels that accumulation of the gas of such an interaction is necessary to have an explosion – ". . . confinement is a first essential for steam pressure." Macdonald (1972) indicates, however, that violent eruptions are more often the result of a rapid generation of gas than they are the result of accumulation. He further points out that most volcanic explosions are really a sustained outrushing of gas measurable in seconds, minutes, or even hours. While no clear evidence is available in the case of King's Bowl crater, it is likely that the rapid generation of gas was possibly coupled with a restriction of outflow of some sort.

The outrushing of gas at King's Bowl may or may not have been preceded by a single violent explosion which carried larger blocks to the surface. It is possible that sufficient pressure was sustained in the outrushing process to pluck even the larger blocks from the walls and carry them out. Whatever the case, lapilli ash tephra was apparently winnowed out by prevailing west winds and carried east of the rift. When the larger blocks fell on the west side, many of them broke through already formed crust of the lake, as well as squeeze-ups. This relationship of bombs to crust and squeeze ups identifies a partial sequence of the eruptive events. It is common to find impact holes in the solidified lava with radiating fractures extending out from them (Figs. 9-7 and 9-8). In some instances, the impacting projectile can

FIGURE 9-7. Small ejecta block thrown from the phreatic explosion that created King's Bowl. The lithic block impacted the crust of the lava lake before it had cooled completely, penetrating the crust to form radial fractures. (Photograph by Ronald Greeley, University of Santa Clara, 1974.)

color is rendered by the presence of large subhedral to anhedral crystals of plagioclase. The lapilli particles themselves are angular to subround in shape and vary from open scoriaceous to a very dense texture. Even when the washed sample has been thoroughly dried, the surface of all grains appear to have a highly reflective, varnish-like veneer. Some of the dense, dark particles give the appearance of being wet. Close examination reveals, however, that this veneer uniformly covers the grains, even being visible on the plagioclase crystal fragments and lining the open scoria cavities.

In thin section, the lapilli grains retain their heterogeneous character. Most of the particles are holocrystalline fragments with the common mineral paragenesis being plagioclase (An_{72-74}) and olivine. A variety of textures characterizes the holocrystalline fragments with the common mineral paragenesis being plagioclase (An_{50-52}), pyroxene, olivine, and an opaque mineral. Some grains are made up of plagioclase laths disseminated in a very fine-grained crystalline matrix. Although no detailed petrographic analysis has yet been made of the lapilli grains, an attempt was made to establish the character of the glassy veneer seen on the washed grains. Even under the highest petrographic magnification (400 x), little could be determined. There appears to be a very thin rind on each particle that is apparently crystalline as it appears birefringent between crossed nicols. A gypsum plate showed that the rind behaved much as a single crystal as the interference color was uniform around the periphery of each grain. It is apparent that more work should be carried out on the lapilli of King's Bowl to (1) detail its exact extent and thickness, (2) determine the size distribution of particles, and (3) define its petrographic characteristics more exactly.

From what is already known about the lapilli, however, it is apparent, based on its lithic character and heterogeneity, that it was derived from a variety of superimposed flows (now exposed in the sides of the rift) during the King's Bowl phreatomagmatic eruption. The lapilli deposits seem to be quite local and of limited thickness, suggesting a tephra ejection event of very short duration.

Volume of Ejecta; The Development of The King's Bowl Crater

A considerable volume of material has been ejected from the King's Bowl crater. However, even if one imagines a throw-out field defined by the maximum distance of ejected lithic fragments (245 m) and the length of the King's Bowl crater (90 m) and assumes it to be covered by an uniform blanket equivalent in depth to the largest blocks presently found nearest King's Bowl (1.5 m), the calculated volume plus the estimated volume of lapilli and ash falls far short of that needed to refill the King's Bowl cavity. This indicates that the King's Bowl crater is not simply the result of forceful ejection of material due to phreatomagmatic eruption. The conclusion must instead be reached that much of the missing volume has collapsed back into the vent.

SUMMARY

The Idaho Rift is made up of a series of rift sets of varying trend and age. One of these rift sets, the King's Bowl rift has many unique aspects associated with it. The Crystal Ice Cave is a natural ice box resulting from subfreezing surface temperatures and snow during part of the year. Some of the snow accumulates in a protected area in the rift; spring melt water and possibly rain percolating through the lava into this cold setting resulted in an accumulation of ice columns and a variety of ice stalagmites and stalactites. The ice accumulation is a recent event but conceivably could mark a process that was initiated as much as 1800 years ago. Development of the Crystal Ice Cave has opened access of the rift to a depth of 46 m.

King's Bowl crater is an explosion vent on the King's Bowl rift. It is one of several vents on the rift that erupted small lava flows. King's Bowl is unique in that it is the largest explosion crater along the rift. Lava flows erupted from the

FIGURE 9-8. Squeeze up with a hole formed by the impact of an ejecta block from King's Bowl. Scale is 10 cm long. (Photograph by John S. King, SUNY at Buffalo.)

still be found in place beneath the crust, while in other instances, the ejected blocks are wedged into fractured crust and squeeze ups which they did not fully penetrate.

King's Bowl Lapilli-ash

The lapilli-ash tephra from the King's Bowl is concentrated on the east side of the rift (Figs. 9-1 and 9-9). In a sample taken from the surface in the vicinity of one lava mound, buff-colored lapilli particles range in size from less than 1 mm to about 28 mm, although most particles are less than 5 mm in size. The characteristic color of the lapilli is caused by a coating of fine, light brownish dust. This finer material washes off the larger particles readily and, lacking it, the particles are seen to be quite heterogeneous. The color of the lapilli is either black or red, although on some a lighter gray

FIGURE 9-9. Vertical aerial photograph of the King's Bowl lava field showing the distribution of ash and other tephra (light-toned area) associated with King's Bowl; arrow marks the entrance to Crystal Ice Cave. (U. S. Department of Agriculture Photograph CYN-78-103.)

FIGURE 9-10. View across King's Bowl lava field showing lava lake crust, drainage of lake and devolatilization resulted in subsidence of the crust, causing it to break into large, irregular slabs. Edge of flow is visible near the horizon. (Photograph by Ronald Greeley, University of Santa Clara, 1975.)

fissure at King's Bowl were briefly held in a lava lake (Fig. 9-10), the location of which is marked by two confinement areas indicated by lava mounds, believed to be remnants of the confining levees of the lava lake. The King's Bowl phreatomagmatic eruption occurred following emplacement, crusting, and fracturing of the lava lake. Block and bomb-sized ejecta directed toward the west in many instances broke through crustal plates of the lava lake, as well as penetrating lava which had squeezed up through fractures in the crustal plates. Lithic lapilli-sized fragments were carried eastward of the rift by prevailing west winds. It appears that there exists a greater void in the King's Bowl crater than can be accounted for by the volume of ejecta, indicating an internal collapse during and following cessation of eruptive activity at the King's Bowl vent.

REFERENCES

Greeley, R. and J. S. King, 1975. Rift zones in the south-central Snake River Plain, Idaho: Geol. Soc. Amer. abstracts with program, vol. 7, no. 5, p. 610-611.

Halliday, W. R., 1976. Depths of the Earth. Harper and Row, New York, 432 p.

Jagger, T. A., 1949. Steam blast volcanic eruptions: Special Report of Hawaiian Volcano Observatory, 137 p.

Macdonald, G. A., 1972. Volcanoes. Prentice Hall, Englewood Cliffs, N. J., 510 p.

Prinz, M., 1970. Idaho Rift System, Snake River Plain, Idaho: Geol. Soc. America Bull., vol. 81, p. 941-948.

10. STRUCTURE OF AN ICE STALAGMITE FROM CRYSTAL ICE CAVE, IDAHO

Erick Chiang
Ice Core Laboratory
State University of New York at Buffalo
Amherst, New York 14226

10. STRUCTURE OF AN ICE STALAGMITE FROM CRYSTAL ICE CAVE, IDAHO

Erick Chiang
Ice Core Laboratory
State University of New York at Buffalo
Amherst, New York 14226

An ice stalagmite from the Crystal Ice Cave in Idaho was collected and returned to the Ice Core Laboratory in Buffalo for petrographic examination. The ice was taken from the Idaho rift at a depth of 46 m from a location just north of the "Hanging Balcony" (J. S. King, personal communication). Temperatures within the cave fluctuate around 0°C (± 0.5°C) while surface temperatures during the summer often range from 32° to 38°C. Runoff from the previous winter's melting snow seeps into the cave contributing to the continuing development of the ice forms.

The general investigation of cavern ice, in particular stalactites and stalagmites, has been primarily conducted in the U.S.S.R., discussed in Dorsey (1940) and Shumskii (1964). Shumskii compiled all natural occurrences of ice types in a genetic classification in which stalactites and stalagmites are included as a form of *congelation ice* within the subgroup of extruded ice. Such ice is formed primarily by the "freezing of water draining along a (cold) solid surface." The type ice referenced is found in the Kungar Ice Caves in the Ural Mountians.

The crystal structure of the stalagmite from the Crystal Ice Cave was examined to determine in which of two ways growth proceeded: 1) that of rapid and sporadic freezing, or 2) that of slow and continuous freezing. If the ice developed in the former manner, it would be cloudy and possibly concentrically layered due to entrapment of air bubbles between the layers. Crystallization would produce many small individual ice grains with their optic axes in random orientation. If, however, the ice formed as a result of a slow and continuous process, it would be transparent due to the gradual expulsion of all dissolved air. Large single crystals would be able to develop through migratory recrystallization and the orientation of the optic axes of the newly accreted ice would be parallel to the optic axis of the parent crystal. These processes eventually produce a single, optically uniform crystal.

Initial observations of the small stalagmite of ice (Fig. 10-1) from the Crystal Ice Cave show it to be clear and essentially bubble-free (0.915 gm/cm^3 vs 0.9165 gm/cm^3 for bubble-free ice at 0°C, Dorsey, 1940) but interspersed with soil particles and macro scale fractures. This suggests that the ice formed through a slow and continuous process. The clarity of the ice makes it possible to trace the individual crystal boundaries through thick sections when they are placed under crossed polaroids (Fig. 10-2). A further examination of the optical characteristics detail the internal structure and development of the stalagmite.

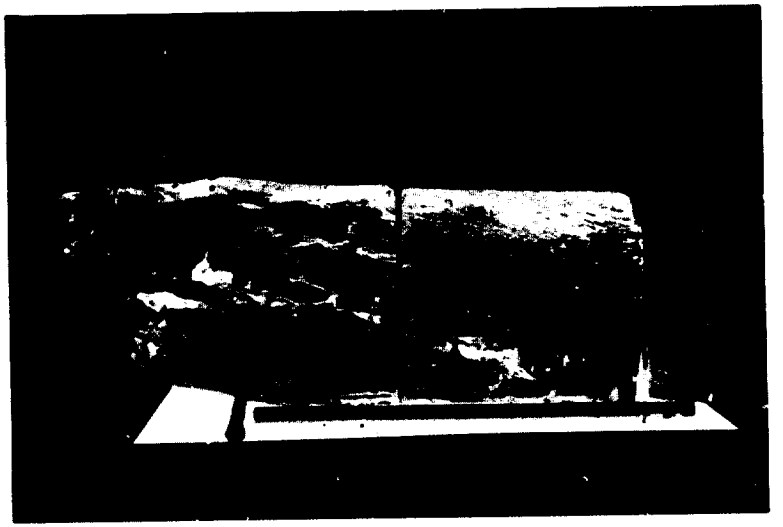

FIGURE 10-1. The ice stalagmite sample. The sample is 30 cm long x 13 cm diameter.

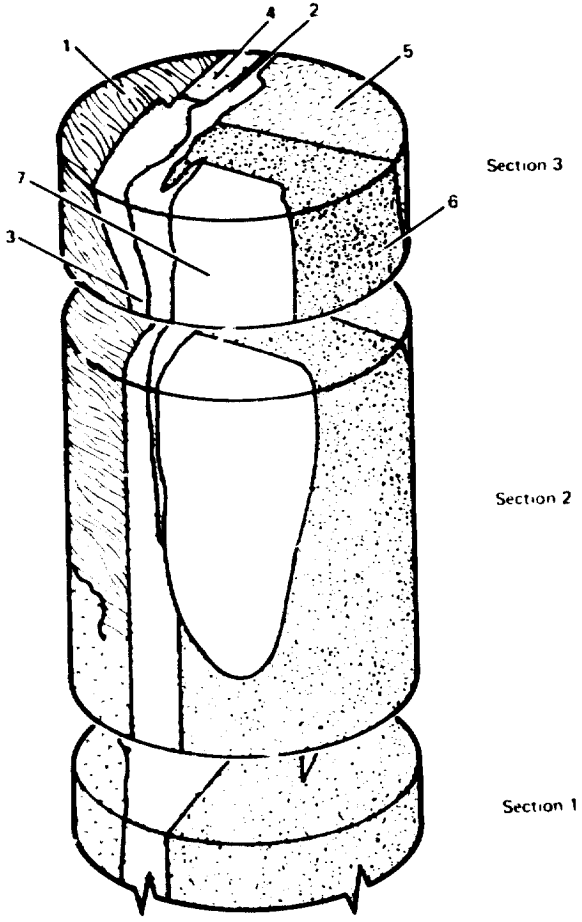

FIGURE 10-2. Diagram of ice stalagmite sample.

LABORATORY PROCEDURE

Three horizontal cuts were made through the sample, of which two are shown in Figure 10-1. The third cut was made approximately midway between the tip of the stalagmite and top of section 2 (Fig. 10-2). Horizontal thin sections were prepared from the bottom and top of section 2 and 3 respectively and placed under crossed polaroids and photographed (Figs. 10-3 and 10-4).

FIGURE 10-3. Horizontal thin section of the basal ice structure as seen through crossed polaroids.

A fourth vertical cut was made through section 2, normal to the grain direction (trend of elongation in the horizontal plane) to demonstrate a portion of the intercrystalline boundary relationships (Fig. 10-5). A superposition of the thin section photographs along with the observation of the crystal outlines made possible the depiction of the ice sample and its internal structure (Fig. 10-2).

The thin section prepared from the top of section 3 (Fig. 10-4) exhibited the greatest number of individual crystal boundaries. The crystal boundaries can be distinguished through rotation on a Rigby universal stage. Seven separate bounded forms were recognized by this method (Fig. 10-2). Sections labeled 1 and 2 are optically uniform as are sections

FIGURE 10-4. Horizontal thin section of the ice structure as it appears near the top of the sample. Similarity in color indicates similarity in optical uniformity.

4 and 5. The azimuth extinction angles for sections 3, 6, and 7 vary from those of 4 and 5 by 6, +2 and -2° respectively. Orientation measurements performed on the separate grains indicate that the optic axes of all the crystals are oriented in the horizontal plane. The crystal boundaries of sections 1 and 2 coincide with the fracture planes observed in the sample.

FIGURE 10-5. A vertical thin section through the center of section 2, as seen through crossed polaroids.

RESULTS AND DISCUSSION

The entire sample is composed of seven or eight large crystals which exhibit a complex intercrystalline boundary structure. The crystals are nonuniform in shape but are strongly oriented in the vertical direction.

The results of the orientation measurements indicate that all the crystalline forms are close to behaving as if they were optically uniform, i.e., as a single large crystal, with the exception of sections 1 and 2, which although showing horizontal orientation, lie in the N–S plane, 90° removed from the remaining crystals in the stalagmite.

It is considered th:t the crystals are secondary features which resulted from ongoing accretion and migratory recrystallization. Continued internal alteration would most readily proceed along the fine boundary lines (marked by small differences in extinction angles) separating section 5 and 6, and section 6 and 7 (Fig. 10-2).

REFERENCES

Dorsey, N. E., 1940. Properties of Ordinary Water-Substance. Reinhold Publishing Corp., New York, 673 p.

Shumskii, P. A., 1964. Principles of Structural Glaciology. Dover Publications, Inc., 497 p.

11. GUIDE TO THE GEOLOGY OF KING'S BOWL LAVA FIELD

Ronald Greeley
Department of Geology and
Center for Meteorite Studies
Arizona State University
Tempe, Arizona 85281

Eilene Theilig
Department of Geology
Arizona State University
Tempe, Arizona 85281

John S. King
Department of Geological Sciences
State University of New York at Buffalo
Amherst, New York 14226

11. GUIDE TO THE GEOLOGY OF KING'S BOWL LAVA FIELD

Ronald Greeley
Department of Geology and
Center for Meteorite Studies
Arizona State University
Tempe, Arizona 85281

Eilene Theilig
Department of Geology
Arizona State University
Tempe, Arizona 85281

John S. King
Department of Geological Sciences
State University of New York at Buffalo
Amherst, New York 14226

The King's Bowl lava field (Greeley and King, 1975 and Chapter 9) is one of the youngest flows on the Snake River Plain, having been dated at 2130 ± 130 years B.P. (Prinz, 1970) on the basis of charcoal recovered from beneath one of the flow units (Fig. 11-1). Despite the small size of the field, it exhibits an abundance of fresh basaltic features, including spatter cones, feeder dikes that can be traced vertically from the fissure into the flow, drainback of lava into the fissure, squeeze-ups, "grooved" lava, cross cutting relations of lava and fractures, overlap relations of flow units, and a phreatic explosion crater. Thus, in a relatively short period of time (and distance) a wide variety of volcanic features can be seen.

The King's Bowl lava field is a compound, fissure-fed lava flow that was erupted both as sheets of lava from the fissure and as localized eruptions from numerous point sources along the fissure, identified by small spatter cones. Overlap relations of flow units show that different parts of the fissure were active at different times; however, the separation in time may have been a matter of only hours.

Some of the flow units were impounded as lava lakes contained by self-constructed natural levees. In some cases the lava broke through the levees, flowed to a lower level (5 to 10 m lower) and formed "perched" lava lakes. Repeated activity of this type resulted in terraced lava lake surfaces. This is particularly apparent in the flows east of South Grotto where at least four terraces can be recognized (Fig. 11-2).

Although the tour over the field could begin and end almost anywhere, the convenient place to start is at the visitor facility at Crystal Ice Cave, where permission should be obtained to walk off the main trails. *Please note* that a certain amount of care should be exercised in walking across the lava to protect yourself (the lava is rather sharp and jagged, and there are deep holes and cracks in the field) and to preserve the fragile volcanic features.

Several walking tours of the King's Bowl lava field are feasible, depending on the length of time available. In order of increasing lengths, possible tours are given in Table 11-1. Figure 11-3 is a geologic map of the field; Figure 11-4 is an aerial photograph showing station numbers.

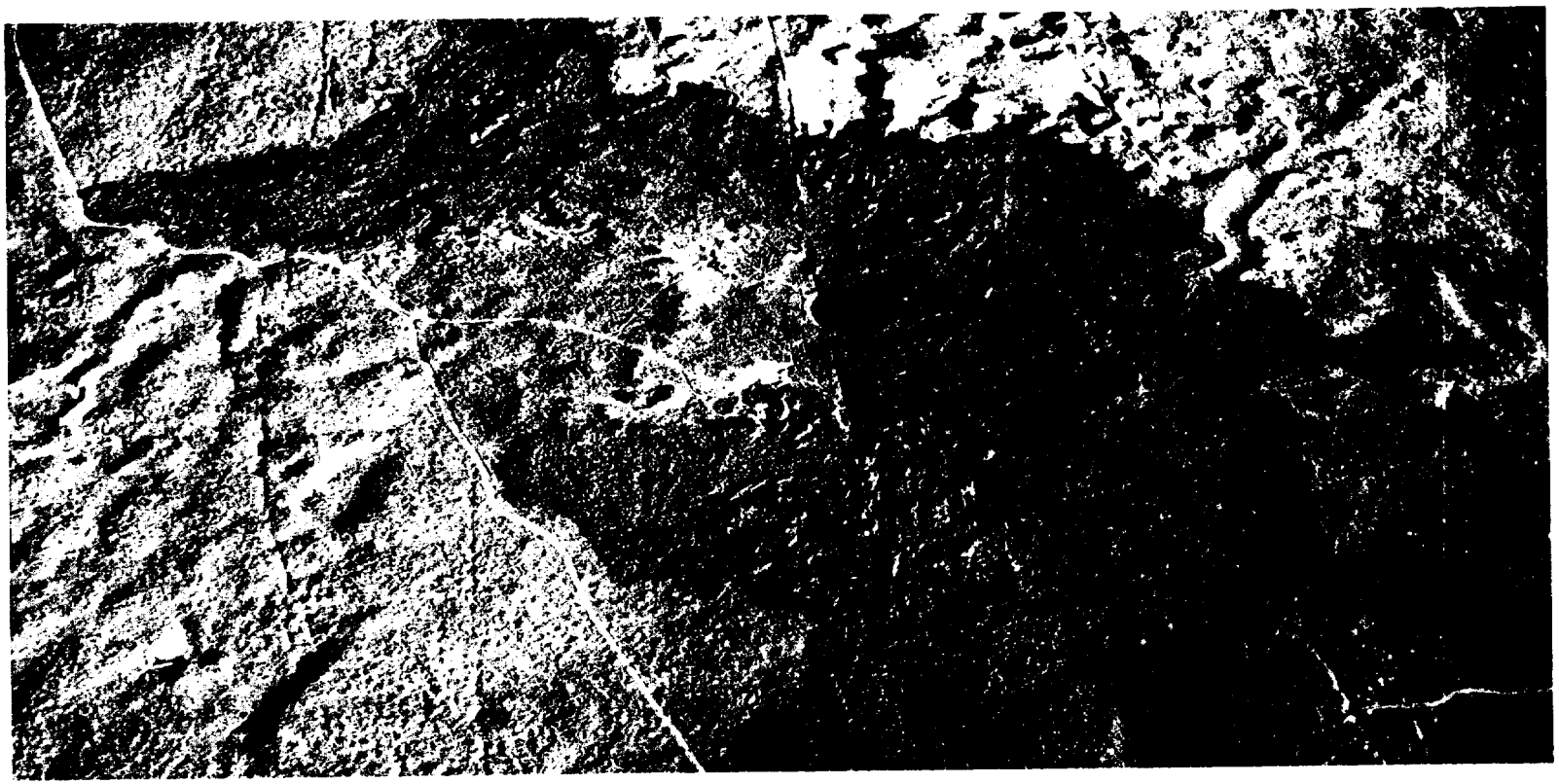

FIGURE 11-1. Oblique aerial view southward of part of the King's Bowl Flow, the main fissure and sets of parallel extensional fractures that have been covered by lava. NASA-Ames photograph by Ronald Greeley, 1969.

FIGURE 11-2. View southwestward of South Grotto, the southern end of the King's Bowl lava field (Station 11), showing several perched lava lakes (light-toned areas) contained by lava levees; linear features in foreground are extensional fractures that parallel the main fissure. Spatter cones mark the main fissure. Photograph by Ronald Greeley, University of Santa Clara, June, 1977.

TABLE 11-1
GEOLOGIC TOURS OF THE KING'S BOWL LAVA FIELD

Key (Figs. 11-3, 11-4)	Features	Time and Distance
1. Stations 1, 4, 5	Lava "mounds," channel-flow, lava lake crust, squeeze-ups, ejecta block field, phreatic eruption crater, vesicle cylinders, compound lava flows, feeder dikes	1.5 hours, 1 km
2. Stations 1, 2, 3, 4, 5	As above, plus lava lake levee, superposed fresh flows, tensional fractures, age relations of flows and fractures	2.5 hours, 2.3 km
3. Stations 1, 2, 2A, 3, 4, 5	As above, plus a lava lake	3.5 hours, 3.9 km
4. Stations 1, 2, 3, 4, 5, 6, 7, 14	Same as 2 plus drainback of lava into fissure, change in flow texture at flow front, exposure of tephra	4 hours, 3.7 km
5. Stations 1-14	Same as 4 plus *en echelon* fissure; spatter ramparts; terraced, "perched" lava lakes	All day, 6 km

STATION 1 (Viewing area Crystal Ice Cave)

This station gives a good overall perspective across the field (Fig. 11-5). The view west and southwestward is across the surface of a former lava lake. The rock platform is built of material excavated from the Ice Cave tunnel and piled on one of the *lava mounds* (see Chapter 9). Although the origin of these mounds is not wholly resolved, some appear to be remnants of a levee that contained a lava lake. Several lava mounds are visible north of the lookout and on the horizon; examination of their distribution (Fig. 11-4) shows the possible relationship to the former lava lake.

Leave the lookout and walk north along the fissure, noting the different flow units. At least two, and possibly three, thinly bedded flow units overlie pre-rift, massive flows. The swirling pattern observed in some of the young flow units is characteristic of near-vent areas (see Fig. 11-6 and Station 5) and are collapsed shelly pahoehoe flows, similar to those described by Swanson (1973). The contact between the pre-rift flow and the younger fissure flows is marked by a prominent soil horizon which often supports vegetation in the rift. It is from this soil horizon that charcoal was obtained for the C^{14} date for the King's Bowl flows. This date applies to the earliest flow unit in the vicinity of King's Bowl.

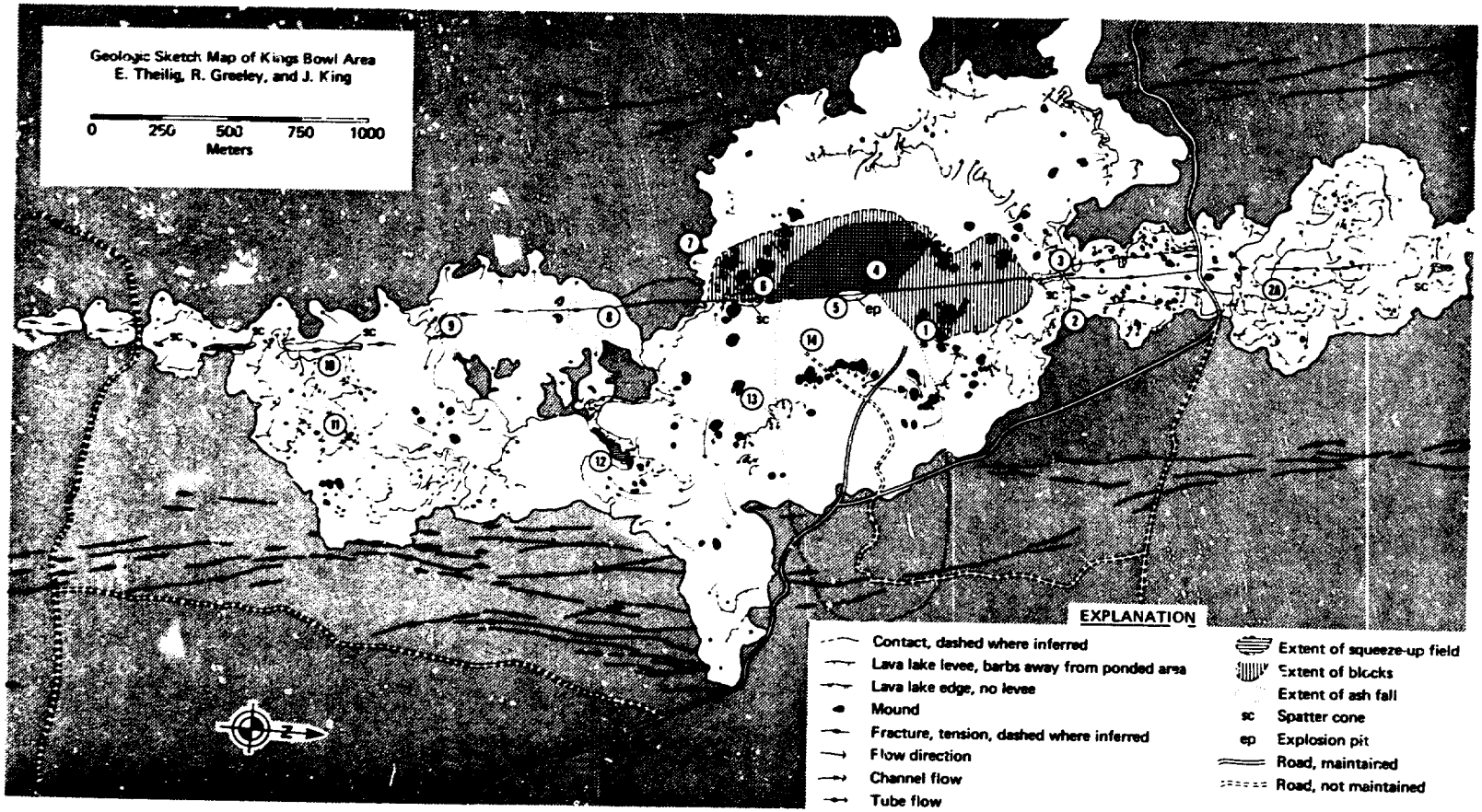

FIGURE 11-3. Geologic sketch map; circled numbers are keyed to text.

FIGURE 11-4. Aerial photomosaic corresponding to Figure 11-3. NASA-Ames photographs 878-2-15,16,17; October, 1968.

FIGURE 11-5. Oblique aerial view westward across the Crystal Ice Cave visitor center and the King's Bowl fissure; arrow marks Station 1 (visitor overlook); dark hills are lava mounds. Photograph by Ronald Greeley, University of Santa Clara, June, 1977.

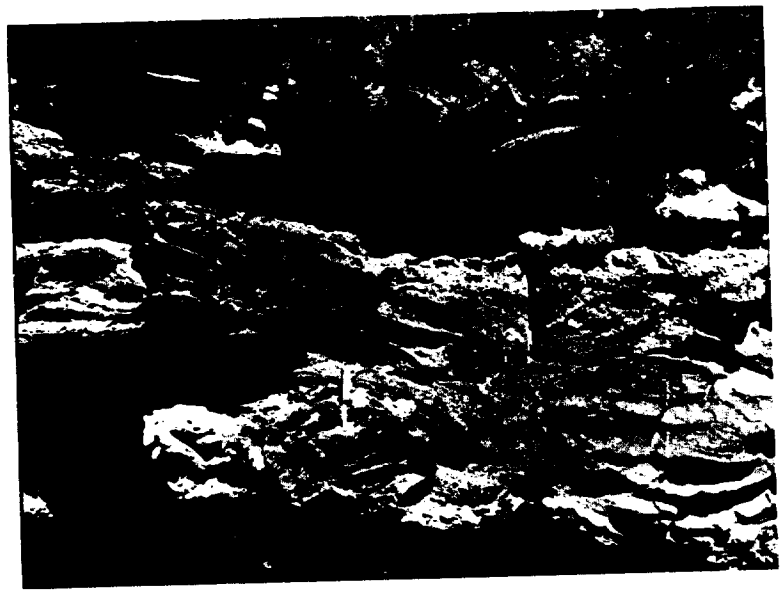

FIGURE 11-6. Swirling pattern in thin flow units exposed in the wall of King's Bowl (Station 5); the pattern represents collapsed shelly pahoehoe blisters, as described by Swanson (1973) in Hawaii. Pocket knife indicates scale.

Note the vertical gouges and grooves in the walls of the rift (Fig. 11-7), formed by phreatic eruption(s) from the rift. Blocks and smaller sized tephra can be seen on both sides of the fissure in this area. Continue along the fissure to Station 2.

FIGURE 11-7. Vertical grooves and gouges (arrows) in the wall of the fissure formed by ejecta from phreatic eruptions (near Station 1).

STATION 2

The age relationship of the younger King's Bowl flow to the older King's Bowl flow is apparent here by superposition. Note that the inner set of fractures cut the older flow and is in turn overlapped by the younger lava lake flow, indicating that extension occurred in the time between the emplacement of the two flow units. Follow the fissure northward across the road to Station 2A.

STATION 2A

This station marks the Creon's Cave area which includes a small lava lake, a small spatter cone, and several "perched" lava ponds. The flows from this eruption center also postdate the older flow that has been cut by the inner fractures. The Creon's Cave flows may be contemporaneous with the lava lake at Crystal Ice Cave, but as the two are not in contact, the exact age relation cannot be determined.

Several small flows which erupted from "point sources" can be seen along the fissure an additional 2 km north of this area.

Return south along the fissure to Station 3.

STATION 3

Levees constructed by lava lake activity are well displayed here. As observed in active flows in Hawaii (Fig. 11-8a,b), momentary halts in advancing flow fronts cause lava to congeal and become fixed in place so that it forms a barrier to later surges in the flow. Mobile crusts on the flow, however, are often shoved over the congealed flow front by the surge and pile up, plate by plate, to form a levee. Occasional lava overflow of the juvenile levee forms lava tubes and channels (as seen here), adding to the levee. Thus, under certain conditions, substantial levees are built.

Proceed southward along the fissure to Station 4.

FIGURE 11-8a. An actively growing levee, Mauna Ulu, Hawaii; tongues of pahoehoe are overflowing the levee at many points. This levee consists mostly of such tongues, although some plates of crusted lava from the lake surface have been pushed to the top of the levee as well. The fountain feeding this lake is visible in the upper left. Photograph by R. T. Holcomb, U. S. Geological Survey, January 21, 1974; from Holcomb and others, 1974.

FIGURE 11-8b. Lava lake levee forming at the Mauna Ulu summit by accretion of slabs of lake crust that are shoved laterally. Photograph by Ronald Greeley, University of Santa Clara, November, 1973.

STATION 4

Four features are of particular interest in this area: lava mounds, the lava lake surface, ejecta blocks and squeeze-ups. The lava mounds are all at about the same level, possibly indicating an origin related to the lava lake. Note the "flow-outs" between the mounds. The lava lake crust is very smooth and flat in this area. As the lava lake subsided by outflow, degassing, and drainback into the fissure, the crust settled and was broken into the plate-like masses observable

today. Squeeze-ups are the bulbous masses of lava (Figs. 11-9 and 11-10) ranging in size from 0.5 m to more than 2 m across; many are hollow. The squeeze-ups resulted from molten lava oozing through cracks on the lava lake crust, possibly in response to the pressure generated by the crust as it subsided.

FIGURE 11-9. Field of lava squeeze-ups on the King's Bowl flow. Many of the squeeze-ups are hollow, and some have been impacted by ejecta from King's Bowl. Squeeze-ups range from 0.2 to more than 1.0 m across. Several "lava mounds" are on the horizon. Ejecta blocks (arrow) litter the surface.

FIGURE 11-10. Linear squeeze-up formed on the crust of the lava lake, Station 4.

Lithic blocks are scattered over this general area, increasing in frequency toward the fissure. The largest blocks are more than 2 m across and are found nearest King's Bowl. Although blocks (Fig. 11-11) are found on both sides of the fissure, they are prevalent on this, the west side. This is due, first, to their partial burial in tephra on the east side (described at Station 5) and, second, to a "sport" of a few years ago, before the area was declared a National Landmark, when

FIGURE 11-11. View across the King's Bowl lava flow showing part of ejecta block field that resulted from the phreatic explosion of King's Bowl. Blocks range up to 2 m across. "Lava mounds" are on the horizon.

FIGURE 11-12a. Small ejecta block (left of pocket knife) thrown from King's Bowl which impacted the still-molten lava squeeze-up, indicating nearly contemporaneous phreatic explosion and lava effusion.

"four-wheelers" would push blocks into King's Bowl and into the fissure (J. Papadakis, personal communication). Blocks on the west side were protected by their relative inaccessibility.

The blocks were thrown out by phreatic eruptions, contributing to the creation of King's Bowl in the process. Many of the blocks penetrated squeeze-ups and parts of the lava lake crust when the lava was still plastic, indicating near-contemporaneity of the lava effusion and phreatic activity (Fig. 11-12).

Cross the fissure (*take care*) and proceed to Station 5.

STATION 5

This station is a tourist overlook for King's Bowl (Fig. 11-13, Chapter 9) which is a 85 m long, 30 m wide, 30 m deep crater on the main fissure, formed partly by a phreatic explosion. The depression was enlarged by collapse, perhaps in

FIGURE 11-12b. Ejecta block that impacted the lava lak[illegible] crust.

FIGURE 11-13. Aerial view of the Crystal Ice Cave visitor center and King's Bowl, a phreatic explosion crater; numbers refer to stations in the field guide. Photograph by Ron Papson, University of Santa Clara, June, 1977.

response to withdrawal of magma. The small hole at the north end of the crater near the tourist wall displays a feeder dike in the fissure that can be traced laterally into the King's Bowl flow (Fig. 11-14).

The surface from the fissure eastward across the flow has been blanketed by fine-grained tephra erupted during the phreatic explosions. Prevailing westerly winds caused its deposition to the east.

Follow the trail southward to the entrance of King's Bowl and descend into the crater. The walls of the crater provide an excellent opportunity to observe Snake River Plain lava flows in cross section (Fig. 3-4), a rare occasion in an area so little eroded. At the point where the trail enters the crater (south end of crater on east side), the upper flows show a swirling pattern (Fig. 11-6). This has been described by Swanson (1973) as resulting from the collapse of fragile shelly pahoehoe, a flow variety characteristic of near-vent activity where devolatilization creates gassy blisters in the lava. Subsequent lav[illegible] on the top of the blisters cause them to collapse, producing the texture observed here.

A prominent soil horizon is visible at a lower level. This horizon can be traced laterally along the wall and gives some appreciation of the hummocky surface of the older lava flow and the wide variation in soil thickness. Beneath the soil horizon is a massive compound flow composed of several flow units. Note the vesicle patterns (Fig. 11-15) in these units.

FIGURE 11-14. View of dike-filled rift near King's Bowl overlook. Dike-lavas are clearly seen feeding the King's Bowl lava flow, both to the west (beneath figure) and to the east. "Lava mounds" are on the horizon.

FIGURE 11-15. Vesicle cylinders exposed in the wall of King's Bowl.

At the bottom of the trail, a dike is exposed in the fissure in the north end of the crater (Fig. 11-16). Proceed (with care) over the rock pile northward into the fissure to observe the grooved walls of the fissure.

Retrace the trail out of the crater and continue south along the fissure to Station 6. Note the drainback of the lava into the fissure (Fig. 11-17). In some places, drainback formed small lava tubes which emptied into the fissure.

STATION 6

This area marks several lava mounds (Fig. 11-18) and the southern boundary of the innermost lava lake (Chapter 9). Note the channelled flow between the mounds.

STATION 7

This area marks the edge of the young flow. Note the stratigraphic relations of the two flows in contact and the rugged relief on the older flow, then extrapolate that relief beneath the younger flow and compare with observations made of the flow cross sections in King's Bowl Crater.

This station is near one of the several prominent pressure ridges formed in the older flow. Pressure ridges typically have a medial fracture along their axes.

Follow the flow contact back to the fissure and continue to Station 8.

FIGURE 11-16. View of the dike in the fissure at the north end of King's Bowl.

FIGURE 11-17. North end of main part of King's Bowl flow, showing part of flow that drained back into the fissure (dark area); figure is on a levee formed on a channel that emptied into fissure. Summit of Grand View low shield is on horizon.

STATION 8

Examine the aerial photograph of this area (Fig. 11-4) and note the "blurred" appearance of the surface deail. This area is blanketed by ash which was probably erupted from the fissure. It has not been determined if this eruption was contemporaneous with the phreatic eruption of King's Bowl; however, the ash field appears to be overlain by the King's Bowl flow.

FIGURE 11-18. View of a typical lava mound on the King's Bowl Flow. Lava mounds range from about 1.5 to 3.5 m high and are "plated" with smooth pahoehoe lava.

STATION 9

At this point, the prominent fissure ends. Walk eastward a few dozen meters to pick up the next segment. This *en echelon* arrangement of fissures and fractures is typical along the rift sytem.

STATION 10

This station is identified by the series of prominent spatter cones aligned over the fissure (Fig. 11-2). The southernmost spatter cone has been breached to the south and east by subsequent flows. South Grotto is the area where the greatest descent was made into the rift (Prinz, 1970). From this area, the fissure may be traced southward an additional 1-2 km beyond the road where small, isolated flow units and spatter cones are present.

STATION 11

From Station 10 to Station 11, the path descends a series of lava lakes arranged in terraces. Note the levees and flow-out relations from one lake to the next (Fig. 11-2). Squeeze-ups are present on many of the lakes (Fig. 11-19).

FIGURE 11-19. Slab of grooved lava that was thrust up through the crust as a squeeze-up on one of the lava lakes in the South Grotto area (Station 11).

STATION 12

Contact between the flows from the King's Bowl area and fissure flows from South Grotto is seen here (Fig. 11-20). The age relations between flow units are not always clear. Observations of active flows in Hawaii (Fig. 11-21) show that young flows sometimes squeeze beneath older flows; thus, apparent superposition of flow units along the contact may not be a reliable indication of age.

East of this point, the fissure flows cover the outer set of extensional fractures (note on aerial photograph).

FIGURE 11-20. Oblique aerial view northwestward across the King's Bowl field, showing the contact between the King's Bowl flows (solid arrows) and the flows from South Grotto (open arrow) at Station 12; arrows indicate flow direction.

FIGURE 11-21a. Fresh pahoehoe flow from Mauna Ulu, Hawaii, showing edge of flow that is raised above the surface, evidently as a result of contraction during cooling. Later flows can push beneath raised flow margins, as shown in Figure 21b. Photograph by Ronald Greeley, University of Santa Clara, August, 1971.

FIGURE 11-21b. Contact relation of two flows on Mauna Ulu, Hawaii. Younger flow (platy texture on left) has shoved beneath older flow on the right.

STATION 13

This station marks the levee of the lava lake associated with King's Bowl.

STATION 14

Borrow pit in the tephra, showing thickness of ash in this area to be about 1 m. Tephra ranges in size from ash to lapilli (pea-gravel sized; see Chapter 9). The rounded masses to the east are "mounds" that have been blanketed by tephra.

Continue to parking lot. End of trip.

REFERENCES

Greeley, R. and J. S. King, 1975. Geologic field guide to the Quaternary volcanics of the south-central Snake River Plain, Idaho: Idaho Bur. Mines and Geology, Pamphlet 160, 49 p.

Holcomb, R. T., D. W. Peterson, and R. I. Tilling, 1974. Recent landforms at Kilauea volacano–A selected photographic compilation *in* Greeley, R., ed., Geologic Guide to the Island of Hawaii: A field guide for comparative planetary geology: NASA CR 152,416, p. 50-86.

Prinz, M., 1970. Idaho Rift system, Snake River Plain, Idaho: Geol. Soc. Amer. Bull., vol. 81, p. 941-947.

Swanson, D. A., 1973. Pahoehoe flows from the 1969-1971 Mauna Ulu eruption, Kilauea volcano, Hawaii: Geol. Soc. Amer. Bull., vol. 84, p. 615-626.

12. THE ORIGIN OF SPLIT BUTTE, A MAAR TYPE CRATER OF THE SOUTH-CENTRAL SNAKE RIVER PLAIN, IDAHO

Michael B. Womer
Department of Geological Sciences
State University of New York at Buffalo
Amherst, New York 14226

12. THE ORIGIN OF SPLIT BUTTE, A MAAR TYPE CRATER OF THE SOUTH-CENTRAL SNAKE RIVER PLAIN, IDAHO

Michael B. Womer
Department of Geological Sciences
State University of New York at Buffalo
Amherst, New York 14226

Split Butte is a volcanic structure of recent origin located in the south-central Snake River Plain at latitude 43°N, longitude 113°20' W. It lies approximately 13.5 km west of King's Bowl and 22 km north of the Snake River. The Butte overlies basalt flows of the undifferentiated Snake River Group, which are Upper Pleistocene to Recent in age.

The surface of the flows in the south-central plain are typically of low relief and locally slope about 6.0 m per km from northeast to southwest. The lavas were probably very fluid, as indicated by the low slopes and large areas covered by the flows. A single flow may cover several hundred km^2 of the plain (Stearns, Crandall and Steward, 1938). Russell (1902) estimated the thickness of the individual flows in the Snake River Group at 50 to 80 m; however, Stearns, Crandall and Steward (1938) estimate thicknesses of 3 to 25 m for most of the flows. The nearby Wapi lava field basalts flow over fissures of the King's Bowl fracture set (Champion, 1973) which implies that they are among the most recent flows in the area. The recent origin of the King's Bowl fracture set is indicated by the age of one of the earliest flows to emanate from it, which has been dated at 2130 ± 130 years (Prinz, 1970). The young Wapi flows encroach upon Split Butte from the southeast, indicating that the Butte predates the Wapi.

A veneer of loess mantles all but the most recent flows of the Snake River Group, but many of the prominences on the lava surface remain exposed.

Split Butte (Fig. 12-1) is a volcanic construct consisting of a tephra ring 550 m in diameter which at one time retained a lava lake. The tephra ring has a maximum relief of approximately 50 m relative to the surrounding plain. It is moderately asymmetrical and shows a greater accumulation of ash on the northeast, the result of prevailing southwesterly winds during the eruption. The tephra, which consists of partially palagonitized sideromelane and lithic fragments, is thinly bedded and dips radially away from the center of the crater. A large "split" or gap 150 m wide occurs in the eastern section of the tephra ring (Fig. 12-2). The ring is in disconformable contact with the basalt of the lava lake and is discontinuous, as the lake basalt appears to have overflowed a section of the tephra on the southwest. The lake crusted and solidified to an unknown depth, after which the central portion of the lake subsided, apparently due to withdrawal of magma in the subsurface. This resulted in an inner pit crater 420 m in diameter and approximately 20 m deep. A small cluster of spatter cones lies on the circular fracture along which collapse occurred, and colluvium from the fracture scarp together with unconsolidated loessal sediments cover the pit crater floor. Three parallel basalt dikes cut the tephra ring along the northwest rim of Split Butte. The thin, nearly vertical dikes are traceable for nearly 200 m before disappearing beneath unconsolidated sedimentary cover to the northeast.

TEPHRA RING

Outcrop Description

The Split Butte tephra forms a low, asymmetric ring which has the greatest accumulation on the northeast side of the structure. The ring is also slightly elliptical, with the major axis oriented northeast-southwest, evidently reflecting the prevailing wind direction during eruption.

The tephra, which varies in color from black to reddish-brown, occurs in two basic types: thickly bedded to massive

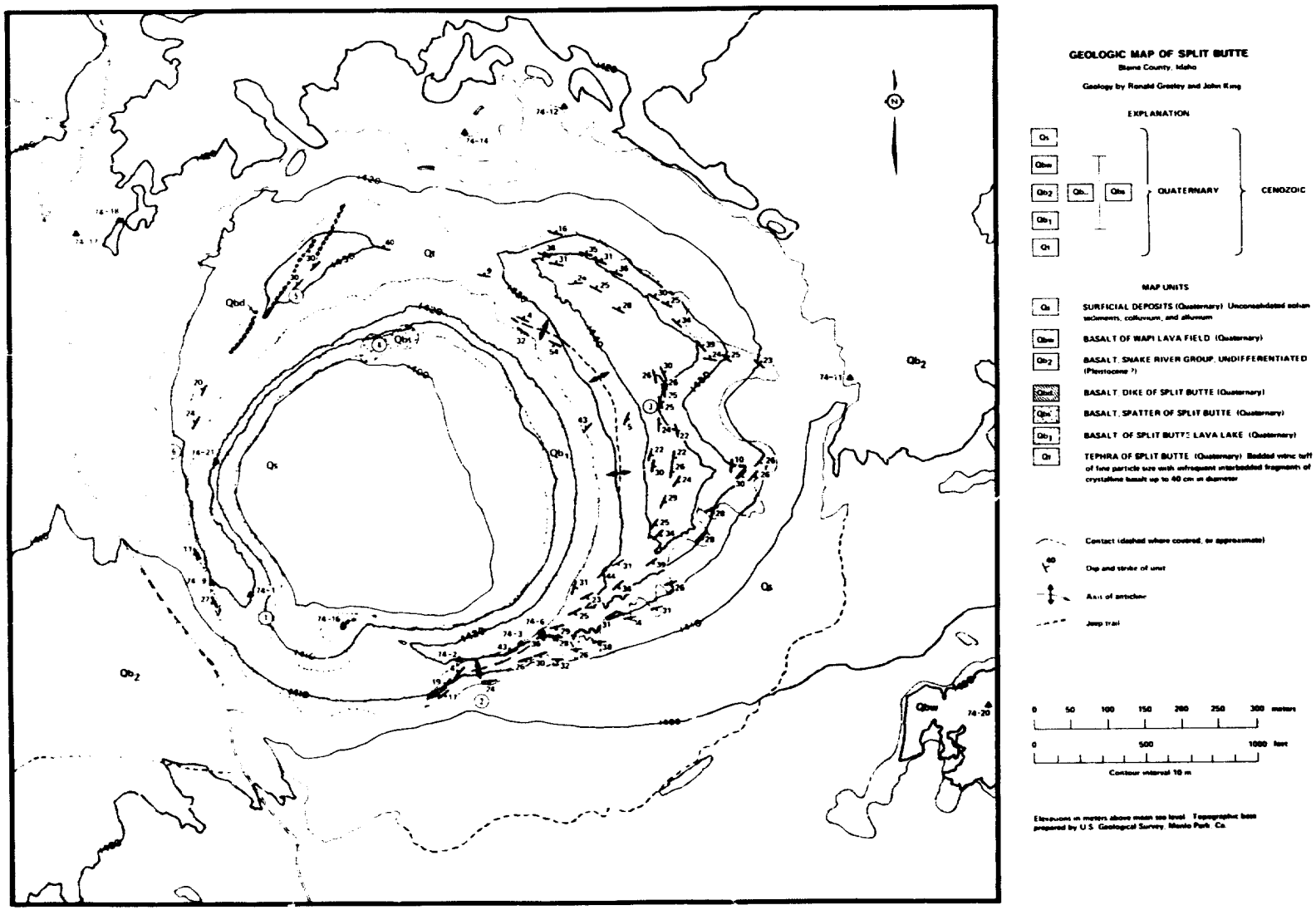

FIGURE 12-1. Geologic map of Split Butte.

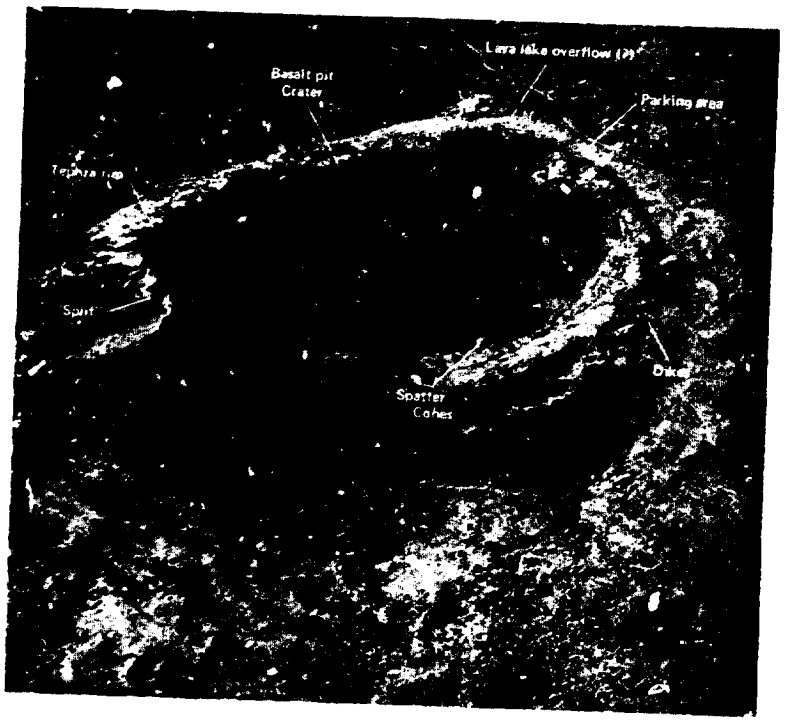

FIGURE 12-2. Oblique aerial view southwestward across Split Butte.

FIGURE 12-3. Bedding sag in tephra below basalt ejecta block.

basal layers which are poorly sorted and extensively palagonitized; and, above this, thin planar beds of well-sorted ash. The thinly bedded tephra, which comprises the bulk of the ring, dips 20^{o} to 40^{o} radially outward from the center of the crater. Individual layers are from 2 to 10 cm thick and are the result of variations in grain size, sorting, and color of constituent materials. The thin layers also vary in resistance to erosion and this accentuates the bedding. Erosion of less resistant layers results in low ridges and shelf-like projections of resistant material. Individual beds vary somewhat in thickness, but lack dune forms and cross bedding. Numerous lithic fragments up to 1.25 m in diameter are found in the tephra and cause bedding sags in the layers below them (Fig. 12-3).

Reversal of dip of the ash occurs close to the lava lake contact, with the tephra layers changing from their outward dip to an inward dip of 25^{o} to 35^{o} toward the center of the vent. The layers thus form an anticlinal-like structure, the axis of which is visible at several points around the ring (Greeley and King, 1975). This dip reversal is depositional and represents the opposing primary dips of the eruption rampart.

The Split Butte tephra is very porous and typically quite friable. Erosion of the outer dip slopes of the tephra ring has produced a very irregular dissected topography that is most prominent in the thick eastern deposits. A large gap, or

"split," occurs in the eastern section of the tephra ring. The "split," after which the Butte was named, occurs at the point of greatest accumulation of the tephra and is either the result of removal of a large volume of tephra from the ring, or deposits never accumulated in this area.

Petrographic Description

In thin section, the tephra consists of round glass grains which lie in a matrix of angular clasts and very finely divided dark brown material. The glass grains, which comprise 30 to 45% of the tephra, range in size from 0.5 to 4.0 mm in diameter, with an average size of approximately 2.0 mm. The glass grains are highly vesicular with the vesicles showing local flattening and stretching. Deformation of the light brown isotropic glass is also indicated by flow banding and trains of opaque inclusions (Fig. 12-4). The grains frequently contain inclusions of plagioclase and olivine, which comprise 3-5% of the tephra.

The vesicular grains lie in a matrix composed of smaller angular glass clasts which constitute 20 to 30% of the tephra, and very finely divided glass which is rich in opaque minerals. The angular clasts range in size from 0.05 to 0.5 mm in maximum dimension and are composed of light to medium brown glass having an average refractive index of 1.612. Utilizing the relationship of the refractive index of natural volcanic glasses versus per cent SiO_2 (Williams, Turner and Gilbert, 1954), the SiO_2 content of the glass from Split Butte is estimated at 47%. The clasts are less vesicular than the larger grains, with the vesicles, where present, typically spherical and generally less than 0.1 mm in diameter (Fig. 12-5). A thin layer of palagonite rims the glass grains in several of the samples studied and slight devitrification is ubiquitous. Secondary mineralization is also present in some samples, as evidenced by the presence of cryptocrystalline calcite, radiating clusters of elongate quartz crystals, and very fine-grained buff material filling many of the void spaces.

FIGURE 12-4. Plastic deformation in large glass grains in tephra (X 30).

INNER LAVA LAKE

A lava lake consisting of an undetermined thickness of layered basalts was confined by the tephra ring (Fig. 12-6). The lava lake appears to have overflowed a section of the tephra ring on the southwest (Holcomb, personal communication), causing the ring to be discontinuous. The lava lake is preserved as a continuous shelf of basalt which is covered by float and aeolian and colluvial sediments. The medium gray, fine-grained basalts are moderately vesicular and are composed of phenocrysts of labradorite (An 55-65%) and forsteritic olivine (Fo 78-88%) in a matrix of clinopyroxene and intersertal glass (Fig. 12-7).

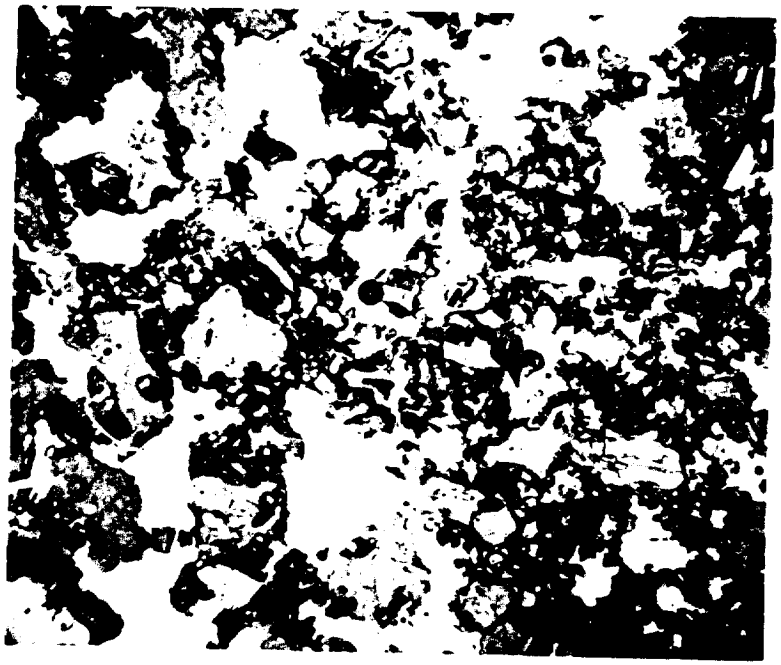

FIGURE 12-5. Photomicrograph of glass clasts exhibiting blocky shapes and arrested vesicle growth (X 30).

The central portion of the lake has subsided, forming a flat-bottomed pit crater 20 m deep and 420 m in diameter. The pit crater is roughly circular and is bounded by the nearly vertical walls of the fracture scarp. A small cluster of spatter cones lies on the pit crater fracture. The spatter consists of highly oxidized, scoriaceous basalt which is very glassy and rich in iron oxide. These spatter basalts were apparently the last volcanic activity at Split Butte.

BASALT DIKES

Three parallel basalt dikes tangentially cut the tephra ring along the northwest rim of Split Butte (Greeley and King, 1975) (Fig. 12-1). The nearly vertical, curviplanar dikes are

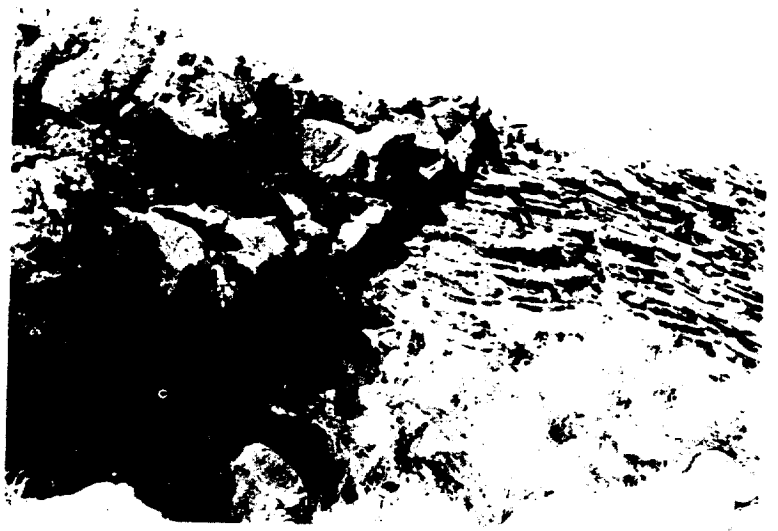

FIGURE 12-6. Lava lake basalt in disconformable contact with dipping tephra layers.

20 to 30 cm thick and are traceable for over 200 m before being covered by unconsolidated sediments. The dikes are more resistant than the tephra they cut and form ridges standing 30 to 45 cm above the tephra (Fig. 12-8). The dikes have dense, glassy chilled margins 5 cm thick. Flow structure is frequently visible in the center of the dikes, which are moderately vesicular. The tephra in contact with the dikes exhibits an approximately 8 cm thick baked zone which consists of tephra altered to a black, cindery layer.

In thin section, the basalts consist of subhedral phenocrysts of plagioclase (An 54-60%) and olivine (Fo 86-90%) in a glassy, opaque-rich groundmass (Fig. 12-9). Minor amounts of clinopyroxene and secondary calcite are also present.

SURFICIAL FLOWS

Surface flows of the undifferentiated Snake River Group have encroached Split Butte and completely surrounded it.

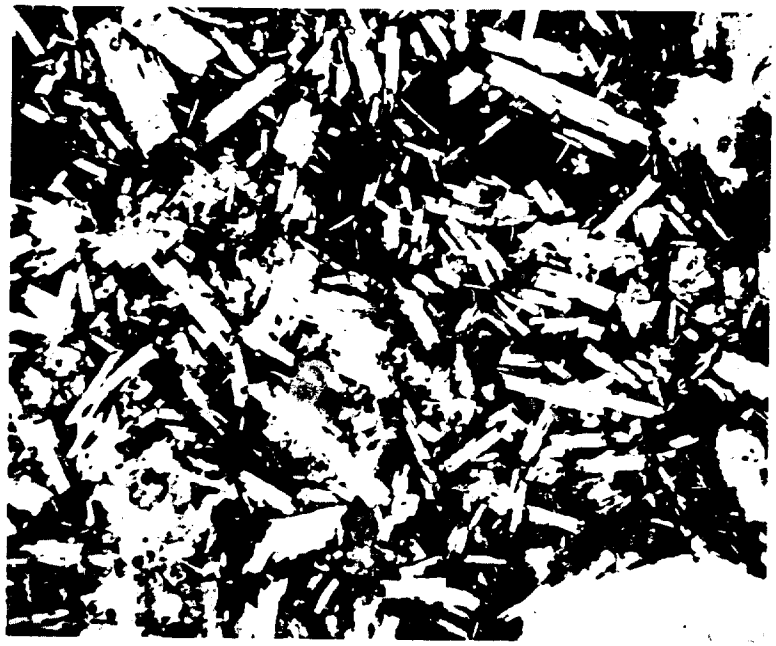

FIGURE 12-7. Photomicrograph of lava lake basalt (X 30).

The advancing lava stopped where it encountered the outer slopes of the Butte and formed a moat-like depression 2-5 m deep around the Butte. Numerous small pressure ridges up to 5 m high are aligned with their axes perpendicular to the flow direction. The flows are covered by discontinuous aeolian sediments, with prominences on the lava surface remaining exposed.

A lobe of the Wapi flow basalts encroaches Split Butte in the southeast (Fig. 12-1). These Holocene basalts overlie Snake River Group basalts and are free of sediment cover. Although they are undated, Wapi flows cover fissures of the King's Bowl fracture set (Champion, 1973) which may be as young as 2130 years ± 130 years (Pranz, 1970). The flow surface is very irregular and has well developed ropy pahoehoe texture.

FIGURE 12-8. Curviplanar, nearly vertical basalt dike exhibiting vesicular core and baked contact zone in the adjacent tephra.

FORMATION OF SPLIT BUTTE

Based on field studies and subsequent petrographic observation and grain size analysis of its tephra, Split Butte is believed to be a maar crater resulting from the phreatomagmatic eruption of magma. Although there is little agreement on the definition of maars, they may be described as landforms which are caused by volcanic explosion and consist

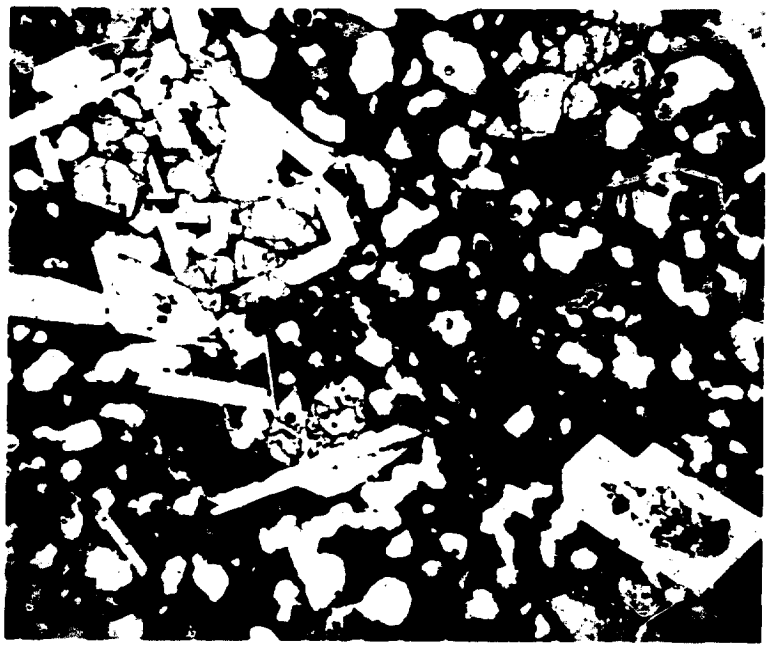

FIGURE 12-9. Photomicrograph of the dike basalt (X 30).

of a crater, which reaches or extends below general ground level and is considerably wider than deep, and a surrounding rim constructed of material ejected from the crater (Ollier, 1967).

Maars are commonly attributed to phreatomagmatic eruptions or explosions resulting from the generation of steam from the interaction of groundwater with erupting magma (Walker and Croasdale, 1971). Ollier (1974) adds the restriction that juvenile magmatic material must be present in the ejecta.

The phreatomagmatic nature of the eruption which formed Split Butte is indicated by the following observations:

The major component of the tephra is clear, light to medium brown sideromelane, which occurs as fragments containing 3-5% crystalline material. Conversion of magma to such a glassy deposit suggests extremely rapid cooling, as would be achieved by quenching in water. The glassy fragments in the tephra occur in two forms, large vesicular grains and small dense clasts. The small clasts have few vesicles; the vesicles tend to be spherical and rarely show flow stretching. This is explained in other maar craters by rapid arresting of bubble growth in the magma as it was quenched (Heiken, 1971). Stretched vesicles are diagnostic of cinder-cone pyroclastics, which Walker and Croasdale (1971) term Strombolian type deposits.

The clasts are shattered fragments of glass formed by quenching magma in water. They are blocky and commonly have straight to slightly curved edges. In contrast, the ejecta from non-phreatomagmatic cinder cones is composed primarily of achelith–particles whose form is controlled by surface tension rather than fracture planes (Walker and Croasdale, 1971) and have shapes ranging from spherical to filamentous. No such particles were seen among the clasts in the Split Butte tephra.

The tephra of Split Butte contains numerous glassy grains ranging in size from 0.5 to 4.0 mm. These rounded and vesicular grains commonly show well developed flow structure in the form of stretched and flattened vesicles. The surfaces of these grains appear to be fluid boundaries rather than fracture planes. The evidence indicates that the larger grains were chilled less quickly than the clasts and therefore originated under conditions of limited water interaction.

Numerous crude accretionary lapilli are present in the tephra. They consist of nuclei of glass grains which are coated with thin layers of fine ash (Fig. 12-10). Moist conditions are necessary for the accretion of ash around a nucleus (Stearns, 1925) and Moore and Peck (1962) indicate that water-rich ash clouds are primarily associated with

C-3

FIGURE 12-10. Photomicrograph of tephra showing well-developed accretionary lapillus (X 30).

phreatic eruptions of basaltic magma. The presence of accretionary lapilli in the tephra of Split Butte, therefore, provides additional evidence of a phreatomagmatic phase of activity.

It is also possible to differentiate phreatomagmatic and non-phreatomagmatic basalt ashes on the basis of their grain size parameters. Walker and Croasdale (1971) have demonstrated that phreatomagmatic ash is generally finer grained and more poorly sorted than non-phreatomagmatic ash. Plotting median grain size versus variance reveals that ash from Split Butte falls in a distinctly different field than that occupied by known non-phreatomagmatic ash in a similar plot (Fig. 12-11). The tephras from Split Butte have consistently higher variances and finer median grain sizes than non-phreatomagmatic ash. Comparison of plots of ash from Split

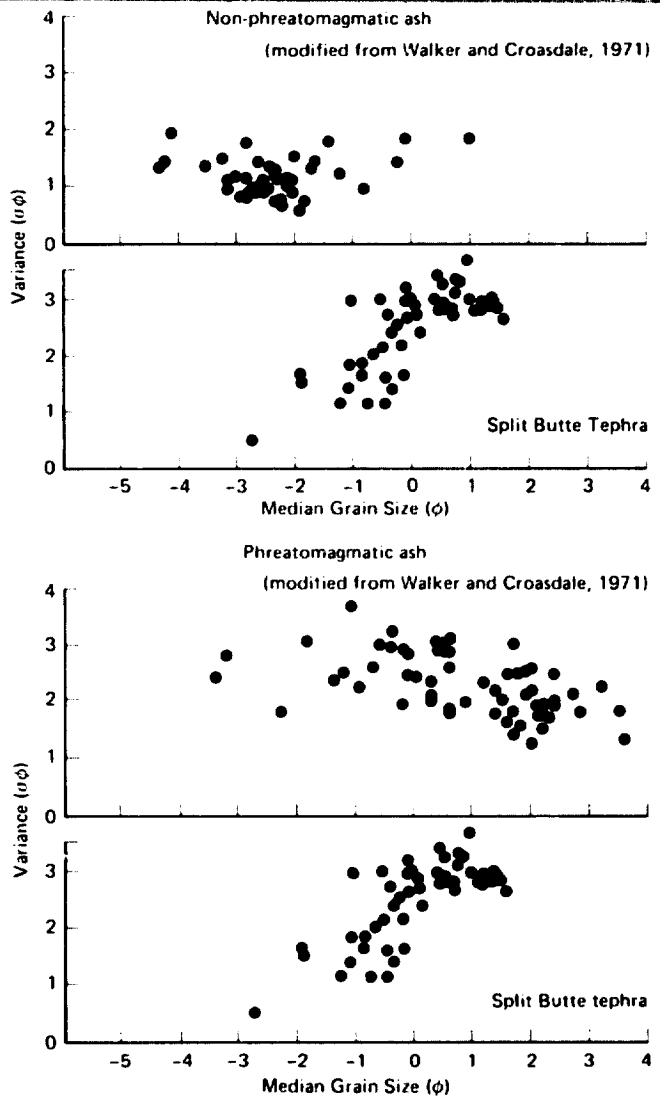

FIGURE 12-11. (Upper) Plots of variance (σ φ) versus median diameter (Md φ) for known non-phreatomagmatic ash and Split Butte tephra. (Lower) Plots of variance (σ φ) versus median diameter (Md φ) for known phreatomagmatic ash and Split Butte tephra.

Butte with plots of known phreatomagmatic ash reveals a much greater correlation (Fig. 12-11). The sorting and median grain size, therefore, indicate that Split Butte tephras are phreatomagmatic in origin.

Other indications of water-rich conditions associated with a phreatomagmatic eruption at Split Butte are: 1) plastic deformation of impacted ash layers below basalt ejecta blocks; 2) the massive nature and extensive palagonitization and secondary mineralization of the basal ash layers (Fig. 12-12); and 3) an estimated original height-width ratio of approximately 1:10 of the ash ring. However, since the amount of erosion is unknown, and the extremeties of the ramparts have been concealed by recent basalt flows, an accurate determination of the height-width ratio is not possible.

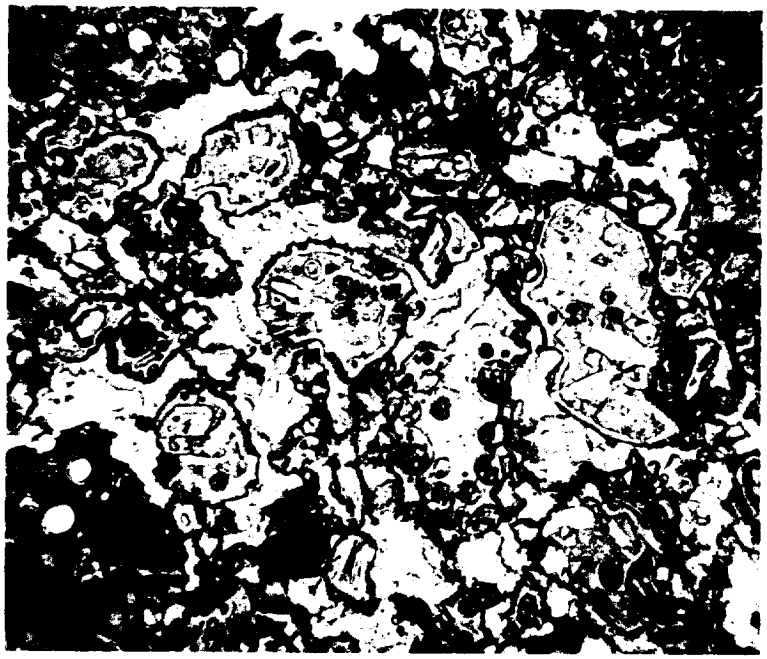

FIGURE 12-12. Sample of tephra from lower, massive ash layer exhibiting extensive palagonitization and secondary mineralization (X 30).

There are two basic mechanisms which form pyroclastic deposits: air fall or flow processes (Walker, 1971). Base surge is one type of flow process which is often associated with phreatomagmatic eruptions (Moore, 1967; Lorenz, 1973). It is defined as a basal cloud of pyroclastic debris spreading radially outwards from a crater as a density flow (Moore, 1967).

Studies by Sheridan (1971) and Walker (1971) indicate that statistical parameters may be used to differentiate air fall pyroclastics from flow deposits. Their data indicate that air fall deposits are coarse-grained and well sorted while flow deposits are fine-grained and poorly sorted.

Comparison of the distribution parameters of ash from Split Butte with Walker's data (Fig. 12-13) indicates that the tephra of Split Butte seems to correlate fairly well with known flow deposits, although some air fall pyroclastics seem to be present as well.

In conclusion, the primary mechanism of emplacement of the tephra is considered to be air fall based on the lack of dune forms, channelways, and cross bedding in the ash layers, and the presence of abundant accretionary lapilli in the tephra. Grain size analysis of the tephra, however, indicates the presence of base surge during the phreatomagmatic phase of the Split Butte eruption.

SEQUENCE OF EVENTS

The following sequence of events is hypothesized to have produced Split Butte (summarized in Fig. 12-14).

Stage 1: Production of the tephra ring

During Late Pleistocene or Early Holocene, rising basaltic magma erupted at Split Butte as part of the widespread effusive activity of the eastern Snake River Plain. The rising basaltic magma encountered abundant near-surface groundwater, causing the phreatomagmatic explosions which produced the tephra ring. The tephra was deposited primarily by air fall, with some base surge possibly active as well.

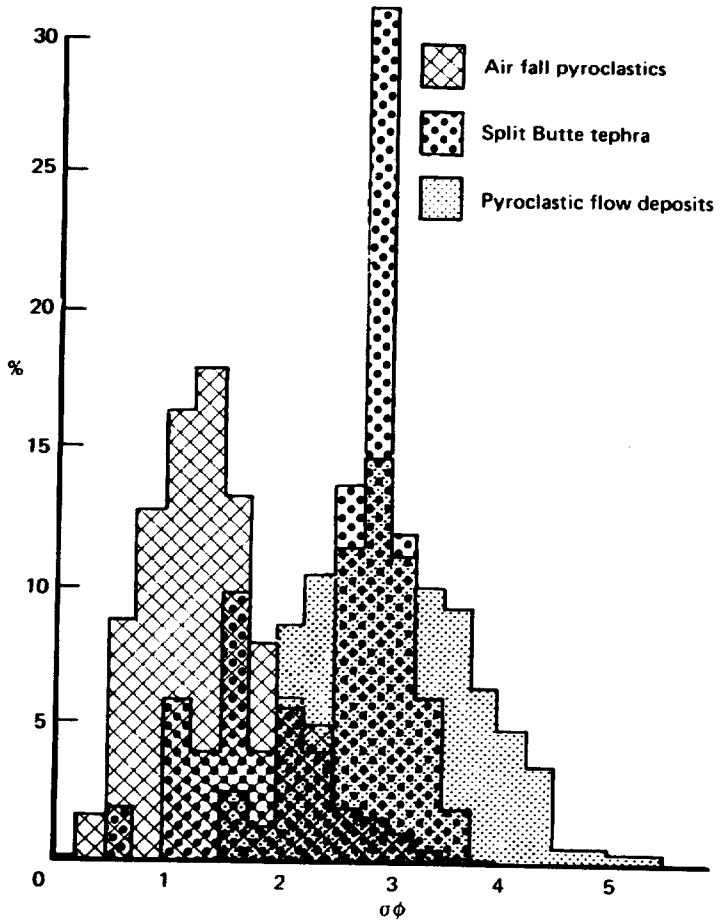

FIGURE 12-13. Range in variance (σ φ), shown by air fall pyroclastics, pyroclastic flow deposits, and Split Butte tephra.

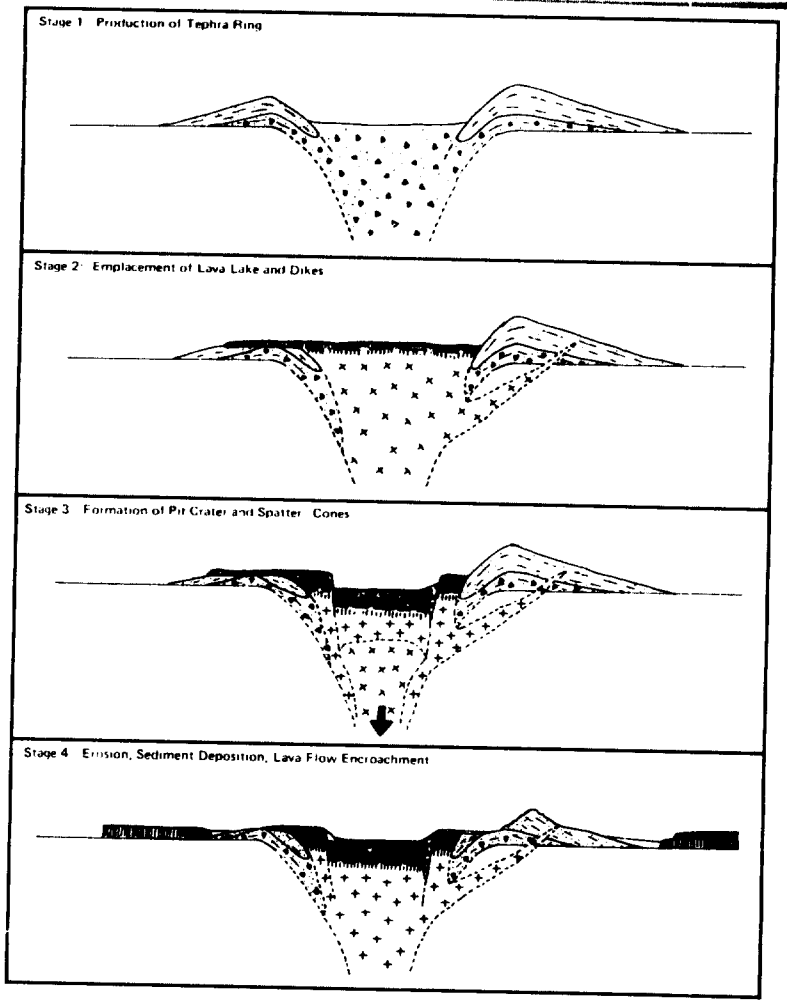

FIGURE 12-14. Sequence of events.

Prevailing southwesterly winds during the eruption resulted in thicker deposits of tephra on the northeast section of the ring.

Stage 2: Emplacement of the lava lake

The second stage in the development of Split Butte was the emplacement of the lava lake, which overflowed a section

of the tephra ring on the southwest. This shift in eruptive style was caused by the cessation of phreatomagmatic activity at the vent.

Phreatomagmatic activity is frequently observed to be followed by a period of eruption during which there is no water-magma interaction (Heiken, 1971). This lessening interaction may be caused by the removal of access of water to the vent, consumption of groundwater supplies by the eruption, or by a greatly increased eruption rate lessening the effect of the water. The cessation of phreatomagmatic activity at Split Butte is considered to be the result of an upward surge of magma. Such an increase in the hydrostatic head of the magma column has the effect of excluding groundwater from the conduit area, causing the phreatomagmatic phase of eruption to cease. Evidence of this increase in magmatic pressure is seen in the high level of the lava lake, which was maintained at a level of approximately 15 m above the surrounding plain.

The emplacement of three parallel basalt dikes is considered to have occurred during this stage of activity. The dikes tangentially cut the ring in the north and could have been propagated along slump fractures caused by the agitated, molten lava lake. The dike basalts bear strong compositional and textural similarities to the lava lake basalts, and it is therefore tentatively assumed that the dikes were fed from the lava lake at depth and are contemporaneous with it.

Stage 3: Withdrawal of the magma

Following partial solidification of the lava lake, the magma withdrew down the conduit. Removal of support resulted in the subsidence of the central portion of the lava lake, forming a circular pit crater 420 m in diameter which is today 20 m deep. As the crater floor is covered by an unknown thickness of aeolian sediments, the original depth of the pit crater is unknown. It is also unclear as to whether the pit crater is the result of a series of collapses or subsidence of a single large block; however, the flat nature of the floor may indicate the latter.

Two coalescing spatter cones formed after the lava lake subsided and represent the last volcanic activity at Split Butte. The spatter deposits are on the ring fracture and may have been a degassing outlet for late stage liquids following subsidence.

Stage 4: Erosion and encroachment of surface flows

The fourth stage in the development of Split Butte was the erosion of the Butte and its encroachment by surface flows.

The soft, porous tephra has been extensively eroded since its deposition. The outer dip-slopes of the tephra have been deeply dissected, producing a very irregular topography. Talus deposits cover the lower 8 to 10 m of the pit crater scarp. They consist of fine-grained sediments and large blocks of basalt which have fallen from the pit crater wall. Aeolian sediments fill depressions in the surface of the surrounding flows and form deposits within Split Butte, where they cover the pit crater floor to an unknown depth.

Flows from Snake River Group basalts and from the Wapi lava field have encroached Split Butte since its formation. The Snake River Group basalts completely surround the Butte and form a ring-like depression 2-5 m deep around the Butte. A small lobe of the Wapi flow has approached to within 400 m of Split Butte in the southeast.

Formation of the Split

The formation of the large split in the eastern section of the tephra ring remains an anomaly. The split has developed in the outer dip-slopes at the point of greatest ash accumulation, and assuming the tephra ring was continuous upon emplacement, represents the removal of a large volume of ash from the ring.

The split may be the result of erosion caused by the prevailing strong southwesterly winds of the area, as there is close correlation between wind direction and orientation of the split. The wind may have been confined by the eastern

section of the tephra ring and funnelled over the rim at the location of the split. The strong winds might notch the ash at the top of the ramparts and continue to erode downward. However, the large volumes of ash which have apparently been eroded are not visible beyond the tephra ramparts.

There is no indication that the split is the result of volcanic activity, either during or subsequent to the deposition of the ash, nor of the tephra being significantly finer-grained or better sorted than at other sections of the ramparts.

SUMMARY AND CONCLUSIONS

Split Butte is a maar crater which consists primarily of a moderately asymmetrical tephra ring with an approximate original height-width ratio of 1:10, an inner lava lake, and a pit crater.

The tephra is composed of partially palagonitized and devitrified sideromelane glass fragments having a silica content of approximately 47%. The tephra is considered to be the result of phreatomagmatic eruptions, based on compositional and textural evidence in the glass grains and clasts. Further evidence of the influence of groundwater is provided by the statistical analysis of grain size data of the ash, which correlates closely with similar data for known phreatomagmatic ash.

The tephra has statistical parameters which indicate the presence of both base surge and air fall pyroclastics. The lack of dune forms, cross-bedding, and channelways, and the presence of accretionary lapilli indicate, however, that air fall was the primary mode of emplacement of the ash.

An inner lava lake apparently formed when groundwater became unable to interact with the erupting magma, possibly as the result of a greatly increased rate of eruption. The lava lake overflowed a section of the tephra ring on the southwest and three basalt dikes were emplaced in the ring during this stage of activity. Withdrawal of the magma caused the subsidence of the central portion of the partially solidified lava lake, forming a shallow pit crater 420 m in diameter. A small cluster of spatter cones lies in the northern section of the circular collapse fracture and represents the last volcanic activity at Split Butte.

Erosion of ash, deposition of aeolian sediments, and encroachment of Split Butte by flows of the Snake River Group and Wapi lava field complete the development of Split Butte.

REFERENCES

Champion, D. E., 1973. The relationship of large scale surface morphology to lava flow direction, Wapi Lava Field, Southeastern Idaho: Master's Thesis, State University of New York at Buffalo, Buffalo, New York, 44 p.

Greeley, R. and J. S. King, 1975. Geologic field guide to the Quaternary volcanics of the south-central Snake River Plain, Idaho: Idaho Bureau of Mines and Geology, Pamphlet No. 160, 49 p.

Heiken, G. H., 1971. Tuff rings: examples from the Fort Rock–Christmas Lake valley basin, south-central Oregon: Jour. Geophys. Research, vol. 76, p. 5615-5626.

Lorenz, V., 1973. On the formation of maars: Bull. Vol., vol. 37, p. 183-204.

Moore, J. G., 1967. Base surge in recent volcanic eruptions: Bull. Vol., vol. 30, p. 337-363.

Moore, J. G. and D. L. Peck, 1962. Accretionary lapilli in volcanic rocks of the western continental United States: Jour. of Geol., vol. 70, p. 182-193.

Ollier, C. D., 1967. Maars, their characteristics, varieties and definition: Bull. Vol., vol. 31, p. 45-73.

Ollier, C. D., 1974. Phreatic eruptions and maars: in Civetta. L. and others, eds., Physical Volcanology. Elsevier Pub. Co., Amsterdam, p. 289-310.

Prinz, M., 1970. Idaho rift system, Snake River Plain, Idaho: Geol. Soc. Amer. Bull., vol. 91, p. 941-948.

Russell, I. C., 1902. Geology and water resources of the Snake River Plains of Idaho: U. S. Geol. Survey Bull. 199, 192 p.

Sheridan, M. F., 1971. Particle size characteristics of pyroclastic tuffs: Jour. Geophys. Research, vol. 76, p. 5627-5634.

Stearns, H. T., 1925. The explosive phase of Kilauea Volcano, Hawaii in 1924: Bull. Vol., vol. 5-6, p. 193-208.

Stearns, H. T., L. Crandall, and W. G. Steward, 1938. Geology and groundwater resources of the Snake River Plain in southeastern Idaho: U. S. Geol. Survey Water Supply Paper No. 774, 268 p.

Walker, G. P., 1971. Grain size characteristics of pyroclastic tuffs: Jour. of Geology, vol. 79, p. 696-714.

Walker, G. P. and R. Croasdale, 1971. Characteristics of some basaltic pyroclastics: Bull. Vol., vol. 35, p. 303-317.

Williams, H., R. Turner, and C. M. Gilbert, 1954. Petrography—an introduction to the study of rocks in thin section: San Francisco, W. H. Freeman Pub. Co., p. 28.

13. MAPPING IN CRATERS OF THE MOON VOLCANIC FIELD, IDAHO, WITH LANDSAT (ERTS) IMAGERY*

Richard H. Lefebvre**
EROS Program Office
U. S. Geological Survey
Reston, Virginia 22090

13. MAPPING IN CRATERS OF THE MOON VOLCANIC FIELD, IDAHO, WITH LANDSAT (ERTS) IMAGERY*

Richard H. Lefebvre**
EROS Program Office
U. S. Geological Survey
Reston, Virginia 22090

ABSTRACT

Lava flows in the Craters of the Moon (COM) National Monument, Idaho, and its surrounding recent volcanic field, show significant radiance variations on LANDSAT (ERTS) images. Preliminary mapping has been conducted using digital LANDSAT imagery in conjunction with analysis of aerial photographs and field observations. The radiance variations are mainly due to three surficial properties of the flows: *surface roughness*, a result of the type of flow (aa, rough-surfaced or pahoehoe, relatively smooth); *surface chemistry and mineralogy* and its effect on the blue glassy coating of the exterior of the pahoehoe flows; and *surface cover* on the pahoehoe flows by weathering, vegetation, and sediment. Surface roughness allows discrimination between aa and pahoehoe flows. Surface chemistry and mineralogy and surface cover make it possible to delineate between pahoehoe flows of different ages. Nearly all of the pahoehoe flows have a glassy crust that is blue due to electron transfer processes near included magnetite crystals. This blue crust gives these young pahoehoe flows an unusual spectra on LANDSAT images – marked decrease in radiance from MSS band 4 to 7. The radiance variations due to the blue crust are diminished with geologic time because of an increased cover on the surface of the flows by vegetation, sediment and weathering.

Digital processing of these radiance variations provides investigators with a broad regional and multispectral perspective for geologic mapping of Holocene flows. The lack of accessibility and the predominance of minor features, such as flow units, make the Craters of the Moon (COM) area and others like it difficult areas to study. Using LANDSAT in conjunction with aerial photographs and field investigations has resulted in the following: The border of the COM volcanic field has been defined by contrast stretching of the light areas on the LANDSAT image. The individual lava flows within the volcanic field have been delineated by contrast stretching of the dark areas. Classification of the LANDSAT digital data supervised by the investigator on interactive computers such as the General Electric Image-100 make it possible to map individual flows in detail.

* *Reprinted fron. Proceedings of the Tenth International Symposium on Remote Sensing of Environment, 1975.*

** *On sabbatical from Grand Valley State College, Allendale, Mich.*

INTRODUCTION

LANDSAT (ERTS) provides geologists with a multispectral tool for geologic maping of broad outpourings of Holocene lava flows in arid to semi-arid areas. The Craters of the Moon (COM) National Monument and Wilderness Area and its surrounding volcanic field is one such area of recent volcanism that is well suited to study by satellite. The COM volcanic field is a large, remote area comprising over 1300 square kilometres in south-central Idaho (Fig. 13–1). Study by aerial photographs requires the scrutiny of numerous individual photographs and, although many lava flow contacts can be discerned, the flows themselves are not easily discriminated. The entire COM volcanic field is contained within a single LANDSAT image. In addition, the LANDSAT Multispectral Scanner (MSS) images span a larger spectral range which is separated into four distinct bands: MSS band 4, 0.5–0.6 μm; 5, 0.6–0.7 μm; 6, 0.7–0.8 μm; and 7, 0.8–01.1 μm. Field investigation in these areas is often arduous and the multiplicity of minor features are confusing from the ground. This is not to say that aerial photographic analysis and field research are not important, but rather that they can be greatly complemented by using LANDSAT images before, during, and after field investigation.

The COM lava flows show significant variability in radiance both within and between the spectral bands of MSS images. Radiance variability between different flows is evident in both single band images and color composites of several bands. Radiance variability of the same flows, particularly the youngest pahoehoe flows of this area, can be observed when the different spectral bands are compared. Such conspicuous band to band radiance differences appear to be uncommon (Rowan and others, 1974; Rowan pers. comm. 1975). Several enhancement and classification techniques were employed to utilize these radiance variations for delineating the volcanic units (mainly lava flows) of the COM area.

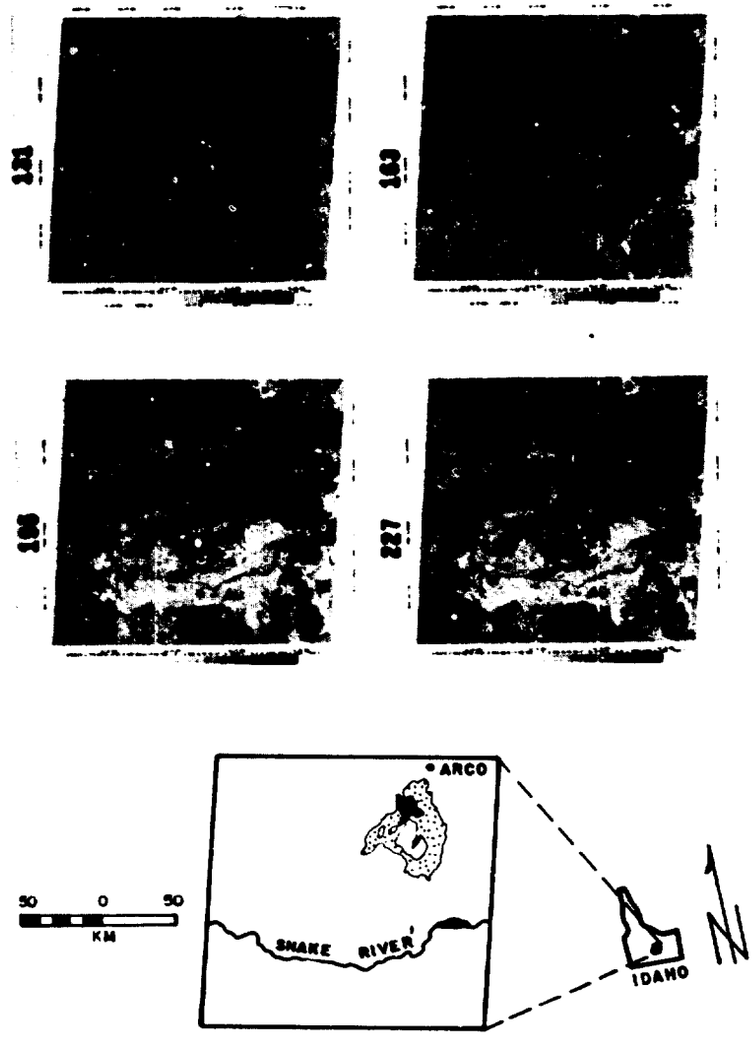

FIGURE 13-1. LANDSAT images (A–D) and a location map (E) of Craters of the Moon (COM) area, Idaho. A–D: MSS bands 4 (0.5–0.6 μm); 5 (0.6–0.7 μm); 6 (0.7–0.8 μm); and 7 (0.8–1.1 μm) of August 27, 1972 scene E–1035–17525. E: Outline map. Craters of the Moon National Monument and Wilderness Area shown by dark area.

GENERAL GEOLOGY

The Craters of the Moon (COM) lava flows are among the most recent eruptions of basaltic lavas that have occurred in the Snake River Plain area. Other nearby areas of a similar nature are Shoshone, Wapi (including King's Bowl), Cerro Grande, and Hell's Half Acre volcanic fields. These eruptive events are superimposed on a thick succession of mainly Pleistocene Snake River Plain (SRP) olivine tholeiites that have filled an arcuate generally east-west downwarp across southern Idaho.

COM lavas are enriched in iron, phosphorous, titanium, and alkalies, and are considered by Leeman and others (1975) to have been evolved from the Snake River Plain olivine tholeiites. According to Leeman and others (1975), they are typically basaltic (olivine ferro-basalts) in composition, but do contain ferro-latites that have as much as 63.5 percent SiO_2.

The two main flow types of the area, aa and pahoehoe, are characteristic of extrusives of this composition. The low viscosity olivine ferro-basalts developed into pahoehoe flows which traveled long distances out from the Great Rift (Fig. 13–2) down the topographic gradient to the east-northeast and more extensively to the west-southwest (Fig. 13–1). Those flows with SiO_2 content around 60 percent (ferro-latites) formed aa flows. Some of these traveled to the northeast, but most also flowed to the southwest, although not as far as the less viscous pahoehoe flows. The surfaces of the COM lava flows are dark reltative to the other geologic units in the immediate area.

Although lava flows predominate, various types of vents were formed along the Great Rift in the COM volcanic field including over 20 prominent cinder cones greater than 100 feet in height (Stearns, 1928). Most of the cones are composed mainly of tephra which ranges in color from light gray to red to black. Large areas of the lighter colored tephra occur as patches along the Great Rift adjacent to the cones. Vegetation, mainly grass and sagebrush, but including trees,

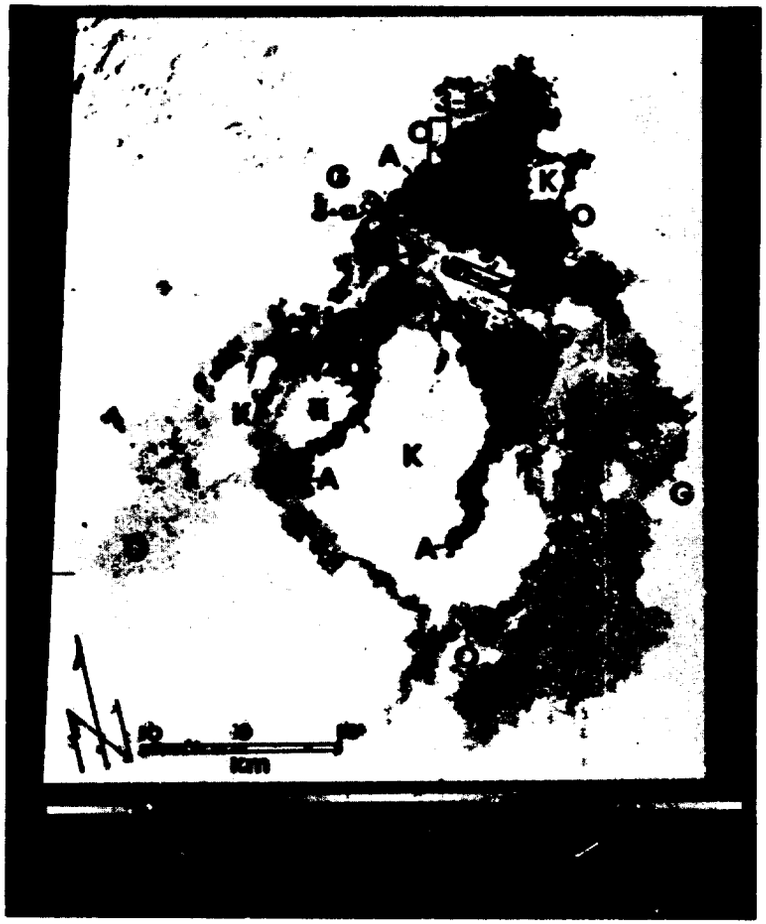

FIGURE 13-2. Portion of MSS band 6 of August 27, 1972, image modified by contrast stretching to increase contrast in dark (lava) areas. A=aa, B=Blue Dragon Flow, G=Great Rift, K=Kipukas (both light SRP lavas and dark COM aa flows), O=Older pahoehoe flows (see Fig. 13–4 for their differentiation), Y=Youngest Blue Dragon-type flows, X=Contact between light and dark facies of youngest Blue Dragon-type flows. 3a–c=areas shown in Fig. 13–3.

grows preferentially on the north slopes of the cones due to the moisture which is held as snow late into the spring. In MSS color-infrared composite images, the cones are pink where they are covered with vegetation.

Kipukas, islands of older rock surrounded by younger lava, occur throughout the volcanic field. The more obvious of these in the LANDSAT image (Fig. 13–2) are large light-colored areas of older Snake River Plain (SRP) lavas, but there are also many smaller kipukas of COM lava and tephra surrounded by younger COM flows.

Only the youngest of the COM lavas have been dated radiometrically. The flows and pyroclastic deposits of this volcanic field probably were extruded in a relatively short period of time, culminating with the flows dated around 2000 years b.p. by Bullard and Rylander (1970, 1971). No dates for the older COM flows have been published.

METHODOLOGY

There are a number of high-quality LANDSAT 1 images of the COM area. Scene E-1035-17525, acquired August 27, 1972, was selected for study, although other images were also examined. One of the fastest and least expensive techniques entails making color composites from diazo transparencies using 9 inch positive black and white film transparencies. A variety of different effects can be produced by varying the exposure for the various bands. In this investigation many of the initial observations were made using this process and later corroborated by more sophisticated techniques. The color additive viewer, also used in this study, produces results similar to those of the diazo technique only it is an additive process rather than a subtractive process and is much quicker, more versatile, and can yield a better photographic product.

Computer compatible tapes (CCT's) were used extensively in a digital analysis of scene E-1035-17525. These tapes contain all the radiance data collected by the satellite and therefore provide a more complete record than the multigeneration photographic products of limited dynamic range used in the diazo and color additive techniques. Classification maps of the flows were made using a General Electric Image-100 (Fig. 13–3).

Additional computer image processing was done by California Institute of Technology's Jet Propulsion Laboratory (JPL) at Pasadena, California. JPL's VICAR processing programs first geometrically rectifies and removes noise or imperfections in the data (Goetz and others, 1975). Contrast stretching proved to be a very useful technique for delineating the lava flows in the COM area. Contrast stretching is a procedure which allows the investigator to examine only those parts of the dynamic range of the image of interest (Goetz and others, 1975). In this study, the input radiance values were reassigned to new gray levels to increase the contrast of the dark portions of the image at the expense of the light portions (Fig. 13–2 and Fig. 13–4) and conversely to increase the contrast of the light portions of the image at the expense of the dark portions.

RADIANCE CHARACTERISTICS OF FLOWS ON LANDSAT IMAGES

The radiance variability of the COM lava flows and related pyroclastic deposits make it possible to map much of the volcanic field directly from the LANDSAT data. Field and laboratory investigation and the use of high- and low-altitude aerial photography must be incorporated into any complete and final mapping of this area just as they were used in this preliminary feasibility study. What the LANDSAT perspective offers beyond these more traditional approaches is it's multispectral broad regional coverage.

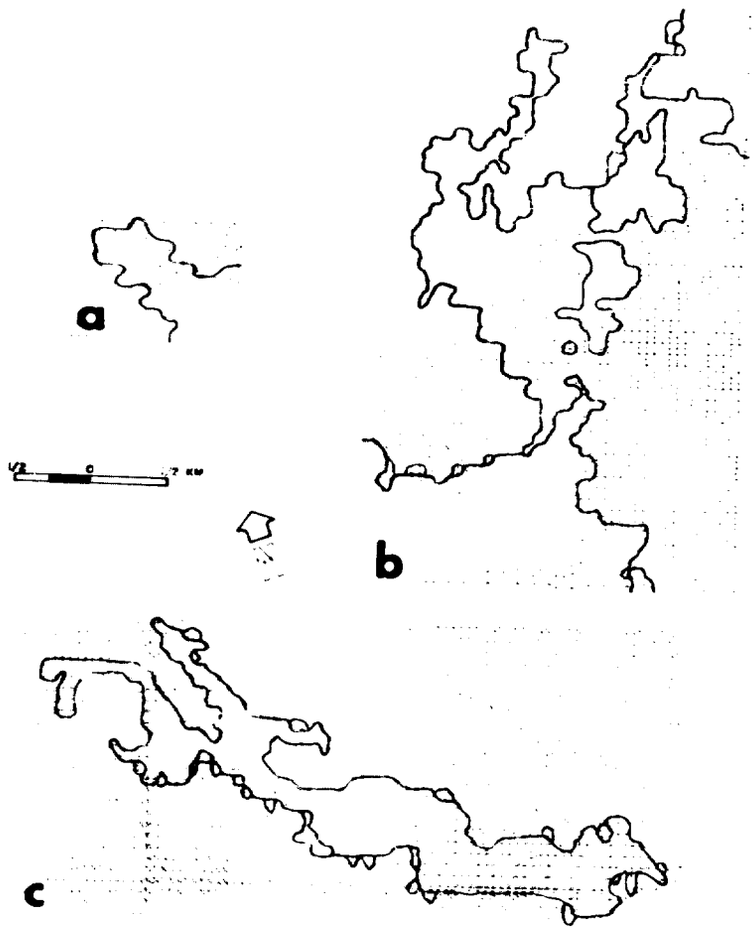

FIGURE 13-3. Selected alphanumeric classification maps from GE Image 100 (See Fig. 13-2 for location). = cinder, vegetation, &/or older covered pahoehoe flows. 1 & 2 = youngest pahoehoe flows, (a = aa. a. Highway flow surrounded by cinders, b. young Blue Dragon-type pahoehoe flow (no name) superimposed on older aa flow (Serrate Flow) and still older pahoehoe flow (Sunset Flow), c. Little Prairie Aa flow (with pahoehoe flow units on edge) surrounded by cinders.

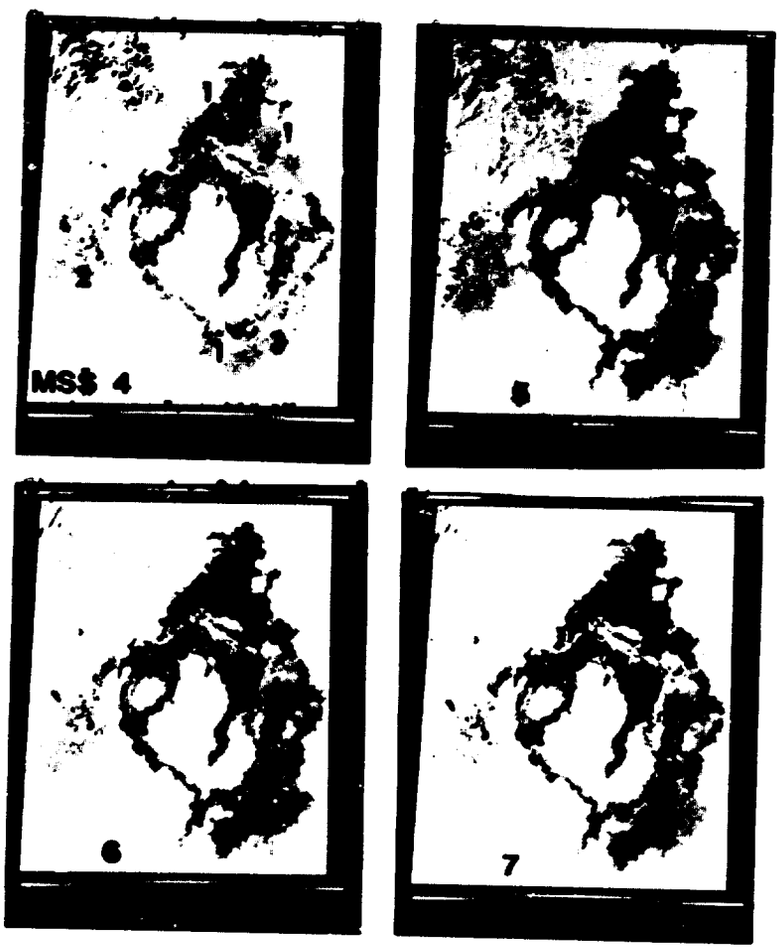

FIGURE 13-4. Identical portions (all 4 MSS bands) of August 27, 1972, image modified by contrast in dark (lava) areas. MSS 6 same as Fig. 13-2. Note changes in radiance values from band 4 through band 7 in areas delineated in Fig. 13-2, especially light and dark facies of youngest pahoehoe flows (Y on Fig. 13-2, 4 on this figure) 1-4 refer to different age (on the basis of radiance) pahoehoe flows (1 = oldest).

The radiance variations of the flows on LANDSAT images are due mainly to three properties of the flow surface: surface roughness, chemistry and mineralogy, and cover. Surface roughness allows discrimination between aa and pahoehoe flows. Surface chemistry and mineralogy and surface cover make it possible to delineate different age pahoehoe flows.

Flow Surface Roughness

Surface roughness is much greater on aa flows than on pahoehoe flows. Not only do aa flow surfaces consist of blocks that range up to more than a metre on a side, but the surfaces of these flows typically have undulations with a relief of several metres. The amount of direct sunlight reflected from a rough surface is less than the sunlight reflected from a smooth surface, other factors being held constant. Therefore, the rough-surfaced aa flows of the COM area have a dark appearance on LANDSAT images which is mappable by digital classification techniques (Fig. 13–3c).

In contrast to aa flows, the surfaces of the pahoehoe flows are relatively smooth and glassy. Irregularities may exist on the surface of pahoehoe flows and, of course, ropelike deformations a few centimetres in relief are common but even when pahoehoe flows develop irregularities, such as when they break up into slabs, the large broken sections often retain their smooth pavementlike character. If pahoehoe flows become so viscous they break up completely, then they must be classified as aa flows. Therefore, it is not unusual to have an aa facies in the distal portions of a pahoehoe flow. These can best be resolved by careful examination of aerial photographs and/or field investigation.

A third flow type, block lava (Finch 1933), makes up a small proportion of the COM volcanic field. Block lava flows have a significantly higher percentage of SiO_2, were more viscous during extrusion, and have more regular and typically larger blocks on their surfaces than do aa flows. Typically their flow margins in plan view are smoother than aa and pahoehoe flows. The Highway Flow just north of U. S. Highway 20-26Alt. 93 near the monument entrance is a block lava flow (Fig. 13–2 and Fig. 13–3a). By visual examination of this flow on black and white prints in the four MSS bands and classifications performed on the G. E. Image 100, it was found that this flow has radiance characteristics of both aa and pahoehoe flows (Fig. 13–3a). It is not known whether this is an universal characteristic of block lava flows.

Surface Chemistry and Mineralogy

Pahoehoe flows characteristically have a glassy crust. In the COM area this crust has an unusual blue color. One flow, in what is now the COM Wilderness Area, was named the Blue Dragon Flow (Fig. 13–2) by Russell (1902, p. 106) because it displayed this blue glassy coating over its entire surface. Faye and Miller (1973) have offered an explanation for this blue glassy crust. Their findings indicate that the blue color is being reflected from the vicinity of partly-oxidized microscopic magnetite crystals in the outer glassy crust of the Blue Dragon Flow. They propose that electron transfer processes (Fe^{2+}–Fe^{3+} and probably Fe^{2+}–Ti^{4+}) due to partial oxidation create absorption in the 0.55–0.7 μm region (Fig. 13–6a). A reflectance spectra (Fig. 13–6b) of the surface sample of the Blue Dragon Flow run on a Beckman DK2-A Spectrometer at the Jet Propulsion Laboratory indicates that this increasing absorbance (decreasing reflectance) extends out beyond the 0.7 μm limit, used by Faye and Miller, into bands 6 and 7 of LANDSAT. This trend corresponds to the decreasing radiance (Area 4, Fig. 13–4, observed in bands 4 through 7 of the LANDSAT images). This area of pahoehoe flows (Area 4, Fig. 13–4) also makes an exception to the generality established in a preceding section that aa flows are darker than pahoehoe flows on LANDSAT images. Examination of area 4 on Fig. 13–4 shows that these flows are as dark as aa flows on MSS band 7.

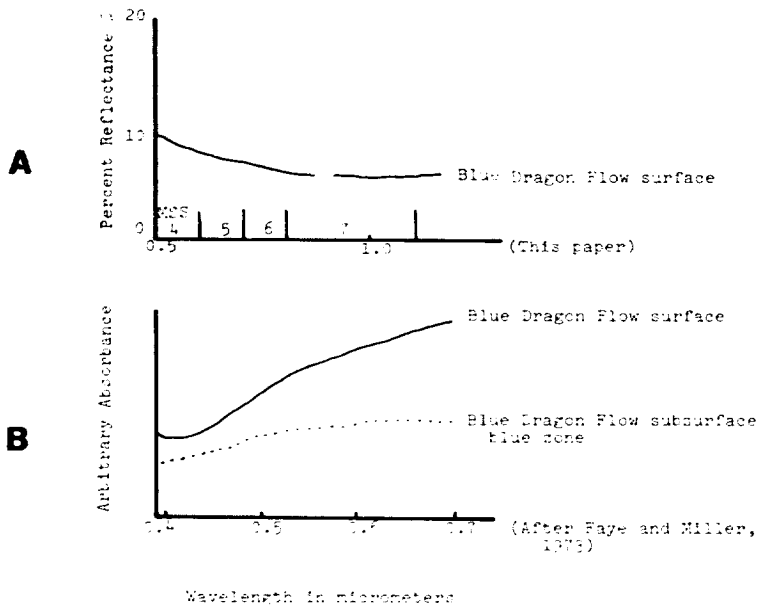

FIGURE 13-6. Reflectance (A) and Absorbance (B) Spectra of Blue Dragon Flow. A. Beckman DK2–A Spectrometer chart with range extended to include LANDSAT MSS bands 6 and 7. B. From Faye and Miller (1973).

When Murtaugh (1961) mapped the flows within the Craters of the Moon National Monument, he delineated an area only a few kilometres in length on the west side of Big Cinder Butte as the Blue Dragon Flow. Before the field work of this investigation, examination of the enhanced LANDSAT images indicated that a much larger area (Area 4, Fig. 13–4) both inside and outside the monument had a similar Blue Dragon-type crust. Field work bore out this hypothesis by demonstrating that a very large area exists (Fig. 13–2 and Fig. 13–4) in which very young Blue Dragon-type lavas cover all the other lavas and cinder areas with which they are in contact.

All the dates determined on COM lavas (Bullard and Rylander, 1970; 1971) have been from these young Blue Dragon-type flows. The young Blue Dragon-type flows also can be differentiated into light and dark facies in the LANDSAT images (Fig. 13–2). The cause of this difference is due to the more striking lighter blue crust of the light facies. An untested observation is that there also appear to be differences in the lichen types growing on the two facies. The two facies are nearly penecontemporaneous with the lighter facies always having a field relationship which indicates that it is the younger of the two (e.g., as squeeze-ups and pahoehoe toes where they are in contact).

These young Blue Dragon-type pahoehoe flows are easily differentiated on enhanced LANDSAT images (Fig. 13–2 and Fig. 13–4) and can be mapped on either the enhanced images (Fig. 13–2 and Fig. 13–4), or the classification maps (1 and 2, Fig. 13–3). The light and dark facies, however, are not easily separable. Since the source of the light facies (2, Fig. 13–3) has not yet been discovered in the field and its relationship to the dark facies when in contact seems to be typically as squeeze-ups, it may have been fed through lava tubes within the dark facies which has hidden its source. Only extensive field work can test this hypothesis.

Surface Cover

Aa flows and pahoehoe flows are affected very differently by surface cover in the COM area. The aa flows show little effect of cover by either sediment, vegetation, or weathing and retain their dark color, so that they are commonly considered to be younger than the pahoehoe flows with which they are in contact. Field relationships clearly indicate that their eruptions alternated with the pahoehoe flows and that they can be either younger or older than a particular nearby pahoehoe flow. Their barren nature is due, in part, to the scant annual rainfall (25–45 cm) in the COM area. Many flows erupted during historic times in the wet parts of Hawaii

already have a mantle of vegetation (Stearns, 1928, p. 19) but this reasoning applies to both kinds of flows. The rubbly surface and extremely permeable nature of the aa flows must account for their inability, compared to pahoehoe flows, to develop grass and sagebrush populations. Any sediment or water that encounters the surface of these flows sifts or runs down into the innumerable cracks. Only trees have managed to grow well on the aa surface suggesting that they are able to take seed in the deep cracks and grow up to within reach of the sunlight better than the smaller plants.

Pahoehoe flows develop a cover of sagebrush and grass more quickly than aa flows, although the young 2000 year-old Blue Dragon-type pahoehoe flows are still nearly barren of vegetation. Field work made it clear, however, that while the other older pahoehoe flows have varying amounts of surface cover by sediment, weathering products and vegetation, nearly all of them also have a Blue Dragon-type crust. The effect of this Blue Dragon-type crust on the spectral radiance of these flows in LANDSAT images has been diminished by their surface cover of sediment, vegetation, and weatheirng products (See O, Fig. 13–2). The greater the amount of cover, the lighter are the pahoehoe flows in the images and the less is the change in radiance from MSS bands 4–7 (Fig. 13–4).

Three and perhaps four major pahoehoe eruptive phases have been differentiable by this method (See 1–4, Fig. 13–4). The most recent set of flows of this sequence is the previously described young Blue Dragon-type pahoehoe flows that are around 2000 years old (See 4, Fig. 13–4). The LANDSAT images thus appear to be useful as a relative age-dating tool for these flows (Fig. 13–3b). Age, however, is not the only factor which controls the amount of weathering, vegetation and sediment that cover these flows. Both water and wind have an impact and can be especially troublesome factors if they vary areally. The greatest effect of water is along the base of the Pioneer Mountains. The Great Rift with its greater amount of unconsolidated pyroclastic material is the area where wind plays a dominant role. Across most of the area, water's effect is controlled by the rainfall because streams traverse nor springs issue from the area. Rainfall, therefore, could be a major control on the weathering and vegetation cover (mainly sagebrush and grass on the pahoehoe). The rainfall decreases 20 cm (45 cm to 25 cm) from north to south across the volcanic field but it has not been possible, at this stage, to measure the effects of this on the vegetation growth and, therefore, the radiance values in the LANDSAT images. It would be an interesting study to make randomly selected sagebrush counts on low-altitude infrared photographs of the major pahoehoe flows. This would not only indicate whether there is an areal distribution due to factors like climate, but could provide a measure of flow age based on the abundance of sagebrush in randomly selected plots on the 3 or 4 different pahoehoe flow types.

Geologic Mapping of Digital LANDSAT Images

Digital analysis techniques found to be most useful in this study are classification and contrast stretching. Examples of classification have already been touched upon in the preceding discussion (Fig. 13–3). The ease with which these maps can be produced preliminary to field investigations and re-classified with new field data afterwards makes this a powerful tool in mapping Holocene flows.

Contrast stretching (Fig. 13–2, Fig. 13–4, and Fig. 13–5) delineates flows within the volcanic field (with results similar to classification techniques discussed above) and emphasizes the outer contact between the COM volcanic field and the older Snake River Plain lavas surrounding it. The details of flows within the volcanic field are delineated by contrast stretching of the dark areas at the expense of the light areas (Fig. 13–2 and Fig. 13–4). The border of the volcanic field is delineated by contrast stretching of the light areas at the expense of the dark areas (Fig. 13–5). Standard LANDSAT products show the outer boundary for much of the perimeter but after field work were found to be insufficient in some areas, particularly where the oldest pahoehoe

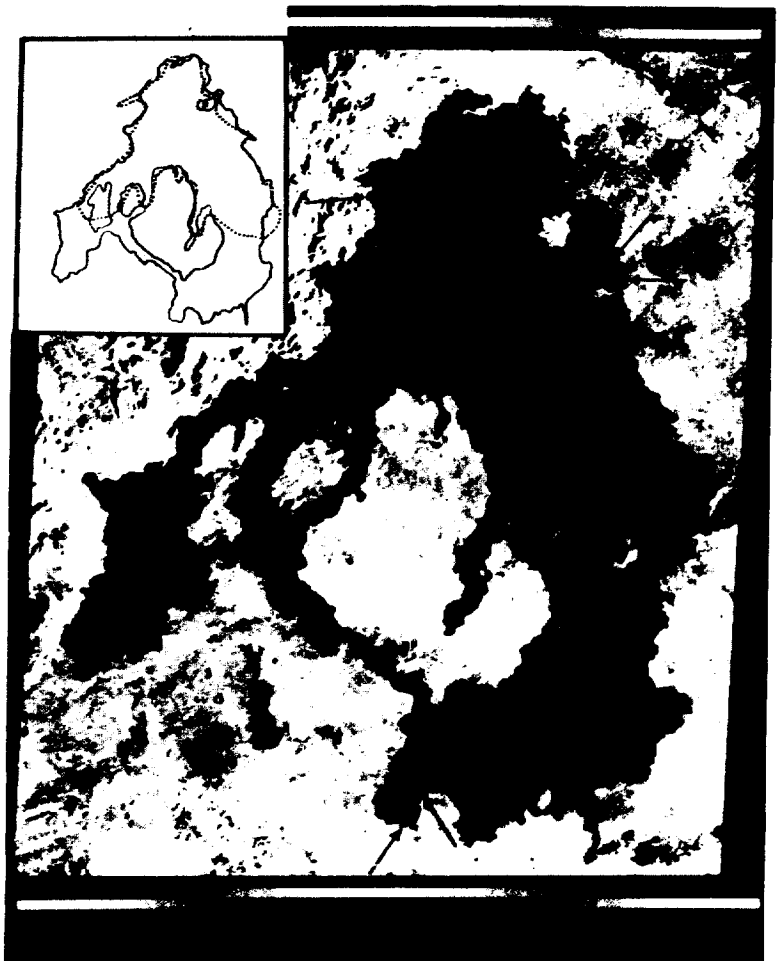

FIGURE 13-5. Portion of MSS band 7 of August 27, 1972 image modified by contrast stretching to increase contrast in bright areas. Most of the Craters of the Moon volcanic field oversaturated black. Arrows show contact between COM lavas and SRP lavas "not apparent" on standard EROS products. Inset shows boundary as it appears on the 1947 State Geologic Map of Idaho (dotted) compared to boundary (solid) drawn from modified image and corroborated in field.

flows are exposed in isolated patches beneath the younger flows (see arrows, Fig. 13–5). This boundary (Fig. 13–5) is a marked improvement over the one shown on the 1947 State Geologic Map of Idaho (Ross and Forrester, 1947).

SUMMARY AND CONCLUSIONS

Digital processing of LANDSAT images of basaltic lava flows in arid to semiarid regions can provide investigators with a broad regional and multispectral perspective for geologic mapping. Field research should be planned and carried out with the aid of LANDSAT images. The difficult accessibility of many volcanic areas as well as confusion caused by the predominance of minor features, such as the multiplicity of flow units, can be wholly or at least partly alleviated by using LANDSAT.

The following observations have been made using digital techniques supported by aerial photography analysis and field work in the COM area:

1. Rough-surfaced aa lava flows (low radiance) can be differentiated (Fig. 13–2) from the relatively smoother pahoehoe flows (higher radiance). Contrast stretching of the dark areas on the LANDSAT image emphasizes these differences and allows individual flows to be delineated.
2. Blue Dragon-type crusts are found on nearly all the pahoehoe flows in the COM area. This blue crust on the youngest (2000 yr. b.p.) pahoehoe flows causes them to have a marked decrease in radiance from LANDSAT MSS bands 4 through 7 thus making them distinctive on LANDSAT images (Fig. 13–4). This conspicuous change in radiance seems to be uncommon for rock units.
3. Blue Dragon-type crusts on older pahoehoe flows do not result in a marked spectral radiance variation (from MSS 4-7) because of the blanketing effect of surface cover by sediment, vegetation and weathering products.

Consequently, establishing a general eruption sequence may be possible for the entire volcanic field because of the essentially time-dependent blanketing effect by surface cover. Three or more major pahoehoe eruptions (Fig. 13–4) alternated with three or more major aa eruptions. Although the pahoehoe eruptive phases can be differentiated with respect to age, the aa age relationships must be determined by other means, e.g., by superposition determined on aerial photographs or in the field. At the present time, the 1300 square kilometres of the COM volcanic field has not been mapped in this detail.

4. Analysis of selected small areas shows that LANDSAT imagery can be used to map, in detail, several flows that are in juxtaposition (Fig. 13–3). This mapping has been found reliable even to the point of differentiating small pahoehoe flow units on the edges of aa flows (Fig. 13–3c).
5. The outer contact of the volcanic field with the older Snake River Plain lavas can be mapped with confidence (Fig. 13–5) by using field checks and contrast stretching of the light portions of the imagery.

ACKNOWLEDGEMENTS

This study was supported by the Earth Resources Observation Systems (EROS) Program Office of the U. S. Geological Survey and by Grand Valley State Colleges. The author is particularly indebted to Dr. Richard S. Williams who suggested the problem and gave encouragement throughout the course of the study. Special thanks go to all the members of the EROS staff for their support and suggestions.

Initial image analysis was done on the General Electric Image–100 at the EROS Data Center in Sioux Falls, S. Dak., and on the M–DAS at the Rosslyn, Va., Office of the Bendix Corporation. Extensive image processing (enhancement) was done by Mr. M. J. Abrams of California Institute of Technology's Jet Propulsion Laboratory of Pasadena, California. The author is grateful to all the people involved at these facilities.

REFERENCES

Bullard, F. M. and D. L. Rylander, 1970. Holocene volcanism in Craters of the Moon National Monument and adjacent areas, south–central Idaho (abs.): Geol. Soc. America, Abs. with Programs, v. 2, no. 4, p. 273–274.

Bullard, F. M. and D. L. Rylander, 1971. Volcanic history of the Great Rift, Craters of the Moon National Monument, south–central Idaho (abs.): Geol. Soc. America, Abs. with Programs, v. 3, no. 3, p. 234.

Faye, G. H. and R. M. Miller, 1973. "Blue Dragon" basalt from Craters of the Moon National Monument, Idaho: Origin of color: American Mineralogist, v. 58, nos. 11–12, p. 1048–1051.

Finch, R. H., 1933. Block Lava: Jour. Geology, v. 41, p. 769–770.

Goetz, A. F. H., F. C. Billingsley, A. R. Gillespie, M. J. Abrams, R. L. Squires, E. N. Shoemaker, I. Lucchitta, and D. P. Elston, 1975. Application of ERTS images and image processing to regional geologic problems and geologic mapping in northern Arizona: California Inst. Technology, Jet Propulsion Lab. Tech. Rept. 32–1597, 188 p.

Leeman, W. P., C. J. Vitaliano, and M. Prinz, 1975. Petrology and origin of "evolved" lavas from Craters of the Moon lava field, Snake River Plain (SRP) (abs.): Geol. Soc. America, Abs. with Programs, v. 7, no. 5, p. 622.

Mundorff, M. J., E. G. Crosthwaite, and Kilburn, 1964. Ground water for irrigation in the Snake River basin in Idaho: U. S. Geol. Survey Water-Supply Paper 1654, 224 p.

Murtaugh, J. G., 1961. Geology of Craters of the Moon National Monument: M.S. Thesis, Idaho Univ., Moscow, Idaho, 99 p.

Prinz, M., 1970. Idaho Rift system, Snake River Plain, Idaho: Geol. Soc. America Bull., v. 81, p. 941–947.

Ross, C. P. and J. D. Forrester, 1947. Geologic Map of the State of Idaho (scale 1:500,000): Idaho Bureau of Mines and Geology.

Rowan, L. C., P. H. Wetlaufer, A. F. H. Goetz, F. C. Billingsley, and J. H. Stewart, 1974. Discrimination of rock types and detection of hydrothermally altered areas in south-central Nevada by the use of computer-enhanced ERTS images: U. S. Geol. Survey Prof. Paper 883, 35 p.

Russell, I. C., 1902. Geology and water resources of the Snake River Plains of Idaho: U. S. Geol. Survey Bull. 15, 192 p.

Stearns, H. T., 1928. Craters of the Moon National Monument, Idaho: Idaho Bur. Mines and Geology Bull. 13, 57 p.

(Publication authorized by the Director, U. S. Geological Survey.)

14. GEOLOGICAL GUIDE TO CRATERS OF THE MOON NATIONAL MONUMENT

Ronald P. Papson
Department of Geology
Arizona State University
Tempe, Arizona 85281

14. GEOLOGICAL GUIDE TO CRATERS OF THE MOON NATIONAL MONUMENT

Ronald P. Papson
Department of Geology
Arizona State University
Tempe, Arizona 85281

Craters of the Moon National Monument, a vast area of cinder cones, spatter cones, and other volcanic features, lies along the northern border of the Snake River Plain, midway between Arco and Carey, Idaho. Craters of the Moon was declared a national monument on May 2, 1924, by President Calvin Coolidge. Originally covering about 100 km^2, it now encompasses more than 200 km^2. The monument lies about 29 km southwest of Arco along U. S. Alternate Highway 93 (Fig. 14-1) within Butte and Blaine counties and is administered by the National Park Service. It has an elevation of 1630 m in the southwest and increases northward to approximately 1810 m where the Snake River Plain meets the Pioneer Mountains.

Geological study of the Craters of the Moon area was initiated by I. C. Russell (1902). His description of the numerous "fresh" lava formations led to further examination by Stearns (1926, 1928) and Murtaugh (1961), who gave a more detailed account of the individual flows and geologic history of the area. Recently, Lefebvre (1975) has used Landsat (ERTS) images to differentiate flows and to aid in geologic mapping of Craters of the Moon (see Chapter 13).

Craters of the Moon is an area of Quaternary lava flows, cinder cones, spatter cones, lava tubes, volcanic bombs, tree molds, and other features typical of basaltic volcanism. The dominant style of eruption has been the "plains" type (see Chapter 3). There are 55 cones with associated lava flows and 14 fissures, many with spatter cones. Of the 27 distinct cinder cones, most are asymmetric in plan view, evidently the result of the dominant southwesterly winds at the time of their formation. Numerous other cones lie partly buried by younger flows.

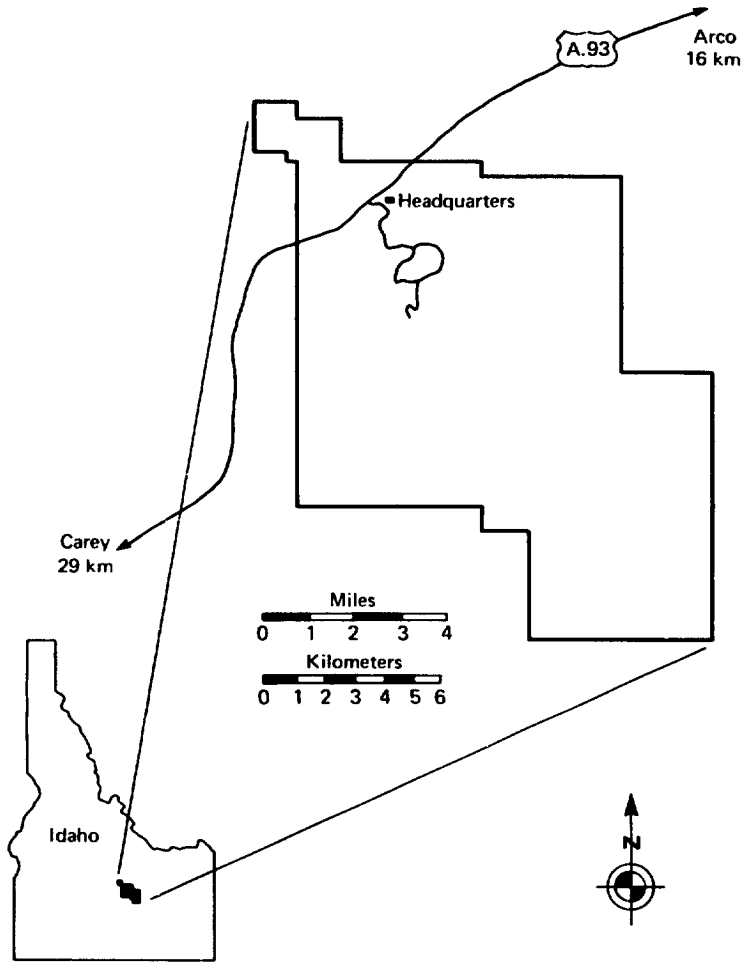

FIGURE 14-1. Index map showing location of Craters of the Moon National Monument.

The Great Rift, part of the *Idaho Rift System* (Fig. 4-5), passes through the monument as a set of *en echelon* fissures which strikes N 35°W and occurs in a zone up to 3 km wide. The entire length of the Great Rift set is 55 km, 21 km of which lie within the monument (Prinz, 1970). These fissures are the major vents for at least the youngest lavas. Raisz (1945) suggests that the fissures are an extension of what he terms the Olympic-Wallowa lineament, an alignment of features from Cape Flattery, Washington, through Craters of the Moon. He suggests that a form of recent tectonism may be the underlying cause of volcanic activity along the Great Rift. Hamilton and Myers (1966) suggest that the rift system is a tensional fracture caused by a northwest drifting crustal plate. Another possibility is that the rift may be a continuation of the tectonic activity associated with underlying older rocks of the southern Basin and Range Province. Thus, the entire rift system may be a continuation of the normal faulting which produced the mountain ranges both north and south of the Snake River Plain.

Few dates have been obtained for the basaltic flows in Craters of the Moon, although geomorphically the uppermost flows and features appear rather young. The Triple Twist Tree (Fig. 14-2) on the North Crater flow has been dated by tree ring counts as 1500 years old. Assuming a certain length of time for a sufficient accumulation of soil to support growth of the tree, the minimum age of this flow is estimated at 1650 years. Recently, Bullard and Rylander (1970) obtained a C^{14} date near the edge of the Craters of the Moon lava field by tunneling beneath a well developed pahoehoe flow (Fig. 14-3) in the vicinity of Blacktail cinder cone to obtain charcoalized rootlets that yielded a date of 2080 ± 85 years B.P. Bullard (1971) found charcoalized roots by excavating the root system of tree molds in Trench Mortar Flat and obtained a date of 2130 ± 80 years B. P. Although these dates are not valid for all recent flows in the area, they do give insight into the age of some of the later activity of Craters of the Moon.

FIGURE 14-2. Triple Twist Tree along Devil's Sewer Trail. Tree ring counts indicate a minimum age for this flow as 1650 years B.P. (Photo by National Park Service.)

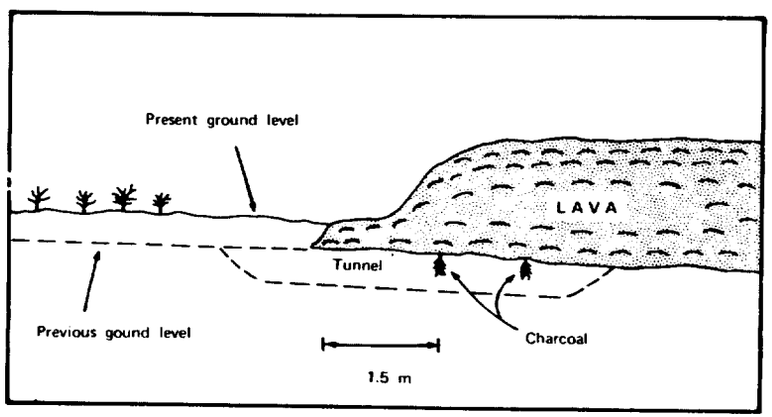

FIGURE 14-3. Diagram showing technique used by Bullard to obtain charred material from beneath Craters of the Moon lava flow; C^{14} dates of this material yielded 2080 ± 85 years B.P. (from Bullard, 1976).

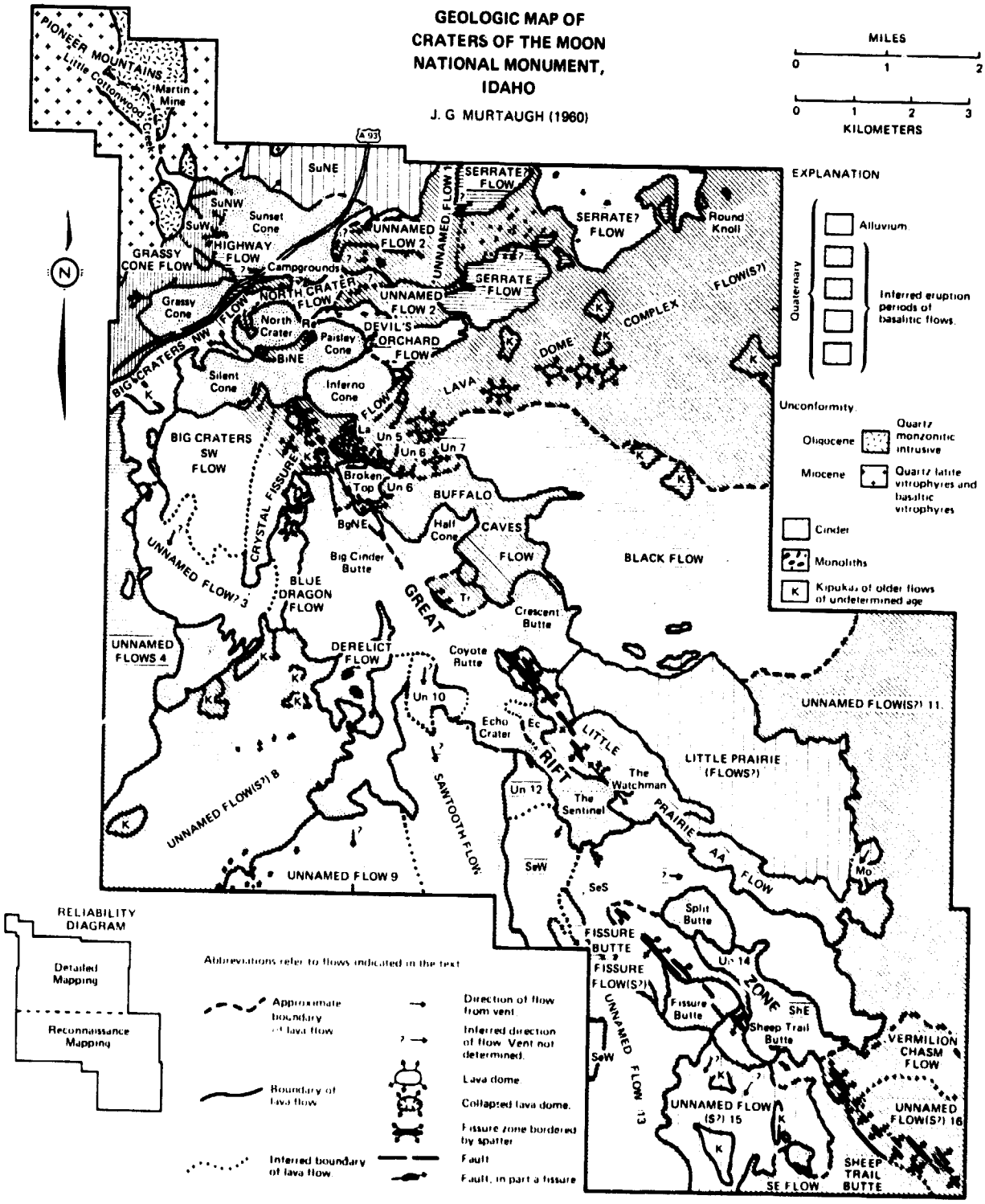

FIGURE 14-4. Geologic map of Craters of the Moon National Monument (Murtaugh, 1961).

Craters of the Moon basalt is a highly evolved olivine basalt of an iron-and-alkali-enriched lava series (Stone, 1969). A sample from the Sunset Cone flow contains phenocrysts of andesine, fayalitic olivine, titanomagnetite, and fluorapatite set in an intersertal brown glass matrix (Stone, 1969). Stone feels that if this represents the residual liquid from the Snake River magma source, more than 80% crystallization of the parent magma is indicated.

Volcanoes in the Mountains

The Pioneer Mountains form the northern boundary of the Snake River Plain in the vicinity of the monument. Within the monument, they consist of two rock types: an older suite of Oligocene quartz latite vitrophyres and basaltic vitrophyres, known collectively as the Challis Volcanics, and a second suite of Miocene quartz monzonite to granodiorite intrusives (Fig. 14-4). Within the monument, small quantities of pyrite, galena, and sphalerite have been extracted from the Martin Mine. Minor amounts of gold and silver are the only valuable metals present. Recent basalt flows from the plain "lap up" against the mountains, forming embayments (Figs. 14-5 and 14-6).

Anderson (1929) describes two volcanic vents in the bounding mountains which lie on strike with the Great Rift. Named the "Lava Creek" vents, they are composed of basaltic scoria and are thought to be an extension of the Idaho Rift System into the Pioneer Mountains. Flows from these vents opened onto the plain, forming a relatively thin aa flow field more than 2 km wide and 16 km long.

FIGURE 14-5. Panoramic view from summit of Big Cinder Butte. Extensive lava flows in the distance embay the northern Pioneer Mountains (1). Great Rift is on the right with Big Crater area (2), Inferno Cone (3), Grassy Cone (4) and Sunset Cone (5).

FIGURE 14-6. Vertical aerial photograph of northwest Craters of the Moon region. Recent plain basalt embays the northern Pioneer Mountains (1). Grassy Cone (2), Sunset Cone (3), and Silent Cone (4) are relatively old cinder cones. The Highway Flow (5), Highway fault (6) and breached North Crater with associated flows (7) represent some of the most recent volcanic activity in the area. (Photograph by U. S. Department of Agriculture, CVO 8T 10, 9-7-57.)

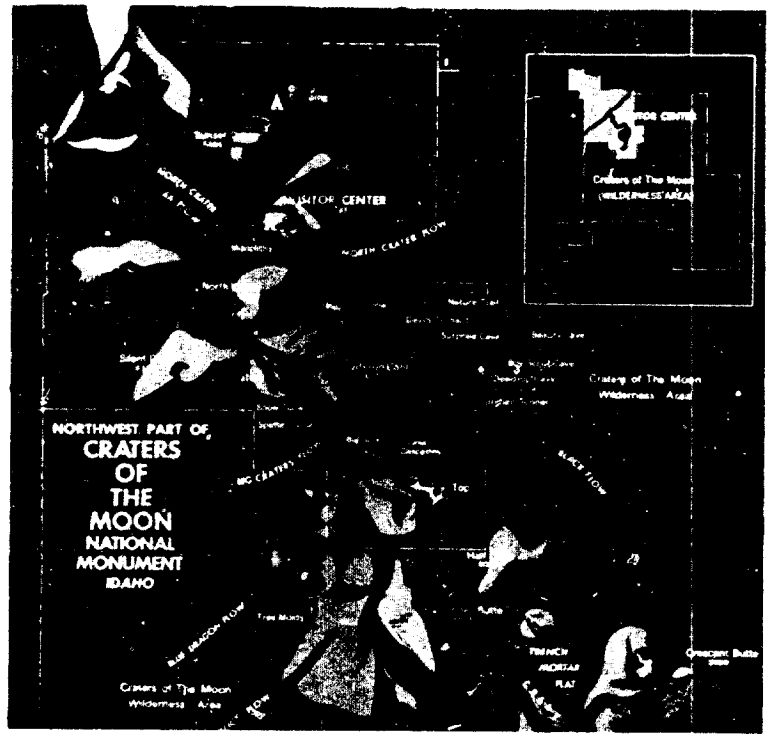

FIGURE 14-7. Map of the northwest part of Craters of the Moon National Monument (National Park Service, November, 1975).

Sunset and Grassy Cones

These cones (Figs. 14-6 and 14-7) are relatively old and rise about 160 m above the surrounding plain. Three flows issue from Sunset cone but are largely blanketed with ash and soil. Two pahoehoe flows breached the crater in the northeast (SuNE) and in the west (SuW). On the northwest flank of the crater, an aa flow (SuNW) approximately 6 m thick issued from a small parasitic cone.

Both cones represent some of the earliest eruptive activity in the monument. Two craters on the north side of Grassy Cone erupted lava simultaneously. The two flows merged and extended northward. A network of lava tubes, some as large as 5 m in diameter, formed within the flows.

North Crater Area

Of the flows described here, only the North Crater flow can be traced with certainty to the North Crater vent (Fig. 14-8). An identifying characteristic of these flows is the presence of monoliths in all except the Highway flow. Monoliths appear to be fragments of cinder cones which have been broken in place or have been rafted to their present position by flowing lava (Fig. 14-9). They range in size from about 0.5 to 200 m long; some are up to 25 m high. Some monoliths protrude as kipukas with younger flows diverted around them.

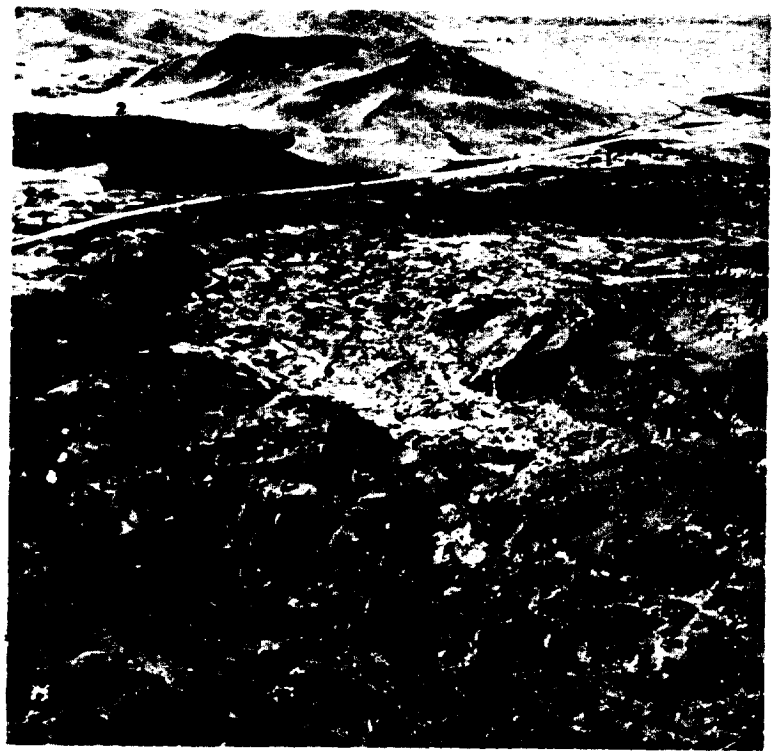

FIGURE 14-8. View northward across North Crater, the breached cinder cone in the foreground. Craters of the Moon National Monument Visitor Center (1), the Highway Flow (2), the Highway Fault (3), Sunset Cone (4), monoliths (5), and North Crater flows (6).

The massive Highway flow (Fig. 14-10) issued northward from the North Crater vent and was confined to the valley between Sunset and Grassy Cones (Figs. 14-6 and 14-11). It has a surface braided with channels 3 to 6 m deep and has flow margins ranging from 3 to 15 m high. Flow units include pahoehoe, aa, and block flows. The Highway fault (Fig. 14-8) near U. S. Alternate Highway 93 forms a distinct scarp 5 to 15 m high which cuts the Highway flow, exposing it in cross section. The fault scarp faces North Crater and must have formed soon after the emplacement of the Highway flow since pahoehoe lava from within the flow is draped over the scarp. The fault may have resulted from post-eruption subsidence.

An unnamed flow, which may have originated from North Crater, contains large andesite xenoliths. These andesite blocks are exposed only in the cross section revealed by the Highway fault and indicate that this flow may have swept past the scarp, picking up talus or transporting blocks which fell onto the flow surface.

The North Crater flow is a recent flow having the "Blue Dragon" crust (Fig. 14-12) on many of the flow units. This term, as proposed by Russell (1902), refers to a glossy, iridescent blue-white crust which is probably a result of weathering soon after extrusion. There are many large circular collapse depressions throughout the flow (Fig. 14-13), some of which are 15-20 m across.

The Serrate flows to the east of Paisley Cone may be associated with North Crater. Each of the flows, including the Devil's Orchard flow, average about 20 m thick and contain several short pahoehoe flow units, although block and aa lavas predominate.

FIGURE 14-9. Photomosaic looking southwest from campgrounds towards North Crater (1). North Crater aa flow in foreground with monoliths (2), North Crater pahoehoe (3), Grassy Cone (4), Highway fault (5), and Inferno Cone (6). (Photograph by Ronald Greeley, University of Santa Clara, June, 1977.)

FIGURE 14-10. Flow front of massive Highway Flow, looking northward toward the Pioneer Mountains. Arrow points to person. (Photograph by Ronald Greeley, University of Santa Clara, June, 1977.)

FIGURE 14-11. Aerial view of the Highway flow looking south toward North Crater. (Photograph by Ron Papson, University of Santa Clara, June, 1977.)

FIGURE 14-12. Ropy pahoehoe with iridescent "Blue Dragon" crust. (Photograph by National Park Service.)

The Registration Waterhole flow (Re) is found in the valley between North Crater and Paisley Cone and has been termed an endogenous dome by Stearns (1926). The sequence of events here includes eruption of pahoehoe lava which was partially covered by a thin aa flow. Registration Waterhole, a perennial fresh water spring is found just below the vent. Several similar springs appear throughout the monument and contain water which is just barely above the melting point of ice. Winter ice trapped in depressions, lava tubes, and channels is insulated against the summer heat by scoriaceous basalt. As the ice slowly melts, it travels through crevices and other openings in the lava until ponding at an impermeable layer of ice or lava. The location of waterholes is unpredictable, depending on annual temperature variations, fracture and joint patterns in the flows, and thermal characteristics of the basalt.

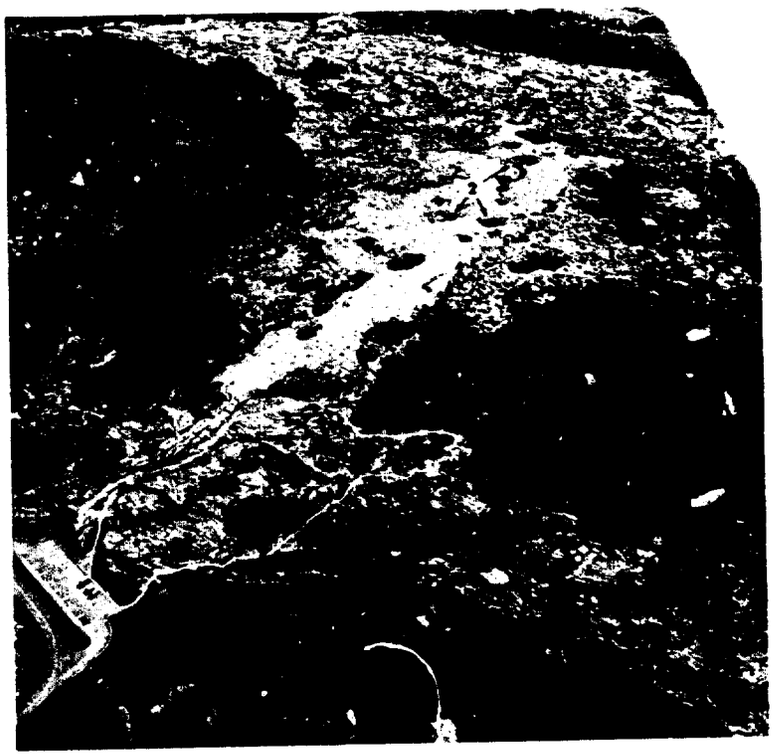

FIGURE 14-13. Low oblique aerial view of the Devil's Sewer trail area, showing pahoehoe flows (light-toned areas and aa flows from North Crater (upper left). Monoliths (1) are fragments of old cinder cone walls that were rafted on the flows. Collapse depressions (2) appear throughout the flow. (Photograph by Ronald Greeley, University of Santa Clara, June, 1977.)

Big Craters

Big Craters is a series of spatter cones and open fissure flows (Fig. 14-14) and is almost identical in size and shape to the vent area produced by the 1960 Kapoho eruption of Kilauea volcano, Hawaii (Parsons, 1970). The slopes of the agglutinate cones are 50-60 degrees near the summit and decrease to about 30 degrees near the base. The upper slopes are angular and rough whereas the lower slopes are smoother and have profiles similar to those of cinder cones (Fig. 14-15). The cones range in height from 12 to 20 m and are aligned with the Great Rift. These spatter cones have chimney-like vent areas, most of which have collapsed, displaying a rubbly interior. Toward the northwest portion of the Big Crater area, however, two complete vents remain intact. They are nearly circular in plan view and show an hour-glass vertical cross section. Some of the vents may be connected by lava tubes at depth. In some cones, ice remains throughout the summer months, protected from the sun by deep cylindrical wells. These "ice wells" were described by Russell (1902) in his initial traverses.

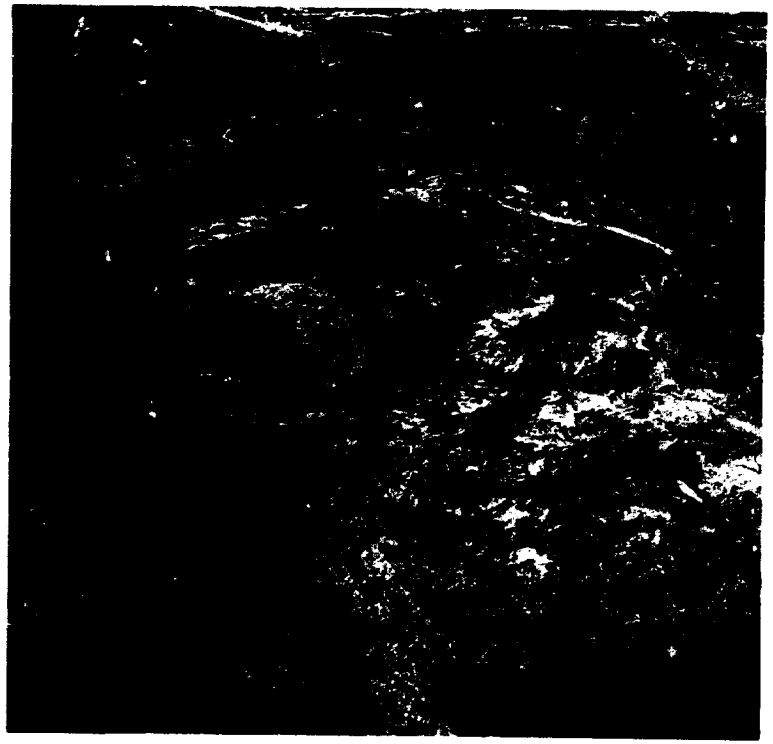

FIGURE 14-14. Low oblique aerial view of Big Craters area. Parking area and trails (white lines) allow inspection of numerous spatter cones. The cones align along a fracture with some flows covering older cinder cones (left center). Inferno Cone (upper right) is composed of black cinders and has no summit crater. (Photograph by Ronald Greeley, University of Santa Clara, June, 1977.)

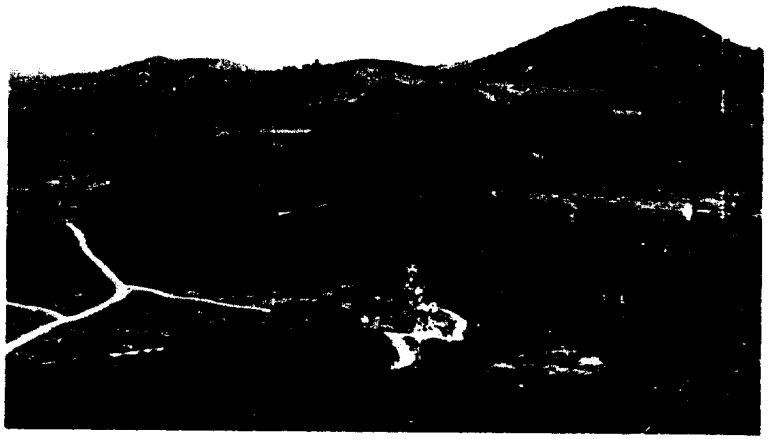

FIGURE 14-15. View of spatter cones in Big Craters area, looking south along the rift. Steep upper slopes are angular and rough, while lower slopes have gentle profiles. Big Cinder Butte (upper right) is the largest cone within the monument and has a total volume of $2 \times 10^8 m^3$. (Photograph by Ronald Greeley, University of Santa Clara, June, 1977.)

Several large pahoehoe and aa flows were erupted from these vents. The northeast flow (BiNE) is a short pahoehoe unit that issued from an open fissure north of the spatter cones. Many of the older flow units are exposed in the walls of the fissure. The northwest flow evolved from flat pahoehoe to slab lava and eventually to a mixture of aa and pahoehoe. Part of this flow extends northward, where it is overlain by the North Crater flow and part extends southward, where it was diverted around Silent Cone. The southwest flow is an extensive aa flow mixed with small pahoehoe subunits which contain numerous channels throughout and overlie the northwest flow.

Lava Cascades

Lava cascades (La) is a large collapsed lava "dome." A "dome" is a gently sloping accumulation of flows with little or no clastic ejecta which forms around a vent from which lava was quietly extruded. Lava cascades formed by surface collapse due to magma subsidence or withdrawal. Short pahoehoe flow units issued from marginal cracks and flowed down into the depression left by the collapse (Fig. 14-16).

FIGURE 14-16. Lava cascades, channelized flow having a "Blue Dragon" crust. (Photograph by National Park Service.)

Tree Molds

Tree molds exist in some flows throughout the monument (Fig. 14-17). As observed in active flows in Hawaii and elsewhere, some lava flows rapidly form crusts that effectively insulate tree trunks from the molten lava, preserving the wood or even preventing death of the tree. Later, the wood rots, leaving a perfect mold of the tree. In some places the grain of the wood has been preserved in lava.

Big Cinder Butte

This cinder cone has a total volume of 2 x $10^8 m^3$ and rises 250 m above the plain—the highest cone within the monument (Fig. 14-10). It has no summit crater and terminates in a rounded cinder knob. A variety of volcanic bombs are found on the cone including cow dung, breadcrust, and spindle types. The rims of five or six older volcanoes are visible around its base.

Several flows issued from Big Cinder Butte. The youngest, the northeast flow (BgNE), originated from a fissure on the north side of the cone and is a "Blue Dragon" pahoehoe flow. The Derelict flow is a short, black aa flow which extends to the southwest and contains numerous monoliths. Southward, an unnamed block lava flow issues near the border of the Derelict flow.

FIGURE 14-17. Tree mold near Big Cinder Butte. Lava flows knock over trees and bury entire portions. Texture is probably that of the tree bark after it was initially burned upon being buried by the lava. (Photograph by National Park Service.)

Lava "Dome" Complex Flows

The area east of Inferno Cone consists of a series of lava "domes." Many of the flow units contain lava tubes, and individual flow units are generally "Blue Dragon" pahoehoe, although some flat scoriaceous pahoehoe is also present. The lava tubes in this area may be part of a giant network in a single flow. Indian Tunnel is one of the largest tubes in the monument, reaching widths of over 15 m (Fig. 14-18). Crescentric rock heaps found in this area (Fig. 14-19) were probably used to secure tepees of the Indian tribes which frequented the caves. Numerous other tunnels and caves are common in this area, ranging in size from centimeters to meters (Figs. 14-20 and 14-21). Natural bridges, which are uncollapsed remnants of tunnel roof sections, occur here and in the southernmost part of the monument. Present uncollapsed sections may be as much as 1 km in length.

FIGURE 14-18. Indian Tunnel lava tube. Many uncollapsed sections of this tunnel exist, some of which have widths up to 15 m. (Photograph by National Park Service.)

FIGURE 14-19. Crescentric rock heaps near Indian Tunnel (lava tube). These were probably used to secure tepees of the Indians who camped in this area. The caves provided protection and cool areas for hot summer days. (Photograph by Ron Papson, University of Santa Clara, June, 1977.)

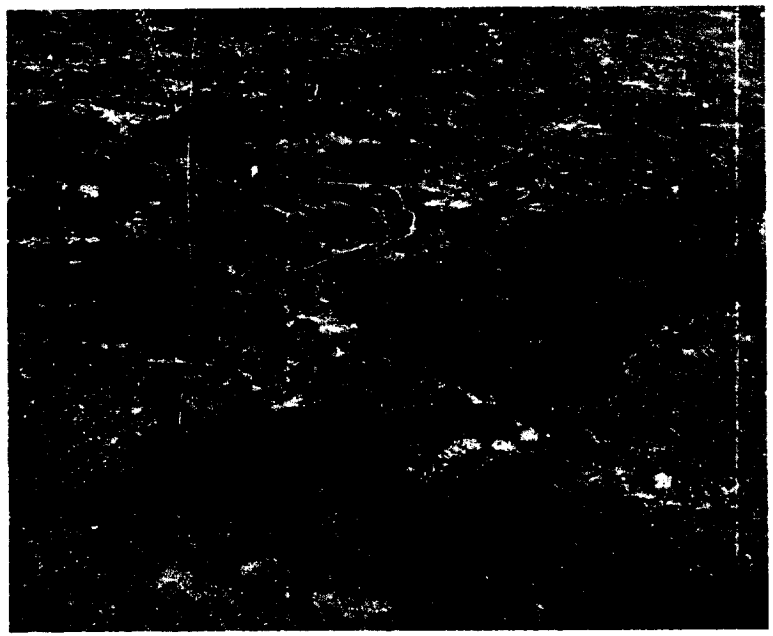

FIGURE 14-20. Arco Tunnel (lava tube), an example of the many tubes within the Cave area.

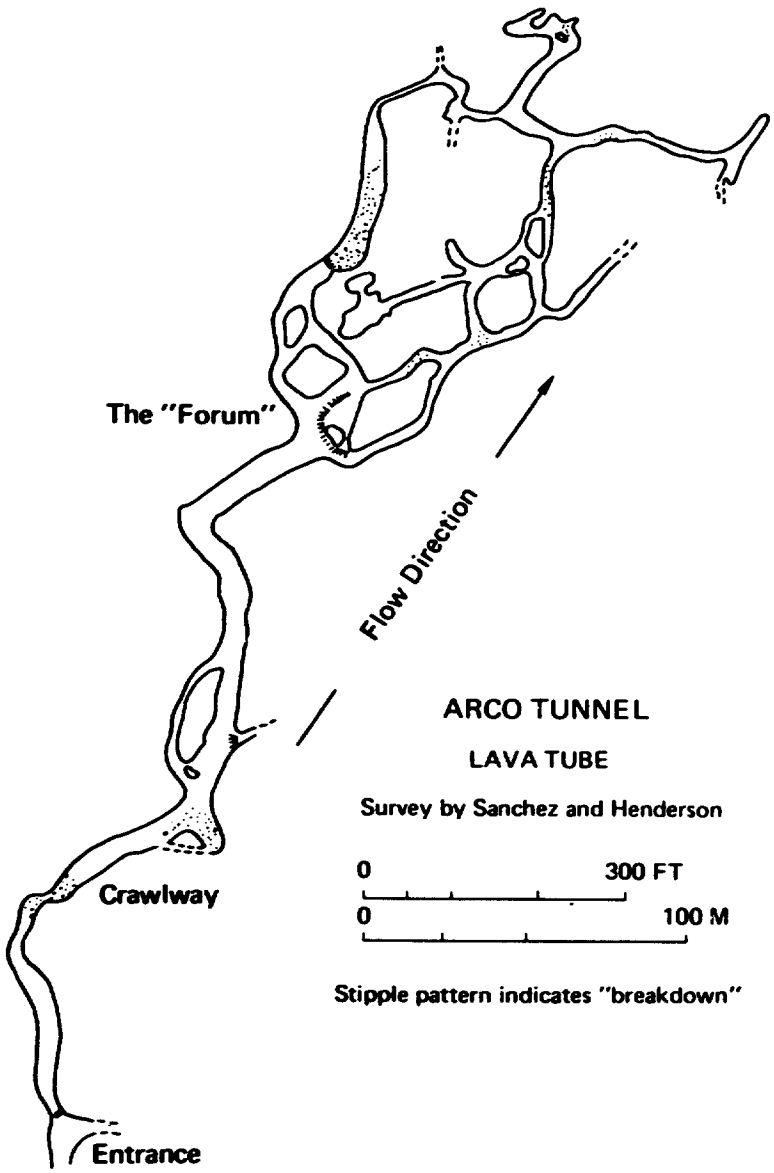

FIGURE 14-21. Arco Tunnel (lava tube), an example of the many tubes within the Cave area.

FLORA AND FAUNA OF CRATERS OF THE MOON NATIONAL MONUMENT

Amy M. Stuart

The first impression of Craters of the Moon National Monument is that the area is barren and desolate, consisting of lavas and cinder cones; however, many plants and animals have successfully adapted to the area, despite harsh climatic conditions.

Paleobotany in the Snake River Plain

Axelrod (1968) examined Eocene and Miocene flora preserved in the beds of adjacent sedimentary rocks associated with Snake River Plain geologic events to determine the timing and topography in the subsidence of the Snake River Plain. The fossil floras investigated represent samples of forest zones existing under different climates. For each epoch, different zones occur as a consequence of elevation differences; therefore, climatic conditions provide a clue for estimating altitudes of the Snake River Plain.

Plants existing in the Eocene forests were hemlock, spruce, pine, maple, birch, aspen, fir, and oak, implying moderately high altitudes. Broad-leaved evergreens, usually associated with more tropical climates, were found on the fringe of what is now the Snake River Plain. Formation of the Snake River basin appeared to have begun during the Oligocene. By the Miocene, the uplands had subsided to a lowland basin. Many of the plants found in the Eocene also occurred in the Miocene, such as spruce, pine, hemlock, and maple, while others, such as the Tree-of-Heaven, beech, and dogwood were not indicated by Axelrod, which suggests a lack of abundance or possibly absence of those species in the area at the time. The paleobotanic evidence of the Snake River Plain subsidence is supported by other geologic features.

Fauna

Numerous animals live in the area despite the harsh environment. The following mammals are most common: cottontail rabbits, chipmunks, squirrels, mule deer, antelope, bats, skunks, pack rats, pocket gophers, and badgers. Other, less visible, animals include bobcat and coyote. Stearns (1928) reports that bears once inhabited the lava caves and that mountain sheep and buffalo were occasionally seen.

Numerous birds also inhabit the area, although some are seasonal. The more commonly seen birds are: mourning dove, sage grouse, killdeer, magpie, raven, crow, Clark's nutcracker, common nighthawk, mountain bluebird, great horned owl, and golden eagle.

Flora

The variety of flowers (Figures 14-22 to 14-28) found at Craters of the Moon National Monument is surprisingly large for such an arid area. Plants must adapt to extremes of heat and cold, dessication from lack of water, lack of nutrients and improper soil acidity, wind, lack of soil, and rooting depth.

Different flowers appear to prefer either the "cinder garden habitat" or the "joint habitat" of the lava flows. On the cinder buttes, plants are rooted in loose tephra deposits mixed with variable amounts of both wind-blown and volcanic dust. The most common plants found here are: dusty maiden or false yarrow (Fig. 14-24), buckwheat (Fig. 14-24), and dwarf monkey flower (Fig. 14-22). On the north-facing slopes of cinder cones where more moisture is available, open stands of timber pine (Fig. 14-26) are found.

The absence of soil and moisture on basalt flows is extremely harsh on many plants. Fractures within lava flows trap soil and provide additional moisture, wind protection, and cooler temperatures than adjacent exposed areas. In the "joint habitat" scabland penstemon (Fig. 14-27) and gland cinquefoil are common, while in deeper crevices, tansybush, bush rockspirea and syringa (Fig. 14-27), Idaho's state flower, will thrive (Urban, 1971).

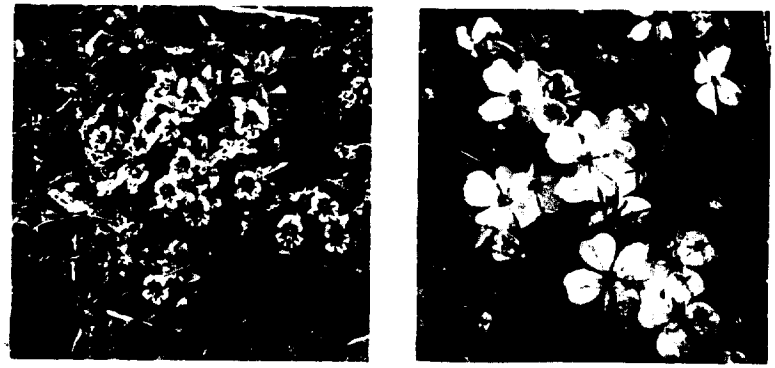

FIGURE 14-22. On left is dwarf monkeyflower (Mimulus nanus), tiny magenta-colored flowers, blooming in late June to early July, rarely greater than 5 cm in height. On right is evening primrose (Oenothera caespitosa), white to pink flowers blossoming from early to mid-June.

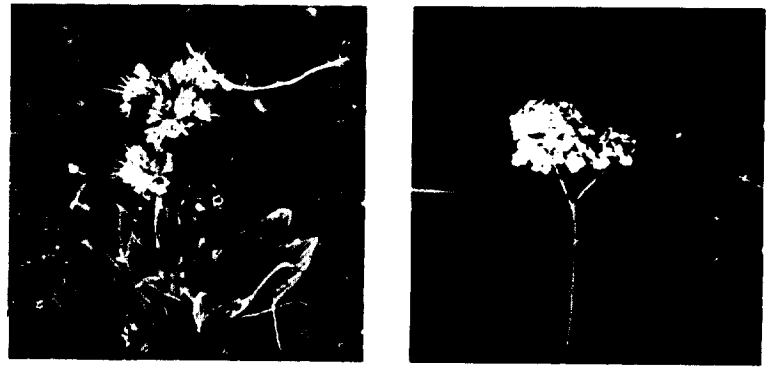

FIGURE 14-23. On left is scorpionweed, lavender flowers curving on stalks like that of a scorpion's tail, blooming from mid-June to mid-July. On right is western yarrow (Archillea millefolium spp. lanulosa), white flat-topped clusters of flowers blooming from late July to early August, usually less than 60 cm tall.

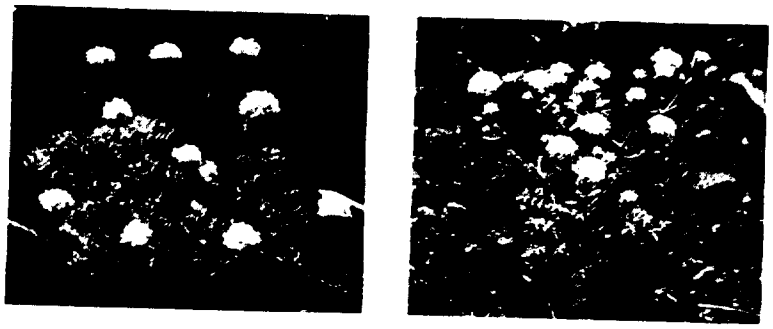

FIGURE 14-24. On left is buckwheat (Eriogonum); flower clusters are pom-pom shaped, blossoming any time from early June to late August, depending on the variety, usually grow to about 25 cm tall. On right is dusty maiden or false yarrow (Chaenactis douglasii), white to pink flowers aggregated in a head-type inflorescence, blossoms from early July to mid-August, usually less than 15 cm tall.

FIGURE 14-26. On left is sunflower (Helianthus annuus), yellow flowers forming in heads about 6 cm in diameter, usually solitary on stems, blooms from August to September, usually 60-120 cm in height. On right is limber pine (Pinus flexilis); needles are bright green and are about 4 cm long, born in clusters of 5.

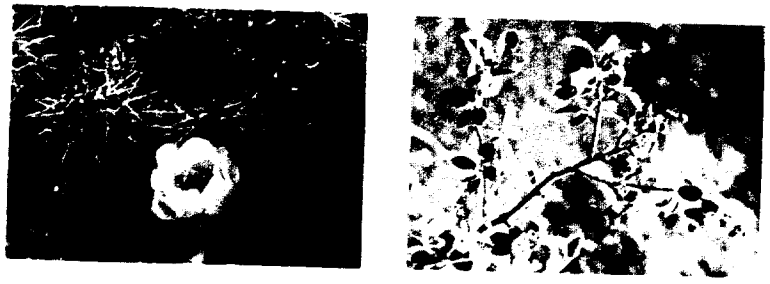

FIGURE 14-25. On left is prickly pear cactus (Opuntia polyacantha), yellow, orange, or red flowers blooming in late June, fruits are edible. On right is squaw currant (Ribes cereum); bright red edible fruits mature in mid-July, leaves usually gray-green and sticky. A close relative, golden currant (Ribes aureum) ripens in late July with orange, edible berries.

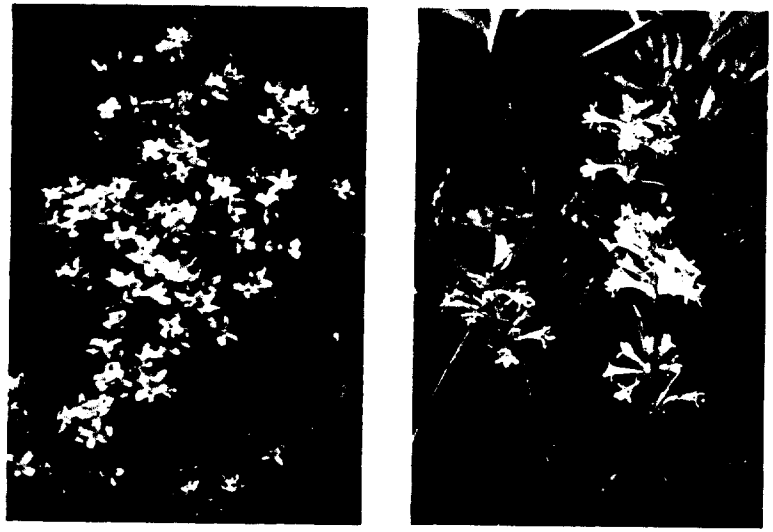

FIGURE 14-27. On left is syringa (Philadelphus lewisii), the state flower of Idaho; its fragrant white petals bloom in early July; the bush is usually less than 120 cm tall. On right is scabland penstemon (Penstemon deustus), white to pink bilabiate blossoms flowering from mid-June to mid-July.

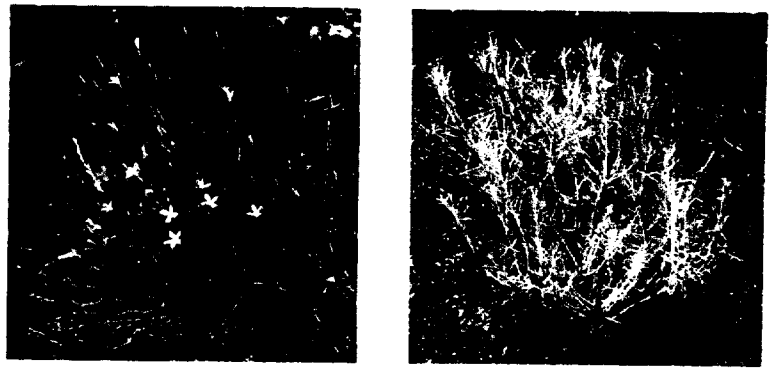

FIGURE 14-28. On left is wire lettuce (Stephanomaria tenuifolia), appearing as branched fragile stems usually about 15 cm high; the pink ray flowers bloom in late July. On right is rabbitbrush (Chrysothamnus naueosus), a shrub with gray-green leaves usually less than 60 cm tall; the small yellow flowers bloom from mid-August to September.

REFERENCES

Anderson, A. L., 1929. Geology and ore deposits of the Lava Creek District, Idaho: Idaho Bureau of Mines and Geology, Pamphlet 32.

Axelrod, 1968. Tertiary floras and topographic history of the Snake River Basin: Idaho Geol. Soc. Amer. Bull., vol. 79, p. 713-734.

Bullard, F. M., 1971. Volcanic history of the Great Rift, Craters of the Moon National Monument, south-central Idaho: Geol. Soc. Amer. Abs. with Programs, vol. 3, no. 3, p. 234.

Bullard, F. M., 1976. *Volcanoes of the Earth.* University of Texas Press, Austin, 579 p.

Bullard, F. M. and D. Rylander, 1970. Holocene volcanism in Craters of the Moon National Monument and adjacent areas, south-central Idaho: Geol. Soc. Amer. Abs. with Programs, vol. 2, no. 4, p. 273.

Hamilton, W. B. and W. B. Myers, 1966. Cenozoic tectonics of the Western United States: Rev. of Geophysics, vol. 4, p. 509-549.

Lefebvre, R. H., 1975. Mapping in the Craters of the Moon volcanic field, Idaho, with LANDSAT (ERTS) imagery: *in* Proceedings of the Tenth International Symposium on Remote Sensing of Environment, Research Institute of Michigan.

Murtaugh, J. G., 1961. Geology of Craters of the Moon National Monument: M. S. Thesis, University of Idaho, Moscow, Idaho.

Parsons, W. H., 1970. Guidebook–Structures and Origins of Volcanic Rocks, Montana-Wyoming-Idaho: Wayne State University.

Prinz, M., 1970. Idaho Rift System, Snake River Plain, Idaho: Geol. Soc. Amer. Bull., vol. 81, p. 941-948.

Raisz, E., 1945. The Olympic Wallowa lineament: Am. Jour. Science, vol. 243-A, Daly Volume, p. 479-483.

Russell, I. C., 1902. Geology and Water Resources of the Snake River Plain of Idaho: U. S. Geol. Survey Bull. No. 199.

Stearns, H. T., 1926. Craters of the Moon National Monument: U.S. Geol. Survey open-file report.

Stearns, H. T., 1928. Craters of the Moon National Monument, Idaho: Idaho Bur. Mines and Geology Bull., No. 13, 57 p.

Stone, G. T., 1969. Preliminary petrologic appraisal of Craters of the Moon, Idaho: Geol. Soc. Amer. Abs. with Programs, vol 1, no. 7, p. 217.

Urban, K. A., 1971. *Common plants of Craters of the Moon National Monument:* Craters of the Moon Natural History Association, Inc., 30 p.

15. POSSIBLE PLANETARY ANALOGS TO SNAKE RIVER PLAIN BASALT FEATURES

Ronald Greeley
Center for Meteorite Studies
and Department of Geology
Arizona State University
Tempe, Arizona 85281

Peter H. Schultz
Lunar Science Institute
3303 NASA Road 1
Houston, Texas 77058

15. POSSIBLE PLANETARY ANALOGS TO SNAKE RIVER PLAIN BASALT FEATURES

Ronald Greeley
Center for Meteorite Studies
and Department of Geology
Arizona State University
Tempe, Arizona 85281

Peter H. Schultz
Lunar Science Institute
3303 NASA Road 1
Houston, Texas 77058

In this chapter planetary features are presented and illustrated as possible analogs to volcanic structures observed in the Snake River Plain. As discussed in Chapter 2, evidence of basaltic volcanism—or volcanism involving lavas with properties similar to basalt—can be cited with varying degrees of confidence for all of the inner planets. Flood lavas are identified on the Moon (Fig. 2-2), Mars (Fig. 2-5), and possibly Mercury. Large shield volcanoes are observed on Mars (Fig. 2-5) and postulated for Venus (Malin and Saunders, 1977).

In addition to flood lavas and shield volcanoes, plains-type basaltic volcanism (as defined in Chapter 3) is identified on the planets based on the types of surface features observed (Fig. 15-1). Many of the mare units on the Moon appear to be the result of "plains" volcanism, particularly mare units of Eratosthenian age (Greeley, 1975). Units of possible volcanic origin cover more than 50 percent of the surface of Mars (Spudis and Greeley, 1976) and many of these units also may be of the basaltic-plains variety.

Basaltic-plains features discussed here include low shields on the Moon and Mars, lava flow textures on the lunar plains, lava tubes and channels in the form of sinuous rilles on the Moon and Mars, and various vent structures, such as pit craters and fissure vents.

FIGURE 15-1. Viking Orbiter image of the Tharsis region of Mars, showing flows interpreted as flood-lavas. Variations in albedo represent differences in aeolian erosion and deposition. Area of image is 160 km by 180 km; north is to the right. (Viking Orbiter II frame 42B31.)

LOW SHIELDS

Viking Orbiter pictures (Carr and others, 1976), taken of the southeastern part of Chryse Planitia during the search for the landing site for Viking Lander I, reveal a field of about 60 small, low-profile structures (Fig. 15-2), tentatively identified as low shields (Greeley and others, 1977; Greeley and Theilig, 1977). The field is the "outwash plain" of a major martian channel of probable fluvial origin. The low shields appear to post-date both the channel and the plains on which they occur and are among the smallest volcanic features observed on Mars. The low shields average 2.5 km across; many have summit knobs—giving a two-part profile—and summit craters.

FIGURE 15-2. Low shield (arrow) about 4.2 km long in southeastern Chryse Planitia; a small "knob" several hundred km across occurs on the southern end of the low shield. (Viking Orbiter I frame 6A36.)

FIGURE 15-3. Enlarged Lunar Orbiter framelets showing coalescing low shields associated with mare deposits (in Lacus Veris) in the Orientale Basin on the Moon. Shields appear to be related to a linear fissure vent; steep features on the fissure are interpreted as pyroclastic deposits. Area of photograph is 22 km by 35 km; north is toward the bottom of photograph. (Lunar Orbiter IV photograph 181 H_2.)

In size and morphology, the martian features closely resemble the low shields of the Snake River Plain, Idaho, such as Pillar Butte (see Chapter 8).

Small shield-shaped features have also been identified on the Moon. Figure 15-3 shows several small coalescing shield-like constructs in the Orientale basin which appear to be associated with a fissure. They are low-profile structures a few km across, some of which have steeper elements near the central fissure that could be spatter and pyroclastic deposits. Other possible small shield volcanoes on the Moon (Fig. 15-4) include structures such as those near Hortensius (Fig. 15-4a) that are circular positive-relief features having central pit craters (Schultz, 1976).

It is emphasized that the low shields described above are rather minor features in comparison to Mauna Loa and Olympus Mons. Rather, the presence of low shields signify plains-type basaltic volcanism.

FIGURE 15-4a. Three small (5 km in diameter) low profile domes (arrows) at 7°N, 332°E, just north of the crater Hortensius on the Moon. The domes have central summit craters, and are interpreted as possible low shields. Open-arrow indicates a line of possible cinder and spatter cones. Area of photograph is about 60 km by 85 km; north is to the bottom of photograph. (Lunar Orbiter IV frame 133 H 1.)

FIGURE 15-4b. Small (6 km across) shield-shaped mass and sinuous rilles on the mare surface near Rima Aristarchus. Note the irregular summit depression on the shield. (Apollo 15 frame 2086.)

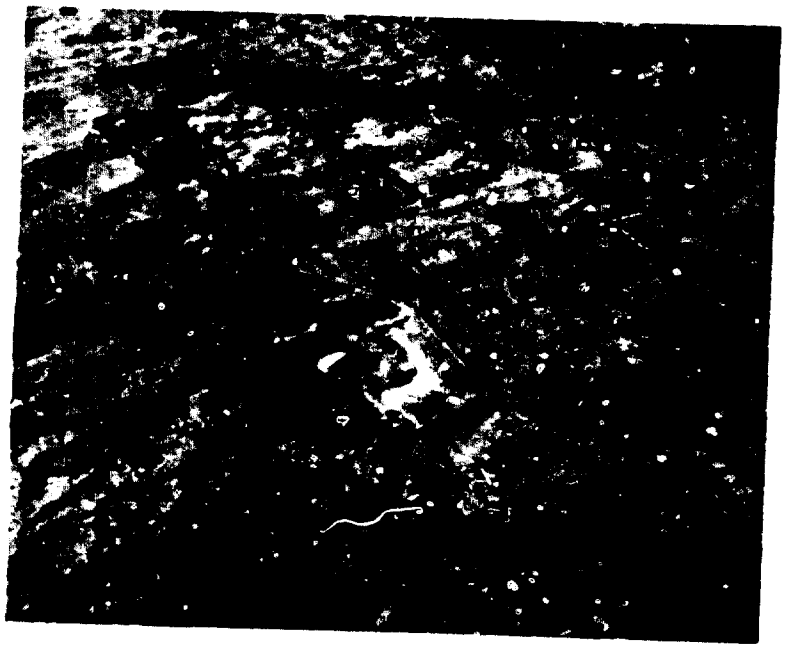

FIGURE 15-4c. Oblique aerial view of a small shield and summit crater on the Snake River Plain; jeep trail indicates scale. (Photograph by Ronald Greeley, University of Santa Clara, 1971.)

LUNAR FLOW TEXTURES AND RING MOAT STRUCTURES

The lunar maria are generally devoid of well-defined lava flow fronts, the Imbrium flows representing notable exceptions (Schultz, 1976; Schaber and others, 1976). However, other features and textures on the maria resemble primary flow morphologies found in terrestrial lava fields, such as those in the Snake River Plain. Pahoehoe basalt flows typically exhibit a ropy texture at fine scales (sub-meter sizes) that could not survive the long-term degradational processes on the Moon. Nevertheless, such flows also exhibit broader scale features (dimensions larger than 50 m) that might survive meteoritic erosion on the younger lunar lavas. These features include (see Fig. 15-5):

1. Tumuli and irregular knobs: maximum size approaching 50 m.
2. Circular collapse depressions: ranging from 10 to 50 m.
3. Irregular plateaus: ranging from less than 50 m to greater than 500 m.
4. Irregular depressions: ranging from less than 50 m to greater than 500 m.
5. Ridges: from very narrow widths to 20 m.
6. Linear depressions (moats) between pre-existing relief and subsequent floors.

The association of these various forms produces a distinctive hummocky surface in several Snake River Plain basalt fields.

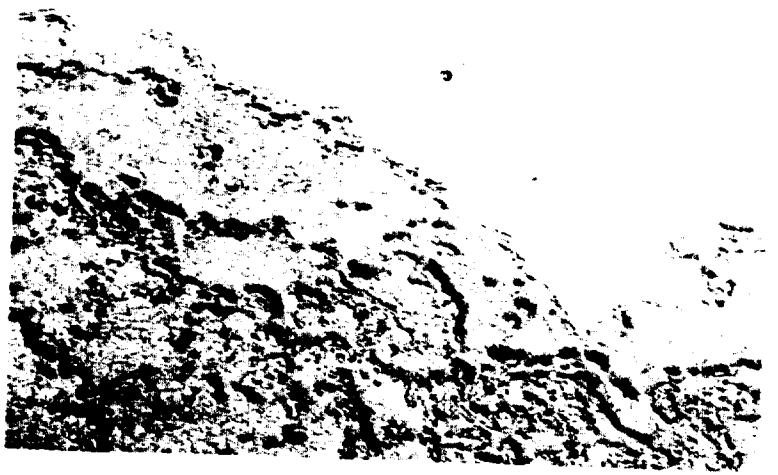

FIGURE 15-5. Pahoehoe surface near the edge of the Wapi lava field. Lava morphology includes irregular plateaus, depressions, and knobs as well as circular dimple-shaped depressions.

Similar hummocky mare surfaces occur on the Moon and are most visible under low solar illumination. Figure 15-6 illustrates in stereo a region in Oceanus Procellarum where a smooth mare surface clearly contrasts with a hummocky mare surface. The hummocky mare unit contains numerous interlinking irregular depressions and commonly exhibits irregular patches of smooth-surfaced units. Although a few regions display a directional trend, more characteristically, a surface grain is absent. Moreover, major sinuous rilles crossing such mare units are notably absent or rare.

The mare-flooded interior of the Flamsteed Ring exhibits a similar hummocky surface that has been interpreted by Schaber and others (1976) as highly degraded lava termini. Figure 15-7 shows a portion of this surface and reveals that the irregular scarps comprise the borders of irregular plateaus or depressions, which resemble the features in certain Snake River Plain basalt fields. In this analogy, the irregular scarps are not the termini of individual flows but are remnants of differential subsidence within a single flow unit.

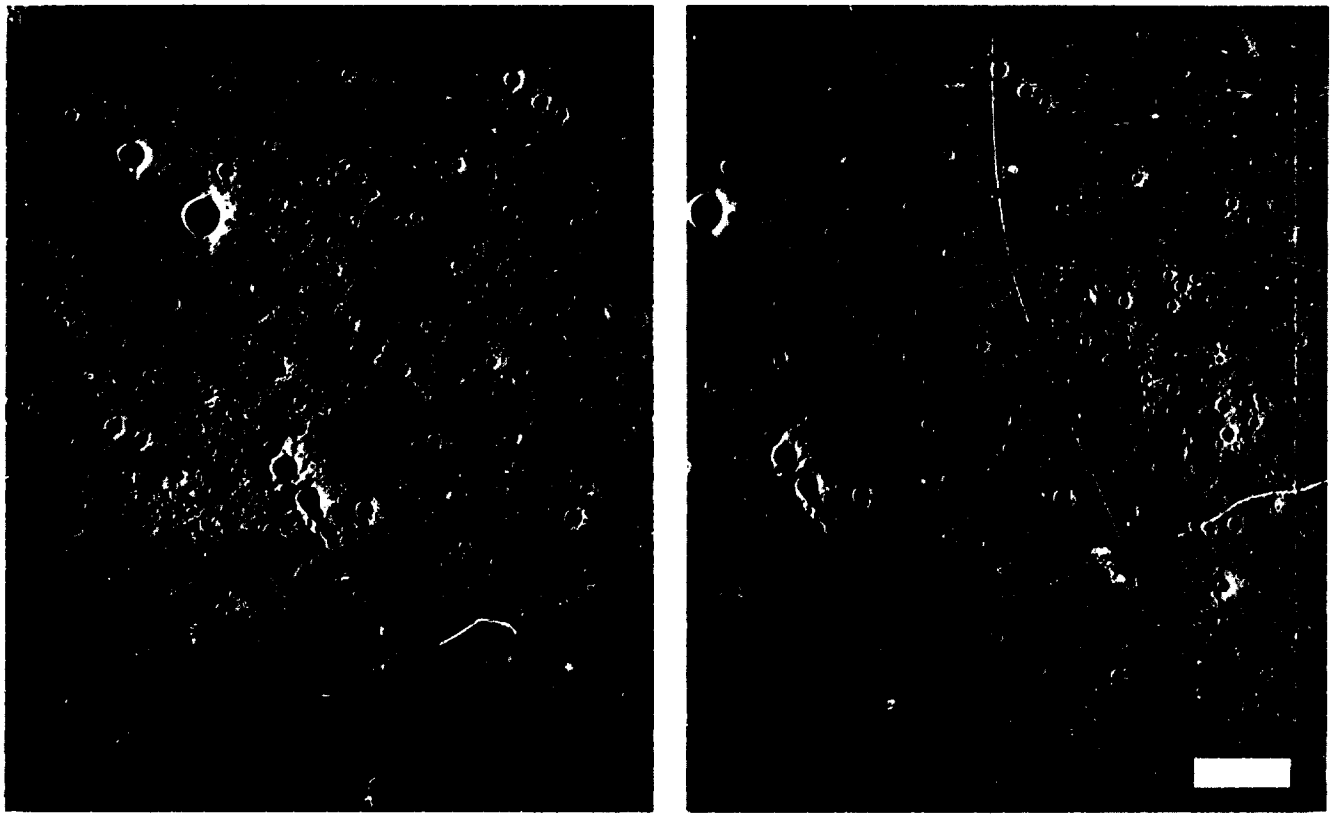

FIGURE 15-6. Stereo view of lunar mare surface in Oceanus Procelarum, west of the Aristarchus Plateau (Apollo 15 frame AS15-2490, left, 2488, right). Smooth-surfaced lava plateaus (A), irregular depressions (B), subdued circular depressions (C), and ring-moat structures (D). Bar represents 0.5 km; illumination from the right (east).

Also within the Flamsteed Ring are numerous, small (50 to 150 m diameter) rings characterized by a narrow depression encircling a low-relief mound (Schultz, 1976; Schultz and Greeley, 1975; Schultz and others, 1976). Such structures are called *ring moats* (Figs. 15-7 and 15-8) and are common within or adjacent to hummocky mare regions and mare regions with low-relief irregular plateaus and depressions. Ring-moat structures fall into three classes: moat surrounding a dome, moat surrounding a dome with subdued summit depression, and moat surrounding an interior mare surface. To date, eight mare regions have been found that display ring-moat structures and generally correspond to young (Eratosthenian age) titanium-rich mare basalts. Isolated examples also are recognized in other regions. The great abundance of such features is illustrated by their spatial distribution within the mare-flooded crater Letronne in southern Oceanus Procellarum (Fig. 15-9).

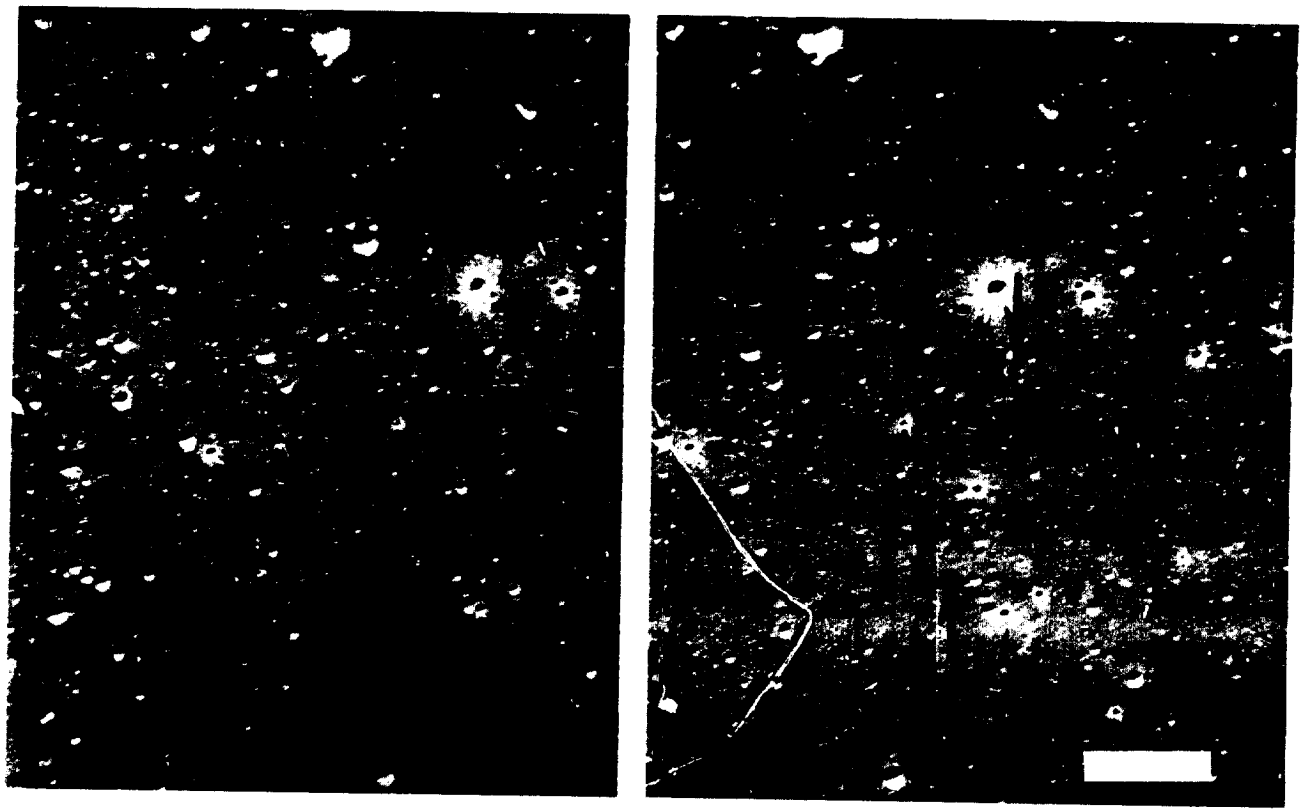

FIGURE 15-7. Stereo view of mare surface within the Flamsteed Ring on the Moon. Arrows locate irregular plateau (A), irregular depression (B), and ring-moat structures (C, D) with central depressions. Bar represents 1.8 km. Illumination from the top (east). (Lunar Orbiter III-191-M, left, III-181-M, right.)

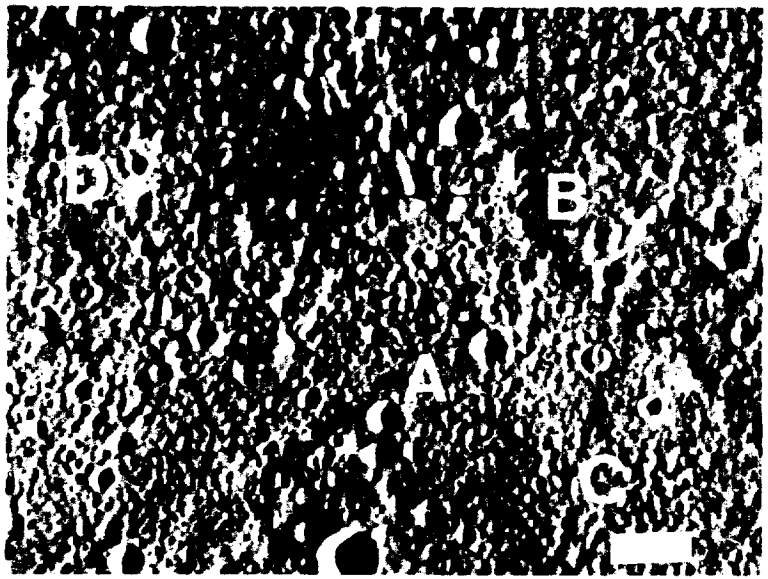

FIGURE 15-8a. Examples of lunar ring-moat structures in Mare Imbrium. Numerous ring-moat structures occur on the edge of one of the Imbrium flows. Examples include moats surrounding low-relief domes (A, B) and pitted domes (C, D). Illumination is from the right (east); bar corresponds to 300 m. (Apollo 15 frame AS15-1699.)

FIGURE 15-8b. Examples of moat-surrounded domes (arrows A, B) within the mare-flooded crater Letronne on the Moon. In addition, note the small dome with summit pit that overlaps the subdued crater (C). Illumination is from the right (east); bar corresponds to 300 m. (Apollo 16 frame AS16-5492.)

Several origins for these features have been postulated (Greeley and Schul' , 1975; Schultz and Greeley, 1976) and fall into two classes: origins at the time of mare emplacement (primary surface features) and origins at later times (secondary features). The preservation of irregular depressions and plateaus of comparable scale suggests that such structures were formed contemporaneous with the emplacement of these units. As primary flow features, ring moats may be produced by the margins of thin (10 m) basalt flows surrounding pre-existing relief such as volcanic cones and tumuli (Fig. 15-10), a process that can be documented in the Snake River Plain basalt fields (Greeley and King, 1975).

FIGURE 15-8c. Viking Orbiter image of ring-moat structures (arrows) in Chryse Planitia on Mars; note "bath tub" ring in the two large craters and the irregular, hummocky surface. These features are considered to be indicative of relatively thin, fluid basalt flows. Area of photograph 25 km by 35 km; north is to the right. (Viking Orbiter I, image 65A56.)

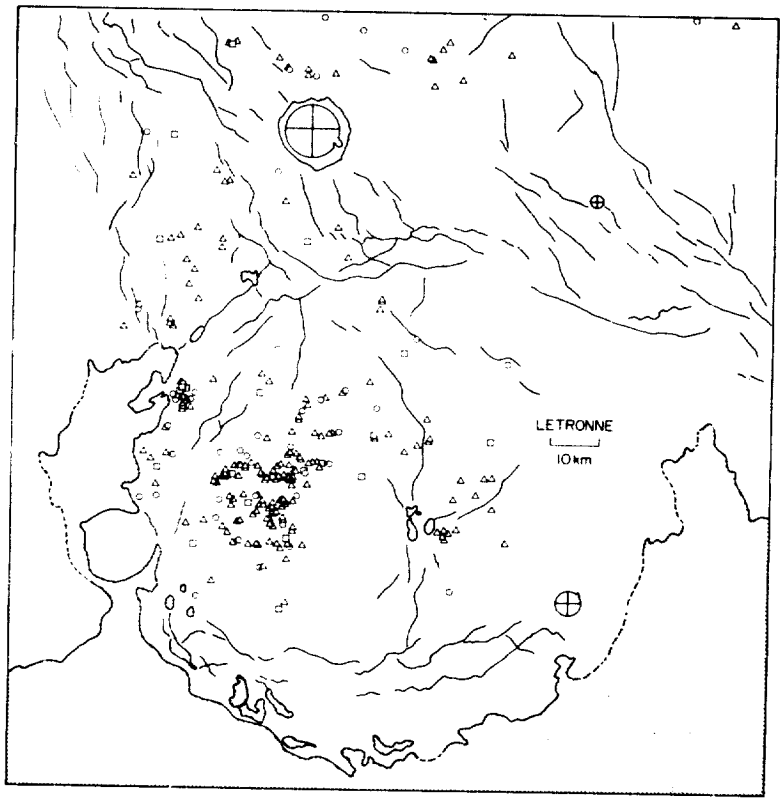

FIGURE 15-9. The distribution of ring-moat structures within the mare-flooded lunar crater Letronne. Diameter of rings range from 30 to 500 m; widths of moats range from 20 to 100 m. Circles indicate ring-moats; triangles, domes surrounded by moats; and squares, pitted domes (cones) surrounded by moats. Circles with interior cross locate craters larger than 1 km in diameter. Sinuous lines correspond to wrinkle ridges. Hachured regions indicate non-mare (crater rim, highlands) surfaces.

FIGURE 15-10. The tephra cone, China Cap (arrow A, 385 m in diameter) and the surrounding lava field in the Snake River Plain, Idaho. The tephra cone has been encroached by basalt flows, thereby producing a moat possibly analogous to the ring-moat structures on the Moon. Moat also occurs around smaller feature. Note the hummocky lava surface and smooth-surfaced plateaus, also similar to certain lunar lava surfaces.

On the Moon, the central relief of larger ring moat structures (diameter greater than 300 m) commonly exhibit central depressions, which may represent volcanic cones (Fig. 15-7). The relief within smaller ring moat structures, however, generally lack such central depressions and may correspond to tumuli. Other possible mechanisms of ring-moat formation include auto-intrusions within thicker (50 m) flow units and the inundation of impact craters. The latter process is believed to be responsible for ring-moat structures approaching 0.5 km to 1.0 km in diameter. These different mechanisms are illustrated in Fig. 15-11.

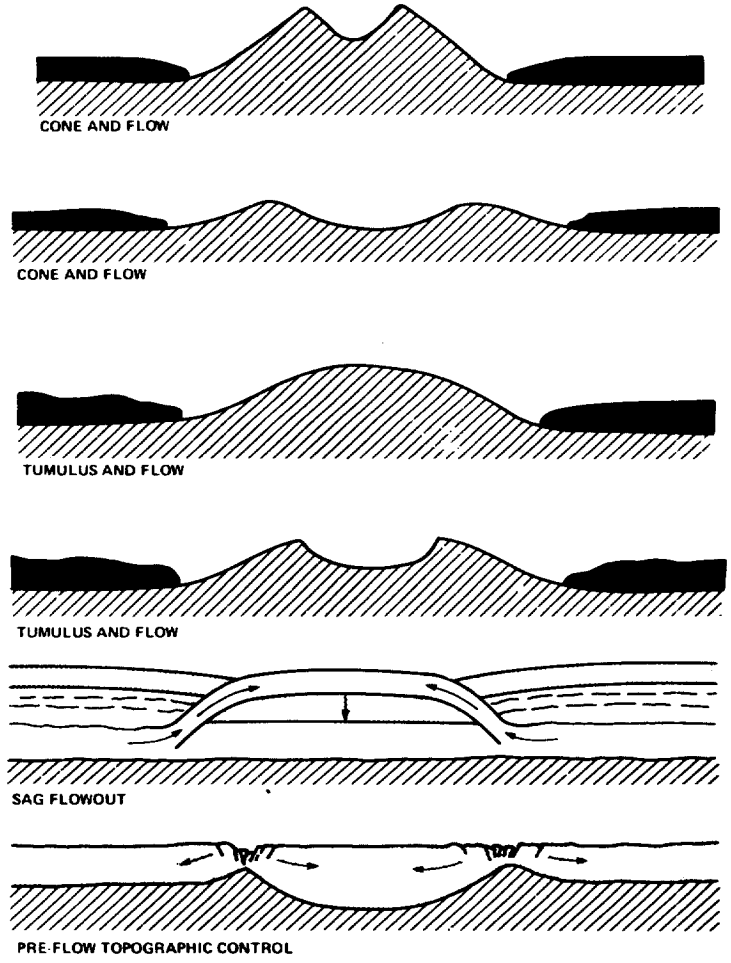

FIGURE 15-11. Mechanisms that might produce lunar ring-moat structures. The first four (top to bottom) mechanisms are recognized in the Snake River Plain where pre-existing relief is encroached by thin lava flows. Sagging of a cooling lava crust with subsequent flowout has been postulated by McKee and Stradling (1970) for ring structures in the Columbia River Plateau near Odessa, Washington. A pre-existing crater rim (bottom) may produce fractures in a cooling lava; this mechanism appears to be appropriate for ring-moat structures larger than 0.5 km in diameter.

Both ring-moat structures and the textured mare surfaces may be providing important clues to the style of mare basalt emplacement where distinct flow termini are absent. By analogy with the Snake River Plain basalts, certain lunar flows represent plains-basalt eruptions characterized by relatively thin (10 m to 20 m) compound lava flows, low viscosity, and numerous local vents (Greeley, 1975, 1976). Moreover, the close association of such regions with titanium-rich mare units recognized in the multi-spectral images of McCord and others (1976) suggests that this was a common late eruptive phase of the western lunar maria.

SINUOUS RILLES, LAVA TUBES, AND ASSOCIATED FEATURES

Many lunar sinuous rilles are considered to be collapsed lava tubes and channels, as discussed by Kuiper and others (1965), Oberbeck and others (1969), Greeley (1971), and others. Analyses of the distribution of lunar sinuous rilles and their relation to other volcanic features show that they are not randomly distributed among the mare units. Some lunar basins, such as Crisium, contain few sinuous rilles, whereas other basins, such as Imbrium, have abundant sinuous rilles. By terrestrial analogy, their presence signals eruptions of plains-type basalts, i.e., sporadic eruptions of lava in contrast to flood-type eruptions. Figures 15-12 and 15-13 show typical lunar sinuous rilles; figure 15-13 is particularly interesting, as it shows the transection of one sinuous rille by a younger rille and the lava flows associated with it. Absence of obvious flow fronts and flow margins indicate the very thin character of the flow units associated with the rille—typical of plains-type basalt flows.

A similar cross-cutting relationship by rille-associated deposits is observed on Mars, illustrated in figure 15-14, where a possible lava channel and associated flows are superimposed over a set of graben. Lava tubes were first recognized on Mars on the flank of Olympus Mons (McCauley and others, 1972; Greeley, 1973). Viking Orbiter pictures show that most of the large martian shield volcanoes are composed of tube-and-channel fed flows (Fig. 15-15), similar to large shields on Earth.

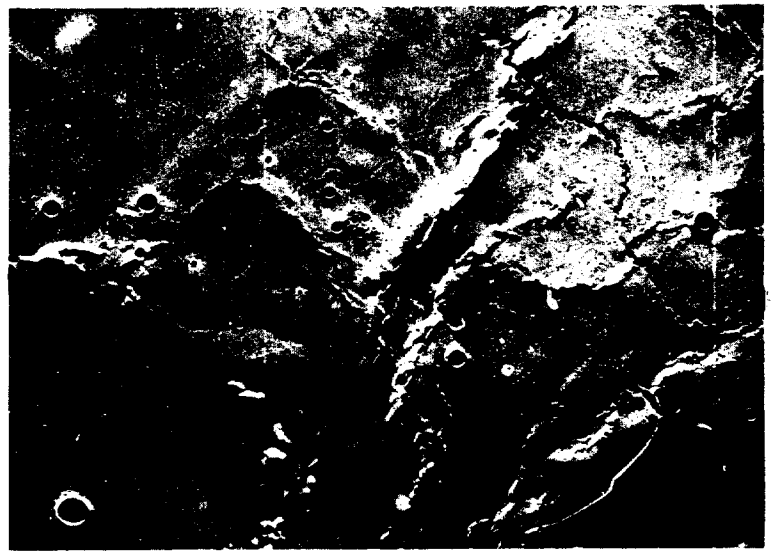

FIGURE 15-12. Region of the Moon near the crater Herigonius showing several lunar sinuous rilles, interpreted as lava channels and collapsed lava tubes. Area of photograph is about 90 km by 120 km; north is to the left. (Apollo 16 metric frame 2837.)

Martian lava tubes are also associated with many of the *patera*, the large, low profile constructs that appear to be unique to Mars (Carr and others, 1977). For example, the western flank of Alba Patera (Fig. 2-4) displays numerous tube-fed flows, some of which can be traced more than 400 km. The roofs of many of the tubes appear to have ruptured during active flow and spilled lava from the rupture as a "rootless" vent to form small domes (Fig. 15-16). Similarly aligned vents, possibly tube-fed, are seen on the Snake River Plain.

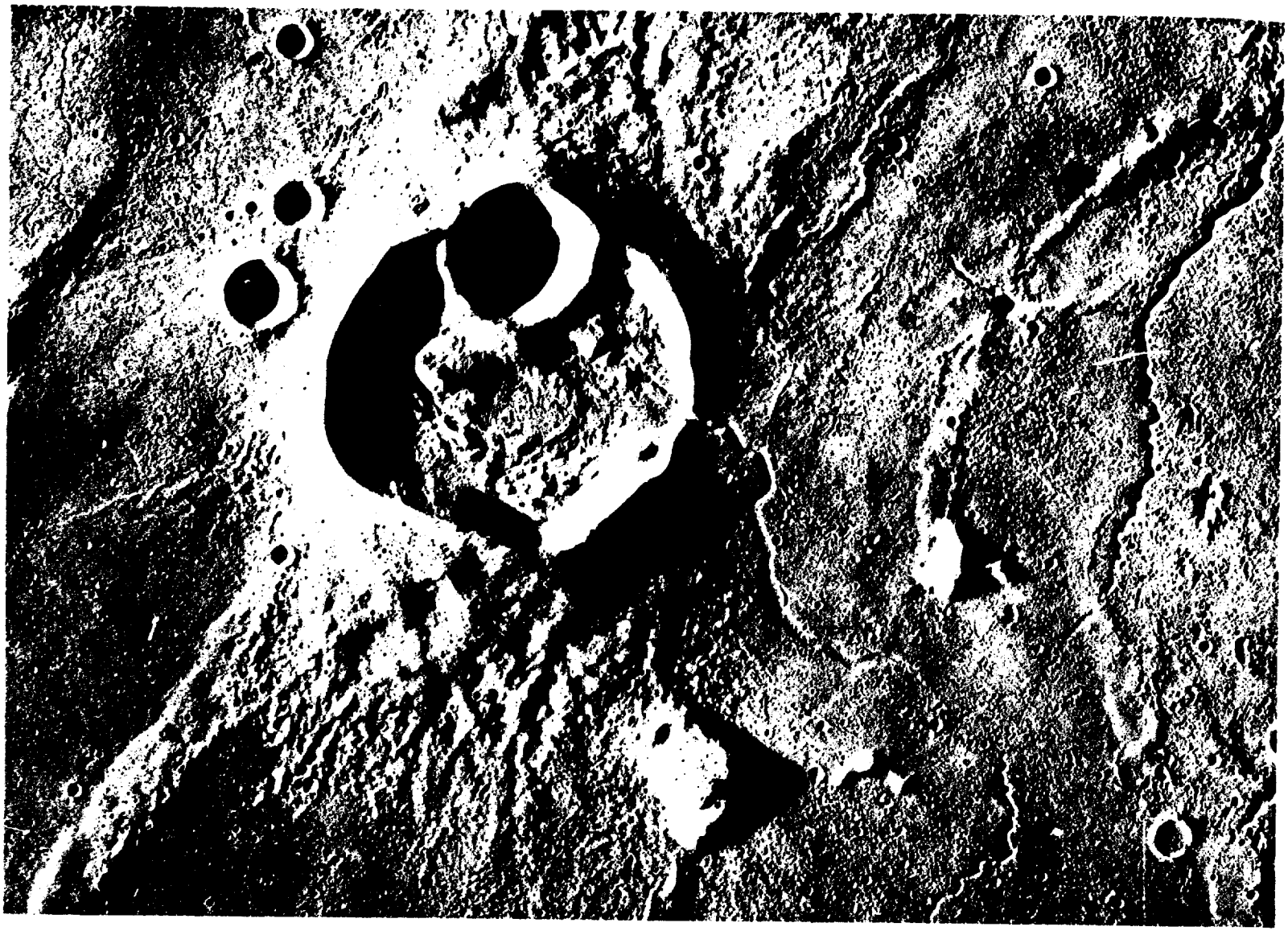

FIGURE 15-13. Apollo 15 photograph of the lunar crater Krieger showing a sinuous rille and probable associated flows that overlap an older sinuous rille on the right side of photograph. Lack of discernible flow margins suggest extremely thin flow units associated with the rille. Area of photograph is 40 km by 50 km; north is to the bottom. (Apollo 15 metric frame 2082.)

FIGURE 15-14. Mariner 9 image of the Ascraeus Mons region of Mars showing a channel and associated deposits that overlie a set of graben. The channel deposits may be volcanic. Area of image is 40 km by 50 km; north is to the top. (Mariner 9 frame DAS 07111373.)

ORIGINAL PAGE IS
OF POOR QUALITY

FIGURE 15-15. Northeast lower flank and basal scarp of Olympus Mons on Mars (22°N, 130.5°W). Note prevalence of well defined leveed flows (as at A) and smooth ridges (B-F), some of which have crater chains or rilles along their crests. Flows completely mantle and greatly subdue basal scarp here. Image height is approximately 80 km (from Carr and others, 1977; Viking Orbiter II frame 47B25.)

FIGURE 15-16. Viking Orbiter mosaic showing lava flows on the northwest part of Alba Patera on Mars. The ridge-mounds appear to be a type of lava tube-fed construct formed by a series of "rootless" vents (after Carr and others, 1977).

CENTRAL VENTS

Central vents on planetary surfaces are generally recognized by their irregular (non-circular) shape and association with other possible volcanic features. Impact craters are more likely to be circular than endogenic depressions and several techniques to assess circularity have been derived. Some endogenic craters, such as maars, may be rather circular and some impact craters, such as those formed by oblique impact, may be non-circular, thus, circularity is not a definitive test for origin. Nonetheless, the technique is a useful tool when used in conjunction with photogeology to assess the origin of craters.

Circularities for several categories of depressions (impact and volcanic craters on Earth, suspected impact and volcanic craters on the Moon) were determined and compared with vents on the Snake River Plain (Fig. 15-17). From this comparison, it is clear that most impact craters have circularity indexes of 1 to 2, indicating a high degree of circularity (1 is a perfect circle), and most volcanic vents are non-circular (index 3 and higher). Most pit crater and collapse depression values fall between 1 and 3 and are difficult to separate from impact craters on the basis of circularity.

Irregular vents have been identified in several areas of the Moon and Mars (Figs. 15-18 and 15-19). Many of these vents have associated sinuous rilles that are probably collapsed lava tubes and channels and appear to be analogous to features on the Snake River Plain.

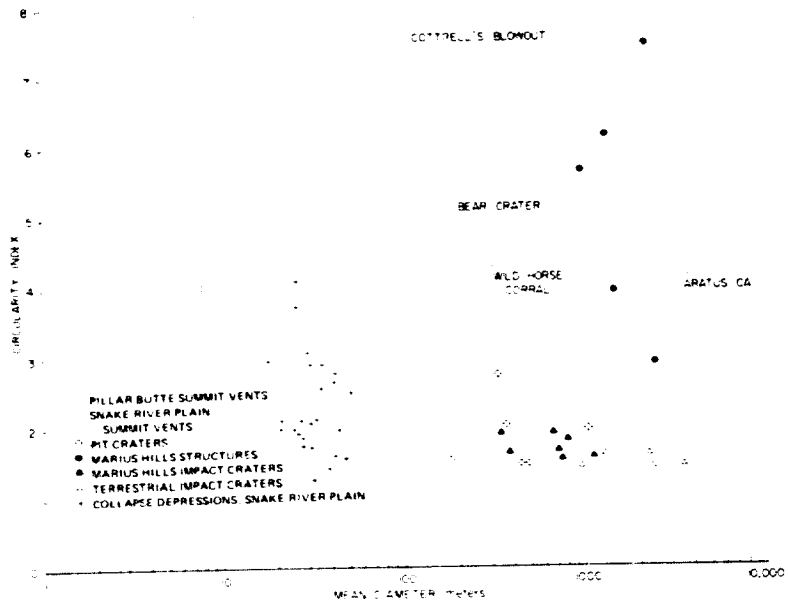

FIGURE 15-17. Comparisons of circularity indices for some endogenic craters and impact craters on the Moon and Earth, using the method of Murray and Guest (1970); crosses indicate values for collapse depressions on basalt flows in the Snake River Plain.

SUMMARY

The identification of volcanic features and distinctive flow textures on planetary surfaces that appear to be analogous to the Snake River Plain suggests similar styles of eruption and modes of emplacement. Features include lava tubes and channels, low shields, cinder and spatter cones, ring-moat structures, and hummocky-textured surfaces. Many of the extraterrestrial features, however, are much larger than their possible Earth analogs. This is normally taken to be a result of differing gravitational accelerations on the planets, but the effect is poorly understood.

Although it is often tempting to apply terrestrial experience directly to the interpretation of extraterrestrial surfaces, caution must be exercised to take into account differences in scaling and environment. Moreover, the possibility of volcanism on the planets in forms not represented on the Earth is very real; while this may make the field frustrating at times, it also makes planetary volcanism exciting.

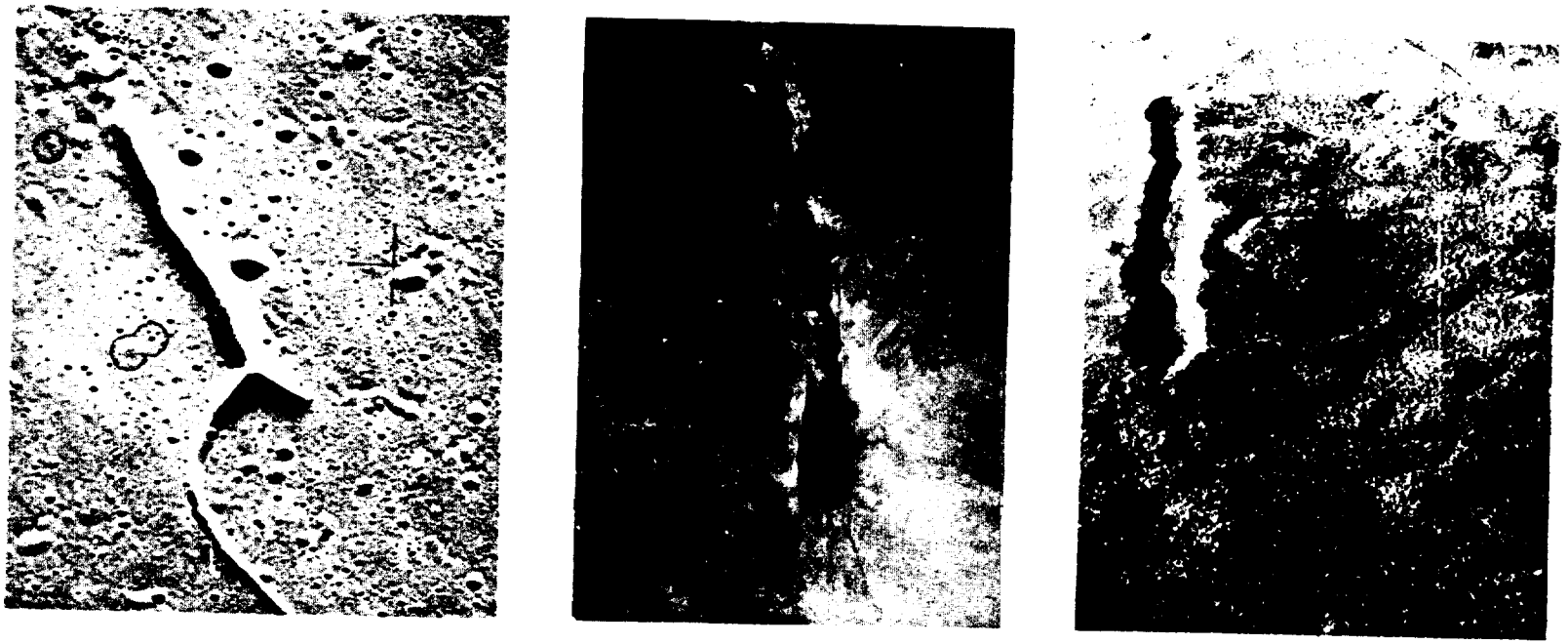

FIGURE 15-18. Comparison of "slot-shaped" vents on the Moon and Earth. Figure on left is part of a suspected vent and associated channel near the crater Delisle on the Moon (Apollo 15 frame AS15-2073); middle photograph is a view of the summit vent of Mauna Ulu in Hawaii; right photograph is an oblique aerial view of an elongate vent southeast of Big Southern Butte on the Snake River Plain. Lunar feature is about ten times larger than the terrestrial features.

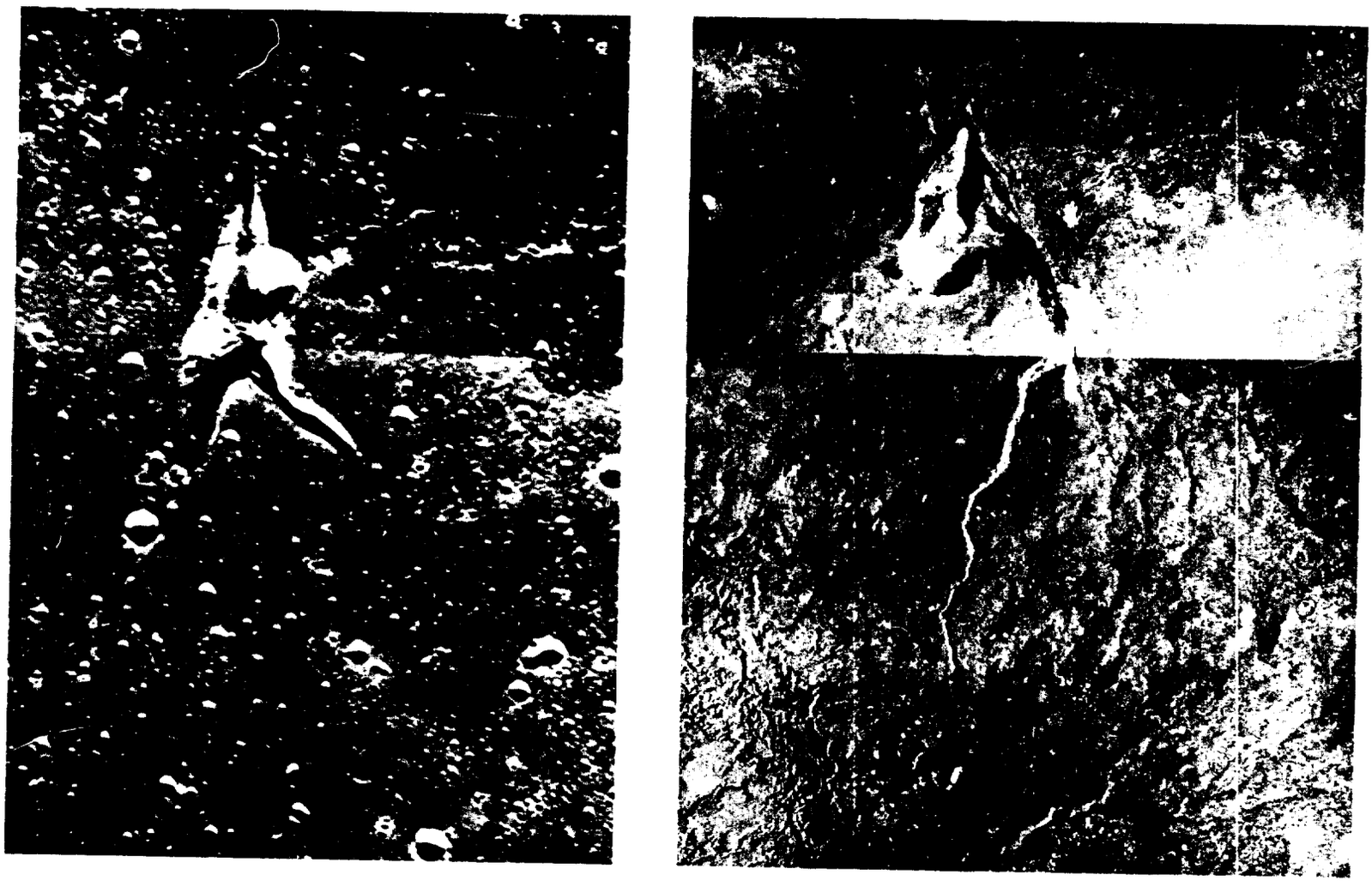

FIGURE 15-19. Comparison of Aratus CA in western Mare Serenitatis on the Moon (right photograph) with Bear Crater on the Snake River Plain. Area of lunar photograph is about 17 km by 25 km; terrestrial photograph is about 2.5 km by 3.3 km. Both features are vents for basaltic lavas (after Greeley, 1973).

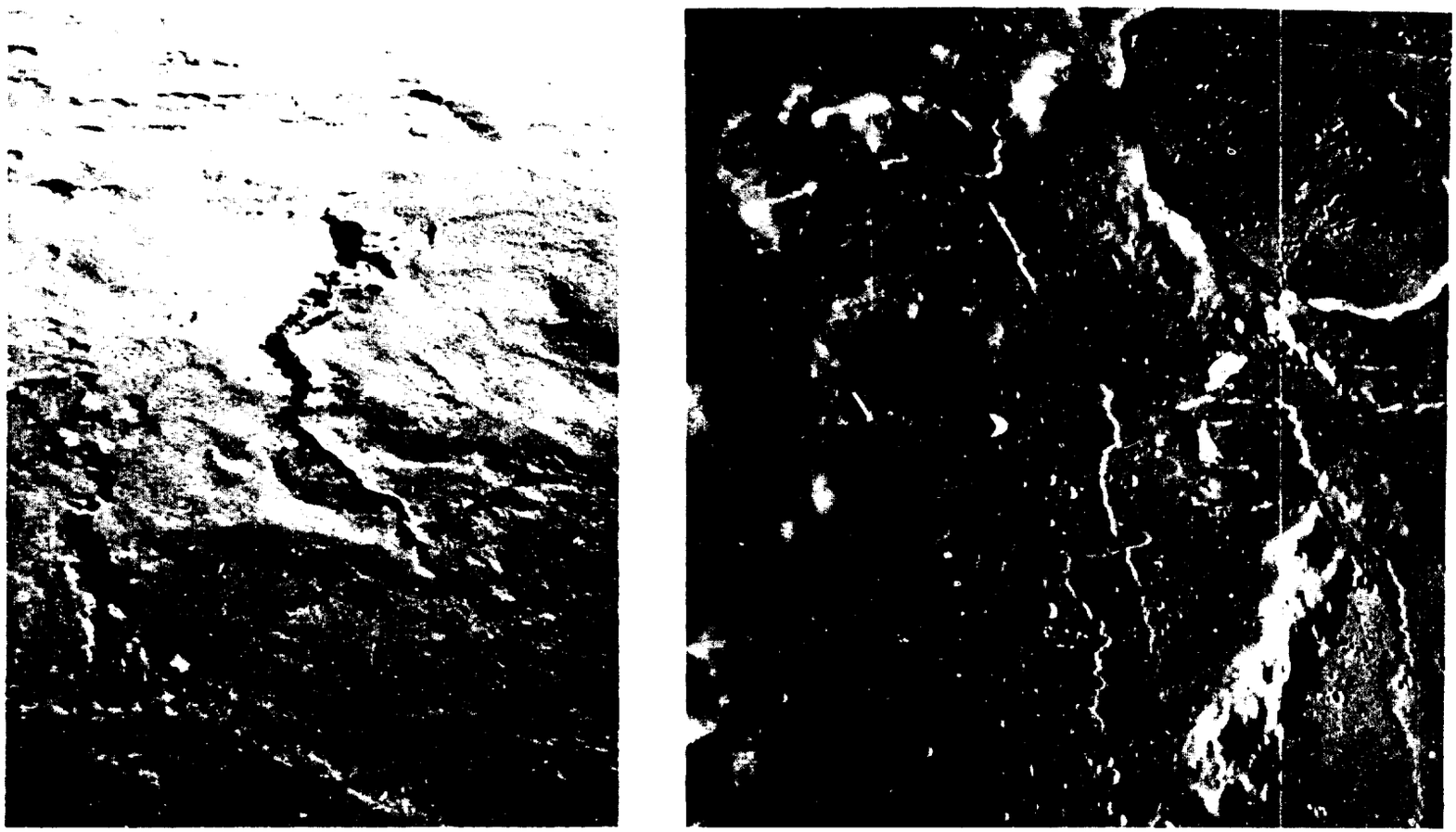

FIGURE 15-20. Crater vent (Inferno Chasm) and associated 1 km long lava channel on the Snake River Plain, compared with similar appearing lunar sinuous rilles (right side) near the crater Prinz. Although their morphology and origin are probably the same, the lunar features are more than two orders of magnitude larger.

REFERENCES

Carr, M. H., H. Masursky, W. A. Baum, K. R. Blasius, G. A. Briggs, J. A. Cutts, T. Duxbury, R. Greeley, J. E. Guest, B. A. Smith, L. A. Soderblom, J. Veverka, and J. B. Wellman, 1976. Preliminary results from the Viking Orbiter Imaging Experiment: Science, vol. 193, p. 766-776.

Carr, M. H., K. R. Blasius, R. Greeley, J. E. Guest, and J. B. Murray, 1977. Some martian volcanic features as viewed from the Viking Orbiters: *in press*, J. Geophys. Res.

Greeley, R., 1971. Lunar Hadley Rille—Considerations of its origin: Science, vol. 172, p. 722-725.

Greeley, R., 1973. Comparative geology of crater Aratus CA (Mare Serenitatis) and Bear Crater (Idaho): *in* Apollo 17 Preliminary Science Report NASA SP-330, p. 30-1–30-6.

Greeley, R., 1973. Mariner 9 photographs of small volcanic structures on Mars: Geology, vol. 1, p. 173-180.

Greeley, R., 1975. A model for the emplacement of lunar basin-filling basalts (abs.): *in* Lunar Science VI, p. 309-310, The Lunar Science Institute, Houston.

Greeley, R., 1976. Modes of emplacement of basalt terrains and an analysis of mare volcanism in the Orientale Basin: Proc. Lunar Sci. Conf. 7th, p. 2747-2759.

Greeley, R. and J. King, 1975. Geologic field guide to the Quaternary volcanics of the South-central Snake River Plain, Idaho: Idaho Bureau of Mines and Geology, Pamphlet No. 160, 49 p.

Greeley, R. and P. H. Schultz, 1975. Lunar ring-moat structures in Letronne and the Flamsteed Ring (abs.): Trans. Amer. Geophys. Union, vol. 56, p. 1015.

Greeley, R., E. Theilig, J. E. Guest, M. H. Carr, H. Masursky, and J. A. Cutts, 1977. Geology of Chryse Planitia: *in press*, J. Geophys. Res.

Greeley, R. and E. Theilig, 1977. Small volcanic constructs in the Chryse Planitia region of Mars: Submitted to the Geol. Soc. Amer., Annual Mtg.

Kuiper, G. P., R. G. Strom, E. A. Whitaker, and W. K. Hartmann, 1965. Interpretation of Ranger VII records: NASA JPL Tech. Rpt. 32-700, p. 9-73.

McCauley, J. F., M. H. Carr, J. A. Cutts, W. K. Hartmann, H. Masursky, D. J. Milton, R. P. Sharp, and D. E. Wilhelms, 1972. Preliminary Mariner 9 Report on the Geology of Mars: Icarus, vol. 17, p. 289-327.

McCord, T., C. Pieters, and M. Feierberg, 1976. Multispectral mapping of the lunar surface using ground-based telescopes: Icarus, vol. 29, p. 1-34.

McKee, B. and D. Stradling, 1970. The sag flowout: a newly described volcanic structure: Geol. Soc. Amer. Bull., vol. 81, p. 2035-2044.

Malin, M. C. and R. S. Saunders, 1977. Surface of Venus: evidence of diverse landforms from radar observations: Science, vol. 196, p. 987-990.

Murray, J. B. and J. E. Guest, 1970. Circularities of craters and related structures on Earth and Moon: Modern Geology, vol. 1, p. 149-159.

Oberbeck, V., W. Quaide, and R. Greeley, 1969. On the origin of lunar sinuous rilles: Modern Geology, vol. 1, no. 1, p. 75-80.

Schaber, G., J. M. Boyce, and H. J. Moore, 1976. The scarcity of mappable flow lobes in the lunar maria: unique morphology of the Imbrium flows: Proc. Lunar Sci. Conf. 7th, p. 2783-2800.

Schultz, P. H., 1976. *Moon Morphology*. University of Texas Press, Austin, 626 p.

Schultz, P. H. and R. Greeley, 1975. Lunar ring-moat structures: constraints on degradational models (abs.): Trans. Amer. Geophys. Union, vol. 56, p. 1015.

Schultz, P. H. and R. Greeley, 1976. Ring-moat structures: preserved flow morphology on lunar maria: *in* Lunar Science VII, p. 788-789, The Lunar Science Institute, Houston.

Schultz, P. H., R. Greeley, and D. E. Gault, 1976. Degradation of small mare surface features: Proc. Lunar Sci. Conf. 7th, p. 985-1003.

Spudis, P. and R. Greeley, 1976. Surficial geology of Mars: A study in support of a penetrator mission to Mars: NASA TM X 73,184, 54 p.

16. IDAHO: INDIAN COUNTRY TO STATEHOOD

Cynthia R. Greeley
Tempe, Arizona

16. IDAHO: INDIAN COUNTRY TO STATEHOOD

Cynthia R. Greeley
Tempe, Arizona

Idaho, the last of the fifty states to be seen by white men (Wells, 1965), is a land of rugged scenic beauty with towering mountains, deep canyons, mineral springs and vast expanses of volcanic lava flows. The physical characteristics of northern Idaho differ greatly from those of southern Idaho with the north having heavily timbered forests and thousands of beautiful mountain lakes. Southern Idaho also has majestic mountains; however, a large portion of southern Idaho, termed the Snake River Plain, is a very inhospitable, dry region covered with sagebrush. Southern Idaho contains huge sand dunes, as well as some of the most recent lava flows in the United States. Great volcanic craters, mountain-like buttes, and deep fissures are stark evidence of the region's active geologic past. Extensive lava flows were active in southern Idaho approximately 2,000 years ago (Greeley and King, 1975). Due to a lack of sufficient rainfall, these lava flows have not decomposed to a great extent, and the barren area is considered to be almost a desert. The Snake River, which flows through southern Idaho, is a tributary of the Columbia River and has played an important part in the history of southern Idaho. The variances in northern and southern Idaho have led to different patterns of settlement, lifestyles, and actual hostilities between the two areas. The purpose of this paper is to trace the development of southern Idaho.

The 1800s in southern Idaho can be roughly divided into three categories. From 1800 to 1860 southern Idaho was basically the domain of the Indians and the fur trappers. The twenty-year period of settlement by the Americans began in 1860. Included in the 1860 to 1880 period were the arrival of the missionaries, the mining boom, the transition period between temporary and permanent settlers, and the colonization by the Mormons. The period of 1880 to 1900 was a time of growth and economic development for all of Idaho. After coming to terms with political and religious controversies, Idaho achieved statehood July 3, 1890.

Indian Country

For the first half of the nineteenth century, the region now known as southern Idaho remained Indian country. Many of the place names currently in use in Idaho have been derived from Indian words, possibly including the name of the state itself. Beal (1942) expressed the popular opinion that the word "Idaho" comes from a Shoshoni Indian expression, *Ee-dah-how*, meaning "the sun is coming down from the mountain tops; however, Etulain and Marley (1974) contend the word has no Indian basis and was, in fact, invented by a politician in 1860.

Southern Idaho was the homeland of several tribes of Shoshoni Indians. They had formerly lived in the Montana and Dakota country but had been driven west by the powerful and unfriendly Blackfoot Nation. The largest Shoshoni tribe in southern Idaho were known as the Snake Indians. Theories vary concerning the origin of the name. Beal (1942) states the Snake Indians were so named because of their characteristic of quickly concealing themselves when discovered, 'like a snake.' Fisher (1937) believes the name originated because the Indians ate snakes and dug their food from the earth, while Trenholm and Carley (1964) contend the name originated when an Indian was asked his tribal sign and made a serpentine movement intended to suggest the weaving method (in and out motion) used for tribal basket and shelter making, but the movement was misinterpreted to mean snakes.

The Snake Indians shared customs with the Shoshoni group, but they also developed particular characteristics. In general, their culture was based on pride, strength and

courage. Superstition appears to have played a large part in their religion and everyday life. Although they were comparatively peaceable to the whites, to become a great warrior was a brave's highest ambition. Leadership came not by heredity, but by cunning, wisdom, and courage. Considerable importance was attached to tribal status, the basic organization of which was the family unit. The women did the majority of the manual labor; they dressed the game and gathered nuts, berries, and camas roots (for making bread), made the clothing, bows, arrows, and even the lodges.

The entire nation of Snake Indians consisted of many hundreds, but it was divided into different bands with vastly different temperaments. Some had a wild nature, while others, derogatorily termed "Diggers" because they used a pointed stake to dig their food from the ground, were considered weak and passive and were looked down upon by the other tribes. The Sheepeaters numbered approximately two hundred and were composed of renegades from the other tribes.

The warlike Bannock Indians are believed to have come to southern Idaho from Oregon. The whites had reason to fear the Bannocks above the other Indians because they were the most fierce and the most willing to fight for their homeland. The name Bannock seems to have originated when a Scottish trapper saw them eating acorn cakes which reminded him of Scotch bannock cake (Beal, 1942). The Bannock tribe was relatively small, but when there was need of numerical strength, such as when they journeyed east over the mountains into Blackfoot country to hunt buffalo, they teamed up with the Shoshoni with whom they maintained a good relationship. The Bannock retained their individual culture and dialect as long as possible, but by the early 1900s, intermarriage with the Shoshoni took its inevitable toll.

Fur Trappers

The trail blazed into Idaho by Lewis and Clark in 1805 was soon followed by the fur trappers and traders. Some of the Indians were friendly toward these mountain men, but the Bannocks could not resist the temptation to harrass those who entered their domain. Peter Skene Ogden, leader of southern Idaho fur trapping expeditions from 1824 to 1829, recorded in his journal for June 8, 1826 that during the preceding ten months the Bannocks had stolen 180 traps and killed thirteen whites (Madsen, 1958).

Frequently, trappers would marry Indian women. The advantages of the so-called squaw men were numerous. Not only did they gain a willing and efficient help-mate for the ardous work, but it was also a way of ingratiating the trapper with a particular tribe, thereby being allowed to trap unharrassed.

Fur trappers seldom worked on an individual basis; they were company men. They would go out in large groups of forty or more, establish a base camp, then spread out in groups of two or three to set their traps. For more than twenty years, from 1824 to 1846, the Pacific Northwest was the territory of the Hudson Bay Company (Rich, 1959). It was Hudson Bay Company policy that no American fur traders would be allowed west of the Rockies, but the westward push of the American Fur Company was a constant threat and led to sharp competition. One tactic used by Hudson Bay Company was to overtrap the Snake River and its tributaries, thereby devastating the beaver population to such an extent that a westward move through Idaho by American trappers would prove unprofitable. Peter Skene Ogden and others carried out this policy in the late 1820s for Hudson Bay, taking as many as 80,000 pelts in one season (Williams, 1971).

Nathaniel Wyeth played an important part in the history of southern Idaho when he established a trading post at Fort Hall in 1834. Wyeth had originally planned to sell his supply of goods to trappers at the 1834 rendezvous in Wyoming, but his plans went awry and he was left with one hundred thirty horses, forty employees, and a large stock of goods. His only alternative was to establish what he hoped to be a successful trading post; he built Fort Hall in southern Idaho, overlooking the Snake River. Hudson Bay Company, which opposed

Wyeth's competition in "their" territory, sabotaged his efforts for success and established their own supply center, Fort Boise, to the northwest of Fort Hall. Hudson Bay Company bought Wyeth out two years later and used Fort Hall as a center for supplying Americans and Indians. This was a reversal of policy on the part of the company. In the past they had refused to supply American trappers, but now they saw Fort Hall as a means of obtaining pelts from Americans as well as Indians. Fort Hall was, therefore, well stocked with British goods.

Wyeth's business failure at Fort Hall actually helped contribute to the American settlement of the West. Several men from Wyeth's company chose to settle the area and established the first farms in the Snake River Country. Also, the strategic location of Fort Hall near what was to become the Oregon Trail established its importance as a supply station for emigrants who by the early 1840s had begun to move westward.

Missionaries

When a new territory was opened, it was usually the missionaries who filled the gap between the explorers and the settlers and so it was in Idaho. With the backing of the American Board of Commissioners for Foreign Missions, a small group of missionaries, including Reverend Henry Spalding and his wife, decided to take the word of God to the Indians of the Pacific Northwest. Mrs. Spalding and another woman in the group thus became the first women to cross the American continent (Lavender, 1963). They followed fur traders westward from Missouri and found themselves at the 1836 rendezvous in Wyoming. At the rendezvous they were joined by a band of Nez Perce Indians who led them westward to Idaho.. The missionary group, which had been existing on dried buffalo meat for lack of other food, pulled into Fort Hall August 3, 1836. They obtained as many supplies as the Fort could spare, including much needed fresh vegetables. The determined missionaries then followed the Snake River into Oregon, but the Spaldings returned to set up a mission at Lapwai, in northern Idaho, in 1836. Their daughter was the first white child born in Idaho.

Emigrants

By the end of the 1830s, stories had drifted back to the East about the Oregon Country and California. The American frontier was then Missouri. The broad and treeless plains of Indian country had temporarily stopped the western migration, but tales of the bountiful country that lay beyond were enough to spark interest for a westward movement.

Obstacles faced by those who wanted to follow the sun were monumental. Huge distances through savage Indian country, deserts and mountains would have to be crossed in one season. Even though wagons had not yet crossed the continent successfully, many still decided to move west, some with their entire families. Some turned back, but for those who reached the southeastern corner of what is now Idaho, near Fort Hall, the decision whether to turn north to Oregon or south to California had to be made. A precedent was set. The California-Oregon Trail was established with Fort Hall as a stopping place. It was a post where food supplies could be obtained, as well as valuable information about the trail and the Indians. It has been estimated that over two hundred thousand emigrants passed by Fort Hall on their way to California and Oregon in the 1840s and 1850s (Beal, 1942). A reconstruction of the old Fort Hall can be visited today. After the California gold rush had run its course, many of the unsuccessful fortune seekers found their way back to southern Idaho to settle.

In the meantime, the heavy emigrant traffic of the late 1840s and early 1850s led to problems. Animosity grew between the whites and the Indians and a series of attacks on the wagon trains followed. By the mid-1850s, stories of massacres were commonplace. An incident which occurred near Soda Springs, southeastern Idaho, in 1961 was typical. A family had fallen behind their wagon train when they

stopped to look for a horse which had strayed. They found that Indians had stolen the horse, but by the time they retrieved it, darkness had fallen. Planning to catch up to the train the following morning, they went to bed. Man, woman, and children were killed in their sleep that night (Anderson, 1940). After the Almo Creek Massacre of 1862 in which 300 whites died, wagon trains through southern Idaho were provided with military escort.

Settlement

The first permanent settlers of Idaho were Mormons who inadvertently thought they were in northern Utah (Wells, 1965). In 1860, thirteen men and women moved north from Salt Lake City and decided on a site on the Cub River they called Franklin. Pioneer life in southern Idaho was difficult. The country was rough and covered by sagebrush. The swift streams were dangerous to cross and the entire area was infested with rattlesnakes and mosquitoes. The people who settled there had to be resourceful and determined; they also had to be able to depend on each other and to cooperate on joint ventures. Group effort was especially important in organizing the irrigation projects so essential to farming in that region. The Mormons possessed the prerequisites for a successful pioneer life: their church bond gave them additional strength to face the hardships. They had been driven out of more lucrative farmlands, but they were determined to make this unhospitable land their home. It was the Mormon's knowledge of irrigation that insured the success of their colony. More Mormon families moved to the Franklin region, and soon a sawmill, gristmill, creamery and various stores appeared. The settlers continued to spread out over the countryside, and their communities thrived. Although the Mormons had attempted to maintain friendly relations with the Bannocks by providing them with food and refusing to quarrel with them, harrassment by the Indians finally led them to ask the military for assistance.

This request, coming on the heels of the Almo Creek Massacre, prompted the United States government in 1863 to send a detachment of infantry with howitzers and a unit of cavalry to southeastern Idaho. After the soldiers won a decisive battle at Battle Creek, the Bannocks were forced to sign a peace treaty and move to a reservation (Beal, 1942). The troubles with the Indians did not end; however, the effectiveness of the Indians to terrorize the settlers was sharply reduced.

Fort Hall, which had to be closed due to Indian attacks in 1855, was destined to become part of the Fort Hall Indian Reservation. In 1868, the Fort Hall Reservation was the home of nearly twelve hundred Bannock and Shoshoni Indians (Madsen, 1958). Generally, the Shoshoni accepted reservation life. The Bannock, however, were not passive and there were frequent instances of their "going off the reservation" in search of food and they were involved in raids against whites as late as 1878.

The year 1860 brought another influx of Americans into Idaho. Gold and silver were discovered and miners who had not hit paydirt in California flocked back to the land they had merely passed through earlier. During the decade from 1866 to 1876, placer mining was extensive in southeastern Idaho. Nearly every stream yielded gold and, along some stretches of the Snake River, there was considerable hydraulic mining. Southern Idaho was very active in mining, but even more extensive mining took place in central and northern Idaho during this period.

Another type of mining took place in southern Idaho. In 1843 emigrants noticed that when water from some of the springs evaporated, salt crystals remained. The area, located in the southeastern part of the state, was named Salt Springs Valley. The settlers later boiled the water in large pans, drained the water off and were left with a residue of pure white salt. The Salt Spring Valley salt mine became one of the earliest organized business ventures in southern Idaho.

With productive mines scattered throughout the area, an organized system of transportation was needed. Stagecoach runs were established, but more substantial methods of moving people and equipment were needed. After 1880 rapid construction of railroads took place. After the Oregon Short Line was built by the Union Pacific across southern Idaho between 1882 and 1884, farming settlements sprang up in all parts of the territory.

Struggle for Statehood

Idaho became a territory of the United States in 1863 but did not achieve statehood until 27 years later. Bitter sectional controversy between northern Idaho and southern Idaho was the primary reason for the long delay.

The volcanic regions of southern Idaho that had at first appeared barren and useless for agriculture proved to be otherwise. It was discovered that cattle and sheep could graze successfully on the abundant grasses that covered the region. Once irrigation came to the Snake River Basin, the area proved to be amazingly fertile and productive. The interests of southern Idaho then lay in the areas of farming, cattle and sheep, while northern Idaho was predominantly concerned with mining.

The controversy between the North and the South also centered around the fact that southern Idaho was dominated by Mormons and northern Idaho was not. Due to a general misunderstanding of concepts, Mormons were traditionally persecuted by both Protestants and Catholics. Open animosity existed between the religious groups. The Mormons were also feared politically because they tended to vote as a solid bloc for their own candidates and could, therefore, wield considerable political strength.

Idaho's territorial legislature met first in Lewiston, which was a mining town in northwestern Idaho. Some of the legislators had to ride horseback several hundred miles to attend the session. When a movement by some of the legislators to relocate the capital to more centrally located Boise was met with resistance, the pro-Boise legislators stole the territorial seal and legislative records and moved to Boise anyway (Winther, 1947). Many of the officials of the early Idaho territorial period were inept, corrupt, or both. Fortunately for Idaho, the caliber of men in high public office improved during the later territorial years.

The clash over permanent location of the capital in 1864 grew into a movement with northern Idaho attempting to join eastern Washington in a new territory to be called Columbia. The attempt failed, but other boundary realignments were attempted during the next twenty years.

After bitter religious and political turmoil, northern Idaho and southern Idaho finally came to terms in 1888. Compromises were made—the location of the capital was to be Boise in the south; the University of Idaho was to be located in the northern town of Moscow. By 1890 the territory of Idaho had gained enough population to become eligible for statehood. The Congress of the United States admitted Idaho as the forty-third state July 3, 1890.

REFERENCES

Anderson, A. C., 1940. *Trails of Early Idaho:* Caxton Printers, Ltd., Caldwell, Idaho.

Beal, M. D., 1942. *A History of Southeastern Idaho:* Caxton Printers, Ltd., Caldwell, Idaho.

Etulain, R. W. and B. W. Marley, eds., 1974. *The Idaho Heritage:* Idaho State University Press.

Fisher, V., 1937. *Idaho: A Guide in Word and Picture:* Caxton Printers, Caldwell, Idaho.

Greeley, R. and J. S. King, 1975. A Geologic Field Guide to the South-central Snake River Plain: Idaho Bureau of Mines and Geology, Pamphlet No. 160.

Lavender, D., 1963. *Westward Vision: The Story of the Oregon Trail:* McGraw-Hill Book Co., Inc., New York.

Madsen, B. D., 1958. *The Bannock of Idaho:* Caxton Printers, Caldwell, Idaho.

Rich, E. E., 1959. *The History of Hudson's Bay Company, 1670-1870, Vol. II: 1763-1870:* The Hudson's Bay Record Society, London.

Trenholm, V. and M. Carley, 1964. *The Shoshonis: Sentinels of the Rockies:* University of Oklahoma Press, Norman, Oklahoma.

Wells, Merle, W., 1965. *Idaho, A Student's Guide to Localized History:* Bureau of Publications, Teachers College, Columbia University, New York.

Williams, G., 1971. *Peter Skene Ogden's Snake Country Journals, 1827-1829:* Hudson's Bay Record Society, London.

Winther, O. O., 1947. *The Great Northwest:* Alfred A. Knopf, New York.

17. ROAD LOG FROM POCATELLO TO CRATERS OF THE MOON NATIONAL MONUMENT

Ronald P. Papson
Department of Geology
Arizona State University
Tempe, Arizona 85281

17. ROAD LOG FROM POCATELLO TO CRATERS OF THE MOON NATIONAL MONUMENT

Ronald P. Papson
Department of Geology
Arizona State University
Tempe, Arizona 85281

The trip starts at the southern boundary of the Snake River Plain and continues northwest to the northern boundary near Craters of the Moon National Monument (Fig. 17-1).

The Snake River Plain volcanics are varied and include both rhyolitic members (Big Southern Butte, East Butte, and possibly Middle Butte) and extensive basaltic members (e.g., Hell's Half Acre, Cerro Grande, and Craters of the Moon lava fields). The relation of volcanic activity to the structural framework of the plain has been explored previously in this guidebook and is only briefly mentioned while describing particular features along the route.

Mileage		
Cumulative	Difference	
0.0	0.0	Head north on I-15 at junction with I-15W. The mountains to the right are part of the Pocatello Range; the highest peak here is Camelback Mountain (2006 m). The mountains consist of Precambrian metasediments, plus Cambrian marine sediments; limestone being the dominant rock type. Alluvial sediments to the right are part of the Tertiary Salt Lake Formation and consist of poorly consolidated sand, silt, and gravel. From here to Blackfoot, these sediments have been highly dissected, forming cliffs up to 30-50 m high.
5.4	5.4	Ferry Butte (Fig. 17-2) at approximately 10 o'clock. This basaltic shield is part of the Snake River basalt group. Rising 130 meters above the surrounding plain, it was a prominent landmark for early travelers along the Oregon Trail. Until the advent of modern dams and bridges, the Ferry Butte crossing was one of the few places that the Snake River could be forded safely.
7.3	1.9	Cutoff to Fort Hall; continue straight. Built by Nathaniel Wyeth in 1834, the Fort Hall trading post was the only outpost for hundreds of miles. It was later sold to the Hudson's Bay Company and used as a base for fur-trading operations. As fur-trading declined, Fort Hall became a welcome post for emigrant trains. Although the original fort (21 km west of here) burned to the ground in 1856, a reconstruction of the old adobe fort has been built at Ross Park in Pocatello.

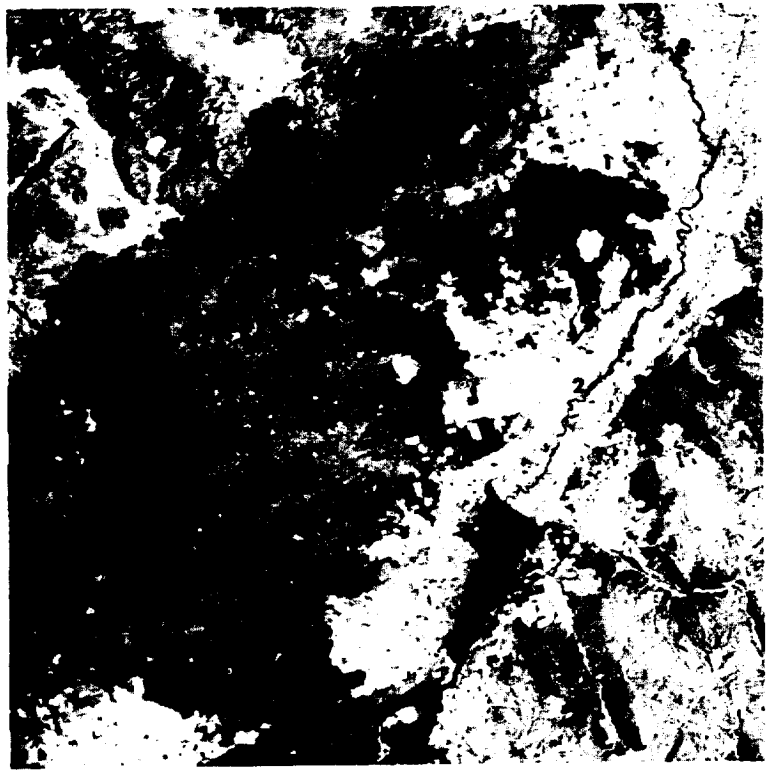

FIGURE 17-1. Landsat (ERTS) photograph of the eastern Snake River Plain. Hell's Half Acre flow (1), Snake River (2), American Falls reservoir (3), East and Middle Buttes (4), Big Southern Butte (5), Cerro Grande lava field (6), Wapi flow and King's Bowl Rift (7), Craters of the Moon lava field (8), Lost River Range (9). Arrows indicate trend of the Great Rift system. Area shown is 136 km by 142 km.

FIGURE 17-2. High altitude (U-2 aircraft) vertical aerial view of Ferry Butte (1) with the Snake River (2) meandering to the west. Large circular patches (3) are caused by circular pivot irrigation (CPI) systems. Photograph is approximately 12 km by 14.6 km. (NASA-Ames Photograph 72-186, frame 5676, October, 1972.)

Mileage		
Cumulative	Difference	
13.9	6.6	Terrace in the Salt Lake Formation. Mountains on the right are the northernmost extension of the Portneuf Range and consist primarily of Triassic volcanic rocks with subordinate Jurassic sandstones and limestones.
17.7	3.8	Blackfoot River.
20.0	2.3	Exit from I-15 and junction with Route 26, heading northwest toward Arco.
20.6	0.6	Snake River. The Snake River (Fig. 17-1), the largest tributary of the Columbia River, is the main drainage channel for southern Idaho. Dams along its length impound water for both agricultural and recreational uses. The Snake River has had an ever-changing course. Once flowing along the northern border of the plain, the Snake River was diverted southward by successive lava flows.
24.8	4.2	Hell's Half Acre flow. The lava field (Fig. 17-1) is basalt of recent origin and covers approximately 400 km^2. The basalt is an olivine tholeiite with 5 to 10 percent olivine and plagioclase phenocrysts in a matrix of olivine, plagicclase, augite, and glass. Some areas contain large numbers of olivine gabbro xenoliths, presumably torn from the feeding conduit at depth during eruption. All flows on the field have apparently issued from a central vent (Fig. 17-3) (see Chapter 7).
26.9	1.2	Two prominent buttes (Fig. 17-4 and Chapter 6) appear on the horizon at approximately one o'clock. East Butte (Fig. 17-5) on the right rises 300 m above the surrounding plain and has a basal diameter of 3.4 km. It is a rhyolitic dome of almost uniform composition. The rock typically consists of large (2-5 mm) phenocrysts of sanidine, quartz, and plagioclase in a fine-grained to glassy matrix. Inclusions of basaltic and rhyolitic fragments are common. Armstrong and others (1975) have dated the butte at 0.6 ±0.01 m.y. Middle Butte (or West Butte) to the left rises nearly as high as East Butte and lies 6.4 km west of it. Middle Butte (Fig. 17-6) has no exposed rhyolite and appears as an upraised block of stratified basalt dipping 10° to the south. The basalt is similar to other Snake River Plain basalts and contains abundant feldspar, olivine, and pyroxene.
36.3	9.4	Big Southern Butte (Fig. 17-7), which lies at the southern end of the Arco rift zone (Kuntz, 1977), can be seen at approximately eleven o'clock. This rhyolitic dome, similar to East Butte, has a basal diameter of 8 km and rises 760 m above the plain. The entire butte is elongate northwest-southeast (Fig. 17-8) and consists of two separate cumulo domes aligned N45°W. The southeast dome is a lavender-gray to light gray spherulitic, lithoidal rhyolite with some chloritization present. This older dome may have formed by internal expansion with flow outward from the center. The base has talus accumulations of non-sorted, non-bedded, angular clasts in a fine-grained matrix, which is indicative of gradual expansion. The younger dome (northwest) consists of white massive rhyolite with some small basaltic inclusions, possibly torn from the conduit. Remnants of a possible central crater 800 m in diameter are visible at the summit. Large sections of basalt, which may have been pushed up and tilted during development of the dome, dip 45°N 45°W (see Chapter 6).

FIGURE 17-3. Vertical air photograph of Hell's Half Acre vent area. The caldera-like vent is elongate in line with other features, suggesting a rift zone eruption. Photograph is approximately 2.7 km by 3.1 km. (U. S. Department of Agriculture Photograph CXO-1GG-31, May, 1966.)

FIGURE 17-5. Vertical aerial photograph of East Butte. Area shown is approximately 3 km by 3 km. (U.S. Geological Survey Photograph GS SWEZ, 7-84, October, 1971.)

FIGURE 17-4. View northeast from Route 26. East Butte is on the right and Middle Butte is on the left. (Photograph by Ronald son, University of Santa Clara, June, 1977.)

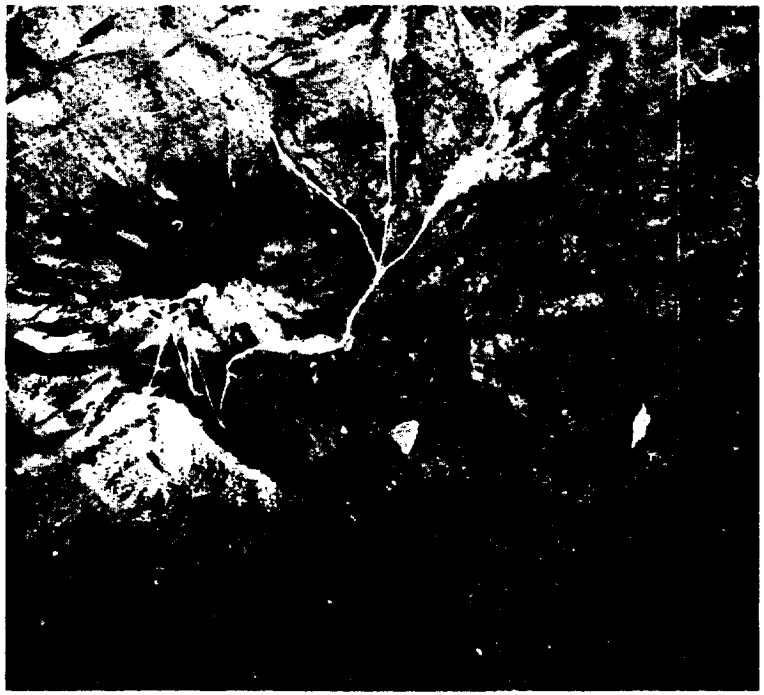

FIGURE 17-7. Oblique aerial view of Big Southern Butte, looking north. Vent area for Robber's basalt (1) is along the Arco Rift Zone. (Photograph by Ronald Greeley, University of Santa Clara, June, 1977.)

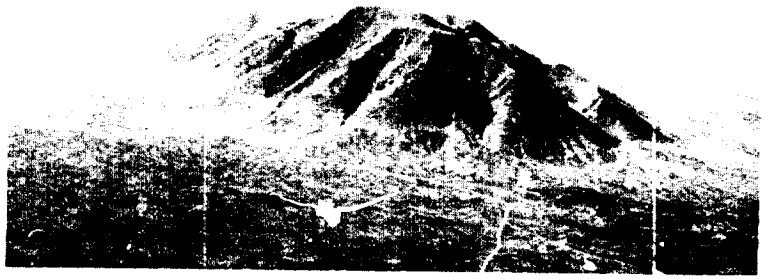

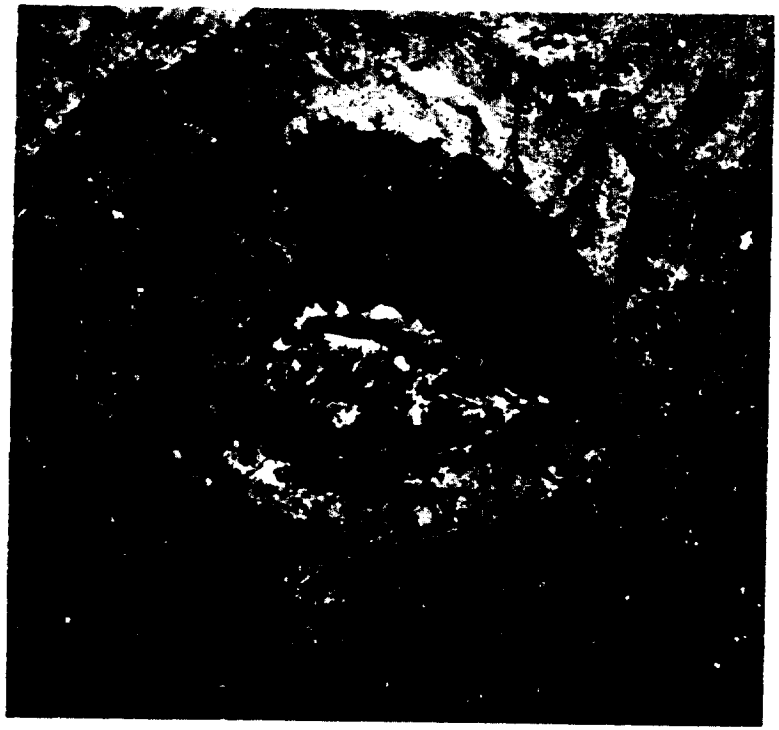

FIGURE 17-6. Vertical aerial photograph of Middle Butte. Area shown is approximately 3 km by 3 km. (U. S. Geological Survey Photograph, GS-SWEZ, 7-86, October, 1971.)

FIGURE 17-8. Vertical aerial photograph of Big Southern Butte. The older dome (1) and the younger dome (2) align N45°W. The alluvial fan (3) and emergency landing strip (4) are visible in the upper left-hand corner. Area covered is about 3.0 by 3.3 km. (Army Map Service Photograph 4416, 1953.)

Mileage		
Cumulative	Difference	
38.8	2.5	The summit region for an unnamed low shield is seen to the left (Fig. 17-9).
45.8	7.0	View of Middle and East Buttes to the right.
47.2	1.4	Cedar Butte vent area visible on the left. Cedar Butte (Fig. 17-10) is an andesitic lava cone relatively old in appearance, with flows covering about 26 km^2. The Cedar Butte andesite consists of a few feldspar phenocrysts with occasional olivine and pyroxene phenocrysts within a matrix of stubby oligoclase crystals in brown or green glass (Niccum, 1969). Explosive eruption activity here is associated with ring and radiating fractures in the older andesites (Niccum, 1969). During the final stages of eruption, the eastern half of the vent area was downthrown along a north-south trending normal fault, leaving a scarp as much as 60 m high in places. One of the last andesite flows cascaded down this scarp. The last stage of activity was the formation of cinder cones along three fissures. One of these was breached and the exposed throat exhibits dike-like coatings along the King's Bowl Rift. The recent Cerro Grande basalt flow laps up against the north-south fault scarp previously mentioned.
47.5	0.3	Atomic City on road to left.
48.0	0.5	Entering National Reactor Testing Site (NRTS), Energy Research and Development Administration (ERDA) facilities. The center covers approximately 2300 km^2 and since 1946, over 50 experimental reactors of various types have been in operation. Originally under the jurisdiction of the Atomic Energy Commission, the newly formed ERDA presently controls operations. The NRTS contains the "sinks" for Birch Creek, Big Lost River, and Little Lost River. In conjunction with site selection for the NRTS, many geologic studies of subsurface conditions were undertaken (Walker, 1964). Well logs indicate an interlayering of lava and sediments. In the southeastern portions of NRTS, basaltic lavas are interbedded with a few thin layers of sediment, whereas to the northwest (in a zone trending northeast), large accumulations of sedimentary material are interbedded with the lava. This may be a function of extensive basalt flows in the south that created a depositional trough northward where sediments of the mountains accumulated. Sediments in this main trough occur mainly in three large bodies intercalated with basalt: 1) the upper mass, exposed at the surface in places, locally more than 100 m thick, 2) another mass approximately 70 m thick with a basal elevation of about 1250 m, and 3) a large deposit, locally 170 m thick, with its upper margin at 1200 m elevation. These large deposits may all be the result of runoff accumulations of glacial periods; the upper deposits associated with the Pinedale Glaciation and the deeper ones with the Bull Lake and Buffalo Glaciations (Walker, 1964) Major recent basalt flows include Furey basalt, Atomic City basalt, Cerro Grande basalt, and Robber's basalt—all of which lie between Big Southern Butte and Middle Butte. The Robber's basalt flows issue from a rift that trends southeast from Big Southern Butte (Fig. 17-7). Legends suggest that the area was the scene of a stage robbery in the early mining days and that three gold ingots are still buried somewhere in the area.

FIGURE 17-9. Unnamed basalt vent showing low shield typical of Snake River Plain basalts. (Photograph by Ronald Greeley, University of Santa Clara, June, 1977.)

FIGURE 17-10. Oblique aerial view showing Cedar Butte vent area (1) and Cerro Grande basalt vent area (2). (Photograph by Ronald Greeley, University of Santa Clara, June, 1977.)

Mileage		
Cumulative	Difference	
49.8	1.8	Lost River Range in the distance at twelve o'clock. The Lemhi Range lies immediately to the east; Saddle Mountain reaches an elevation of 3290 m.
53.1	3.3	Road cut through Cerro Grande basalt. This flow covers 195 km^2 (Fig. 17-1) and is 76 m thick near the vent; flow margins are about 3-6 m high. The flow originated from a fissure 10 km southeast of Big Southern Butte (Fig. 17-10).
54.5	1.4	Junction with Route 20. Turn left, towards Arco.

Mileage		
Cumulative	Difference	
59.9	5.4	Road on left leads to the Experimental Breeder Reactor-I (EBR-I), a national historic landmark administered by ERDA and the National Park Service. EBR-I was the first reactor in the world to generate usable amounts of electricity. On December 20, 1951, enough power was generated to light four light bulbs. The next day, the experiment was repeated and sufficient energy was produced to power the entire EBR-I building. Within the next ten years, the facility demonstrated the feasibility of nuclear power.
61.4	1.5	Lost River: for most of the year, this river bed is dry, the water being diverted for agricultural and irrigation purposes upstream. The Big Lost River and Little Lost River enter the Snake River Plain through the valley north of Arco. In the wetter seasons, the Lost Rivers flow through this channel to an area where the water percolates through the underlying basalt, about 33 km east of Arco. This water is believed to reappear at the Thousand Springs area along the Snake River, some 150 km southwest.
74.3	12.9	Junction with Routes 22 and 88; continue north on Route 20.
75.6	1.3	Craters of the Moon volcanic vents can be seen at ten o'clock.
76.2	0.6	View of Arco Peak (Fig. 17-11) at about one o'clock. Dipping beds contain Carboniferous marine carbonate rocks with some quartzites. Many of the Paleozoic rocks throughout the Lost River Range are strongly folded and faulted by normal and thrust faults.
83.0	6.8	Junction with Route 93A in Arco. Turn left toward Craters of the Moon. Arco has the distinction of being the first city in the world to be completely powered by nuclear energy.
84.5	1.5	The original site of Arco, built in 1879, was just south of here. Being the intersection of two stage lines, it was originally called "Junction." The post office, however, did not accept the name and it was subsequently changed to Arco.
86.7	2.2	To the right a young lava flow blocks the valley of the Big Lost River to the north.
88.0	1.3	Road to right was originally part of the old state highway connecting Carey and Arco. It still serves as an access to the Lava Creek mining district, now mostly inactive. The mines contained various metals such as silver, gold, lead, zinc, copper, and tungsten, but are principally known for the silver ore produced from 1883 to 1887.
94.6	6.6	Margins of relatively fresh lava flows. The basalts here are typical of the Snake River Plain. Road cuts show the internal structure and cooling units within the flows. The mountains to the right are the Pioneer Mountains and consist primarily of the Tertiary Challis volcanics, a suite of quartz latite and basaltic vitrophyres.
99.0	4.4	Enter Craters of the Moon National Monument (Fig. 17-12).
100.8	1.8	Headquarters and visitor center. The monument is situated on the Great Rift and has 14 fissures marked by both cinder and spatter cones. Most flows within the monument are Recent and contain numerous tubes with collapsed and uncollapsed sections. (See Chapters 13 and 14.)

FIGURE 17-11. Arco peak showing dipping beds of Carboniferous marine sediments. (Photograph by Ronald Greeley, University of Santa Clara, June, 1977.)

FIGURE 17-12. Craters of the Moon National Monument showing U. S. Alternate Highway 93 (1), Visitor Center (2), campground (3), Devil's Sewer trail (4), North Crater flow (5), and Sunset Cone (6). (Photograph by Ronald Greeley, University of Santa Clara, June, 1977.)

REFERENCES

Armstrong, R. L., W. P. Leeman and H. E. Malde, 1975. K-Ar dating, Quaternary and Neogene volcanic rocks of the Snake River Plain, Idaho: American Jour. Sci., vol. 275, p. 225-251.

Kuntz, M. A., 1977. Extensional faulting and volcanism along the Arco Rift Zone, eastern Snake River Plain, Idaho: Geol. Soc. Amer., Abs. with Programs (Rocky Mountain Section), vol. 9. p. 740-741.

Murtaugh, J. G., 1961. Geology of Craters of the Moon National Monument. Master's Thesis, University of Idaho, Moscow, Idaho, 99 p.

Niccum, M., 1969. Geology and permeable structures in basalts of the east central Snake River Plain near Atomic City, Idaho: Master's Thesis, Idaho State University, 135 p.

Walker, E., 1964. Subsurface geology of the National Reactor Testing Station, Idaho: U. S. Government Printing Office, Washington, 22 p.

U. S. Geological Survey and Idaho Bureau of Mines and Geology, 1959. Geologic Map of the State of Idaho, 1 sheet.

18. ROAD LOG ALONG PLEISTOCENE LAKE BONNEVILLE FLOODPATH

Ronald P. Papson
Department of Geology
Arizona State University
Tempe, Arizona 85281

18. ROAD LOG ALONG PLEISTOCENE LAKE BONNEVILLE FLOODPATH

Ronald P. Papson
Department of Geology
Arizona State University
Tempe, Arizona 85281

The road log follows the course of the Lake Bonneville flood (Fig. 18-1) and is split into two parts. The first half is approximately 90 miles in length, round trip, starting in Pocatello, heading south toward Red Rock Pass, and then returning to Pocatello. Many flood effects, such as channeling, scouring, and deposition of boulder bars, can be seen. The second half of the trip is approximately 35 miles, one way, starting at the north end of Pocatello, then heading southwest towards American Falls, and ending at Massacre Rocks State Park. Flood features along the Snake River will be examined as well as local stratigraphy.

Pleistocene Lake Bonneville overflowed at Red Rock Pass near Downey, Idaho. Flood waters washed through Marsh Creek Valley and eventually to the Portneuf River Valley, scouring and eroding the surfaces. As waters entered the ancestral American Falls lake, an extensive gravel delta was deposited. This additional inflow to the Snake River eventually broke through the basalt dam which had previously impounded waters. Erosion from these waters produced the many features (e.g., abandoned spillways, boulder bars, channels, and terraces) seen from American Falls to Massacre Rocks.

Mileage		
Cumulative	Difference	
0.0	0.0	The field trip starts at Upper Ross Park, heading south on Business Route I-15, at the southern end of Pocatello.
0.4	0.4	Turn right onto Interstate Highway I-15, heading south. The cliffs on the right cut the basalt of the Portneuf River valley, two superimposed flows informally termed the McCammon Basalt (Ives, 1964). These flows, which at one time filled the valley, appear to be continuous southeastward beyond Lava Hot Springs and may have originated from vent structures near Alexander, Idaho, on the Bear River. The flows entered the Portneuf valley near McCammon and spread southward a short distance toward Arimo and northward about 30 km. The dark gray to black basalt locally displays well developed diktytaxitic texture. Throughout the valley the two are each about 15 m thick and exhibit columnar structure. Well logs near Pocatello indicate that the lower basalt flowed over valley alluvium approximately 10 m thick (Trimble, 1976). Organic material from beneath the lower flow has been dated at 33,000 $\pm$ 1600 years B.P. and 35,000 $\pm$ 3000 years B.P. (Ives, 1964). To the south, near McCammon, the flows dammed Marsh Creek forming a temporary lake. Mollusks from these lake beds have been dated at 32,500 $\pm$ 1500 years B.P. (Ives, 1964). The upper surface of the McCammon Basalt was scoured by Lake Bonneville floodwaters and thus is older than the flood.

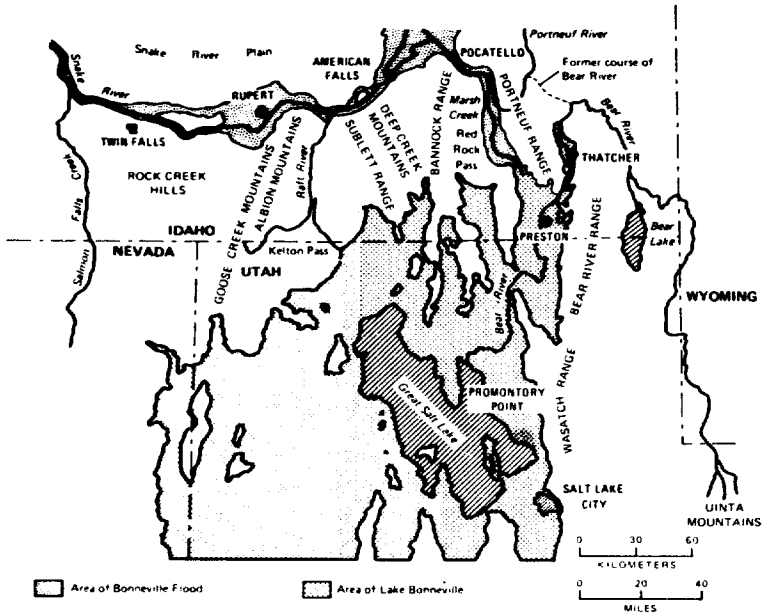

FIGURE 18-1. Map showing northern extent of Pleistocene Lake Bonneville and area covered by subsequent Bonneville floodwaters. The diversion of the Bear River into Lake Bonneville by basalt flows north of Thatcher evidently caused the initial spillover at Red Rock Pass. (From Malde, 1968.)

Mileage		
Cumulative	Difference	
3.4	3.0	In the valley to the right lies the Portneuf River which empties into the American Falls reservoir to the north. The Portneuf originates in the mountains on the east side of the Pocatello Range, flows southward to Lava Hot Springs, westward towards McCammon, then finally northward toward Pocatello.
4.7	1.3	At this point, the road veers left through a canyon-like constriction. Rocks on either side are members of the Precambrian Pocatello Formation (Fig. 18-2). On the left are primarily dark gray to black siltstones and slaty argillites; to the right is a "tillite series" (Ludlum, 1942), consisting of thick layers of metadiamictite interstratified with a few beds of limestone and dolomite (Trimble, 1976). The constriction is termed the Portneuf Narrows and confined the floodwaters of Lake Bonneville to a depth of 120 m (Malde, 1968).

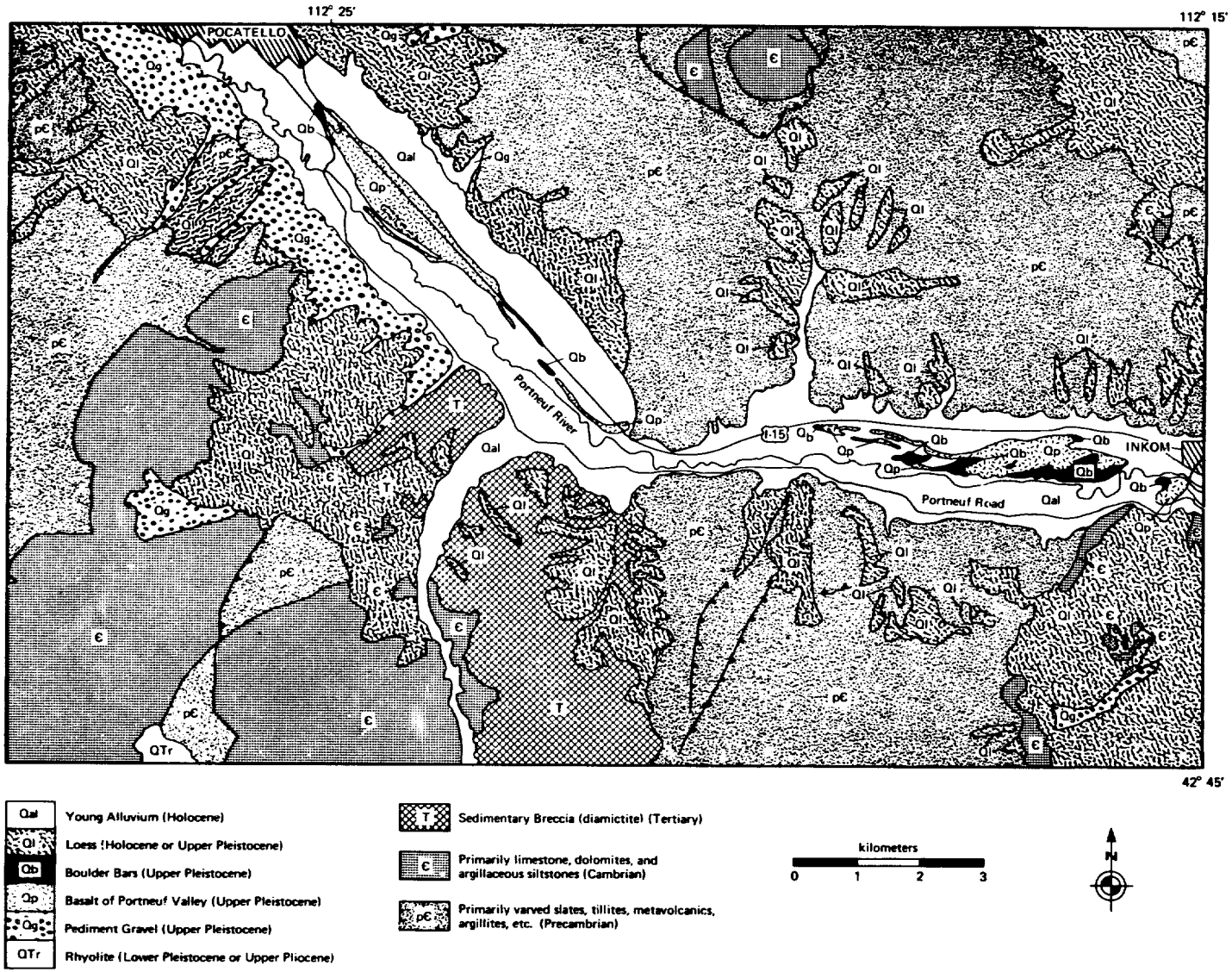

FIGURE 18-2. Generalized geologic map of the southern section of the Pocatello quadrangle, Idaho. McCammon basalt (Qp) and boulder bars (Qb) predominate in the valley between Pocatello and Inkom. Precambrian metasediments (PE) constricted the Bonneville floodwaters at Portneuf Narrows. (From Trimble, 1976.)

Mileage		
Cumulative	Difference	
10.4	5.7	Inkom. To the left are prominent basalt cliffs which display well developed columnar jointing (Fig. 18-3). The basalt west of the river has been stained white by dust from a local cement plant.
11.3	0.9	Bridge crossing over the Portneuf River, which veers southward toward McCammon. Marsh Creek, the only major tributary of the Portneuf River, has cut the wide valley to the right.
11.8	0.5	The interstate crosses the surface of the McCammon Basalt. The basalt forms a plateau which is dissected to the east by the Portneuf River and to the west by Marsh Creek (Fig. 18-4).
20.4	8.6	Intersection of Route 30N. Lava Hot Springs (to the east) was used by Indians as a source of hot water. Continue south on Interstate Highway I-15 toward Red Rock Pass.

FIGURE 18-3. Oblique aerial view of basalt cliffs southeast of Inkom along Interstate Highway I-15. The basalt extended from Pocatello to McCammon, covering the entire valley. Subsequent erosion has produced the vertical cliffs along the river valleys, exhibiting excellent columnar jointing. The Portneuf River is in the foreground with the cement plant in the lower left corner. Photograph by Ronald Greeley, University of Santa Clara, June, 1977.

FIGURE 18-4. Oblique aerial view looking southward toward Red Rock Pass (1). The Portneuf River (2) and Marsh Creek (3) dissect the McCammon basalt, forming a plateau (4). Interstate Highway I-15 crosses the plateau and heads south toward Elkhorn Peak (5). Water from Lake Bonneville overflowed Marsh Creek valley and spilled over to the Portneuf River, cutting channels (6) in the surface. Photograph by Ronald Greeley, University of Santa Clara, June, 1977.

Mileage		
Cumulative	Difference	
28.4	8.0	The flow edge of the McCammon Basalt can be seen to the right. The extensive basalt flows dammed Marsh Creek to the west and formed a lake, deposits from which are as much as 30 m deep and extend about 3.2 km south of Arimo. The Bonneville Flood, which occurred in the Late Pleistocene, is one of the latest geologic events along the Snake River in southeastern Idaho. To understand the catastrophic effects caused by the voluminous discharge of Pleistocene Lake Bonneville, we must first trace the events which ultimately led to the overflow at Red Rock Pass. The Bear River, which heads in the Uinta Mountains of Utah (Fig. 18-1) presently accounts for 43 percent of runoff into Great Salt Lake. Bear River, however, was at one time a tributary to the Snake River by way of the present day Portneuf River (Fig. 19-1). The ancestral Bear River was subsequently dammed and diverted by several basalt flows issuing from vents near Alexander. The impounded waters formed Lake Thatcher (Fig. 18-5) within a basin between the Bear River Range and the Portneuf Range. Periodic overflow at the northern rim of Lake Thatcher allowed discharge into the Portneuf River. Successive basalt flows, however, soon raised the north rim to a higher elevation than that of the south rim (1660 m) thus forcing the lake to overflow southward and cut through a quartzite divide to Lake Bonneville. This greatly augmented inflow caused by the capture of the Bear River, initiated the rise in the level of Lake Bonneville, and caused its eventual spillover at Red Rock Pass. Other factors–such as changes in regional climate–may also have influenced Lake Bonneville, but the Bear River inflow is seen as the most important (Malde, 1968).
36.4	8.0	Exit Interstate Highway I-15 onto Route 91, heading toward Preston. The conical mountain is Elkhorn peak with an elevation of 2743 m.
42.5	6.1	View of Red Rock Pass ahead.
44.2	1.7	Red Rock Pass. This was the outlet of Pleistocene Lake Bonneville. The pass divides the northern Malad Range to the west with the Portneuf Range to the east. The outlet channel is 120 m wide at the top and 100 m deep. The initial overflow of Lake Bonneville quickly cut through an old alluvial barrier at Red Rock Pass, and probably accounts for the catastrophic effects of the flood. Removal of these unconsolidated materials proceeded rapidly and the tremendous discharge of water continued until a resistant rim of Paleozoic shales, limestones, and dolomites (Fig. 18-6) was encountered. Discharge diminished and erosion of these more resistant rocks continued at a slower rate. The elevation of Lake Bonneville at time of overflow has been estimated at 1565 m (Williams, 1952). The pass has now been graded to the Provo shoreline elevation of 1457 m (Malde, 1968). Estimates on the age of the flood vary; Bright and Rubin (1965) estimate 18,000 years B.P. while Malde (1968) believes 30,000 years B.P. is more reasonable. Reverse direction and head north toward Pocatello.

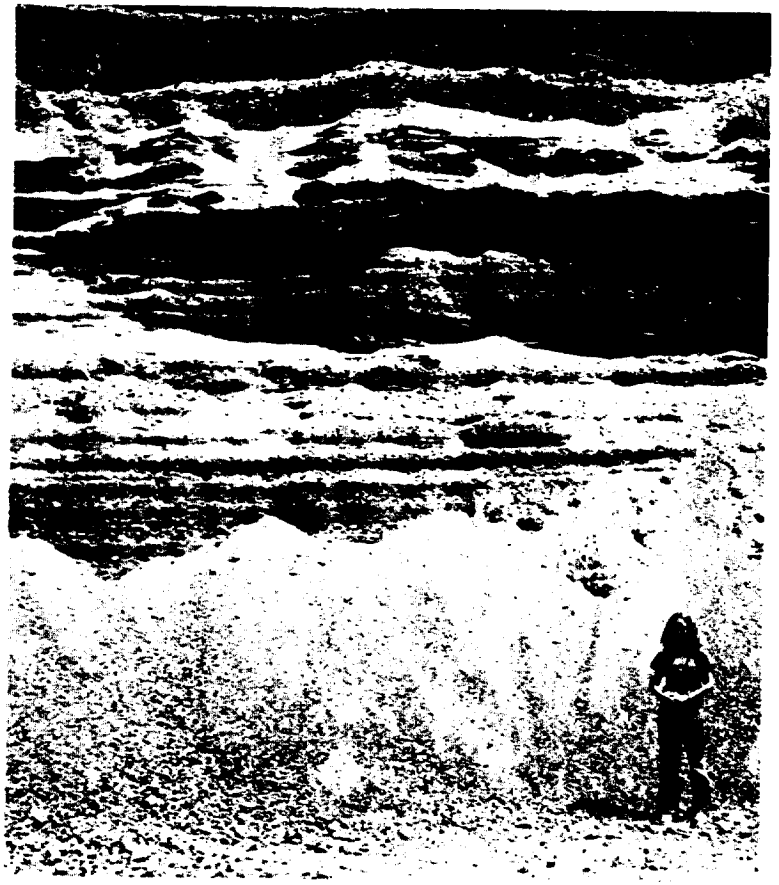

FIGURE 18-5. Large gravel deposits in Lake Thatcher lake beds near the Bear River. Photograph by Ron Papson, University of Santa Clara, June, 1977.

FIGURE 18-6. Eroded remnants of Paleozoic shales, limestones, and dolomites at Red Rock Pass. As overflow waters from Lake Bonneville reached these more resistant rocks, the flood diminished and subsequently cut down to the present level at a reduced rate. Photograph by Ron Papson, University of Santa Clara, June, 1977.

Mileage		
Cumulative	Difference	
50.0	5.8	Downey. As much as 5.5 m of bouldery cobble gravel was deposited in this area as a result of the flood (Bright and others, 1965). Water filled the valley from wall to wall, depositing boulders and cobbles along its path. The velocity of the water at this point has been estimated at 7.6 m/sec. The maximum discharge has been calculated at approximately 4.3 x $10^5 m^3$/sec with a total flow volume of about 1600 km^3 (Malde, 1968). In comparison, discharge over Niagara Falls is only 5.5 x $10^3 m^3$/sec, a factor of 75 less. Malde (1965) believes that the catastrophic flooding effects continued for a few weeks with voluminous discharage continuing for at least one year.
52.0	2.0	Junction with Interstate Highway I-15; head north toward Pocatello through Marsh Creek valley. Pediments and high level alluvial fans border the mountain ranges.
68.0	16.0	Exit Interstate Highway I-15 at junction with Route 30N. Turn left toward Indian Rocks State Park.
68.2	0.2	Indian Rocks State Park. Shoshone Indian petroglyphs (or "rock carvings") are found here.
68.6	0.4	Road veers right and descends along a basalt cliff of Marsh Creek Valley. As water from Lake Bonneville descended the valley, it met this constriction cut into the McCammon basalt. The highly erosive floodwaters plucked and stripped basalt from the cliffs and widened the valley. During periods of very high discharge, water overflowed the basalt plateau (Fig. 18-4), scouring its surface. Overflow waters cut channels on the plateau (Fig. 18-4), spilling into the Portneuf River to the east. View of Scout Mountain (2654 m) straight ahead.
68.9	0.3	Cross Marsh Creek.
69.4	0.5	Veer right onto Marsh Creek Valley Road.
71.2	1.8	Basalt cliffs across valley on right.
76.4	5.2	Boulder train (boulder bar) extends from cliff. Canyon constriction along the flood path intensified the flow and increased the erosion. Basalt boulders (Fig. 18-7) were torn from the cliffs and were deposited in more tranquil water, sometimes several kilometers downstream. The immense size of these boulders (up to 5 m in diameter) is evidence of the tremendous power of the flood.
77.4	1.0	Sag in basalt flows along cliff (Fig. 18-8).
78.2	0.8	View of Marsh Creek emptying into the Portneuf River.
79.0	0.8	Stop just south of the cement plant. Examine the basalt surface here and observe scour patterns (Figs. 18-9 and 18-10). Water laden with debris pitted and fluted the surface.
79.4	0.4	Turn left onto Portneuf Valley Road. Road to right passes the cement plant and terminates in Inkom.
79.5	0.1	Boulders on right.
80.6	1.1	Note basalt cliffs across the valley. Boulder bars are streamlined in the direction of the flood.

FIGURE 18-7. Typical boulder bar along the Bonneville floodpath. High velocity waters tore these boulders from exposed cliffs, transported them downstream (as much as a few kilometers), and then deposited them in more tranquil waters. The large size (up to 5 m in diameter) indicates the tremendous force of the flood. Photograph by Ron Papson, University of Santa Clara, June, 1977.

FIGURE 18-8. Basalt cliff along Marsh Creek showing flow sag (arrow) and typical columnar jointing. Photograph by Ronald Greeley, University of Santa Clara, June, 1977.

FIGURE 18-9. Scour and fluting on basalt surface near Inkom. Photograph by Ronald Greeley, University of Santa Clara, June, 1977.

FIGURE 18-10. Scour and fluting caused by floodwaters of Lake Bonneville. Photograph by Ronald Greeley, University of Santa Clara, June, 1977.

Mileage		
Cumulative	Difference	
83.0	2.4	View of basalt scarps across the valley. At one time the entire valley was covered with basalt. Portneuf Narrows (Fig. 18-11) can be viewed downstream. The narrows is a constriction which impeded the floodwaters, causing the waters to build up to a depth of 120 m.
83.4	0.4	Veer left.
85.0	1.6	Exit Portneuf Narrows.
85.4	0.4	Cross Fort Hall Road.
86.7	1.3	Veer right.
87.1	0.4	Turn right onto Bannock Highway.
88.4	[illegible]	View of channel cut into surface of basalt of Portneuf Valley (Fig. 18-12).
88.6	0.2	Turn right onto Cheyenne Avenue.
89.0	0.4	Cross Portneuf River.
89.1	0.1	Road curves left. Basalt cliffs begin and continue northward.
90.1	1.0	Boulders at base of basalt cliff (Fig. 18-13) on right.
90.4	0.3	Lower Ross Park. End of first half of field trip. Walk around the park and examine scoured basalt cliffs and rounded boulders. Rounded quartzite boulders can be found resting upon basalt surfaces. Upper Ross Park can be reached by short trails up the cliffs; the reconstruction of the Old Fort Hall is in the Upper Park.

The second half of the field trip will follow the path of the Lake Bonneville floodwaters downstream along the Snake River. Bonneville overflow entered the Snake River through ancestral American Falls lake at the north end of the Portneuf Valley.

FIGURE 1° 11. View of Portneuf Narrows looking west from Portneuf Road. Water was 120 m deep at this construction during periods of maximum discharge. Photograph by Ronald Greeley, University of Santa Clara, June, 1977.

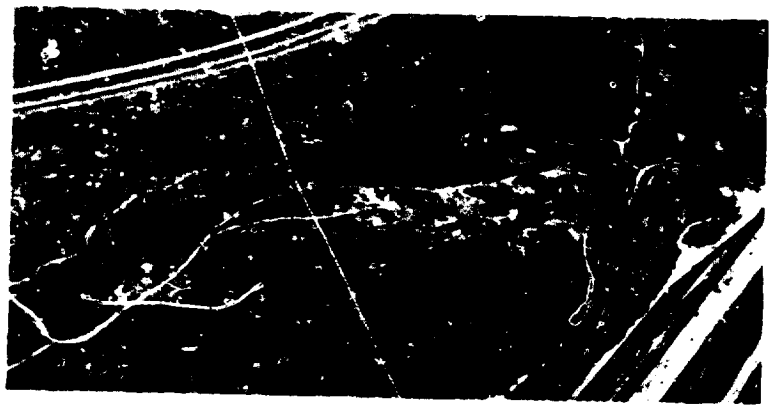

FIGURE 18-12. Oblique aerial view of channel cut in the McCammon basalt near Pocatello. Photograph by Ron Papson, University of Santa Clara, June, 1977.

FIGURE 18-13. Typical boulder transported by the Bonneville Flood. Water erosion rounded these boulders in short distances (several km maximum) and short periods of time (approximately six weeks) during the maximum discharge of water. Photograph by Ron Papson, University of Santa Clara, June, 1977.

Mileage	
Cumulative	Difference
0.0	0.0
0.9	0.9

Start the second half of the trip heading west on Interstate Highway I-15W at junction with I-15. Pass beneath Route 91. Waters from Lake Bonneville entered ancestral American Falls lake in this area, forming the deltaic deposits of the Michaud Gravel. This deposit extends approximately 29 km, almost to American Falls and rests conformably on the surface of the American Falls lake beds. The Michaud Gravel is 15 to 24 m thick and grades from boulders about 3 m in diameter near Pocatello to cobble sized sediments toward Michaud (Fig. 18-14). Calculations indicate that the water velocity near Pocatello was approximately 11 m/sec and 3-4 m/sec near Michaud. A minimum age for the deposition of the gravel is 29,700 ± 1000 years B.P. (Trimble and Carr, 1961).

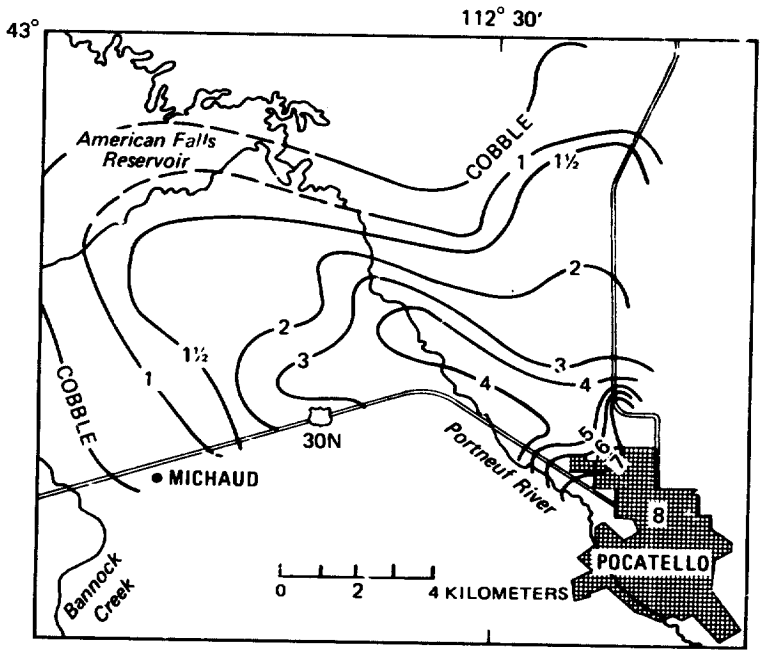

FIGURE 18-14. Diagram showing the Michaud delta northwest of Pocatello, Idaho. Contour lines show the longest dimension (in feet) of the largest boulders. (From Trimble, 1976.)

Mileage		
Cumulative	Difference	
1.7	3.8	FMC Corporation on left. The road to right leads to a gravel pit in the Michaud Gravel. Quarries such as this are found throughout the Michaud flats and expose the poorly sorted gravel deposits in cross section (Fig. 18-15). The lithology of the gravel is mostly basalt and quartzite. Deposits locally contain mollusks and in a few places, specimens of *Bison alleni* have been found (Hopkins, 1951).
7.4	2.7	Pocatello airport to right.
9.7	2.3	Bannock Creek (Fig. 18-16). West of here the Michaud deltaic deposits consist of pebbly sand, eventually decreasing in grain size to a fine sand. Bannock Range to the east.
14.9	5.2	To the right for the next few miles Big Southern, Middle and East Buttes are visible in the distance. Studies are currently being conducted to determine the origin of the buttes and their relation to the surrounding Snake River volcanics (Chapter 6). American Falls Reservoir is on the right (Fig. 18-16).
17.0	2.1	Bridge over the Union Pacific railroad tracks. The Grandview Terrace can be seen across the reservoir (Fig. 18-16). Deposits are tan, brown, or pinkish silt and fine sand, and are probably marginal deposits formed on the margin of the Pleistocene American Falls lake. These deposits may be fine-grained equivalents of the Michaud Gravel (Carr and Trimble, 1963).
21.4	4.4	Continue west on Interstate Highway I-15W. Route 39 heads north toward the city of American Falls. The completion of the American Falls dam in 1927 allowed 110,000 acres of new land to be irrigated. Presently, the dam is being partly reconstructed to provide additional hydroelectric power and to reinforce the old dam.
24.9	3.5	Ferry Hollow (Fig. 18-17) on the right. Excellent exposures of the Pliocene Walcott Tuff are visible in the valley walls (Fig. 18-18). The underlying Neeley Formation was laid down in a shallow lake and consists primarily of pink siliceous tuffs and tuffaceous sandstones (Stearns and Isotoff, 1956). Minor amounts of marl, silty clay, and conglomerate are often interbedded with the volcanic beds. The Walcott Tuff (formerly called the Eagle Rock Tuff) overlies the Neeley Lake Beds with a slight disconformity and consists primarily of rhyolitic welded tuff, typical of *nuée ardente* volcanic activity. Four distinct phases of the formation have been described by Stearns and Isotoff (1956) and can be seen at this outcrop. Phase 1, the lowest, is a thin layer of loose white and gray ash grading upward to a black well-bedded glass shard tuff. Phase 2 is a hard black obsidian contining numerous spher... ... 3-6 mm in diameter. Phase 3 (Fig. 18-19) consists of friable gray to black, fine-grained obsidian shards honeycombed with lithophysae up to 5 cm in diameter. Phase 4 is a dark red brittle pitchstone at the top of the formation.

FIGURE 18-15. Outcrop of Michaud Gravel in Union Pacific quarry near junction of Interstate Highway I-15W and Route 30N. Well-rounded, poorly sorted rocks were deposited as the Bonneville floodwaters entered the ancestral American Falls Lake. Photograph by Ron Papson, University of Santa Clara, June, 1977.

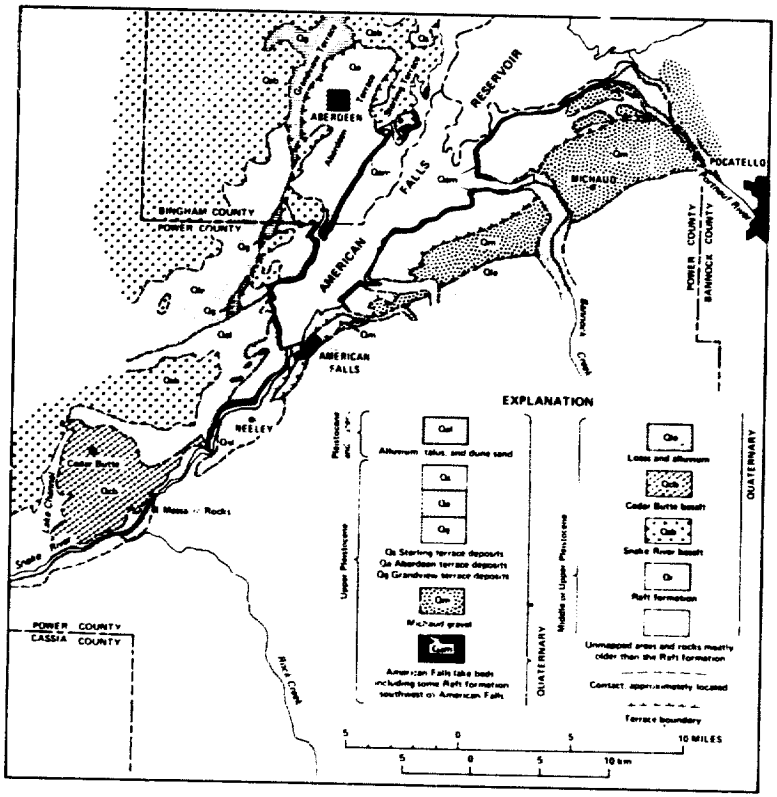

FIGURE 18-16. Geologic sketch map along the Snake River in the American Falls area. (After Trimble and Carr, 1961.)

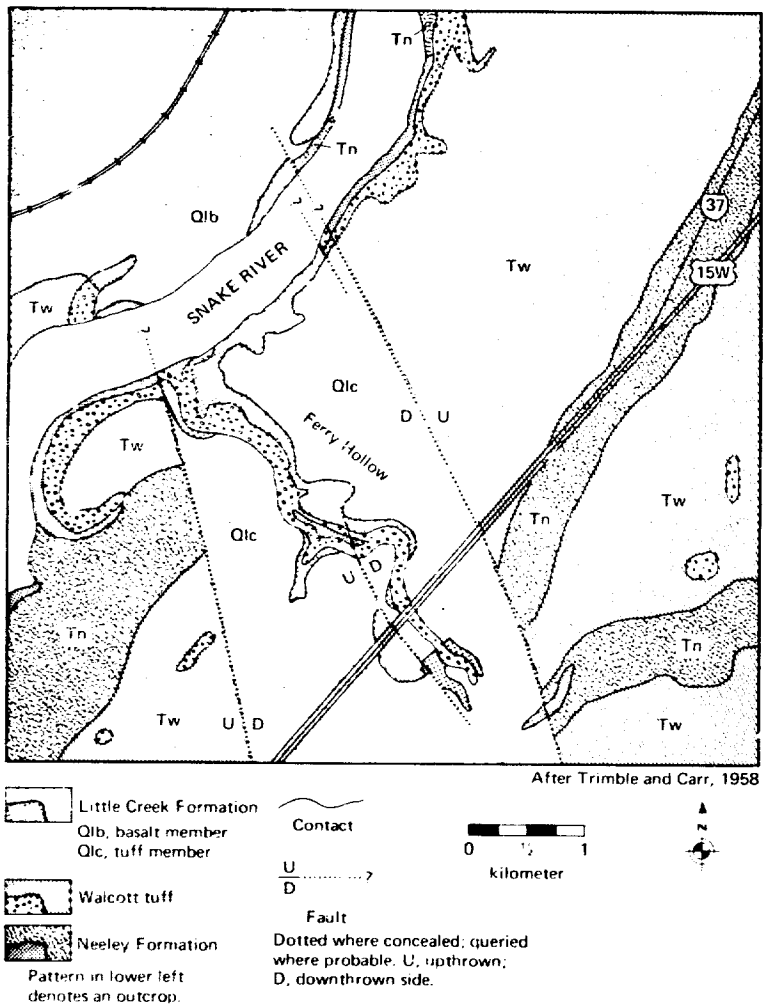

FIGURE 18-17. Geologic sketch map of Ferry Hollow area. Outcrops of the Neeley Formation, Walcott Tuff, and Little Creek Formation are exposed in the valley walls. (After Carr and Trimble, 1958.)

FIGURE 18-18. Outcrop of Walcott Tuff (lower dark layer) and Little Creek Formation (upper light area) in Ferry Hollow. Photograph by Ronald Greeley, University of Santa Clara, October, 1977.

Mileage

Cumulative Difference

Above the Walcott Tuff, with a slight disconformity, lies the Little Creek Formation (Fig. 18-18). The lower part of this unit is a tan, fine-grained rhyolitic tuff containing reworked fragment of the Walcott Tuff. The upper part consists of light-gray to tan basaltic tuff and ash mixed with varying amounts of sand and clay (Fig. 19-20). The following geologic history of this area has been proposed by Stearns and Isotoff (1956):

1) Deposition of Neeley lake beds and volcanic tuffs. An ephemeral lake confined in a shallow basin received ash fall from several volcanoes. In addition, streams washed loose ash into the basin.
2) The area underwent uplift which caused Neeley Lake to drain. Slight erosion of the lake beds took place at this time.
3) Deposition from a *nuée ardente* of the Walcott rhyolitic tuff. Basal white ash indicates quick chilling of hot material with the colder ground.
4) Deposition of pink siliceous silt (Little Creek Formation) containing weathered blocks of the Walcott Tuff. There are indications that Neeley Lake was revived and deposition of rhyolitic ash occurred. All these events occurred in the late Tertiary.

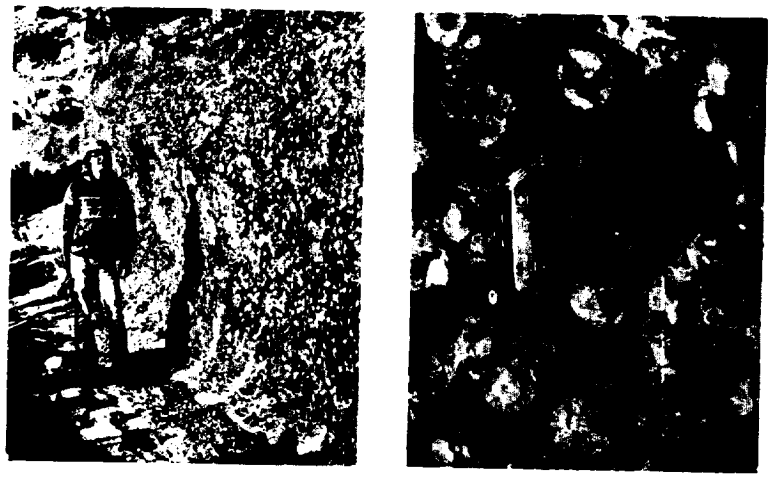

FIGURE 18-19. Left–Phase 3 (Stearns and Isotoff, 1956) of the Walcott Tuff. This friable obsidian layer is honeycombed with lithophysae up to 5 cm in diameter. Right–Close-up of lithophysae in obsidian shard matrix. Photographs by Ronald Greeley, University of Santa Clara, October, 1972.

Mileage		
Cumulative	Difference	
29.2	4.3	American Falls lake beds and Cedar Butte basalt dam on right. To the northwest is the Cedar Butte vent area (Fig. 18-21). Extensive basalt flows from the vents extended northward and abutted the Big Hole Basalt. Lava also entered the Snake River channel forming a basalt dam. Prior to the eruption, the Snake River occupied a channel roughly parallel to the present channel but was a few kilometers to the north (Stearns and others, 1938). The river was restricted and formed ancestral American Falls lake with an elevation of approximately 1356 m. The lake extended almost 64 km northeast, to the present city of Blackfoot and was approximately 19 km wide. The American Falls lake beds (Fig. 18-22) were deposited behind this basalt barricade, the maximum elevation of deposition being approximately 1341 m. They consist of a lower coarse gravel layer grading upward to a fine-grained sand and silt layer. Above this are interbedded layers of calcareous and noncalcareous clay with some sand. Occasional overflow and seepage occurred throughout the history of the lake. As Bonneville floodwaters entered American Falls lake, depositing the Michaud Gravel, the augmented inflow caused the dam to be breached, with initial overflow diverting northward, around the Cedar Butte vents, and southward in the approximate position of the present Snake River channel (Fig. 18-23a). The overflow produced a series of cataracts along the present Snake River, and along abandoned channelways, such as the old Lake Channel (Fig. 18-24) and erosion produced narrow channels with scalloped shaped alcoves upstream (Fig. 18-25). Lake Channel was cut and eventually abandoned as floodwaters subsided. The course of subsequent flow is indicated in Figures 18-23b and 18-23c and represents the final stages of the flood. Normal river erosion finally broke through the Cedar Butte basalt dam (Fig. 18-26). The softer lake beds behind the dam were easily eroded and produced the steep cliffs across the river. The present course of the Snake River (Fig. 18-25d) reflects the long history of diversion by volcanic activity and erosion by the Lake Bonneville flood. The alcoves at the heads of channels, as well as the channels themselves, may not be a result of the Bonneville flood. Stearns and other (1938) believe these coves are a result of a "sapping" process where water percolating through a weak, permeable basalt layer removes parts of that layer causing the overlying basalt to collapse into the resulting void. Successive collapse would cause the retreat of these springs and form a channel along its path. In the case of Lake Channel, water was supplied by percolation from ancestral American Falls Lake.
33.8	4.6	Historic site on right. On the way west for John Jacob Astor's Pacific Fur Company in 1811, a group of men led by W. P. Hunt explored the Snake River Valley. They passed here on October 26 and headed downstream where rapids overturned their canoes. One man and much gear was lost, but after splitting into three parties, they continued afoot to Fort Astoria at the mouth of the Columbia River. From this point, a stratigraphic section of the area can be seen upstream (Fig. 18-27).

FIGURE 18-20. Exposure of the Pleistocene Little Creek Formation showing typical weathering surfaces. Photograph is approximately 5 m high along right margin. Photograph by Ron Papson, University of Santa Clara, June, 1977.

FIGURE 18-21. Vertical air photograph of area covered by overflow of ancestral American Falls Lake. Cedar Butte vents (1) were the source of lava which dammed the Snake River. Floodwaters cut Lake Channel (2) and the numerous alcoves found here (3). Many abandoned spillways (4) and abandoned waterfalls are found north of the Massacre Rocks vents (5). Recent sand dunes can be seen as high albedo areas trending in an east-west direction. U. S. Geological Survey Photograph GS-VEI, 1-117, October, 1954.

FIGURE 18-22. View of cliff in American Falls lake beds exposed on north bank of the Snake River near Neeley, Idaho. These beds were deposited behind the Cedar Butte basalt dam (arrows) in the ancestral American Falls Lake. Photograph by Ron Papson, University of Santa Clara, June, 1977.

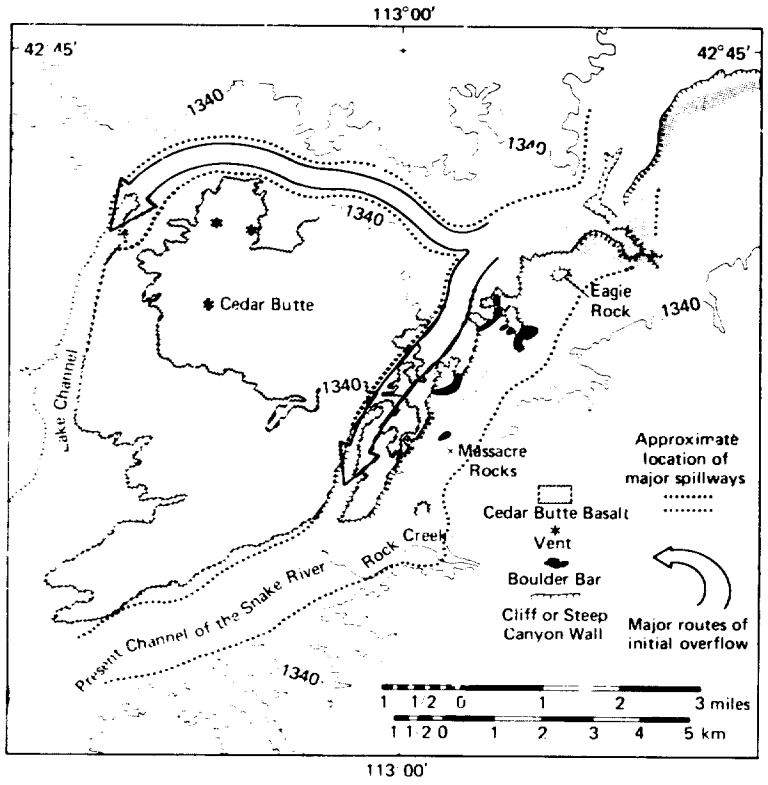

FIGURE 18-23a. Routes of initial American Falls Lake overflow as a result of Bonneville floodwaters.

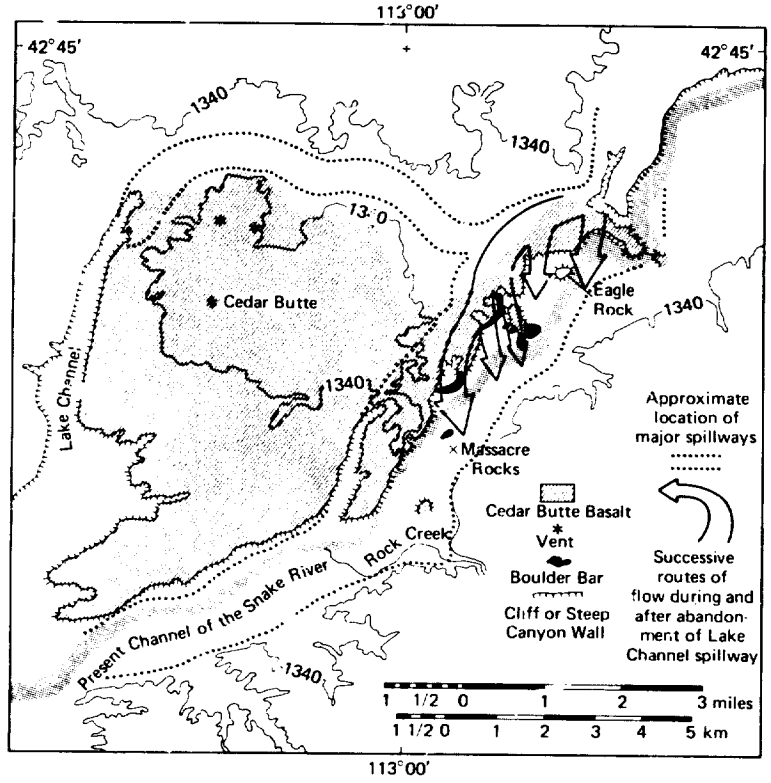

FIGURE 18-23b. As overflow diminished, Lake Channel was abandoned and successive water routes drained toward the south.

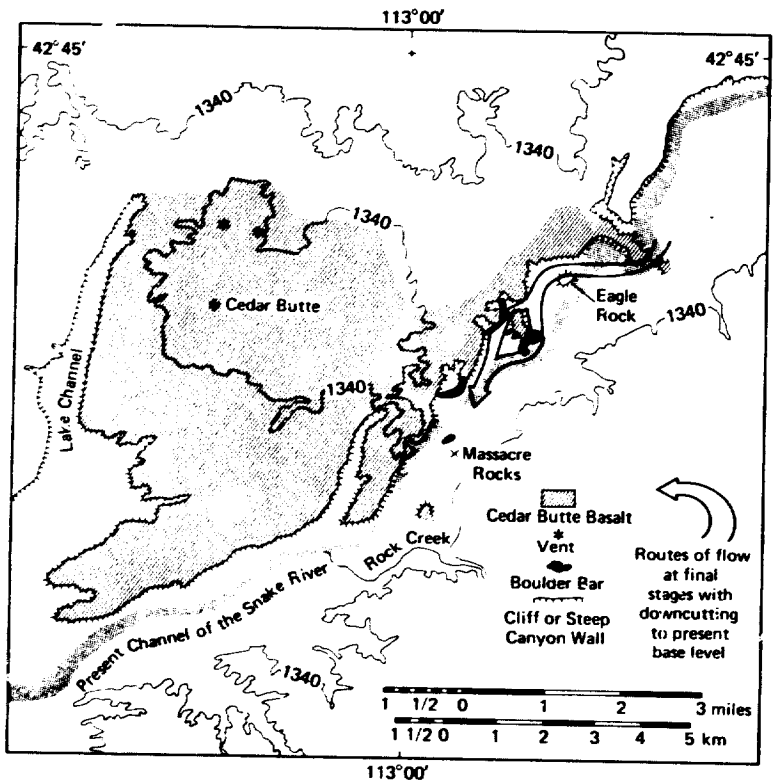

FIGURE 18-23c. After the catastrophic effects of the Lake Bonneville flow ceased, waters slowly downcut the Cedar Butte dam until the Snake River reached its present base level.

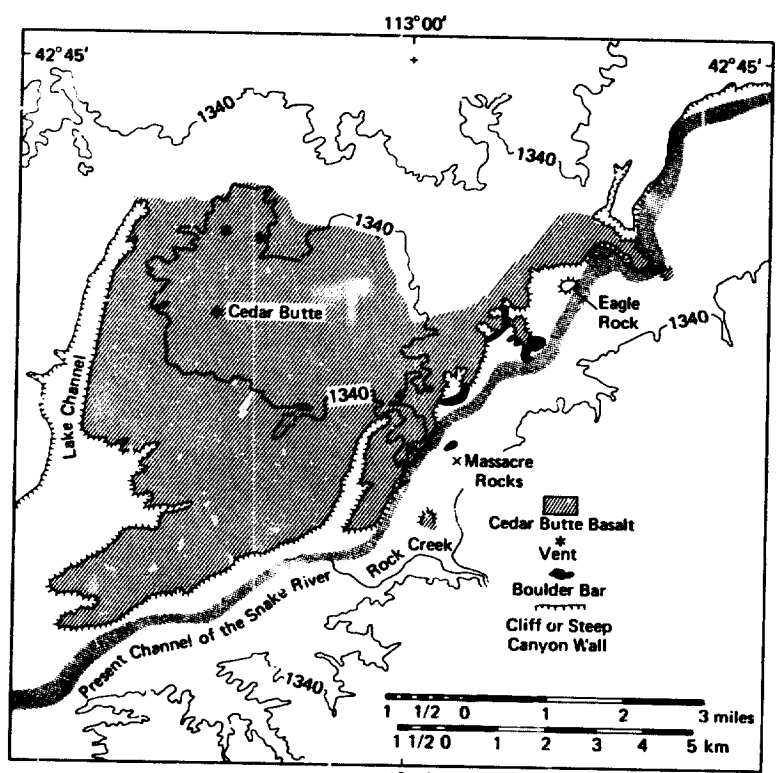

FIGURE 23d. Sketch map of Massacre Rocks area. Lake Channel and other abandoned spillways end in steep cliffs. Areas of major boulder bar depositions can be seen. The Cedar Butte vents and maximum extent of associated flows is also visible. (After Carr and Trimble, 1963.)

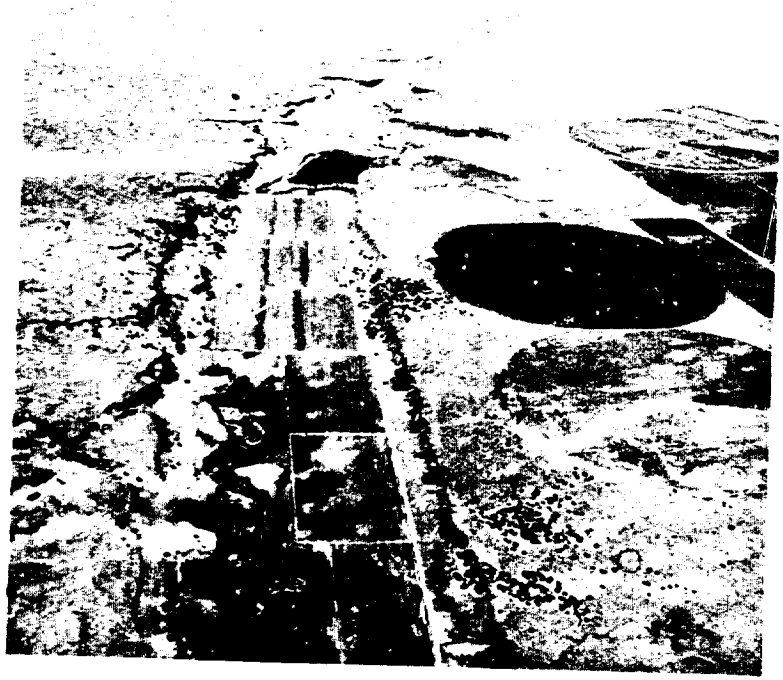

FIGURE 18-24. Oblique aerial view of Lake Channel, an abandoned spillway for ancestral American Falls Lake. Photograph by Ronald Greeley, University of Santa Clara, June, 1977.

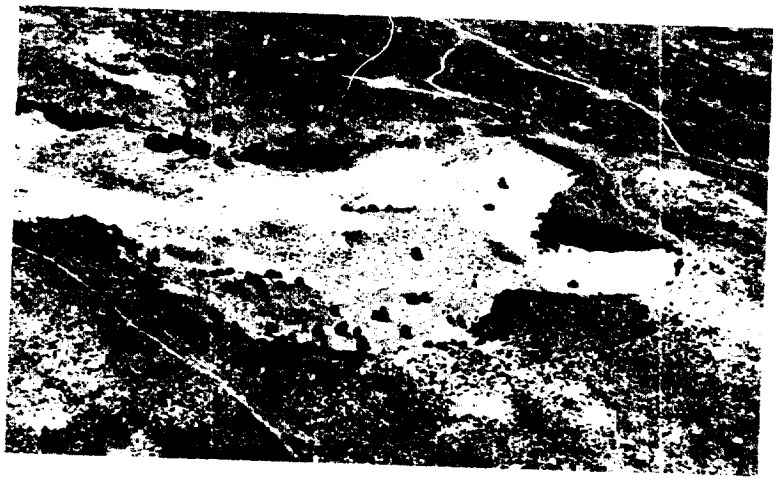

FIGURE 18-25. Oblique aerial view of alcoves which occur throughout this area. Photograph by Ronald Greeley, University of Santa Clara, June, 1977.

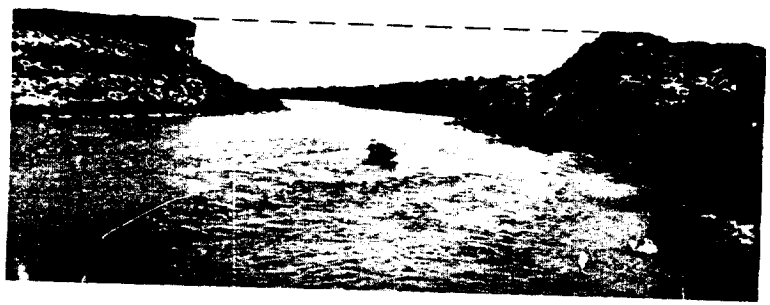

FIGURE 18-26. View upstream of breached Cedar Butte basalt dam (old level is in dashed line). Deposition of the American Falls Lake beds occurred behind this dam. Photograph by Ron Papson, University of Santa Clara, June, 1977.

FIGURE 18-27. View upstream at Hunt Party historic site with exposure of local stratigraphy in southern bank; Neeley Lake beds (1), Walcott Tuff (2), Little Creek Formation (3), and Massacre volcanics (4).

Mileage		
Cumulative	Difference	
35.3	1.5	Main entrance to Massacre Rocks State Park. The name refers to an 1862 ambush, supposedly by Indians, of an emigrant train at this point.

The rocks southwest of the entrance represent the eroded vents for the volcanic rocks in this area (Fig. 18-21). The wide distribution of material from these vents, extending more than 50 km^2, suggests that the original cone was more than 300 m high and several km in diameter (Stearns and others, 1938). These "Massacre Volcanics" are younger than the Walcott Tuff and consist of basaltic cinders and fragments of basement rocks. Following deposition, a period of gentle folding and faulting occurred, as evidenced by offsets in pyroclastic beds in the area. Subsequent eruption of the Cedar Butte vents mentioned above buried the Massacre volcanics and presently form the rimrock along this section of the Snake River channel. As Bonneville floodwaters poured over the basalt, the Snake River channel was deeply eroded, leaving many abandoned spillways and waterfalls (Fig. 18-21), the remnants of which can be seen along the northern bank of the river. Boulder bars, similar to those farther south, appear near the visitor center and are also scattered along the flood path (see Fig. 18-25d).

In the upper campground an unique geologic feature, called the "Devil's Garden," consists of pinnacles of resistant material. A possible explanation of this feature is that hot gases (rich in silica) rose through previously deposited pyroclastic material and precipitated silica, cementing the particles together.

End of road log.

REFERENCES

Bright, R. C. and M. Rubin, 1965. In G. M. Richmond, R. Fryxell, J. Montague and D. E. Trimble, Guidebook for Field Conference E, Northern and Middle Rocky Mountains: Internat. Assoc. Quaternary Res., 7th, p. 105-106.

Bright, R. C. M. Rubin and D. E. Trimble, 1965. In G. M. Richmond, R. Fryxell, J. Montague and D. E. Trimble, Guidebook for Field Conference E, Northern and Middle Rocky Mountains: Internat. Assoc. Quaternary Res., 7th, p. 103-104.

Carr, W. J. and D. E. Trimble, 1963. Geology of the American Falls Quadrangle, Idaho: U. S. Geol. Survey Bull. 1121-G.

Hopkins, M. L., 1951. *Bison (Gigantobison) latifrons and Bison (Simobison) alleni* in southeastern Idaho: Jour. Mammology, vol. 32, p. 192-197.

Ives, P. C., B. Levin, R. D. Robinson, and M. Rubin, 1964. U. S. Geol. Survey, Radiocarbon Dates VII: Radiocarbon, vol. 6, p. 37-76.

Ludlum, J. C., 1942. Pre-Cambrian formations at Pocatello, Idaho: Jour Geology, vol. 50, no. 1, p. 85-95.

Malde, H. E., 1965. In Wright, H. E., Jr., and D. G. Frey, *The Quaternary of the United States:* Princeton University Press, p. 255-263.

Malde, H. E., 1968. The catastrophic Late Pleistocene Bonneville Flood in the Snake River Plain, Idaho. U. S. Geol. Survey Prof. Paper 596.

Stearns, H. T., L. Crandall, and W. G. Steward, 1938. Geology and groundwater resources of the Snake River Plain in southeastern Idaho. U. S. Geol. Survey Water Supply Paper 774.

Stearns, H. T. and A. Isotoff, 1956. Stratigraphic sequence in the Eagle Rock volcanic area near American Falls, Idaho: Geol. Soc. Amer. Bull., vol. 67, p. 19-34.

Trimble, D. E. and W. J. Carr, 1961. The Michaud Delta and Bonneville River near Poatello, Idaho. In Short Papers in the Geologic and Hydrolic Sciences: U. S. Geol. Survey Prof. Paper 424-B, p. B164-B166.

Trimble, D. E., 1976. Geology of the Michaud and Pocatello Quadrangles, Bannock and Power Counties, Idaho: U. S. Geol. Survey Bull. 1400.

Williams, J. S., 1952. Red Rock Pass, Outlet of Lake Bonneville (abs.): Geol. Soc. America Bull., vol. 63, p. 1375.

19. ROAD LOG FROM AMERICAN FALLS TO SPLIT BUTTE*

Ronald Greeley and John S. King

Department of Geology and
Center for Meteorite Studies
Arizona State University
Tempe, Arizona 85281

Department of Geological Sciences
State University of New York at Buffalo
Amherst, New York 14226

19. ROAD LOG FROM AMERICAN FALLS TO SPLIT BUTTE*

Ronald Greeley and John S. King
Department of Geology and Department of Geological Sciences
Center for Meteorite Studies State University of New York at Buffalo
Arizona State University Amherst, New York 14226
Tempe, Arizona 85281

Driving time, with stops: approximately 6½ hours
Driving distance, round trip: 89 mi (143 km)

On this field trip we will examine some of the Quaternary volcanic features of the south-central Snake River Plain (Fig. 19-1). Specific features include King's Bowl Lava Field and other features of the Idaho Rift System (one of the longest exposed rifts in the United States), Bear Trap Cave (an uncollapsed section of Bear Trap lava tube, one of the major tubes on the Plain, traceable for more than 21 km), and Split Butte (a young tephra cone crater which once contained a basaltic lava lake).

After leaving the paved road about 18 km from American Falls, the trip continues on gravel and graded dirt roads that are generally passable for moderate-clearance passenger cars. If the area has received much rain, the dirt roads beyond Crystal Ice Cave may require four-wheel drive vehicles.

The road log was developed when the route crossed the Snake River via the 1927 dam, rather than via the new highway bridge; thus, differences in mileage may occur.

Mileage		
Cumulative	Difference	
0.0	0.0	Initiate road log; mid-town American Falls, traffic light at junction of Business Interstate I–15W and Idaho Rt. 39. Proceed west on Idaho 39 (sign reads Idaho 39 North) toward Aberdeen across the Snake River, following the signs to Crystal Ice Cave.

* After Greeley and King, 1975.

Mileage		
	Cumulative	Difference

C-4

The American Falls reservoir was created in 1927 with the completion of the American Falls dam. The project was begun in 1923 with the aim of putting 110,000 acres of new land under irrigation (Beal, 1942). The dam was planned and erected across the Snake River below the old town site of American Falls, then on the east bank. This meant that the entire established city of American Falls had to be moved to a new location farther to the east. The 1927 dam was constructed at a cost of $3,060,000. It was 1593 m long and 25 m high. When the reservoir filled, it contained 1,700,000 acre feet of water. Presently, the dam is being reinforced and partially reconstructed.

1.3 1.3

STOP 1. Turn left to parking area for field trip orientation and to examine the stratigraphic section exposed in banks of Snake River a hundred meters downstream from the railroad bridge. Cross the Snake River below the American Falls dam. A local stratigraphic section is exposed in the north bank of the river but is presently inaccessible due to construction. Figure 18-16 is a geologic sketch map around American Falls.

Although our interest is in Holocene volcanic features, the general geologic history for the area can be summarized as follows (after Prinz, 1970, supplemented by Stearns and Isotoff, 1956; Trimble and Carr, 1961; Carr and Trimble, 1963):

1. Deposition of the Pliocene *Starlight Fm.* (the nearest exposures are about 2 km SW of American Falls); consists mainly of rhyolitic tuff, welded tuff, and tuff breccia, and locally numerous basalt flows and layers of basaltic tuff.
2. Erosion, followed by deposition of the Pliocene *Neeley Fm.*; consists of light tan to orange brown, fine- to coarse-grained rhyolitic tuff.
3. Deposition of the Middle Pliocene *Walcott Tuff* (exposed in river bank); consists of a lower member of white to gray bedded friable tuff containing spherulites and an upper dark obsidian welded tuff; conformably overlies the Neeley Fm., which may have been deposited in a quiet lake (Carr and Trimble, 1963).
4. Some faulting, local erosion, and possibly some folding.
5. Deposition of the Pleistocene (?) Little Creek Fm. (uppermost units on west side of river); consists of interbedded basaltic and rhyolitic tuffs, with rhyolitic material more prevalent at the base. Diatoms common in some layers indicate accumulation in lakes or ponds for some parts of the formation.
6. Explosive eruption of Pleistocene *Massacre Volcanics* and associated basaltic lavas (vents at Massacre Rocks, Eagle Rock, and Table Mountain, all southwest of American Falls), marks the earliest *extensive* basaltic activity in this part of the Plain and consists of basaltic flows, dikes, agglutinated cinder tuffs, cinder beds, and tuffs.

Mileage		
Cumulative	Difference	

7. Faulting, gentle folding, erosion; erosion of steep-sided canyons.
8. Deposition of the Pleistocene *Raft Fm.* (nearest exposure is about 1.7 km south on the east bank of the Snake River); consists of light-colored calcareous bedded quartz silt and fine sand of predominantly fluvial deposition, although some parts of the formation accumulated also in lakes.
9. A long period of erosion, in which the Snake River cut an ancestral valley in the weakly resistant Raft Formation.
10. Eruption of the Pleistocene *Big Hole Basalt,* a series of undifferentiated lava flows erupted from numerous vents on the Plain west of the Snake River. Deposition of loessal deposits appears to have followed the emplacement of the Big Hole Basalt. The loess is commonly less than 9 m thick, but 6.5 km south of American Falls, it may be at least 30 m thick. The loess may have been derived from the Raft Fm,

    Deposition of the *Sunbeam Formation,* consisting of alluvial and colluvial deposits of silt and minor interstratified sand and gravel.
11. Eruption of the Pleistocene *Cedar Butte Basalt* from vents about 17 km southwest of American Falls. The predominantly olivine basalt built up a low shield and filled the Snake River Valley. North, the flows abutted the Big Hole Basalt. The basalt dammed the river and impounded the water to a maximum level of about 1356 m above sea level, forming ancestral American Falls lake. The lake was more than 60 km long, extending nearly to Blackfoot. Overflow poured around the margins of the dam through two major spillways (Fig. 18-23), one to the north of Cedar Butte, the other approximately along the present channel.
12. Deposition of the Upper Pleistocene *American Falls Lake Beds* (exposed along the Snake River and along the shore of American Falls Reservoir); consists of light-colored calcareous sand, silt, and clay, and a layer of white diatomaceous clay.
13. Overflow of Lake Bonneville through Red Rock Pass 80 km southeast of Pocatello. By this time, American Falls Lake (see 11 above) was about two-thirds filled with sediments. The water from Lake Bonneville entered the shallow lake near Pocatello, depositing the *Michaud Gravel,* a deltaic sand and gravel deposit about 30,000 years B.P.
14. The catastrophic flood of Lake Bonneville greatly increased the discharge at the dam and accelerated downcutting of the spillways, particularly along the southern channel so that eventually the northern passage was abandoned.
15. Just before the northern channel was abandoned, the *Grandview terrace* was cut (between 1350 and 1360 m elevation). At later stages the *Aberdeen terrace* (between 1338 and 1350 m elevation) and *Sterling terrace* (between 1329 and 1338 m elevation) were cut.

Mileage		
Cumulative	Difference	
		16. The dam was finally breached and the lake drained as the river cut into soft sediments.
		Return to Idaho 39 and continue toward Aberdeen.
2.7	1.4	View of Big Southern Butte at eleven o'clock. This well-known landmark, 70 km distant, is about 8 km in diameter and rises nearly 80 m above the Plain. It is a kipuka composed dominantly of rhyolite flows and explosion debris with some basalt. The degree of erosion indicates an age older than the surrounding basalt flows.
3.3	0.6	On the left is a center pivot irrigation system (CPI) developed by Frank Zyback around 1950. A central water source supplies a series of sprinklers set on an aluminum pipe. The pipe rotates around a central point producing a circular field of irrigation. These systems are completely automatic and require very little attention.
6.0	2.7	Road junction, take left branch.
6.3	0.3	Road junction, turn left on North Pleasant Valley Road.
7.8	1.5	Potato shed on right. These distinctive structures are common in southern Idaho. The sprinkler systems seen throughout the area are called *wheel lines.*
12.7	4.9	End of pavement (as of July, 1977).
14.7	2.0	Road junction, turn right. Cemetery on right.
15.7	1.0	Road bears left.
17.6	1.9	Pillar Butte is in view on the horizon at one o'clock. Pillar Butte is composed of predominantly agglutinated lava and marks the summit of the lava cone of the Wapi lava field. The flows immediately surrounding Pillar Butte are both pahoehoe and aa.
18.0	0.4	Turn right.
19.7	1.7	Pillar Butte and part of the Wapi lava field in view to the left.
19.8	0.1	CAUTION—blind hill. This circular depression appears to have been a lava lake.
20.6	0.8	Cattle guard, take left fork.
21.7	1.1	Cattle guard.
23.8	2.1	Pressure ridges on right.
24.7	0.9	Road junction. Dirt track to left goes to Wapi Park (Fig. 19-1), which is the best approach to Pillar Butte; 4-wheel drive is required to reach Wapi Park.
25.2	0.5	STOP 2. Overview of general area. Park on side of road and walk up the hill to the right of the road to the rim of Grandview Crater. Facing generally north, the trailers at the rift mark Crystal Ice Cave. With the trailers at twelve o'clock, the other features can be identified by "clock" directions (Fig. 19-2).

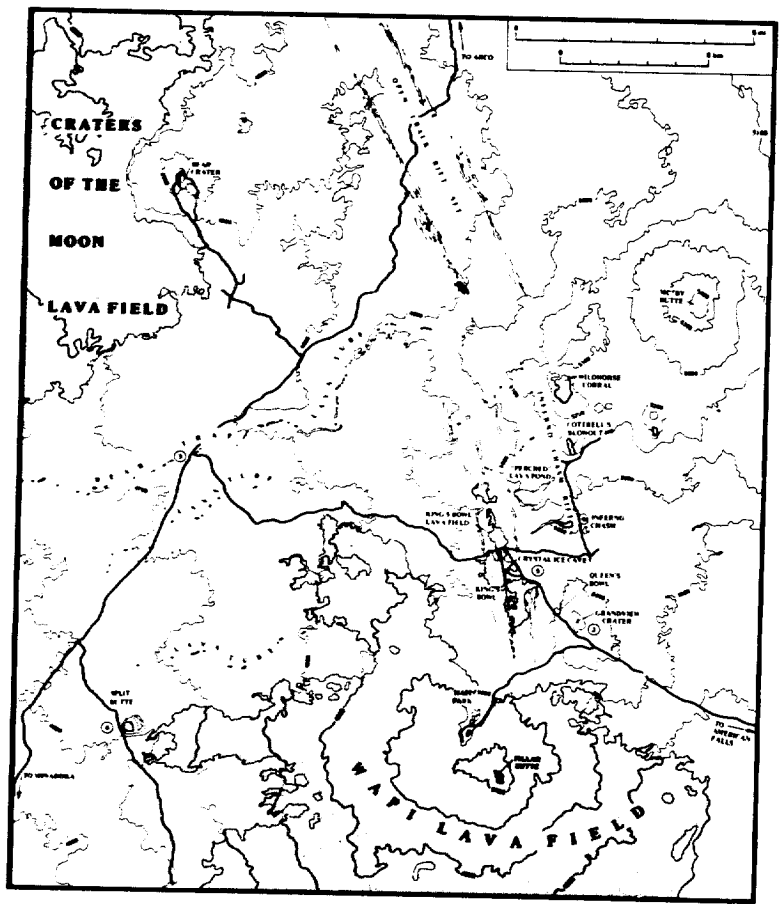

FIGURE 19-1. Sketch map of field area showing the location of named features and field trip stops. The major Holocene lava fields are stippled. Main roads are shown as heavy lines; however, the roads beyond Crystal Ice Cave (from American Falls) are often impassable to conventional vehicles.

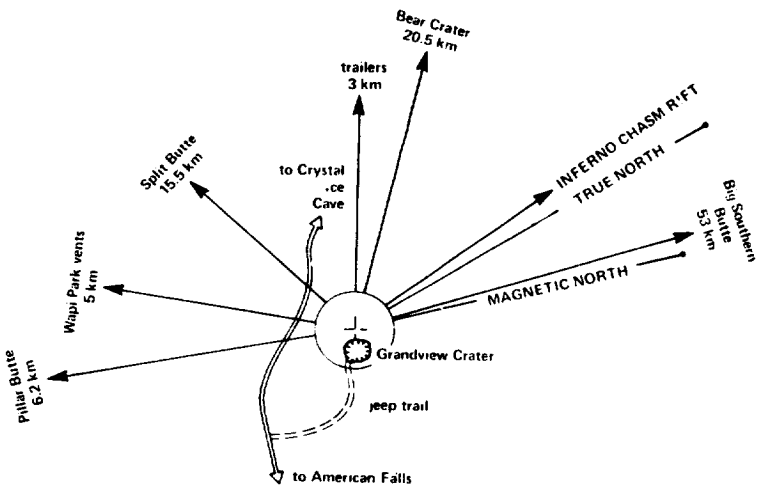

FIGURE 19-2. Stop 2. "Clock diagram," keyed to the various features in the field area as viewed from the rim of Grandview Crater. Diagram is oriented with trailers (Crystal Ice Cave) at twelve o'clock.

Mileage		
Cumulative	Difference	
		Pillar Butte at eight o'clock marks the only known vent area for the Wapi lava flow. The typical low profile for the flow and the steeper slopes of the summit lava cone are well displayed here. The Wapi flow is one of the youngest on the Plain and probably typifies the flow–lava cone structures that make up most of the Plain. Most of the Wapi flow is composed of pahoehoe lava. The steeper slope near the vent can be attributed partly to the accumulation of more viscous aa lava flows. A series of unnamed vents is visible at nine o'clock. These have been partly flooded by the Wapi flow.
		Split Butte is visible across the Wapi flow at between nine o'clock and ten o'clock. From about ten o'clock to one o'clock, the King's Bowl lava field and other features of the King's Bowl rift set are visible. This area is described below at Stop 6.
		A low lava shield is visible at one o'clock. This is the summit area of Bear Crater. On a clear day, the Pioneer Mountains, marking the northern boundary of the Snake River Plain, are visible on the horizon beyond Bear Crater.
		From about one o'clock to two o'clock, a series of low topographic profiles mark large, aligned vents that are approximately parallel to the King's Bowl rift set. These vents include Wildhorse Corral, Cottrel's Blowout, and Inferno Chasm.
		Big Southern Butte is visible between two o'clock and three o'clock.
25.8	0.6	Queen's Bowl Crater on the right.
26.9	1.1	Holocene flows of pahoehoe basalt erupted from the Great Rift are on the left.
27.1	0.2	Road junction, Crystal Ice Cave road and BLM (Bureau of Land Management) road to Minidoka. In wet weather, 4-wheel drive vehicles are recommended for the trip from here to Split Butte and return.
27.9	0.8	Road climbs about 1.5 m onto pahoehoe flows of the King's Bowl Lava Field.
28.0	0.1	Road crosses the east set of tensional fractures that parallel the King's Bowl rift.
28.2	0.2	Road leaves the King's Bowl Lava Field.
28.5	0.3	Road crosses rift fractures.
31.5	3.0	Margin of the Wapi flow can be seen a few hundred meters to the left.
34.3	2.8	Road begins to climb the axis of an unnamed lava tube system (Fig. 19-1). Lava tubes commonly form broad topographic highs along their axes.
35.3	1.0	On crest of lava tube axis. View ahead is across small valley that separates this lava tube from Bear Trap lava tube a few km away (Fig. 19-3).
35.4	0.1	Road junction. Continue straight on the main track.
36.2	0.8	A collapsed section of Bear Trap lava tube is to the right of the road.

Mileage		
Cumulative	Difference	
36.3	0.1	Road junction, turn left (toward Minidoka). Note that road crosses the axis of Bear Trap lava tube.
36.5	0.2	STOP 3. BEAR TRAP LAVA TUBE (Figs. 19-3 and 19-4). (See separate section on lava tubes). CAUTION: Rattlesnakes often inhabit the basalt ledges around lava tube entrances. This is an uncollapsed segment of a 21 km long lava tube that appears to have originated in the vicinity of the Idaho Rift. The tube trends westward where it is eventually buried by Holocene lava flows from Craters of the Moon. Bear Trap and other lava tubes were important in the emplacement of the extensive lava flows in the Plain because they were effective mechanisms to feed advancing flow fronts miles from the source with very little drop in lava temperature.

Continue westward on the side road along the axis of the tube in the downflow (Fig. 19-3) direction 2 km to a second (and better) uncollapsed section of tube.

The segment of Bear Trap lava tube exposed here displays many features common to lava tubes. Walls on both sides of the tube and the roof section exposed over the entrance display typical "layered" lava of Ollier and Brown (1965). They attribute this layering to horizontal partings that develop along shear planes in a single flow. Whether or not one chooses to accept this "shear plane concept," layering does develop within single flows as can be demonstrated by tracing the partings laterally to points where they merge. Conversely, single layers often bifurcate into two layers, which may remerge (?) to form one layer. Thus, layering such as this cannot be attributed to multiple flows. However, multiple flows and flow units are also present here, evidenced by oxidized and brecciated zones between units.

A short distance inside the entrance, the layered lava walls (Fig. 19-5) are covered with a *lava-tube lining*, (a layer of lava that accretes to the tube interior during active flow). In general, linings range in thickness from less than one inch (approximately cm) to a few more than several feet (approximately m). Multiple linings often accrete when the tube serves as a conduit by repeated eruptions. The lining here at Bear Trap shows peculiar pitting which has been observed elsewhere (Greeley, 1971) but has not been explained.

The shelf that occurs approximately 1 m above the floor may represent a period when the flow through the tube was constant enough for accretion to occur along the wall. Alternatively, it may represent downcutting by active flow below a previous level. Lateral erosion has been demonstrated in other areas (Greeley and Hyde, 1972; Greeley and Baer, 1971), and indirect evidence has been cited for downcutting (Swanson and Peterson, 1974), in active lava tubes.

The original floor of Bear Trap tube here is covered with colluvium and other detritus to an unknown depth. The end of the tube is about 50 m from the entrance. It is marked by a sudden "plunge" of the roof in a smooth downward arc. This "roller coaster" profile has been noted in other lava tubes; however, Bear Trap tube is too weathered to determine if this is the case.

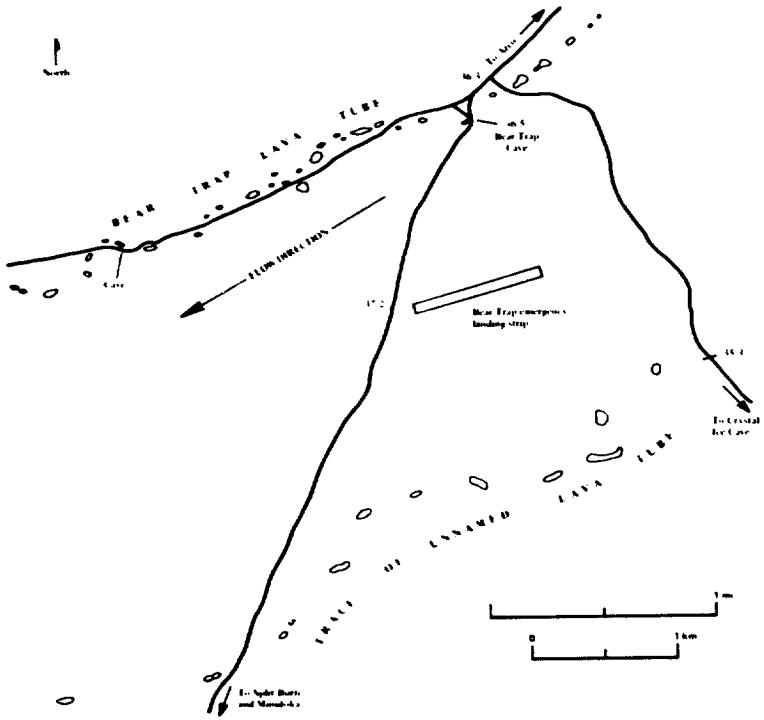

FIGURE 19-3. Stop 3. Sketch map of the Bear Trap lava tube area. Bear Trap Cave is adjacent to the road junction at mileage 36.5. A second cave is about 2 km west.

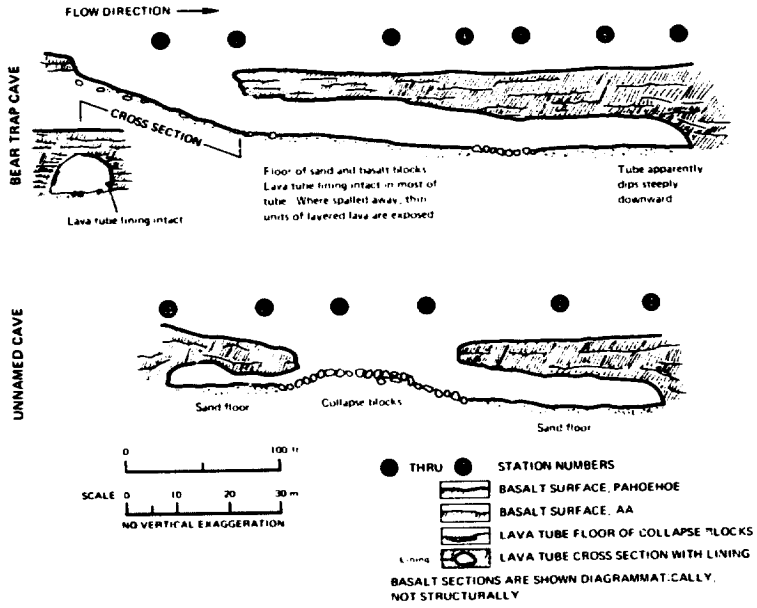

FIGURE 19-4. Longitudinal profiles of two uncollapsed sections of Bear Trap lava tube (Stop 3, Road Log). Surveyed by R. Greeley, M. Lovas, K. Oas, and J. Papadakis, 1969.

Mileage		
Cumulative	Difference	
		Turn vehicles around and retrace the jeep track eastward (Fig. 19-3) back to the first cave (2 km) and resume the road log. NOTE: The mileage from the first cave to the second and return is NOT on the log.
36.8	0.3	Split Butte is visible ahead at eleven o'clock.
37.2	0.4	Road junction, Bear Trap emergency landing strip to the left. Continue straight.
41.2	4.0	Road junction, turn left off main road, toward Split Butte.
42.4	1.2	Road junction, continue straight.
43.2	0.8	Road junction, take right branch.
43.7	0.5	Road junction, turn left and park.

STOP 4. SPLIT BUTTE (See Chapter 12).

Although Split Butte is one of the older exposed features in this part of the Plain, it is still young enough that its salient features are well preserved. This guide is keyed to a walk counter-clockwise around the crater rim, beginning from the parking area (Figs. 12-1 and 19-6).

Station 1:

Walk to the top of the crater rim, up the jeep trail. Recapping from the geologic history of Split Butte given earlier, the earliest event discernible is the eruption of tephra, visible as the "Split," opposite this point, which built a tephra cone; prevailing westerly winds resulted in the asymmetric distribution of tephra on the east rim. This was followed by the formation of a lava lake whose center was slightly offset from the center of the tephra cone which contained it. The lava lake appears to have spilled over the tephra rim in about this area, evidenced by *in situ* basalt on the outer flank of the crater rim. Weathering prevents tracing the lateral extent of the overflow. Withdrawal of magma resulted in the formation of the central pit crater in the former lava lake. Concurrent with, or subsequent to, the lava lake activity, three *en echelon* basalt dikes intruded the tephra on the northwest side of the crater. Following the formation of the pit crater, minor fountaining produced low spatter-and-cinder mounds on the flow and bank of the crater, on the west side. The flanks of the cone-crater were encroached by younger lava flows, the youngest of which are the Wapi flows to the southeast.

FIGURE 19-5. Interior of Bear Trap lava tube, showing typical layered lava (left half of photograph, behind figure) and in situ lava tube lining that covers the layered lava (right half of photograph). From Greeley, 1971.

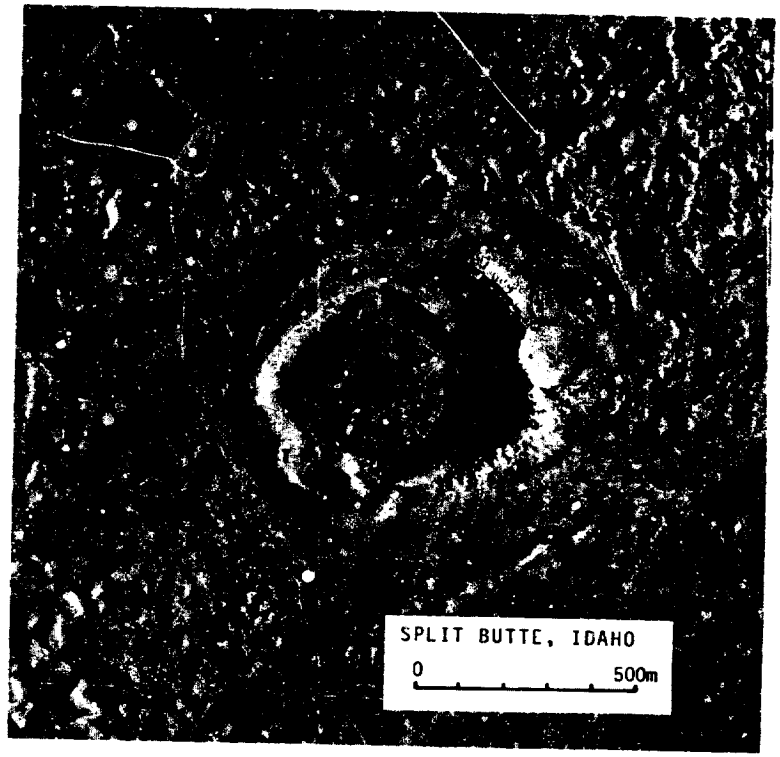

FIGURE 19-6. Vertical air photograph of Split Butte. This structure consists of an outer tuff cone which enclosed a basaltic lava lake. Withdrawal of magma and the subsequent subsidence of the lava lake resulted in the interior pit crater. (NASA-Ames Research Center photograph 951-1-4, May 1969.)

Mileage		
Cumulative	Difference	
		Station 2:
		Beginning near this point and continuing counter-clockwise around the outer crater rim about a hundred meters, both inward-dipping and outward-dipping tephra exposures occur and their relation to the basalt can be established. In several places, the tephra has eroded to expose the "underside" of the lava lake. Near the beginning of the exposed contact with the basalt, the tephra is visible as a broad arch, demonstrating the "turn over" of the tephra layers from the crater interior, over the rim, to the outward-dipping flank of the crater. Split Butte is one of the few places where this relationship is clearly demonstrable. Here, also, the axis of the tephra rim plunges slightly westward, beneath the zone where the basalt lake appears to have spilled over the rim.
		Station 3:
		Continue to the "split." The tephra in this area contains several very large (larger than 30 cm in diameter) basalt blocks which were ejected with the finer-grained material. From this point, the Holocene Wapi flows and Pillar Butte are visible eastward.
		Station 4:
		Proceed northwest to the pit crater rim. This area contains two prominent mounds of red cinder and spatter that represent the last known volcanic activity at Split Butte. The cone may have formed during the subsidence of the lava lake, or from much later activity. East and West from the cinder-spatter cones are exposures of the lava lake basalts in the walls of the pit crater. The surface of the lava lake in the pit crater is buried by colluvial and alluvial material to an unknown depth.
		Station 5:
		Continue an additional 150 meters westward to the tephra outcrop. Near the rim crest, watch for the narrow (30 cm) dikes. The three dikes are nearly vertical and can be recognized as standing above the tephra. Figure 19-7 shows the best exposure, on the northwest part of the rim. From here to the "split," the outcrop of the tephra is more extensive. Note the variations in color and grading of particle sizes.
		Station 6:
		Proceed counterclockwise around the *outside* crater rim along the base of the basalt scarp. Most of the tephra that contained the lava lake has been eroded on this, the windward crater flank, leaving the basalt scarp. However, some remnants of the inward dipping tephra is visible in several places along the base of the scarp.
		Return to the vehicles. Retrace route back to road junction to Crystal Ice Cave (mileage point 27.1), as follows:
43.7		Split Butte parking area. Proceed north on dirt track.

Mileage		
Cumulative	Difference	
44.2	0.5	Road junction, take left branch.
45.0	0.8	Road junction, continue straight.
46.2	1.2	Road junction, turn right onto main Minidoka-Arco road (turn toward Arco).
50.2	4.0	Road junction, continue straight.
50.9	0.7	Bear Trap lava tube (Stop 3), continue on main road.
51.1	0.2	Road junction, turn right.
52.0	0.9	Road junction, continue straight.
60.3	8.3	Road junction, turn right to Crystal Ice Cave.
60.6	0.3	STOP 5. KING'S BOWL LAVA FIELD AND CRYSTAL ICE CAVE (Chapters 9, 10, 11).
		At this stop we will examine the King's Bowl rift set and consider its relationship to the Great Rift system. Individual features include King's Bowl, a phreatic explosion crater formed in the rift, cinder-spatter cones on the rift, bulbous squeeze-ups, and other fresh lava flow features in the King's Bowl Lava Field. We will also be guided through Crystal Ice Cave to examine the cross-section exposed in the walls of the rift and secondary features, such as the spectacular ice formations.
		Return to vehicles and retrace route back to American Falls.
89.0	28.4	American Falls. END OF TRIP.

FIGURE 19-7. South rim of Split Butte showing the outward dipping tephra layers (on the right) in disconformable contact with the younger basalts of the lava lake that was partly contained by the tephra cone.

REFERENCES

Beal, M. D., 1942. *A History of Southeastern Idaho:* Claxton Printers, Caldwell, Idaho, 443 p.

Carr, W. J. and D. E. Trimble, 1963. Geology of the American Falls Quadrangle, Idaho: U. S. Geol. Survey Bull., 1121-G, 43 p.

Greeley, R. and R. Baer, 1971. Hambone, California, and its magnificent lava tubes (abs.): Abstracts, Geol. Soc. Amer., vol. 3, p. 128.

Greeley, R., 1971. Geology and morphology of selected lava tubes in the vicinity of Bend, Oregon: State of Oregon, Dept. of Geology and Mineral Industries, Bull. 71, 47 p., 33 figs., 3 pls.

Greeley, R. and J. H. Hyde, 1972. Lava tubes of the Cave Basalt, Mount St. Helens, Washington: Geol. Soc. Amer. Bull., vol. 83, p. 2397-2418.

Ollier, C. D. and M. C. Brown, 1965. Lava caves of Victoria: Bull. Volcanol., vol. 28, p. 215-229.

Prinz, M., 1968. Volcanic geology of the American Falls area: in Structures and origin of volcanic rocks, Montana, Wyoming, and Idaho: Guidebook: Wayne State University, W. H. Parson, ed., p. 56-63.

Prinz, M., 1970. Idaho Rift system, Snake River Plain, Idaho: Geol. Soc. Amer. Bull., vol. 81, p. 941-947.

Stearns, H. T. and A. Isotoff, 1956. Stratigraphic sequence in the Eagle Rock volcanic area near American Falls, Idaho: Geol. Soc. America Bull., vol. 67, p. 19-34.

Swanson, D. and D. Peterson, 1974. Observed formation of lava tubes: Studies in Speleology, vol. 2, pt. 6, p. 209-223.

Trimble, D. E. and M. J. Carr, 1961. Late Quaternary history of the Snake River in the American Falls Region, Idaho: Geol. Soc. America Bull., vol. 72, p. 1739-1748.

NASA-Langley, 1977